Stable gut hormones and related analogues for treatment of fragility fractures associated with type 2 diabetes

A thesis for the degree of

Doctor of Philosophy

in

School of Biomedical Sciences

Faculty of Life and Health Sciences

Ulster University

By

Sagar Shankar Vavahare BVSc and AH, MVSc and AH, MSc

January 2018

I confirm that the word count of this thesis is less than 100,000 words

TABLE OF CONTENTS

CHAPTER 2

MATERIALS AND METHODS

CHAPTER 3

EFFECTS OF GIP, GLP-1, XENIN AND HYBRID PEPTIDES ON SAOS-2 CELLS *IN VITRO*

CHAPTER 6

IMPACT OF BONE-SPECIFIC GIP/XENIN HYBRID PEPTIDES ON METABOLIC CONTROL AS WELL AS BONE QUALITY AND STRENGTH IN HIGH-FAT FED MICE

ACKNOWLEDGEMENTS

My PhD would not have been completed without blessings of my mother and father. I am eternally grateful to them who have stood beside me everytime. I am grateful to my sister who has constantly motivated me throughout my PhD.

I am blessed to have Dr. Nigel Irwin as my supervisor. He is not just a supervisor but much more than that. He accepted me as a student even though I was transferred from another group. He is father-figure, friend and very positive human being who has understood me and had been so patient during my PhD. He constantly stood besides me and helped me to develop myself in many ways. He always reminded me to keep working towards my goal help me develop scientific temparement and positive mental attitude. He believed in me always and encouraged me every single time. I consider lucky to have Nigel as my supervisor.

I am grateful to Professor Peter Flatt who provided valuable guidance and advice during my PhD. I am thankful to Dr. Guillaume Mabilleau and Professor Daniel Chappard who gave me opportunity to work in their lab at University of Angers. I got chance to learn in one of the best labs in Europe in the field of bone biology.

I would like to thank my wife, Mayuri who has never complained to me and had been so patient during my PhD. She is my support system and belief system. She has tolerated me and my mood swings patiently. My father-in-law and mother-in-law have helped me in my ups and downs. I am grateful for their help and support.

I am thankful to James, Rob, Glen, Lisa, Danny, Velma, Keith and Rhonda who helped me in different ways during my PhD.

I am than.kful to all post-doc staff Tony, Charlotte and Vadivel who provided their valuable guidance during my PhD. I am thankful to my colleagues, Annie, Michael, Chris, Ryan, Vishal, Galyna, Dawood, Shruti, Neil, Rachael, Paul, Andrew, Dipak and Prawez. I really had great time with them and enjoyed working with them.

Sagar Shankar Vyavahare

SUMMARY

Type 2 diabetes mellitus plays a crucial role in causing bone impairments and fragility fractures. Incretin hormones such as glucose-dependent insulinotropic polypeptide (GIP) and glucagon-like peptide 1 (GLP-1) are known to augment insulin secretion from pancreatic beta-cells. There is mounting evidence which points out that these incretin hormones do have positive effects on bone. Especially, GIP is known to have dual action on bone as it enhances osteoblasts which are bone forming cells and reduces bone resorption by osteoclasts. There are mixed results regarding effects of GLP-1 on the bone and the mechanism of action is less clear. However, one cannot rule out the positive findings of several studies highlighting beneficial effects of GLP-1 on the bone. The scientific community is taking an interest in designing oligopeptide as a promising approach in the treatment against bone fractures. The main focus of this thesis is to assess the potential beneficial effects of bone-specific oligopeptides and its analogues on sarcoma osteogenic SAOS-2 cells as well as assess the impact of these analogues on bone directly through *in-vivo* studies. Furthermore, the use of highly advanced sophisticated imaging techniques provides deeper understanding of bone tissue microarchitecture and bone integrity. (D-Ala^2)GIP and bone-specific (D-Ala^2)GIP-Asp enhanced bone biomarker-alkaline phosphatase activity in human osteoblastic SAOS-2 cells. Bone-specific analogue (D-Ala^2)GIP-Asp possessed similar insulin secretory actions as (D-Ala^2)GIP in BRIN-BD11 cells. Treatment with (D-Ala^2)GIP-Asp improved glucose homeostasis and insulin sensitivity in high fat fed mice. (D-Ala^2)GIP-Asp increased bone mineral content (BMC) in tibia highlighting positive effects of (D-Ala^2)GIP-Asp on bone. Bone matrix properties such as bone marrow diameter, total area and cortical thickness were increased in the mice treated with (D-Ala^2)GIP-Asp. Collagen cross-linking was enhanced by (D-Ala^2)GIP-Asp. The results of xenin analogue on bone were inconsistent. The bone-specific analogue namely, Xenin-25[Lys^{13}PAL]-Asp did not showed any beneficial effects on bone but overall, Xenin-25[Lys^{13}PAL] and Xenin-25[Lys^{13}PAL]-Asp showed beneficial metabolic effects in lean as well as high fat fed mice. Further studies need to be carried out to assess the positive impact of Xenin-25[Lys^{13}PAL]-Asp on bone. Varying degrees of benefit of the bone-specific hybrid peptide, namely GIP/Xenin-Asp and GIP/Xenin-Glu, were found on bone in high-fat fed mice. Once daily administration of GIP/Xenin-Asp and

GIP/Xenin-Glu enhanced tibial bone mineral density. GIP/Xenin treatment increased trabecular bone volume and number of trabeculae in high fat fed mice. No effects of GIP/Xenin-Asp and GIP/Xenin-Glu were seen on bone matrix and tissue material properties. This thesis sheds light upon immense potential of incretin-based therapeutic treatments for bone fragility fractures associated with type 2 diabetes.

ABBREVIATIONS

(*db/db*)	Diabetic (*db/db*) mice
µg	Microgram
µl	Microlitre
µm	Micrometer
AGEs	Advanced glycation end products
Ala	Alanine
AlkP	Alkaline phosphatase
ANOVA	Ananlysis of variance
Asp	Aspartic acid
AUC	Area under the curve
B.Dm	Bone diameter
BMC	Bone mineral content
BMD	Bone mineral density
BMDD	Bone mineral density distribution
BMSCs	Bone marrow stromal cells
BSE	Back-scattered electron
BTM	Bone turnover markers
BV	Bone volume
bw	Body weight
cAMP	Cyclic adenosine monophosphate
cm	Centimeter
CSMI	Cross-sectional moment of inertia
Ct.Th	Cortical thickness
DCC	Dextran coated charcol
DEXA	Dual-energy x-ray absorptiometry
dl	Decilitre
DM	Diabetes mellitus
DM	Marrow diameter
DPP-4	Di-peptidyl peptidase 4
FBS	Fetal bovine serum
FDA	Food and drug administration
g	Gram

GIP	Glucose-dependent insulinotropic polypeptide
GIPR	Glucose-dependent insulinotropic polypeptide receptor
GLP-1	Glucagon-like peptide-1
GLP-1R	Glucagon-like peptide-1 receptor
h	Hour
HAP	Hydroxyapatite
HBSS	Hanks buffer saline solution
HPLC	High performance liquid chromatography
IBMX	3-isobutyl-1-methylxanthine
IGF-1	Insulin- like growth factor 1
ip	Intraperitoneal injection
kg	Kilogram
KO	Knock-out mice
KRBB	Krebs ringer bicarbonate buffer
kV	Kilovolt
l	Litre
LDL	Low density lipoprotein
Ma.Dm	Marrow diameter
mg	Miligram
microCT	X-ray microcomputed tomography
min	Minutes
ml	Mililitre
mm	Milimeter
mmol	Milimolar
MMP	Matrix metalloproteinase
mN	Milinewton
MPa	Megapascal
mrna	Messenger RNA
MSC	Mesenchymal stem cell
N	Newton
nm	Nanometer
OPG	Osteoprotegerin
PDX-1	Pancreas duodenum homeobox-1
PI-3k	Phosphotidyl inositol 3 kinase

PMMA	Polymethylmethacrylate
PPAR-γ	Peroxisome proliferator activated-gamma
qBEI	Quantitative back-scattered electron imaging
qXRI	Quantitative x-ray imaging
RANKL	Receptor activator on nuclear factor-Kappa B ligand
RIA	Radioimmunoassay
ROI	Region of interest
rpm	Revolutions per minute
SAOS-2	Sarcoma osteogenic
s-CTX	Serum C-terminal telopeptide
SEM	Standard error of the mean
SGLT-2	Sodium-glucose co-transporter-2
s-P1NP	Serum-procollagen type I N propeptide
SSTR2	Somatostatin receptor type 2
T1DM	Type-1 diabetes mellitus
T2DM	Type-2 diabetes mellitus
Tb.N	Trabecular number
Tb.Sp	Trabecular separation
Tb.Th	Trabecular thickness
TGF-β	Transforming growth factor-beta
TRAP	Tartrate-resistant acid phosphatase
TV	Trabecular volume
U	Unit
WnT	Wingless-related integration site
Z	Atomic number
α-MEM	alpha-minimum essential medium

DECLARATION

"I hereby declare that for 2 years following the date, on which the thesis is deposited in Research Student Administration of Ulster University, the thesis shall remain confidential with access or copying prohibited. Following expiry of this period I permit

1. the Librarian of the University to allow the thesis to be copied in whole or in part without reference to me on the understanding that such authority applies to the provision of single copies mase for study purposes or for inclusion within the stock of another library.
2. the thesis to be made available through the Ulster Institutional Repository and/or EThOS under the terms of the Ulster eTheses Deposit Agreement which I have signed.

IT IS A CONDITION OF USE OF THIS THESIS THAT ANYONE WHO CONSULTS IT MUST RECOGNISE THAT THE COPYRIGHT RESTS WITH THE UNIVERSITY AND THEN SUBSEQUENTLY TO THE AUTHOR ON THE EXPIRY OF THIS PERIOD AND THAT NO QUOTATION FROM THE THESIS ANS NO INFORMATION DERIVED FROM IT MAY BE PUBLISHED UNLESS THE SOURCE IS PROPERLY ACKNOWLEDGED."

Chapter 1

Introduction

1. 1 DIABETES MELLITUS

Diabetes mellitus is a metabolic disease where the pancreas cannot produce sufficient insulin, or bodily tissues cannot effectively utilise it (Effoe *et al*. 2017, Moon *et al* 2017 and Kodama *et al*. 2017). Hence, blood glucose levels are elevated in the body in diabetes. There are two major forms of diabetes mellitus; type 1 diabetes mellitus (T1DM) and type 2 diabetes mellitus (T2DM). Currently, there are more that 400 million people in the world affected by diabetes (International Diabetes Federation, 2015). It is projected that, in 2035, 592 million individuals will be affected with diabetes imposing tremendous burdens on health care systems. According to Diabetes UK, from November 2016, there are almost 3.6 million people who have been diagnosed with diabetes in United Kingdom (Northern Ireland-88,000; Wales-188644; England-3,033,529 and Sctoland-280,023). There are various well-characterised complications associated with diabetes which include retinopathy, neuropathy, nephropathy, cardiovascular diseases. (Diabetes UK, 2014). As well as there is growing evidence to suggest that diabetes can cause bone fragility and increase the risk of bone fractures (Palmero *et al*. 2017, Westberg-Rasmussen *et al*. 2017 and Sanches *et al*. 2017). Various studies have pointed out that diabetes can cause severe impairment of bone microarchitecture, reduce bone mineral density (BMD) and bone mineral content (BMC) in T1DM patients. In T2DM patients, BMD is found to be slightly elevated, but increased fracture risk still persists (Vestgaard 2007, Ponti *et al*. 2017 and Perez-Saez *et al*. 2017). There are inconsistencies with BMD, but without doubt diabetes plays an important role in causing bone fractures (Jiao *et al*. 2015). This whole new frontier of diabetes and bone fragility fractures needs to be studied extensively in order to develop an effective new treatment approach.

1.1.1Type 1 diabetes mellitus (T1DM)

T1DM is mostly seen in young adults and accounts for 10% of the cases of diabetes worldwide (International Diabetes Federation, 2014). Type 1 diabetes mellitus is characterised by inability of body to produce sufficient insulin due to autoimmune destruction of pancreatic β cells (American Diabetes Association Definition). Therefore, the patient has to depend on exogenous insulin to maintain blood glucose concentration after ingestion. It is believed that over expression of $CD4^+$ and $CD8^+$ T cells by pancreatic β cells, ultimately leads to destruction of insulin producing β cells in T1DM (Graham *et al*. 2012). Genetic and environmental factors do play an important role in pathogenesis of T1DM. Genetic factors mainly include major histocompatibility complex human leukocyte antigen (HLA) alleles, such as DR3-DQ2 and DR4-DQ8 that strongly contribute to T1DM (Atkinson & Eisenbarth 2001). Environmental factors, such as viruses which can cause abnormal activation of immune system, has been shown to lead to the generation of β cell specific auto-antibodies (Napoli *et al*. 2016).

1.1.2 Type 2 diabetes mellitus (T2DM)

T2DM is characterised by inability of β cells to produce sufficient insulin coupled with an ineffective utilisation of insulin by peripheral tissues (Bolen *et al*. 2017, Powers *et al*. 2017). T2DM accounts for 90% cases of diabetes worldwide and is generally reported in middle aged and older individuals (Fareed *et al*. 2017, Pan *et al*. 2017). In order to maintain normal blood glucose levels, compensatory bodily mechanisms come into action, which respond to insulin resistance by secreting more insulin to maintain steady blood glucose levels (Drucker 2006). However, eventually beta-cell exhaustion occurs and the body cannot produce sufficient insulin, leading to overt

hyperglycemia. There are several environmental factors that contribute to T2DM that include pregnancy, ageing, obesity, physical inactivity and poor diet (Balcerczyk *et al*. 2017, Romieu *et al*. 2017). Genetic associations also exist, and genetic predisposition are linked to mutations in *TCF7L2, PPARG, CAPN10, MC4R, FTO, KCNJ11* and *KCNQ1* genes (Valeria *et al*. 2007, Taharani *et al.* 2011, Basil *et al*. 2014, Prasad & Groop 2015). The biggest concern regarding T2DM is that it can progress symptom free for many years before clinical diagnosis (Wilmot & Idris 2014, Chaudhury *et al*. 2017).

1.1.3 Diabetes and fracture risk

Bone fracture risk is elevated in diabetes, and is considered to be higher in T1DM than T2DM (Moayeri *et al*. 2017). Several studies have clearly revealed reduced BMD in T1DM patients (Hampson *et al*. 1998, Miazgowski & Czekalsi 1998, Vestergaard 2007, Rakel *et al* 2008). In contrast, T2DM patients have normal or sometimes elevated BMD (Schwartz *et al*. 2000, Petit *et al*. 2010 and Asokan *et al*. 2017). Even though T2DM patients have elevated BMD, they are still at higher risk of bone fractures (Moseley 2012). As such, focus on potential for bone fracture should not be entirely dependent upon BMD, as there are many other factors such as neuropathy and retinopathy could lead to higher risk of falling in diabetic patients (Schwartz *et al*. 2002) and postural instability (Moseley 2012). In addition, Yamagishi *et al*. reported interaction of advanced glycation end products (AGEs) and collagen in bone reduces bone strength, leading to osteoporosis in diabetic patients (Yamagishi *et al*. 2005, Alikhani *et al*. 2007). Further, AGEs may stimulate apoptosis of osteoblasts, causing defective bone formation (Asokan *et al*. 2017). Some studies have pointed out that low levels of vitamin D and altered vitamin D metabolism may lead to osteoporosis and eventually increased fracture risk in diabetes (Wientroube *et al*. 1980, Vogt *et al*. 1997, Caprio *et al*. 2017).

BMD is strongly associated with body weight, ageing and lean mass, which are all important in the diagnosis and progression of diabetes (Ooms *et al*. 1993, De Laet *et al*. 2005, Hirschfeld *et al*. 2017). Figure 1.1 summarises the major factors that may be responsible for increased bone fracture risk in T2DM (Mosenzon *et al*. 2015).

1.1.4 Existing treatment for diabetes

The current approved treatment for T1DM is daily injections of exogenous insulin (Heise *et al*. 2017). As well as insulin injection, there are other treatment options for T1DM which mainly include islet-cell transplantation. Transplantation is an issue in T1DM because of the altered immune systems in this individual and possible organ rejection (Kolb & Herrath 2017). In addition, drugs that are used to prevent organ rejection have been shown to have negative effects on beta-cell insulin secretion (Langsford *et al*. 2017). Moreover, there is short supply of organs, and until new sources of functional islets are found, the future remains uncertain. Regarding T2DM, several drugs, or drug combinations, have been approved. Although, there are some inconsistencies regarding effective dosing and related side effects, most of these drugs are fairly well tolerated by patients (Table 1.1). However, the impact of these drugs to help prevent bone fractures are not yet well established (Table 1.2). In addition, it should be remembered that the normal measures of BMD to assess fracture risk, are likely not be appropriate in diabetes (Wasserman & Gordon 2017).

Figure 1.1 Factors responsible for higher fracture risk

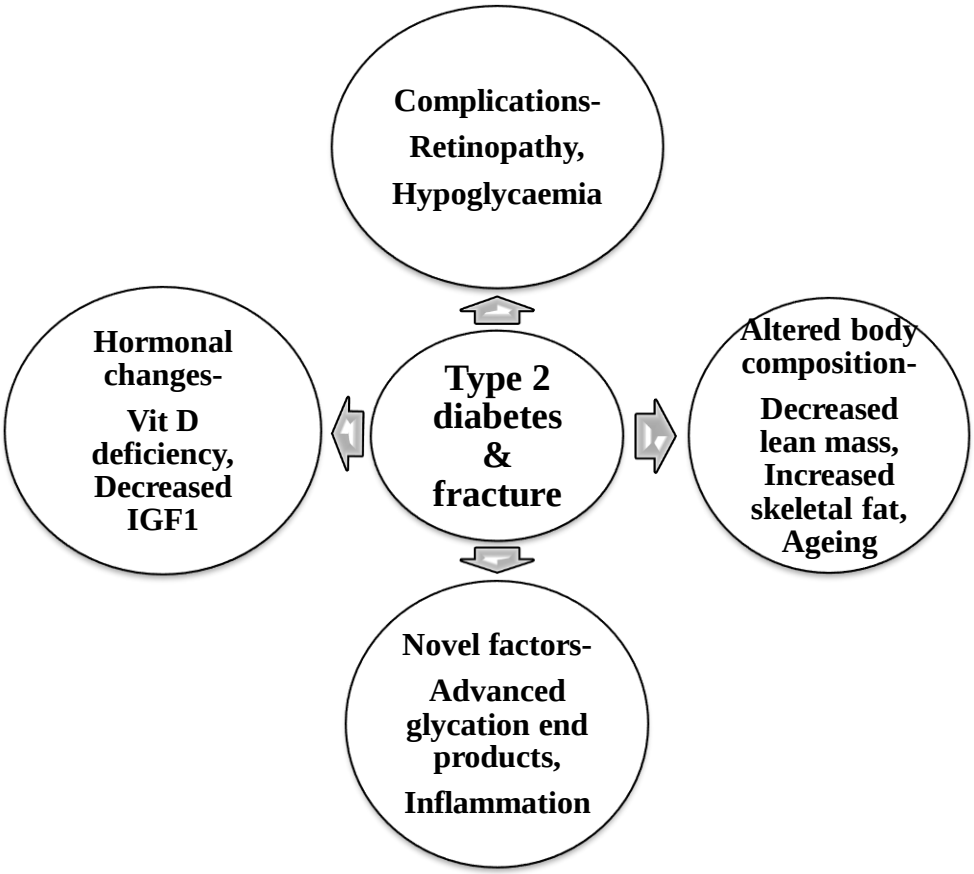

Schematic representation of factors responsible for increase fracture risk in diabetes

Table 1.1 Summary of available treatment options for T2DM

Principal mechanism of action	Class of medication	Active compound	Dosing	Frequency	Mechanism of action	Side effects
Insulin Sensitizer	Biguanide	Metformin	500-1000 mg	Twice/Three times	Activation of AMPK that results in suppression of hepatic glucose production and increase in insulin sensitivity	Diarrhoea, abdominal cramping, risk of lactic acidosis, Vitamin B_{12} deficiency
	Thiazolidine-dione (TZD)	Pioglitazone	15-30 mg	Once a day	Activation of the transcription factor PPARγ involved in the transcription of genes regulating glucose and fat metabolism	Weight gain oedema / heart failure Bone fractures
		Rosiglitazone	2-8 mg			
Insulin secretagogue	Sulphonylureas	Glyburide	5-15 mg	Once or twice a day	Binds to sulfonylurea receptors and closes K_{ATP} channels on beta cell plasma membrane resulting in influx of Ca^{2+} and stimulation of insulin release	Hypoglycemia Weight gain
		Glimepiride	1-4 mg			
		Glipizide	5-15 mg			
		Gliclazide	40-320 mg			
	Meglitinide	Nateglinide	60-120 mg	With each meal	As for sulphonylureas	Hypoglycemia Weight gain
		Repaglinide	1.5-16 mg			
	DPP-4 inhibitor	Alogliptin	25 mg	Once or twice a day	Inhibits DPP-4 action and causes an increase in concentrations of GLP-1 and GIP	Angio-oedema Association with pancreatitis
		Linagliptin	5 mg			
		Saxagliptin	5 mg			
		Sitagliptin	50-100 mg			
		Vildagliptin	50 mg			
	GLP-1r agonist	Exenatide	5–10 µg	Twice a day	Increase in glucose-dependent insulin secretion, glucagon suppression,	Vomiting, pancreatitis and medullary thyroid tumors in animals
		Liraglutide	06-1.8 µg	Once a day		
		Lixisenatide	10-20 µg	Once a day		
		Albiglutide	30 mg	Once a week		
		ExenatideLAR	2 mg	Once a week		

					slowing gastric emptying and reducing appetite	
Other	SGLT2 inhibitor	Canagliflozin	100-300 mg	Once a day	Inhibits SGLT2 action in the kidney causing reduction in renal glucose reabsorption	Increased risk of genital and urinary tract infections
		Dapagliflozin	10 mg			

AMPK: AMP-Activated protein kinase; DPP-4: Dipeptidyl peptidase-4;; GLP-1r: Glucagon-like peptide 1 receptor; LAR: Long-acting release; SGLT2: Sodium–glucose co-transporter 2; PPAR: Peroxisome proliferator-activated receptor.

Taken from (Tahrani *et al*. 2011, Inzucchi *et al*. 2012, Mabilleau *et al*. 2015)

Metformin is now considered the first-line of treatment agent in T2DM (Upadhyay *et al*. 2017). It is an oral antidiabetic drug that belongs to biguanide class (WHO- Dept of Essential Medicines and Health Products). Its mechanism of action involves activation of AMP-activated protein kinase which results in suppression of hepatic glucose production and increases insulin sensitivity. Metformin directly inhibits the mitochondrial respiratory chain complex through inhibition of mitochondrial glycerophosphate dehydrogenas, which leads to suppression of gluconeogenesis (Madiraju *et al*. 2014). Interestingly, other recent evidence has suggested that metformin benefits in T2DM could be linked to suppression of hepatic glucagon signalling (Miller *et al.* 2013). There is controversial evidence when it comes to the action of metformin on bone. Metformin has been shown to enhance type I collagen and osteocalcin expression, increase alkaline phosphatase activity and promote the bone mineralisation process (Kanazawa *et al*. 2008). Metformin also reduces osteoclast activity by disrupting CaMKK and TAK1 (Mai *et al*. 2011). However, very few clinical studies have reported a reduced risk of fracture with metformin (Meier *et al*. 2008, Melton *et al.* 2008, Vestergaard *et*

al. 2009) and the majority of studies show no effect on fracture risk (Kanazawa *et al*. 2010, Colhoun *et al*. 2012 and Napoli *et al*. 2014).

Sulphonylureas are also extensively used in the treatment of T2DM (Deacon & Lebovitz 2016). Their mechanism of action involves binding to sulfonylurea receptors, which leads to the closure of K_{ATP} channels on the β-cell plasma membrane. Subsequently, this leads to closure of potassium channels and opening of voltage-dependent calcium channels that stimulates insulin secretion (Roder *et al.* 2016, Baumgard *et al.* 2016). There is evidence which suggest that sulphonylureas has some positive effects on osteoblast and enhance alkaline phosphatase activity (Chandran 2017, Lecka-Czernik 2017). However, another most important aspect is that sulphonylureas are associated with higher incidences of hypoglycaemia that increases risk of fall in individuals, and therefore increased fracture risk (Badieh & Mary 2016, Pscherer *et al*. 2016 and Watts *et al.* 2016).

Thiazolidinedione (TZD) mechanism of action involves activation of peroxisome proliferator activated receptor gamma (PPARγ), a transcription factor that facilitates mesenchymal stem cells to differentiate into adipocytes (Lecka-Czernik *et al*. 2002). Several clinical studies have reported a higher incidence of fractures with TZD (Meier *et al*. 2016), and this has been confirmed on numerous occasions (Fujita *et al*. 2016, Shanbhogue *et al*. 2016). Preclinical studies confirm that TZDs are detrimental to bone (Lecka-Czernik *et al*.2002). TZDs reduce the number of osteoblasts-bone forming cells and related bone volume (Rzonca *et al*. 2004). Preclinical studies have reported a neutral effect of SGLT-2 inhibitors on bone with some positive effects leading to increase in bone mineral density (Yokono *et al*. 2014). However, it is conceivable that the effect

of SGLT-2 inhibitors on the levels of circulating ions could ultimately have a negative impact on bone integrity.

Glucagon-like peptide 1 (GLP-1) is secreted by intestinal L-cells in response to nutrient absorption (Steinert *et al.* 2017). GLP-1 enhances glucose–stimulated insulin secretion through binding to specific GLP-1 receptors (GLP-1r) on beta-cells. The GLP-1r is also present in various tissues including the brain, heart, kidney and gastrointestinal tract (Holst *et al.* 2004, Green & Flatt 2007). GLP-1 also causes glucagon suppression, slows gastric emptying and reduces appetite (Amalia *et al.* 2017). Some controversy exists as to the presence of GLP-1rs on the bone, although GLP-1 mediated bone effects are acknowledged (Nuche-berrenguer *et al.* 2010). As such, studies in GLP-1r knockout (KO) mice reveal a reduction in osteoclasts (Yamada *et al.* 2008), but it has been reported that bone formation remains almost unaffected in GLP-1r KO mice (Yamada *et al.* 2008). However, others have shown that the GLP-1r is critical for optimal bone mechanical and material properties (Mabilleau *et al.* 2013). SGLLT2 inhibitors such as dapagliflozin and canagliflozin have no effect on the bone (Nauck 2014).

Dipeptidyl peptidase-4 (DPP-4) is an enzyme that inactivates GLP-1, and its sister incretin hormone glucose-dependent insulinotropic polypeptide (GIP), by cleaving an N-terminal dipeptide from both hormones leaving the truncated metabolites GIP(3-42) and GLP-1(9-36) (Drucker 2007). Interestingly, both metabolites are considered to be receptor antagonists (Yanagimachi *et al.* 2017), and a very recent study has fully characterised the antagonistic properties of a DPP-4 cleaved GIP compound in man (Gasbjerg *et al.* 2017). Currently, there are many DPP-4 inhibitors available for clinical use, including Vildagliptin, Saxagliptin, Sitagliptin and Linagliptin (Duez *et al.* 2007). There is conflicting evidence regarding DPP-4 and its use as therapeutic treatment option for reducing bone fractures

in diabetes. Some studies suggest that there is no effect of DPP-4 inhibition on osteoblast differentiation (Sbaraglini *et al*. 2014), while in another study it was found that 12 week treatment with saxagliptin caused a reduction in osteoblasts and osteocyte density and an increase in osteoclast numbers (Gallagher *et al*. 2014). Taken together, the most exciting area in terms of diabetes medications and bone effects, with potential therapeutic implications, relates to the incretin hormones. As discussed above, GLP-1 mimetics have been shown to potentially positively impact bone (Mabilleau, *et al*. 2017). In addition, emerging evidence has revealed an extremely important role for GIP in the maintenance of normal bone function and quality. Therefore, this thesis will focus on the effects of incretin peptides, and related therapies, on bone strength and quality in diabetes.

Table 1.2 Effect of current T2DM treatment options for bone fracture risk

Class of medication	Potential mechanisms bone	Effect on fracture risk
Biguanide	Conflicting results in animals and humans	↔
Thiazolidinediones	Reduction in the number of osteoblasts, osteoclasts	↓
Sulphonylureas and meglinitinides	Animal/human data is conflicting	↔
GLP-1R agonists	Controversial findings; alterations in bone tissue material properties	↔ or ↓
DPPIV inhibitors	Conflicting results in preclinical rodent studies	↔ or ↓
SGLT2 inhibitors	Neutral/no effect	↔

Taken from Irwin & Flatt 2015

1.2 BONE

Bone is a living mineralised tissue that comprises of three major components - fibrous protein collagen, calcium phosphate-based hydroxyapetite and water (Weiner & Wanger 1998). There are many important physiological functions of bone, but the most important is to control mechanical function of the body and act as a storage vessel for calcium and phosphate (Hao *et al*. 2017). Bone undergoes continuous remodelling through sequential activity of bone-forming osteoblast cells and bone-resorbing osteoclast cells (Figure 1.2). This continuous process is governed by various autocrine and paracrine factors, such as IGF-1, IL-6, netrin 1, TGF-β (Bart Clarke 2008, Kini & Nandeesh 2012). Bones undergoes several changes throughout life that can be due to environment, age and disease status (Oishi & Manabe 2016). Some diseases, such as osteoporosis, may

cause alterations in the bone leading to fractures (El-Tawdy *et al*. 2017). However, early diagnosis can prevent further deterioration of the bone and there are several techniques that can be used for assessment of bone in more detail.

Figure 1.2 Bone remodeling cycle

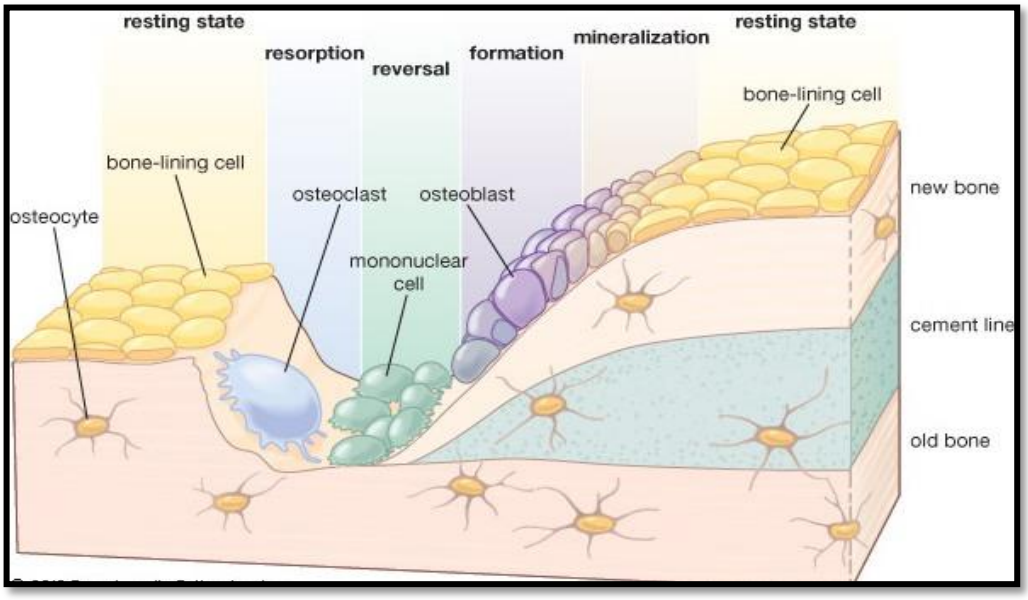

(Taken from Encyclopedia Britannica Inc, 2010)

Bone remodelling is a continuous process and is coordinated by the activity of osteoclasts and osteoblasts through bone resorption and formation, respectively.

1.2.1 Assessment of bone mass

The most commonly used technique to assess bone mass is dual-energy X-ray absorptiometry (DEXA) (Ali *et al*. 2017, Leeuwen *et al*. 2017). DEXA analysis can help in determining bone mineral density (BMD) and bone mineral content (BMC). Bone mineral content and bone mineral density can also be assessed by X-ray microradiograph imaging (Bassett *et al*. 2012). In the general population, increased BMD is considered to be good

thing as it is linked to a lower risk of bone fracture (Unnauntana *et al*. 2010). Unfortunately, this is not the case in diabetes, with both T1DM and T2DM having contradictory effects on BMD. As such, T1DM patients have reduced BMD while T2DM tend to present with unchanged or elevated BMD (Vestergaard 2007, Abdulameer *et al*. 2012, Jackuliak & Payer 2014). Since both forms of diabetes are linked to increased fracture risk, it is clear that BMD does not paint a true picture of fracture risk in these patients. Indeed, BMD is not the only parameter that reflects bone quality, and other characteristics such as bone microarchitecture, mineral matrix ratio, collagen maturity, collagen content and mineral composition can also play important role (Gourion-Arsiquad *et al*. 2009, Wen *et al*. 2015).

1.2.2 Assessment of bone microarchitecture

Microcomputed tomography (microCT) provides a deeper understanding of bone microarchitecture. Essentially, there are three different steps to assess bone microarchitecture. In the first step, the entire bone is scanned leading to a projection of overlaid X-ray images. In the second step, from this stack of X-ray images, a 3D representation of the bone is reconstructed and then finally analysis can be performed (Van't Hof 2012). The main advantage of microCT is that it provides deeper insight into the trabeculae of bone and assesses number of trabeculae, bone volume as well as trabecular thickness (Verdelis *et al*. 2011, Manske *et al*. 2015). This information can provide a much clearer picture of bone quality than simple BMD and BMC measures.

1.2.3 Biomechanical assessment of bone

The two major factors that govern the biomechanics of bone are strength and stiffness (Osterhoff *et al*. 2016). Bone stiffness, or hardness, can be assessed using nanoindentation and ultimate strength by three-point bending (Nyman *et al*. 2016).

Nanoindentation was first used by Oliver and Pharr in 1962. The biggest advantage of nanoindentation is that it can measure mechanical properties of the bone in a very small scale (below micron level), to gain a more accurate reflection of the material properties in bone matrix (Olive & Pharr 1992). The basic principle of three-point bending depends on the relationship between load applied at the midshaft of long bone and displacement of the bone until failure, which produces load displacement curve similar to well-established stress-strain curve (Iepsen *et al*. 2015). This stress-strain curve helps in assessing different variables of the bone, including ultimate load, ultimate displacement, stiffness and work-to-failure ratio (McNerny *et al*. 2016).

1.2.4 Assessment of bone material properties

Scanning electron microscopy can be used to assess bone mineral density distribution (Whitehouse *et al* 1971). Basically, backscattered electrons are reflected by the atoms present in the bone sample. The atoms with high atomic number have stronger interactions with the electrons and they appear brighter in the grey level image derived from the electron scan. The atoms with lower atomic numbers will have fewer interactions and will produce images of less intensity (Chappard *et al* 2011). Another technique that can be employed for assessment of bone material properties is Fourier transformed infrared (FTIR) microscopy. Fundamentally, femurs are cut at mid-shaft and embedded in polymethylacrylate and further subjected to spectral analysis which is carried out by infrared microscope. FTIR is used for examination of mineral to matrix ratio, degree of mineralisation, mineral maturity, crystallinity and collagen maturity (Farley *et al*. 2010, Kourkoumelis *et al*. 2012, Wen *et al*. 2015), all of which can give a clear indication of bone quality.

1.3 INCRETIN EFFECT

The term ‘incretin effect’ is used to describe the fact that oral glucose administration produces greater degree of insulin secretion as compared to intravenous infusion of the same amount of glucose (Nauck *et al*. 1986). Thus, it implies that gut derived factors have an important role to play in insulin secretion and glucose homeostasis (Yang *et al*. 2017). Indeed, the incretin effect is estimated to account for 50-70% of total insulin secretion after oral glucose administration (Kazafesos 2011, Nauck *et al*. 2011). After food ingestion, the incretin hormones, GIP and GLP-1, are released into the blood and directly enhance glucose-mediated insulin secretion from pancreatic β-cells (Fu *et al*. 2013, Smith *et al*. 2014). Although there are many gastrointestinal hormones that can stimulate and release insulin, GIP and GLP-1 are believed to be the only molecules that can do this at physiologically relevant levels, meaning that these two hormones account for the full incretin effect in man (Seino *et al*. 2010).

1.4 GLUCOSE-DEPENDENT INSULINOTROPIC POLYPEPTIDE (GIP)

GIP was initially isolated from porcine small intestine and initially it was known as gastric inhibitory polypeptide, hence the acronym GIP, because of its ability to inhibit gastric acid secretion (Brown *et al*. 1969). However, the main biological role is now considered to be stimulation insulin release in response to food ingestion (Pederson *et al*. 1976), and so was later named glucose-dependent insulinotropic polypeptide to maintain its original acronym, GIP.

1.4.1 Synthesis, secretion and signaling

GIP is a 42-amino acid peptide synthesised by intestinal K-cells, which are found in the upper duodenum and proximal jejunum (Fujita *et al*. 2016). The human GIP gene comprises of 6 exons (Figure 1.3), and most of the sequence for GIP lies in exon 3. The GIP sequence is highly conserved and human GIP shares more than 90% similarity in amino acid sequence with mouse, rat, porcine and bovine GIP (Baggio & Drucker 2007, Mells & Anania 2013).

Figure 1.3 Structure of ProGIP

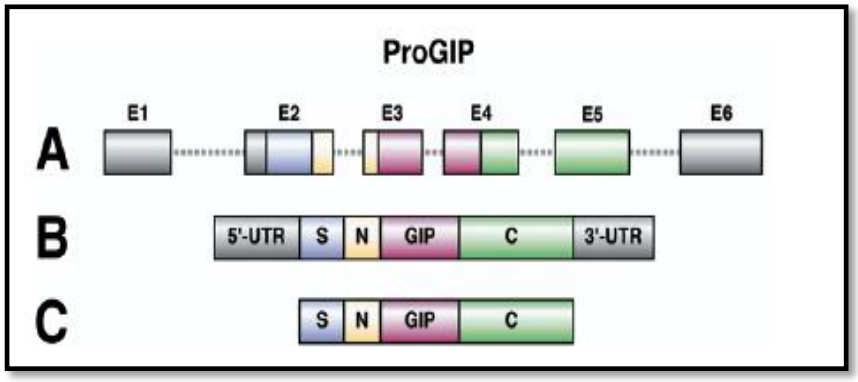

Structures of (A) ProGIP gene, (B) mRNA, and (C) GIP protein. (Taken from Baggio & Drucker 2007)

1.4.2 GIP, β cell and diabetes

The main role of GIP as incretin hormone is to regulate glucose homeostasis (Holst *et al.* 2017). Upon food intake, GIP is secreted by K-cells and then binds to its specific receptor on pancreatic islet β-cells to enhance glucose-mediated insulin secretion (Cavin *et al*. 2017). Activation of GIPR signaling increases cAMP levels and subsequent inhibition of K_{ATP} channels (Figure 1.4). Inhibition of K_{ATP} channels leads to influx of Ca^{2+} and stimulation of insulin secretion by exocytosis (Ding & Gromada 1997). Binding of GIP to its G-protein coupled receptor also activates cAMP-mediated

phosphatidylinositol 3-kinase (PI3K)/protein kinase B (PKB) and MAP kinase signaling pathways which are closely associated with promotion of proliferation, differentiation and inhibition of apoptosis of β -cells (Ugleholdt et al. 2006).

Figure 1.4 Signalling pathways of GIP

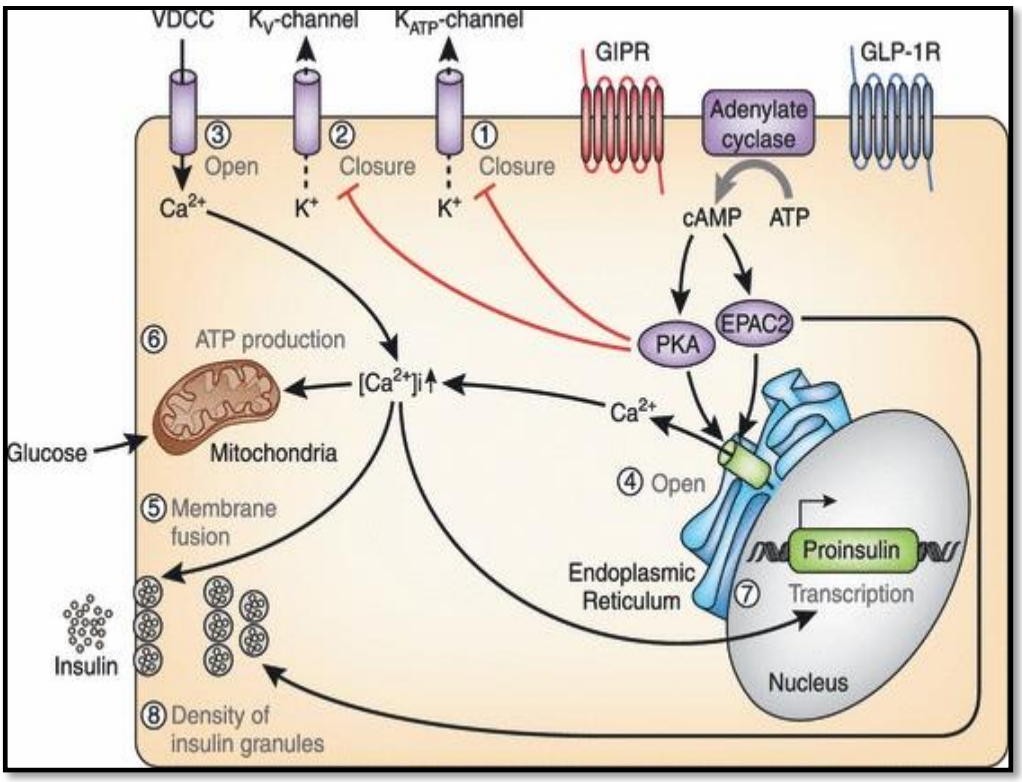

(Taken from Seino *et al*. 2010)

1.4.3 Extrapancreatic action

The main physiological action of GIP is in pancreas. However, the widespread expression of GIPRs in other tissues such as in adrenal cortex, brain, heart, lung, pituitary, adipose as well as bone suggests wider extrapancreatic actions of GIP in the body (Figure 1.5). There is firm evidence revealing that functional GIPRs are present in primary adipocytes and the adipose cell line, 3T3-L1 (Weaver *et al*. 2008, Gogebakan *et al*. 2015).

Figure 1.5 Extrapancreatic action of GIP

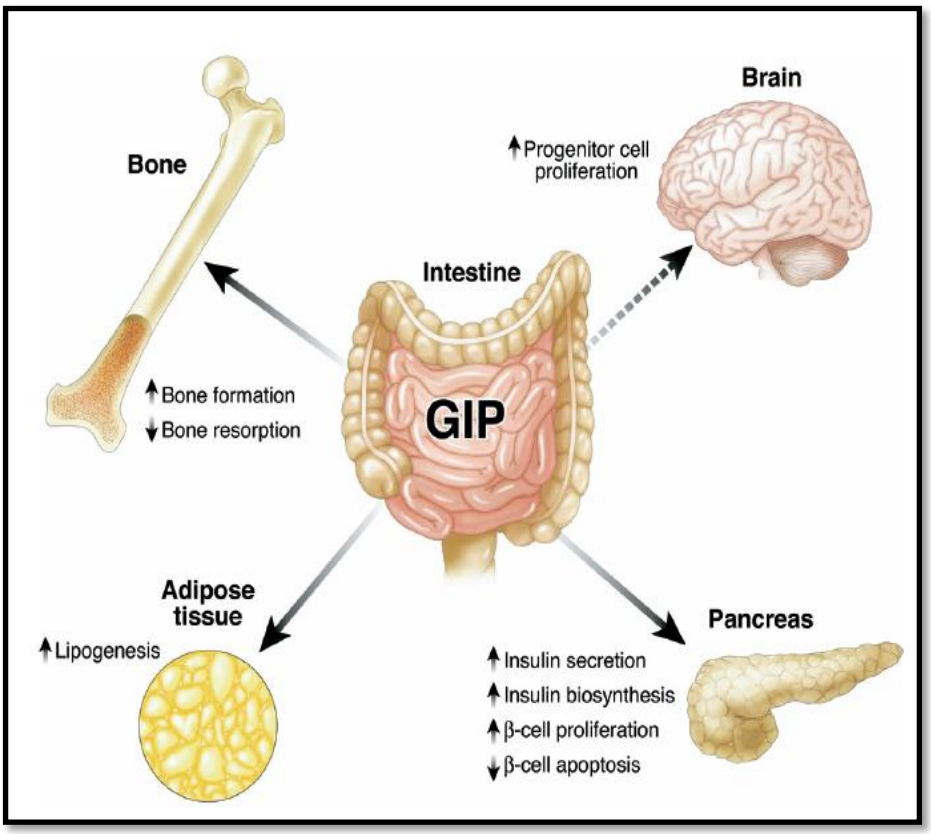

Extrapancreatic effects of GIP by direct interaction with GIPRs on specific tissues. (Taken from Baggio & Drucker 2007)

Effects of GIP have also been shown in the brain. GIPR mRNA and specific binding sites have been detected in the cerebral cortex and hippocampus, including the olfactory bulb (Usdin *et al*. 1993, Kaplan & Viagna 1994). Indeed, several studies have highlighted that GIP plays important role in regulating functions in the brain. In 2007, Nyberg and co-workers demonstrated that administration of exogenous GIP in rats and incubation of GIP with cultured adult hippocampal progenitor cells stimulates the proliferation of hippocampal progenitor cells (Nyberg *et al*. 2007). In addition, GIP-overexpressing transgenic mice display better memory

recognition than normal wild type mice (Ding *et al*. 2006, Li *et al*. 2016). In 2011, Porter and colleagues demonstrated that, administration of a stable GIP analogue for 28 days improved cognitive function in high-fat fed diabetic mice that displayed cognitive dysfunction (Porter *et al*. 2011). Overall, these findings show that GIP does play an important role in regulating certain brain functions.

In terms of bone, functional GIPRs are found on bone-forming osteoblast cells and bone-resorbing osteoclast cells (Bollag *et al* 2000, Zhong *et al* 2007). GIPRs are also expressed on osteocytes (Bollag *et al* 2001) and cultured bone marrow stromal cells (BMSCs) (Ding *et al*. 2008). Genetic knockout of the GIPR in mice has been shown to negatively affect bone quality and strength (Greco *et al*. 2016, Mantelmacher *et al*. 2017, Ramsey & Isales 2017) whereas administration of a stable GIP analogue improves bone quality in normal and diabetic rodents (Millar *et al*. 2016, Hansen *et al*. 2017, Mansur *et al*. 2017). Together, this also reveals an important role for GIP in normal bone physiology.

1.4.4 DPP-4 and GIP metabolism

GIP is secreted immediately after food ingestion, but has a short half-life due to the action of the ubiquitous enzyme DPP-4 (Chon & Gautier 2016, White & baker 2016). In rodents, the half-life of GIP is less than 2 mins (Kieffer *et al*. 1995) while in humans, the half-life of GIP is around 5-7 mins (Deacon *et al*. 2000). DPP-4 is a specialised serine protease that cleaves the penultimate residues from the N-terminal of bioactive proteins that contain alanine or proline residues at position 2 (Mentlein *et al*. 1993). Thus, DPP-4 inactivates biologically active GIP by cleaving at its first two N-terminal amino acids (Tyr^1-Ala^2), leaving truncated metabolite, GIP(3-42) (Kieffer *et al*. 1995, Marvani & Patel 2017, Nongonierma & FitzGerald 2017, Sparre-Ulrich *et al*. 2017). The cleavage of active GIP (1-42) by

DPP-4 leads to eliminates biological activity, and possibly leads to the generation of a GIPR antagonist (Gault *et al*. 2003). In addition to rapid degradation by DPP-4, GIP is also subjected to renal excretion by kidney filtration (Meier *et al*. 2004). In order to overcome the inactivation of GIP by DPP-4, structurally-modified DPP-4 resistant GIP molecules have been designed (Divya *et al*. 2014, Chaurasia *et al*. 2016, O'Harte *et al*. 2016). In addition, renal clearance can be reduced by conjugating the peptide to fatty acid moieties or polyethylene glycol residues (Muppidi *et al*. 2016, Yang *et al*. 2016, Han *et al*. 2017). Together these modifications prolong the pharmacokinetic profile of GIP and dramatically enhance its bioactivity, as detailed below.

1.4.5. Structurally modified GIP agonists

In order to fully exploit the insulinotropic properties of GIP, a substantial number of DPP-4 resistant GIP molecules have been designed and tested (Table 1.3). One of the pharmacological approaches that is extensively used is modification of the N-terminal amino acid residues of GIP to prevent DPP-4-mediated degradation (Irwin & Flatt 2009). Several Tyr^1-substituted GIP molecules that have been generated and tested which include N-acetyl, N-Fmoc, N-gluticol, N-pyroglutamyl and N-palmitate GIP. These analogues have been shown to be resistant to DPP-4 and thus, have enhanced bioactivity as compared to that of native GIP (O'Harte *et al*. 2000, Gault *et al*. 2002, O'Harte *et al*. 2002). Synthesis and characterisation of several Ala^2-modified GIP analogues has also been carried out and these include [Abu^2]GIP, [Gly^2]GIP, [Sar^2]GIP, [Ser^2]GIP and [D-Ala^2]GIP. However, it has been found that only [Gly^2]GIP, [Ser^2]GIP and [D-Ala^2]GIP have notable biological activity and antihyperglycaemic properties as compared to native GIP (Hinke *et al*. 2002, Gault *et al*. 2003a).

Even though N-terminally-protected GIP analogues are resistant to DPP-4-, there is still another hurdle of renal filtration that needs to be addressed. Therefore, in order to overcome this problem, C-16 palmitate fatty-acid (PAL) chain has been attached covalently to the Lys^{16} or Lys^{37} residue of the GIP peptide. There are several fatty-acid GIP derivatives that have been developed to date. These include GIP(Lys^{37}PAL), GIP(Lys^{16}PAL), N-AcGIP(Lys^{37}PAL), N-AcGIP(Lys^{16}PAL), N-pGluGIP(Lys^{37}PAL) and N-pGluGIP(Lys^{16}PAL) (Irwin *et al*. 2005a, Irwin *et al*. 2005b, Irwin *et al*. 2006a) (Table 1.3). The main advantage for attaching C-16 fatty acid is that it encourages non-covalent binding of the peptide to albumin, acting as a drug reservoir that cannot be filtered by the kidneys, thus prolonging biological activity (Irwin & Flatt 2009). Polyethylene glycol (PEG) derivatised GIP analogues have also been characterised and these molecules are also resistant to kidney filtration and display protracted pharmacodynamics profiles (Chen *et al*. 2016).

Table 1.3 GIP agonists that have currently been characterised

Structural modifications giving DPP IV resistance	**Structural modifications aimed at restricting kidney filtration**
N-acetyl-GIP	GIP(Lys^{16})-palmitate
N-pyroglutamyl-GIP	GIP(Lys^{37})-palmitate
N-glucitol-GIP	N-acetyl-GIP(Lys^{16})-palmitate
N-palmitate-GIP	N-acetyl-GIP(Lys^{37})-palmitate
N-Fmoc-GIP	N-pyroglutamyl-GIP(Lys^{16})-palmitate
(Gly^{2})GIP	N-pyroglutamyl-GIP(Lys^{37})-palmitate
(Ser^{2})GIP	GIP [PEGylation]
(Abu^{2})GIP	N-palmitate-GIP(1-30) [PEGylation]
(Sar^{2})GIP	
(D-Ala^{2})GIP	

(Adapted from Irwin *et al*. 2015)

1.5 GLUCAGON -LIKE PEPTIDE (GLP-1)

1.5.1 Synthesis, secretion and signaling

The proglucagon gene has 6 exons and the entire GLP-1 coding sequence lies within exon 4 (Figure 1.6). The proglucagon gene is expressed in pancreatic α-cells, intestinal L-cells and the central nervous system (Jiang *et al*. 2016). Posttranslational processing of the proglucagon gene product generates different peptides, depending on the tissue. In the pancreas, proglucagon is cleaved by prohormone convertase (PC2) to produce glucagon

(GLUC), glicentin-related polypeptide (GRPP), intervening peptide-1 (IP-1) and major proglucagon fragment (MPGF) (Rouille *et al*. 1997a). As a major product of proglucagon in α-cells, glucagon is known to play its role by counteracting insulin action to maintain normal glucose levels (Mayfield *et al*. 2016, Muller *et al*. 2017 and Preiato *et al*. 2017).

In the intestine and central nervous system, the 180-amino acid proglucagon peptide liberates oxyntomodulin, glicentin, GLP-1, intervening peptide-2 (IP-2) and GLP-2. GLP-1 is the major product of proglucagon gene in the intestine and it is one of the important glucoregulatory hormones that control glucose homeostasis (Albrechtsen *et al*. 2016, Drucker 2016). In addition to GLP-1, oxyntomodulin is also released postprandially and the peptide is believed to exert its effects by binding to both GLP-1 and glucagon receptors (Pocai 2012). Activation of glucagon receptor increases blood glucose concentration, whilst simultaneous GLP-1R activation counteracts this effect, thus balancing glucose metabolism in the body. However, there is a suggestion that central activation of glucagon receptors can alter energy turnover and lead to body weight loss (Pocai 2014). For this reason, oxyntomodulin has recently been speculated to have therapeutic potential for diabetes and obesity (Pocai 2014). Similar to GIP, processing of proglucagon precursor to yield GLP-1 is dependent on prohormone convertase PC1/3. Proglucagon is initially cleaved to glicentin and the major proglucagon fragment (MPGF). Subsequent cleavage of MPGF at the monobasic site Arg^{77} and the dibasic site Arg^{109}-Arg^{110} releases GLP-1 (Rouille *et al*. 1997b).

Figure 1.6: Structures of proglucagon

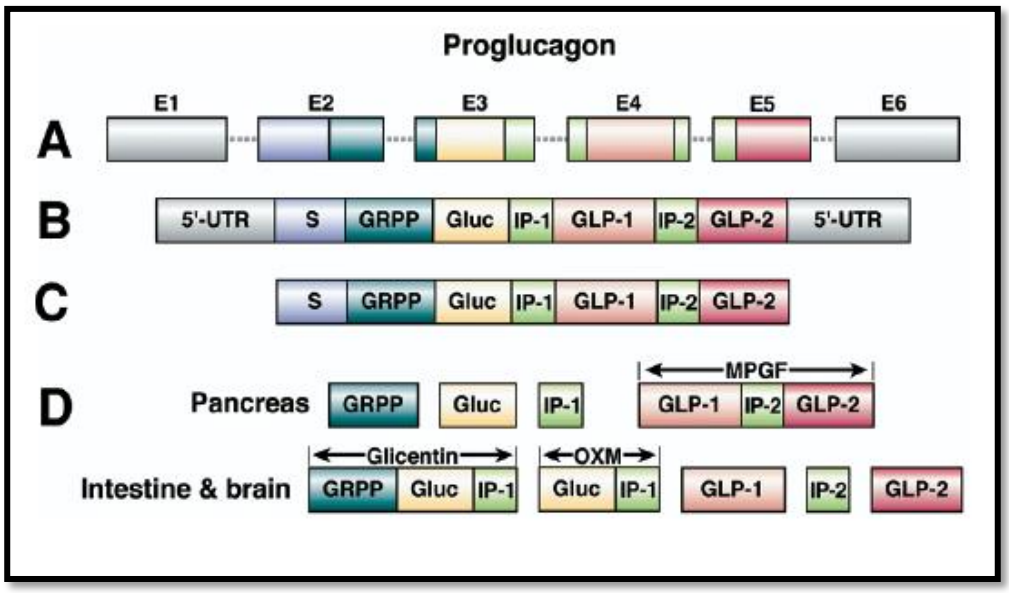

Structures of (A) the proglucagon gene, (B) mRNA, and (C) protein. (D) Posttranslational processing of proglucagon. (Taken from Baggio & Drucker 2007)

1.5.2 Pancreatic actions

The primary physiological action of GLP-1 in the pancreas is to stimulate insulin secretion from beta-cells in a glucose dependent manner (Mojsov *et al.* 1987). Two different signalling pathways are involved in GLP-1-mediated insulin release, either through cAMP-dependent PKA or Epac2 activation, or via cAMP-independent phosphatidylinositol-3 kinase (PI-3K)/protein kinase C (PKC) signalling pathways (Baggio & Drucker 2007). GLP-1 can also encourage insulin gene transcription and synthesis through effects on the pancreas duodenum homeobox 1 (PDX-1) gene (Amatya *et al.* 2017). PDX-1 is an essential transcription factor for pancreatic beta-cell function (Wang *et al.* 1999). GLP-1 also strongly suppresses glucagon secretion from pancreatic α-cells (Holst *et al.* 2011) and its inhibitory action is likely mediated through stimulation of somatostatin and activation of somatostatin subtype receptor 2 (SSTR2) in pancreatic α-cells (de Heer *et al.* 2008, Piro *et al.*

2016, Otter & Lammert 2016, Gylfe 2017, Muller *et al*. 2017, Pradhan & Majhi 2017).

Extrapancreatic actions

Several tissues have been shown to express glucagon-like peptide-1 receptors (GLP-1Rs), such as the heart, brain, liver, intestinal tract, muscle and adipose tissue (Wei & Mojsov 1996, Dunphy *et al*. 1998, Merchenthaler *et al*. 1999 and Green *et al*. 2009). As shown in Figure 1.7, GLP-1Rs are present throughout the body. The glucoregulatory activity of GLP-1 does not only take place in pancreas, but also in other tissues by reducing hepatic glucose production in liver and increasing glucose uptake in muscle and adipose tissue (Larsson *et al*. 1997, Baggio & Drucker 2007). In the brain, activation of GLP-1R signaling enhances neurogenesis, reduces apoptosis and protects neuronal function (Perry *et al*. 2002, Perry *et al*. 2003). It has been reported that GLP-1can also be used as a therapeutic option for treatment of chronic heart failure (McDermott *et al*. 2016). Moreover, improvements in learning and memory activities were observed in rodents when treated with stable GLP-1 mimetics (Cha *et al*. 2016, Millar *et al*. 2017, Palleria *et al*. 2017, Tramutola *et al*.2017). Therefore, GLP-1 could be useful in the treatment of neurodegenerative disorders (Dilan *et al*. 2017, Kim *et al*. 2017 and Muscogiuri *et al*. 2017).

Figure 1.7: GLP-1 actions on specific tissues

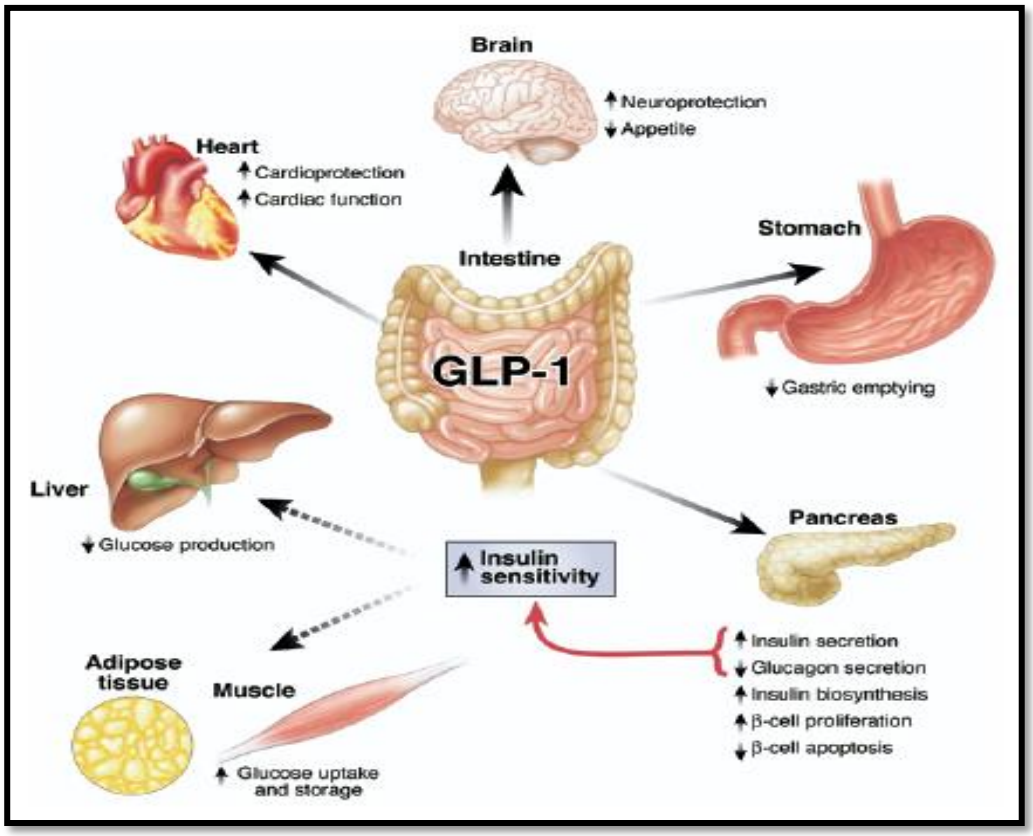

Extrapancreatic effects of GLP-1 by direct interaction with GLP-1Rs on specific tissues. (Taken from Baggio & Drucker 2007)

1.5.4 DPP4- and GLP-1 metabolism

There are several forms of GLP-1 secreted *in vivo* that include GLP-1(1-37), GLP-1(1-36)amide, but only GLP-1(7-37) and GLP-1(7-36)amide are thought to be biologically active (Baggio & Drucker 2007). GLP-1 is rapidly secreted into the blood circulation following feeding; however, the half-life of intact GLP-1 is short, around 2 mins (Kieffer *et al*. 1995), due to the activity of DPP-4. Native GLP-1 contains an alanine at position 2 and therefore alanine acts as a good substrate for DPP-4 (Mirošević *et al*. 2017). The specific cleavage of DPP-4 at N-terminal dipeptides from GLP-1 produces GLP-1(9-36)amide

and GLP-1(9-37) with diminished biological activities (Mentlein *et al*. 1993, Kieffer *et al*. 1995). Similar to GIP, GLP-1 can also be eliminated from circulation by renal filtration (Meier *et al*. 2004). The short half-life of GLP-1 has therefore prompted the need of generation of stable long-acting forms of GLP-1, if the peptide is to be employed therapeutically (Knudsen *et al*. 2000).

1.5.5 Structurally modified GLP-1 agonists

In order to exploit the highly significant glucose-lowering and insulin-releasing properties of GLP-1, various structurally modified GLP-1R agonists have been generated (Green *et al*. 2001). These GLP-1 analogues possess modification of amino acid residues at N-terminus of the peptide, producing GLP-1R molecules that are resistant to DPP-4 activity (Deacon *et al*. 1998). Biological activity of GLP-1 can also be prolonged by delaying renal filtration, and this can be achieved through fatty acid derivatisation (Green & Flatt 2007).

1.5.6 Exendin-4

Exendin-4 (Exenatide / Byetta) is a naturally occurring 39 amino acid peptide which is isolated from the saliva of the lizard *Heloderma suspectum* (Furman BL 2012). Exendin-4 exhibits around 53% similarity in structure to that of mammalian GLP-1. It is resistant to DPP-IV action due to the presence of a glycine residue at position 2 in place of alanine (Drucker & Nauck 2006). Therefore, exendin-4 remains in the blood for longer time as compared to that of native GLP-1 (Chen *et al*. 2017, Peter *et al*. 2017). The biological activity of exendin-4 is similar to that of GLP-1, since it binds and activates the GLP-1R (Koole *et al*. 2017). As such, exendin-4 enhances insulin secretion in glucose dependent manner, delays gastric emptying as well as reduces food intake thereby reducing body weight (Seino *et al*. 2010, Duarte *et al*. 2013, Sharma *et al*. 2015). Exenatide is the

synthetic form of exendin-4 and was approved by US Food and Drug Administration (FDA) in 2005 for the treatment of T2DM (Vishal Gupta 2013, Seungah Lee & Dong Yun Lee, 2017).

1.5.7 Liraglutide

Liraglutide is a GLP-1 analogue that has a high sequence homology (approx. 97%) to native GLP-1 (Jacobsen *et al*. 2016). The half-life of Liraglutide is about 13 hrs due to C-16 fatty acid derivation, and hence it is suitable for once-daily subcutaneous administration in humans (Chaudhury *et al*. 2017, Lorenz *et al*. 2017, Meece 2017). In 2009, Liraglutide was approved by European Medicines Agency for T2DM treatment, and then it was also approved by US Food and Drug Administration in early 2010 (Peterson & Pollom 2010). Several clinical studies of Liraglutide have been carried out and it was demonstrated that once-daily subcutaneous administration of Liraglutide at a dose of 0.6-1.8 mg was well tolerated (Rigato & Fadini 2014, Zang *et al*. 2016). Liraglutide can also be used as single drug or in combination with other drugs such as metformin and/or a sulphonylurea, in poorly controlled T2DM patients (Pfeiffer *et al*. 2014, Marin-Penalvar *et al*. 2016). Moreover, recently Liraglutide has been approved for the treatment of obesity at an elevated dose of 3.0 mg (Nuffer & Trujillo 2014, Scheen 2016).

1.6 XENIN

1.6.1 Synthesis, secretion, signaling and pancreatic action of xenin

Xenin is a 25-amino acid peptide which is secreted by intestinal K-cells in response to the food intake (Wice *et al*. 2012, Martin *et al* 2016). Xenin is synthesised from its precursor proxenin through post translational enzymatic action of Cathepsin-E (Hamscher *et al*.1996; Feurle, 1998). Xenin was first isolated

from human gastric mucosa (Feurle *et al* 1992). Importantly, xenin is known to potentiate the biological actions of GIP which are known to be compromised in T2DM (Taylor *et al.* 2010, Wice *et al*. 2010, Martin *et al*. 2012 and Gault *et al*. 2015).

Xenin is structurally similar to neurotensin because it contains identical C-terminal amino acid sequence which is highly conserved through evolution (Hamscher *et al*. 1996). The major metabolic actions of xenin include effects on gut motility, promoting satiety and reducing food intake (Sterl *et al*. 2016). However, it has also been reported that xenin plays important role in glucose homeostasis and insulin secretion (Taylor *et al*. 2010, Hussain *et al*. 2016). The possible mechanism of GIP mediated insulin release could be through activation of non-ganglionic cholinergic neurons (Wice *et al*. 2010), but effects of cAMP as well as beta-cell membrane potential and intracellular calcium levels are not believed to be important (Taylor *et al*. 2010). The therapeutic potential of xenin is restricted because it is rapidly degraded by aspartic proteases at lysine and argine residues (Martin *et al.* 2012). The C-terminal octapeptide fragment of xenin (xenin-8, but also termed xenin(18-25) was found in circulating in plasma highlighting its potential physiological importance (Martin *et al*. 2014). Xenin-8 retains biological activity and exhibits insulin secretory properties and potentiates GIP mediated insulin release (Martin *et al*. 2014). Interestingly, when xenin-25 and xenin-8 were administered along with (DAla^{2}GIP) this led to improved insulinotropic and glycaemic actions in mice (Martin *et al*. 2014). This GIP potentiating effect of xenin is quite remarkable, because this will help to overcome GIP resistance which is normally seen in T2DM patients (Hasib *et al*. 2017, Kaji *et al*. 2017).

Recently, a study conducted in our laboratory has demonstrated that the amino acid substitution of Lys and Arg residues in

xenin-25 and xenin-8 with Gln, to impede enzymatic degradation, induces superior metabolic effects mice (Parthsarathy *et al*. 2016). In this regard, xenin or related fragments could have therapeutic potential in the treatment of T2DM (Martin *et al*. 2016). Xenin also plays an important role in secretion of various hormones such as pancreatic polypeptide, vasoactive intestinal peptide, insulin and glucagon (Feurle *et al*. 1997), which merits further study.

1.6.2 Extrapancreatic actions

Extrapancreatic effects of xenin revolve mainly around regulation of intestinal motility and food intake suppression (Clemens *et al*. 1997; Nustede *et al*. 1999; Kim and Mizuno, 2010a). No specific receptor for xenin has been reported to date, but neurotensin receptors have been suggested as possible targets for xenin (Bhavya *et al*. 2017). Xenin mediated suppression of food intake have been reported previously in different animal models, as well as humans (Alexiou *et al*. 1998; Cline *et al*. 2007, Chowdhury *et al*. 2014).

1.7 EFFECTS OF TYPE 2 DIABTES ON BONE METABOLISM

There is considerable amount of evidence which suggests type 2 diabetes is associated with increased bone fracture risk even though bone mineral density (BMD) is seen to be unaltered or even increased (Vianna *et al*. 2017, Wallander *et al*. 2017). There are different factors which increase fracture risk in diabetes such as inadequate glycaemic control, greater risk of falling as a consequence of hypoglycaemia, osteopaenia and impairment of bone quality (Sanches *et al*. 2017). Lack of scientific in-depth knowledge makes it difficult to develop a strategy to treat bone fractures in diabetes. Even though type-2

diabetes and osteoporosis are not directly related, they share many common features including genetic predispositions, molecular mechanisms and pathophysiological mechanisms (Billings *et al*. 2012).

According to World Health Organisation, osteoporosis is defined as disease characterised by low bone mass and microarchitectural deterioration of bone tissue leading to enhanced bone fragility and consequent increase in fracture risk. Osteoporosis reduces BMD and affects around 200 million women and accounts for 8.9 million fractures annually in women who are above the age of 50 (International osteoporosis foundation-The global burden of osteoporosis factsheet). The commonly used tools to estimate fracture risk are BMD and a fracture risk assessment tool called FRAX, to help predict 10-year probability of bone fracture risk (Hiller *et al*. 2011, Rubin *et al*. 2013). However, BMD is considered as gold standard by world health organisation (Garg & Kharb 2013). BMD is expressed as a T-score, which is the number of the number of standard deviations that the individual is above or below the average age of a healthy adult (Schwartz *et al*. 2017). On the other hand, FRAX is used to calculate femoral neck BMD T-score (Gadam *et al*. 2013). The FRAX algorithm takes into account several other factors like age, sex, alcohol consumption, arthritis, history of fracture, basal metabolic index and glucocorticoid intake (Cavalli *et al*. 2016). Unfortunately, FRAX does not include Diabetes as a risk factor and hence, the algorithm is not considered to be accurate for this disease (Leslie *et al*. 2012, Oie *et al*. 2015).

In response to food ingestion, incretin hormones are released into blood circulation which enhances glucose-mediated insulin secretion from pancreatic β cells (Irwin *et al*. 2015). There is an intimate relationship between glucose homeostasis and bone metabolism, controlled by many factors including advanced

glycation end products (AGEs), insulin, insulin-like growth factor-1 (IGF-1), peroxisome proliferator-activated receptor gamma (PPARγ), glucose-dependent insulinotropic peptide (GIP), glucagon-like peptide 1 and 2 (GLP-1 and GLP-2), osteocalcin and sclerostin (Sanches *et al*. 2017, Vianna *et al*. 2017).

1.7.1 Advanced glycation end products (AGEs)

Hyperglycaemia contributes to the bone loss as it affects cellular and extracellular bone matrix (Jiao *et al*. 2015). Glucose causes formation of intermediate highly reactive dicarbonyls, through a non-enzymatic glycation process (Napoli *et al* 2014), and ultimately leads to production of AGEs (Singh *et al*. 2001). AGE formation causes impairment of bone matrix (Ahmed *et al*. 2005, Hernandez *et al*. 2005) and increases fracture risk (Epstein *et al*. 2016). Briefly, the mechanism involves binding of AGEs to it receptor known as receptor for AGEs (RAGE) that leads to production of reactive oxygen species, inflammation and macrophage and platelet activation (Figure 1.8). Therefore, bones become more brittle with reduced bone strength. Formation of AGEs causes osteoblast deterioration and enhances osteoclast activation, ultimately decreasing bone mineralisation (Saito *et al*. 2006, Sanguineti *et al*. 2008).

Figure 1.8 Relationship between accumulations of AGEs in the bone

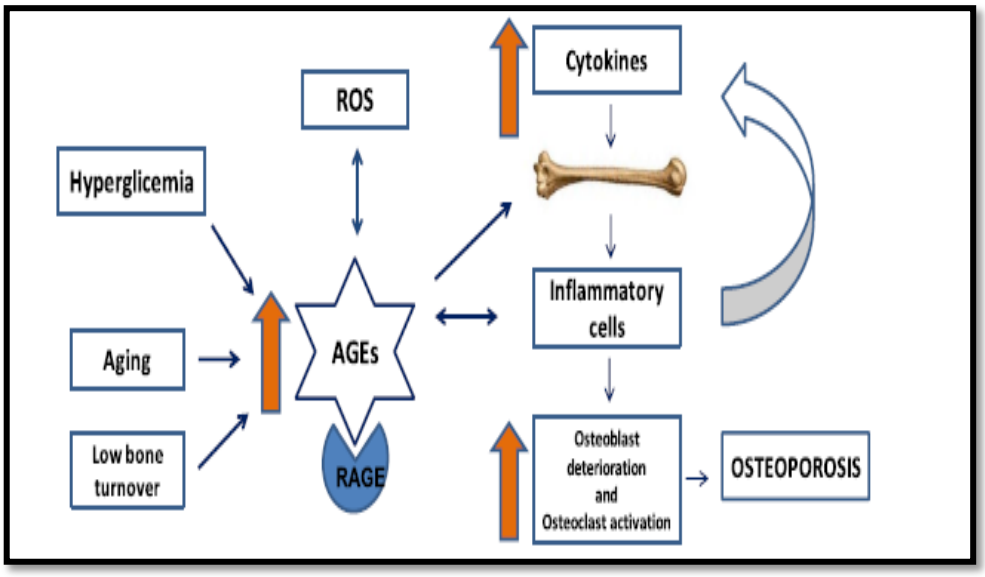

(Taken from Sanguineti *et al*. 2008)

1.7.2 Insulin and Insulin-like growth factor-1 (IGF-1)

Insulin has two receptors, namely insulin receptor 1 and insulin receptor 2, and both the receptors are present on bone (Gallagher *et al*. 2013). Insulin receptors stimulate osteoblast proliferation, bone formation and collagen synthesis (Lee *et al*. 2017). Similar to insulin, insulin-like growth factor-1 (IGF-1) promotes osteoblast proliferation and enhances bone matrix deposition by reducing collagen degradation (Yin *et al*. 2017). Previously, it has been widely reported that there is a positive correlation between IGF-1 and BMD (McCarthy *et al*. 2004, Sanguineti *et al*. 2008).

1.7.3 Peroxisome proliferator-activated receptor gamma (PPARγ)

PPARγ has two isoforms namely- PPARγ1 and PPARγ2 (Wang *et al*. 2017). PPARγ1 is expressed in osteoclasts and helps in differentiation of osteoclasts as well as bone resorption (Chong *et al*. 2007). PPARγ2 regulates mesenchymal stem cell

differentiation (Camp *et al*. 2017). PPARγ induces adipogenesis and suppresses osteoblastogenesis, by inhibiting Runx2 function (Figure 1.9), causing in a reduction of osteoblasts in the bone marrow (Fan *et al*. 2017).

Figure 1.9 Peroxisome proliferator - activated receptor gamma (PPARγ)

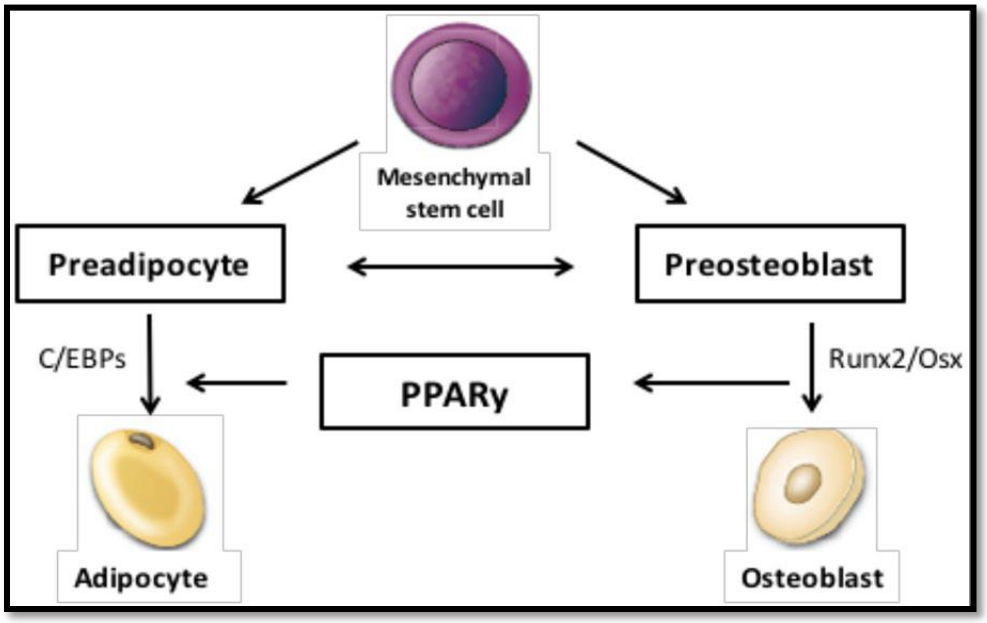

(Taken from Kawai *et al*. 2010)

C/EBPs - enhancer binding proteins, CCAAT-enhancer binding proteins, Osx/ Runx2- runt related transcription factor 2

1.7.4 Vitamin D

Hyperglycaemia causes impairment of renal calcium absorption (Chaiban *et al*. 2015). Further, hyperglycaemia results into reduced number of 1, 25$(OH)_2$D3 (1,25-dihydroxy vitamin D) receptors on osteoblasts (Garcia-Gil *et al*. 2017). Therefore, it becomes difficult for osteoblasts to produce osteocalcein in response to 1, 25$(OH)_2$D3. However, there are some reports that

contest involvement of vitamin D in type-2 diabetes to increase fracture risk (Manigrasso *et al*. 2013).

1.7.5 Osteocalcein

Type-2 diabetes does have an impact on serum bone turnover markers (BTM) particularly, osteocalcein (OC) and amino-terminal propeptide of procollagen type 1 (PINP), as there levels are decreased in type-2 diabetic patients (Rosen *et al*. 1997, Rubin *et al*. 2015). It has been reported that postmenopausal women with T2DM have lower OC and PINP levels (Shu *et al*. 2012, Yamamoto *et al*. 2012, Raska Junior *et al*. 2017). The bone resorption marker CTX (serum C-terminal telopeptide from type 1 collagen), is found to be reduced in type-2 diabetic patients (Oz *et al*. 2006, Rubin *et al*. 2015), while some reports indicate that there is no difference in CTX (Achemlal *et al*. 2005). Of all bone turnover markers, osteocalcein is considered as important when it comes to understand pathophysiology of T2DM, mainly because osteocalcein stimulates insulin secretion and enhances insulin sensitivity (Pittas *et al*. 2009, Booth *et al*. 2013, Zanatta *et al*. 2014, Ippei Kanazawa 2015, Eibhlís M.O'Connor & Edel Durack 2017).

1.7.6 Sclerostin

Sclerostin is expressed by osteocytes (Weivoda *et al*. 2017). Sclerostin inhibits Wnt/ß-catenin pathway and negatively regales bone formation by binding to low-density lipoprotein receptor related protein (LPR) 5 or 6. The Wnt/ß-catenin pathway enhances osteoblast proliferation and bone formation (Kim *et al*. 2017). Wnt/ß-catenin signalling suppresses osteoclasts by inducing osteoprotegerin (Figure 1.10). Wnt/ß-catenin signalling also reduces bone resorption by acting directly on osteoclast precursors. Thus, Wnt has dual effecst on osteoblasts and osteoclasts results in increased bone mass. As such, after binding of sclerostin to Wnt receptors, osteoclasts are

inhibited and osteoblasts promote bone formation (Canalis *et al*. 2013). Type-2 diabetes patients have higher levels of sclerostin which are related with increased fracture risk (Garcia-Martin et.al. 2012, Rubin *et al*. 2015).

Figure 1.10 Canonical Wnt signaling and bone remodelling

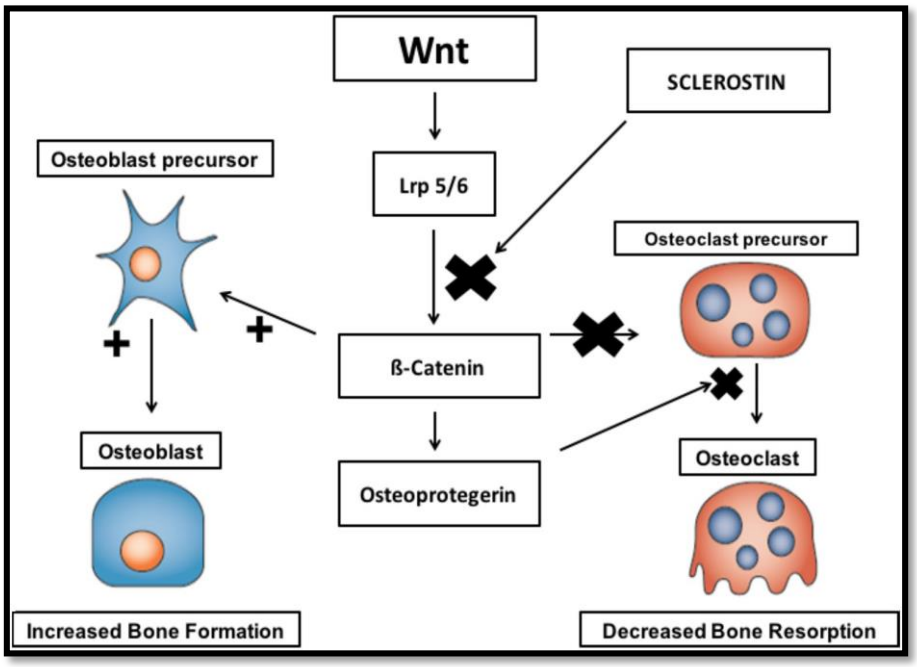

(Taken from Canalis *et al*. 2013)

Canonical Wnt signaling and bone remodelling, Lrp-lipoprotein receptor-related protein

1.7.7 Incretin hormones and bone

Bone formation and bone breakdown are closely related to food ingestion, and upon food intake, biomarkers for bone resorption are reduced (Bonjour *et al*. 2011, Motil *et al*. 2014, Graff *et al*. 2016). GIP and GLP-1 are secreted in response to nutrient intake (Pais *et al*. 20116, Hansen *et al*. 2017, Hutchinson *et al*. 2017) and therefore it is suspected that incretins may play a role in bone turnover. GIP does have direct action on bone as GIPR

mRNA and protein are present in normal bone cells (osteoblast and osteoclast) and progenitor bone cells (Zhong *et al*. 2007, Ding *et al*. 2008, Tokarev *et al*. 2014).

1.7.7.1 GIP

Binding of GIP to GIPR on osteoblasts increases cAMP and Ca2+ concentrations and subsequently elevates expression of bone formation biomarkers, collagen type 1 and alkaline phosphatase activity (Bollag *et al*. 2000, Bart Clarke, 2008, Yutaka Seno &Daisuke Yabe, 2013), indicating a positive action of GIP on bone formation. GIP plays an important role in proliferation of osteoblasts as it was observed that GIP has stimulatory effects on the release of transforming growth factor-β (TGF-β) (Patil *et al*. 2011). Investigation of potential osteoprotective effects of GIP using primary mouse osteoblasts and osteoblastic-like SAOS-2 cells found that pre-treatment with GIP significantly reduced the percentage of apoptotic cells (Tsukiyama *et al*. 2006). Furthermore, there is a possible role of GIP in the early process of osteogenesis by promoting osteoblastic differentiation of bone marrow stromal cells (Meiczkowska *et al*. 2015, Kainuma *et al*. 2016, Fujita *et al*. 2017). With regards to action of GIP on bone-resorbing osteoclast cells, there is limited information. However, it has been reported that GIP inhibits osteoclast activity and differentiation *in vitro* (Zhong *et al*. 2007), suggesting a role of GIP in reducing bone resorption (Berlier *et al*. 2015, Mabilleau *et al*. 2016). This has later been confirmed in studies showing that GIP can reduce osteoclast differentiation and resorption (Mabilleau *et al*. 2016), as well as improving osteoclast function following serum deprivation-induced apoptosis (Berlier *et al*. 2015).

Rodent studies in GIPR knockout mice have revealed reduced bone size and lower bone mass as well as a decrease in bone

formation biomarkers compared with the wild type mice (Xie *et al*. 2005, Shapses & Sukumar 2012, Gilbert & Pratley 2015). Bone histomorphometrical analyses of GIPR-deficient mice demonstrated that the reduction in bone mass was due to increased multinucleated osteoclasts, which are responsible for active bone resorption (Tsukiyama *et al*. 2006). In GIP over expressing transgenic mice, it was found that bone mass, bone size and biomarkers for bone formation were increased while bone resorption biomarkers were decreased (Xie *et al*. 2007, Yu *et al*. 2016, Tsung-Rong Kuo & Chih-Hwa Chen, 2017). These observations are in agreement with *in vitro* data that reported a stimulatory effect of GIP on osteoblasts and inhibitory effect on osteoclasts (Hansen *et al*. 2017). A bone assessment study performed using highly sophisticated imaging techniques found that the bones of GIPR KO have altered microstructure and decreased strength, highlighting the beneficial effects of GIP on bone (Mieczkowska *et al*. 2013). It has been demonstrated earlier that administration of GIP prevented bone loss in ovariectomised rats (Ma *et al* 2014, Wee & Baldock, 2014). In another recent study, it was found that rats injected with a stable GIP analogue appeared to have increased tissue material properties at the cortical bone level (Mabilleau *et al*. 2014, Meiczkowska *et al*. 2015, Mabilleau 2017). A number of additional studies have demonstrated that GIP receptor deficient mice have shown altered bone microarchitecture (Hansen *et al*. 2017, Christensen *et al*. 2017, Palmero *et al*. 2017). A recent study carried out in 2017 by Mantelmacher and colleagues has shown that GIP receptor deficiency results in impaired bone marrow haematopoiesis. The study highlighted that GIP receptor deficient mice affected GIP signaling and showed reduced levels of bone marrow as well as immune cells (Mantelmacher *et al*. 2017).

1.7.7.2 GLP-1

There is conflicting evidence regarding the expression of GLP-1Rs on bone cells (Ceccarelli *et al*. 2013, Mabilleau *et al*. 2013, Yusta *et al*. 2015, Adil *et al*. 2017, Napoli *et al*. 2017). However, the inconsistencies may result from the use of different bone cell lines. GLP-1 appears to affect bone turnover in a beneficial manner, as GLP-1R-deficient mice have reduced bone mass and bone mineral density, while bone resorption biomarkers appeared to be significantly increased (Yamada *et al*. 2008). In addition, GLP-1R knock-out mice also have reduced cortical bone strength, due to alterations of cortical thickness and bone material properties (Mabilleau *et al*. 2013). Other studies demonstrated that bone formation biomarkers were elevated after 3-day subcutaneous administration of GLP-1 or exendin-4 in streptozotocin-induced diabetic rats (Nuche-Berenguer *et al*. 2009, Nuche-Berenguer *et al*. 2010a). These findings do highlight that GLP-1 does have positive effects on the bone. Exenatide, a GLP-1 analogue, has proven to be quiet effective when it comes to bone physiology. As such, a clinical study carried out by Wanq and colleagues in 2017 has revealed that 30 obese patients treated with exenatide for 18 weeks present with reduced bone morphogenic protein-4 (BMP-4) levels. As BMP-4 regulates white adipogenesis and plays important role in fat distribution, the study highlighted the fact that exenatide might have potential when it comes to augmenting bone quality (Wanq *et al*. 2017).

GLP-1 receptor agonists, DPP-4inhibitors and SGLT2 inhibitors are widely used as anti diabetic drugs. It has already been reported that thiazolidinediones have detrimental effects on bone metabolism and fracture risk (Ruppert *et al*. 2017). A recent report published by Eggar and colleagues in 2016,

suggest that SGLT2 causes alteration in calcium and phosphate homeostasis. This alteration is mainly because of secondary hyperparathyroidism induced by increased phosphate reabsorption. These results highlight potential negative effects of SGLT2 inhibitors on skeletal integrity, but not on bone metabolism directly (Egger *et al*. 2016). The role of liraglutide, a GLP-1 analogue, which is widely used in the treatment of type-2 diabetes and obesity in bone formation, was unclear until recently, when it was demonstrated that liraglutide reduces osteoblastic differentiation of MC3T3-E1 cells via modulation of AMPK/mTOR signalling (Hu *et al*. 2016). The study demonstrated that liraglutide upregulated phosphorylated adenosine monophosphate-activated protein kinase (p-AMPK) and downregulated phosphorylated mammalian target of rapamycin (p-mTOR) and TGF-β protein expression levels.

The effect of liraglutide to reduce osteoblastic differentiation was eradicated by AMPK-specific inhibitor, Compound C and mTOR activator, MHY1485 (Hu *et al*. 2016). Recently, it has been reported that GLP-1 receptors affect fat-bone axis by enhancing osteogenic differentiation and inhibiting adipogenic differentiation of bone mesenchymal precursor cells (BMSCs) (Palmero *et al*. 2017). A similar study published by Meng and colleagues in 2016, demonstrated that activation of GLP-1 receptors promoted osteogenic differentiation of bone marrow stromal cells through the β-catenin pathway (Meng *et al*. 2016). There are some studies that reveal conflicting data when it comes to liraglutide and exendin-4 effects on bone. For example, Pereira and colleagues carried out study in overactomised mice where liraglutide (0.3 mg/kg/day) and exenatide (10 μg/kg/day) were injected for four weeks. Both, liraglutide and exenatide increased trabecular bone mass with no effect on cortical bone. But in case of exenatide, the osteoclasts number was increased. In addition, liraglutide and exenatide

stimulated osteoblastic differentiation (Pereira *et al*. 2015). Another study carried out by Lu and colleagues in overactomised female Wistar rats, but without diabetes, assessed the impact of liraglutide on bone mass and bone quality. Liraglutide increased trabecular volume, trabecular thickness, number of trabecular as well as bone mineral density (Hansen *et al*. 2017). Together, these studies highlight the protective positive effects of liraglutide on bone quality.

1.7.8 Diabetes and bone

Diabetes negatively affects bone health by disturbing several underlying pathophysiological pathways which regulate bone physiology (Karpinski *et al*. 2017). Several pathways pertaining to bone formation, bone resorption, collagen formation, inflammatory cytokine, bone marrow adiposity and calcium metabolism are affected in diabetic, patients eventually increasing fracture risk. In type-1 diabetic patients, there is six-fold increase in hip fracture risk and two-fold increase in vertebral fracture risk as compared to that of non-diabetic individuals (Russo *et al*. 2016). In type-2 diabetic patients there is about two- to three-fold increase in hip fracture risk as compared to that of normal individuals (Palmero *et al*. 2017). Interesting, a study carried out in 2017 by Westberg-Rasmussen and colleagues, aimed to clarify whether oral or intravenous administration of glucose affects bone turnover differently. An oral glucose tolerance test was performed, followed by isoglysemic intravenous glucose infusion. Blood samples were analysed for different bone turnover serum markers such as, C-terminal telopeptide of type-1 collagen (s-CTX) and procollagen type IN propeptide (s-P1NP), insulin and gastrointestinal hormones such as GIP, GLP-1 and GLP-2. Oral glucose caused a 50% reduction in s-CTX marker while only 30% reduction

was observed in case of isoglycemic intravenous glucose infusion (Westberg-Rasmussen *et al*. 2017).

Further investigation is needed to realise the untapped potential of incretin hormones and their positive effects on bone. Future clinical trials will be necessary to investigate the relationship between incretin hormones and fracture risk in diabetic patients.

1.8 OLIGOPEPTIDE TAGGING

Targeted drug delivery to the bone can be achieved (Stapleton *et al*. 2017), due to the the physical nature of bone. As such, the majority of the bone is comprised of inorganic compound called hydroxyapatite (HAP) (Florencio-Silvia *et al*. 2015). Evidence shows that targeted drug delivery to HAP can be achieved (Takahashi-Nishioka *et al*. 2008, Newman & Benoit 2016 and Haider *et al*. 2017). In this respect, acidic oligopeptides can serve as novel drug delivery method to increase site-specific drug delivery to the bone (Low *et al*. 2014, Dang *et al*. 2016, Shaikh & Sawarkar 2016, Ulbrich *et al*. 2016). For example, non-collagenous proteins in the bone namely, osteopontin and sialoprotein, have repetitive sequence of acidic amino-acids (L-Asp and L-Glu) that bind to hydroxyapatite (Takahashi *et al*. 2008, Zurick *et al*. 2016, Jiang *et al*. 2017), making introduction of acidic oligopeptides a promising candidate as a bone targeting carrier.

With this idea in mind, the peptides used in the present bone studies were designed in such a way that they were targeted towards by adding six repetitive aspartic amino acid and glutamic amino acid residues to the C-terminal. Along with appropriate parent peptides, the bone-targetting peptides used in these studies were (D-Ala^2)GIP-Asp, (D-Ala^2)GIP-Glu, (D-Ala^2)GLP-1-Asp, (D-Ala^2)GLP-1-Glu, Xenin-25[Lys^{13}PAL]-Asp, GIP/Xenin-Asp and GIP/Xenin-Glu.

1.9 AIMS OF THE THESIS

The primary aim of this thesis was to investigate the impact of diabetes on bone and to characterise the effects of long-acting antidiabetic peptide analogues, with potential bone targeting moieties, on metabolic control as well as bone strength and quality in diabetes.

The specific objectives of this thesis were:

1. Designing bone targeting peptides by adding six repetitive amino aspartic amino acid and glutamic amino acid residues to the C-terminal.
2. Assess *in vitro* effects of the peptides on beta-cell insulin release and human osteoblast cell function.
3. Understand the mechanism of peptide signaling pathways in bone by assessing alkaline phosphatase activity, TGF-beta release, IGF-1 release and cAMP generation.
4. Perform long term animal studies in normal and high fat fed mice with assessment of metabolic parameters such as glucose tolerance, insulin sensitivity, food intake, body weight, body composition as well as bone mineral density and content.
5. Perform assessment of bone-specific parameters in these mice using techniques such as 3-point bending, nanoidentation, FTIRI, microCT and qBEI.

Chapter 2

Materials and Methods

2.1 PEPTIDES

2.1.1 Synthesis of peptides

All peptides were purchased from EZ Biolabs Ltd. (Carmel, IN, USA). The peptides used in these studies were divided into four distinct groups, namely GIP based peptides, xenin based peptides, GIP/xenin hybrid based peptides and GLP-1 based peptides. Specifically, the peptides used were (D-Ala^2)GIP, (D-Ala^2)GIP-Asp, (D-Ala^2)GIP-Glu, (D-Ala^2)GLP-1, (D-Ala^2)GLP-1-Asp, (D-Ala^2)GLP-1-Glu, Xenin-25[Lys^{13}PAL], Xenin-25[Lys^{13}PAL]-Asp, GIP/Xenin, GIP/Xenin-Asp, GIP/Xenin-Glu (Table 2.1).

Table 2.1 Peptides employed within this thesis

Group	Amino acid sequence	Name of the peptide
GIP	Y-(dA)-EGTFISDYSIAMDKIHQQDFVNWLLAQK-HN_2	**(D-Ala^2)GIP**
	Y-(dA)EGTFISDYSIAMDKIHQQDFVNWLLAQKGAA**DDDDDD**-NH_2	**(D-Ala^2)GIP-Asp**
	Y-(dA)-EGTFISDYSIAMDKIHQQDFVNWLLAQKGAA**EEEEEE**-NH_2	**(D-Ala^2)GIP-Glu**
GLP-1	H-(dA)-EGTFTSDVSSYLEGQAAKEFIAWLVKGRG-NH_2	**(D-Ala^2)GLP-1**
	H-(dA)-EGTFTSDVSSYLEGQAAKEFIAWLVKGRGGAA**DDDDDD**-NH_2	**(D-Ala^2)GLP-1-Asp**
	H-(dA)-EGTFTSDVSSYLEGQAAKEFIAWLVKGRGGAA**EEEEEE**-NH_2	**(D-Ala^2)GLP-1-Glu**
Xenin	MLTKFETKSARVK(gamma glutamyl PAL)GLSFHPKRPWIL-OH	**Xenin-25[Lys^{13}PAL]**
	MLTKFETKSARVK(gammaglutamylPAL)GLSFHPKRPWILGAA**DDDDDD**-NH_2	**Xenin-25[Lys^{13}PAL]-Asp**
GIP/xenin hybrid	H-Y-(dA)-EGTFISDYS-IAMHPQQPWIL-OH	**GIP/Xenin**
	H-Y-(dA)-	**GIP/Xenin-Asp**

	GTFISDTSIAMHPQQPQILGAA**DDDDDD**-NH_2	
	H-Y-(dA)-EGTFISDTSIAMH PQQPWILGAA**EEEEEE**-NH_2	**GIP/Xenin-Glu**

2.1.2 Peptide purification, identification and characterisation

All peptides were purified using reverse phase high performance liquid chromatography (RP-HPLC). Briefly, peptides were dissolved in distilled water at a concentration of 1 mg/ml. A peptide solution (100 µl of 1 mg/ml peptide) was then made up to 1 ml using 0.1% (v/v) TFA/water. Next the solution was injected into Kinetex C-18 analytical column (150 x 4.60 mm, Phenomenex, Cheshire, UK) equilibrated with 0.1% (v/v) TFA/water at a flow rate of 1 ml/min. Acetonitrile (70%) was used as the eluting solvent. The concentration of eluting solvent was increased using linear gradients from 0 - 36% acetonitrile over 5 mins followed by 36 - 40% over 15 mins and 40 - 70% over 5 mins and absorbance measured at 214 nm.

The peptides were identified by mass spectroscopy. The molecular mass of all the peptides was confirmed using a Voyager-DE Biospectrometry Workstation (PerSeptive Biosystems, Farmingham, MA, USA). Bone is mainly composed of fibrious protein collagen, water and hydroxyapaptite. Addition of six aspartic acid and glutamic acid residues towards C-terminal increased affinity of peptides to bind to hydroxyapaptite. Parent xenin peptides were carboxylated, but with addition of six aspartic acid and glutamic acid residues all oligopeptides were amidated, as this has proven to main bioactivity of tagged peptodes (Takahashi-Nishioka *et al*. 2008).

2.1.3 DPP-4 degradation profile

DPP-4 degradation profile of the peptides was performed as described by Gault *et al.*, (2011). In short, 30 µl of peptide (1 mg/ml) was incubated with 5 µl of porcine DPP-IV (5 mU,

purchased from Sigma Aldrich, UK) in 50 mM Triethanolamine hydrochloride (TEA-HCl) (pH 7.8; final volume 440 µl) at 37°C for 0, 2, 8, 12 and 24 hrs. The enzymatic reaction was then stopped using 50 µl TFA/H_2O (10% v/v). Degradation profiles were followed using HPLC (as described in Section 2.1.2) and degradation products were analyzed using mass spectroscopy as detailed in Section 2.1.2.

Table 2.2 Identification and characterisation of peptides by mass spectroscopy

Name	Group	Theoretical molecular weight (Da)	Experimental molecular weight (Da)	DPP4 degradation	Retention time (mins)
(D-Ala^2)GIP	GIP	3533.02	3544.02	> 12 hrs	26
(D-Ala^2)GIP-Asp		4421.77	4423.48	> 12 hrs	25.2
(D-Ala^2)GIP-Glu		4506.93	4507.16	> 12 hrs	25.5
(D-Ala^2)GLP-1	GLP-1	3355.76	3353.77	> 12 hrs	27.2
(D-Ala^2)GLP-1-Asp		4245.50	4244.49	> 12 hrs	27.2
(D-Ala^2)GLP-1-Glu		4329.67	4326.20	> 12 hrs	26.7
Xenin-25[Lys^{13}PAL]	Xenin	3336.13	3331.29	> 12 hrs	30.4
Xenin-25[Lys^{13}PAL]-Asp		4219.54	4215.31	> 12 hrs	29.3
GIP/Xenin	GIP/Xenin hybrid	2562.59	2558.02	> 12 hrs	24.6
GIP/Xenin-Asp		3457.69	3451.26	> 12 hrs	22.9

GIP/Xenin-Glu		**3531.65**	**3528.49**	**> 12 hrs**	**22.67**

2.2 CELL CULTURE

2.2.1 BRIN-BD11 cells

BRIN-BD11 cells are immortalised pancreatic beta-cells derived from the electro fusion of rat pancreatic islet cells and tumoral rat insulinoma RINm5F cells (McClenaghan *et al*. 1996). BRIN-BD11 cells were cultured in RPMI-1640 growth medium supplemented with 10% (v/v) foetal bovine serum (FBS) and 1% (v/v) antibiotics – penicillin (100 U/ml), streptomycin (0.1 mg/l) in 75 cm^2 sterile tissue culture flasks (Greiner bio one, UK) and maintained at 37°C and 5% CO_2, in a LTEC incubator (Laboratory technical engineering, Nottingham, UK). Then the culture media was removed from the flasks and cells were washed with 10 ml Hanks buffer saline solution (HBSS). Then the cells were harvested from the surface of the tissue culture flask by using 3 ml trypsin/ EDTA. Then, 7 ml fresh culture media was added to the detached cells and it was pipetted in and out so as to form a single suspension. The cell suspension was centrifuged at 900 rpm for 5 mins and the pellet was re-suspended in 10 ml of pre-warmed culture medium. The counting of cells was performed using Neubauer haemocytometer (Scientific Supplies Co., UK). 100 cell suspension was stained with 100 µl of trypan blue. Viable cells (unstained and bright) were counted in all the four WBC squares and average was calculated to obtain the total number of cells in the suspension.

The acute test was carried out as described by Gault *et al.* (2002). In order to perform acute test, the BRIN-BD11 cells were seeded at 150,000 cells/well seeding density in 24-well

plates. Then the cells were allowed to attach (24 hrs) overnight at 37ºC. The pre-incubation step was carried out using Krebs–Ringer bicarbonate buffer (KRBB) (115 mmol/l NaCl, 4.7 mmol/l KCl, 1.2 mmol/l $MgSO_4$, 1.28 mmol/l $CaCl_2$, 1.2 mmol/l KH_2PO_4, 25 mmol/l HEPES and 8.4% $NaHCO_3$, containing 0.5% (w/v) BSA , pH 7.4) which is supplemented with 1.1mM glucose. Then the test incubations (n=8) were performed in the presence of glucose (5.6mM and 16.7mM) with a range of concentrations varying from 10^{-12} to 10^{-6} M of respective peptides for 20 mins at 37ºC. After incubation, 200 µl aliquots of assay buffer were collected from each well and stored at -20ºC for measurement of insulin by radioimmunoassay (RIA) method.

Iodinated bovine insulin

Iodogen solution was prepared by dissolving 100 µg/ml of 1, 3, 4, 6-tetrachloro-3α,6α-diphenylglycoluril in dichloromethane, followed by dispense of the solvent (100 µl) into Eppendorf tubes. Then the tubes were left in a fume hood to allow evaporation of the solvent and leaving a uniform layer of iodogen at the bottom of the tubes. Bovine insulin solution (125 µg/ml) was prepared by diluting 1 mg/ml solution of bovine insulin in 10 mM HCl with 500 mM phosphate buffer. 20 µl of the bovine insulin solution and 5 µl of $Na^{125}I$ (100 mCi/ml stock) was added to the iodogen-coated eppendorf tubes and left on ice with gentle agitation for 15 mins. The iodogen reaction was stopped by removing the reaction mixture into a fresh Eppendorf tube with an addition of 500 µl of 50 mM sodium phosphate buffer. The solution was kept on ice before carrying out HPLC separation.

HPLC separation was carried out using a Vydac C-8 analytical column (4.6 x 250 mm). The mobile phases used were 0.12% (v/w) TFA (in purified H_2O) and 0.1% TFA (in 70%

acetonitrile-30% purified H_2O). The separation programme was set for 67 mins and 1 ml fractions were collected by fraction collector (Frac-110, LKB). Then 5 µl from each fraction was aliquoted into LP3 tubes. Radioactivity counts were assessed using a gamma counter (Perkin Elmer Wallac Wizard 1470 Automatic Gamma Counter). The fractions with highest counts were kept to perform antibody-binding tests and further pooled together to be used as the ^{125}I-labelled tracer in the insulin radioimmunoassay.

2.2.2 Radioimmunoassay (RIA)

Radioimmunoassay stock buffer was prepared by adding disodium hydrogen with orthophosphate, base (17.035 g in 3 litres of distilled water, i.e. 40 mM solution) and sodium hydrogen orthophosphate, acid (6.240 g in 1 litre of distilled water, i.e. 40 mM solution). Then 0.6 g of thimerosal and 9 g of NaCl were added to the base. The pH of acidic solution was adjusted to 7.4 and both the solutions were stored at 4°C until further use. On the experimental day, working RIA buffer was prepared by dissolving bovine serum albumin (BSA, Sigma) 0.5% (w/v) in stock RIA buffer i.e. 0.5 g in 100 ml, in 40 mM sodium phosphate buffer (pH 7.4). Insulin standards were prepared by serial dilution (0.039 to 20 ng/ml concentration) from frozen rat insulin stock (40 ng/ml) in working RIA buffer. To determine insulin concentration in experimental samples, 180 µl of working RIA buffer was added to 20 µl of unknown sample to give a total volume of 200 µl per LP3 test tube. Guinea pig anti-porcine antibody was prepared by diluting frozen stock (100 µl) to 30 ml with working RIA buffer (i.e. 1/30,000 final concentration). Prepared antibody (100 µl) was then added to unknown and standard samples (triplicate) followed by addition of 100 µl ^{125}I-labelled insulin (10,000 cpm/100 µl in working RIA buffer) into all samples. Then the

tubes were stored at 4°C for 48 hrs in order to allow sufficient time for competitive binding to take place.

Dextran T 70 (5 g) was dissolved in sodium phosphate buffer (5%, without BSA) and 50 g charcoal was added with continuous mixing, making the final volume up to 1l with assay buffer. Stock dextran coated charcoal (DCC) solution was prepared at least 24 hrs prior to use. Working dextran coated charcoal solution was then prepared using a 1:5 dilution of stock DCC with stock RIA buffer. The separation of free from bound ^{125}I-label was achieved by adding 1 ml of working DCC to all the tubes except the total tubes of the standard. All the tubes were then vortexed and incubated for 20 mins at 4°C in cooled centrifuge (Beckmann Coulter) and then further centrifuged for 20 mins at 2500 rpm. The supernatant was discarded and the unbound (free) ^{125}I-labelled tracer was absorbed to black charcoal pellet at the bottom of the tube. Radioactivity was measured using Perkin Elmer Wallac Wizard Gamma Counter. The insulin concentration in the unknown sample was determined from rat insulin standard curve, as shown in Figure 2.1.

Figure 2.1 Typical standard curve of rat insulin standards for radioimmunoassay

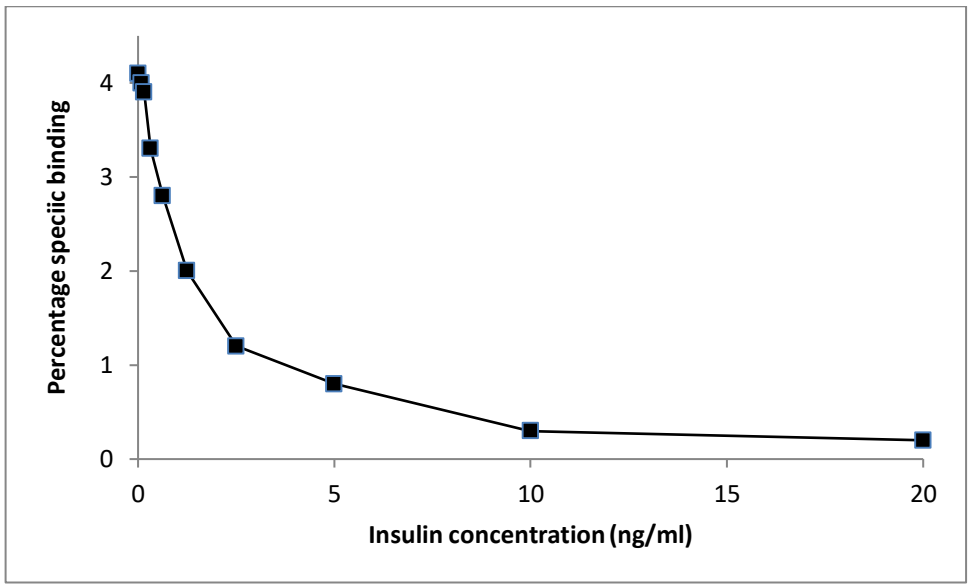

Standard curve of rat insulin for radioimmunoassay

2.2.3 Sarcoma osteogenic SAOS-2 cells

The Sarcoma osteogenic SAOS-2 cell line was procured from ATCC. These cells are derived from primary osteosarcoma of 11 year old Caucasian girl in 1973 by Fogh *et al*. The cells from the stock vial were transferred to small flask very gently. After that, fresh 10 ml of alpha-MEM media was added into the flask. Then after 24 hrs, again the media was changed. SAOS-2 cells were cultured in Minimum Essential Media (MEM) alpha medium, without phenol red (GIBCO, Invitrogen, UK). The MEM alpha medium was supplemented with 10% of foetal bovine serum (FBS) obtained from Lonza (Levallois-Perret, France) and 1% of penicillin/streptomycin (5000 U/ml, 5000 µg/ml). The cells were maintained in sterile large tissue culture

flasks in a controlled atmosphere at 37°C, 5% CO_2. As the cells were 80 % confluent, they were washed and trypsinised. The trypsin was removed by centrifugation at 900 rpm for five mins and re-suspended in pre-warmed culture medium.

2.2.4 Measurement of alkaline phosphatase activity

SAOS-2 cells were seeded at a density of 1 x 10^5 cells/well in 6-well plates and cultured for 72 hrs in growth media. 24 hrs before adding peptide, media was replaced with 2% FBS-containing media. Cells were then incubated with varying concentrations of respective peptides (10^{-6} - 10^{-12} M) in media which was supplemented with 2% FBS, 1% penicillin/streptomycin. After the desired incubation period (24, 48 and 72 hrs), cells were washed 3 times with PBS (Oxford, England). Then 250 µl of 0.2% Nonidet-40 (NP-40) (Sigma) was added into each well and plates were left on an orbital shaker for 10 mins. Using cell scraper (Costar) cells were then scraped and cellular material was homogenised by 3 cycles of freeze (-70°C)-thawing (37°C). The mixture of cells/0.2% NP-40 was collected in 500 µl eppendorf tubes and those tubes were snap-frozen in liquid nitrogen. The tubes were then placed on a shaker for 16 hrs at 4°C. Finally, the contents of the tube sonicated using Soniprep 150 Plus ultrasonic disintegrator for 15 seconds. The sonicated samples were then centrifugated for 15 mins at 13000g at 4°C and supernatant was collected for determination of alkaline phosphatase activity and total protein contents.

2.2.5 Alkaline phosphatase determination

Samples (50 µl) were added to 96-well plates in duplicate and alkaline phosphatase activity was indirectly measured using 4-methyl umbelliferyl phosphate (Sigma) as the substrate. After incubation for 30 mins at 37°C, the reaction was stopped by addition of 100 µl of 0.6 M Na_2CO_3 (Sigma-Aldrich). The basic

principle is that alkaline phosphatase cleaves the phosphate group of the non-fluorescent 4-methylumbelliferyl phosphate (MUP) and this leads to generation of highly fluorescent and stable 4-methyl umbelliferone (MU). Using FlexStation 3 (Molecular Devices) fluorescence was measured at excitation wavelength of 360 nm and an emission wavelength of 450 nm. The cut off was kept at 435 nm. Alkaline phosphatase activity was calculated from a standard curve (0-1000 pmol) of 4-methyl umbelliferone.

2.2.6 Total protein determination

Total protein content in samples (whose alkaline phosphatase activity was measured) was determined using the bicinchoninic acid (BCA) protein assay kit (Pierce). Sample (25 µl) and standard were added to a 96-well plate in duplicate. Reagent AB (200 µl of 50:1) supplied in the kit was added. The plates were then incubated at 37ºC for 30 mins. After desired incubation the plates were then left for 5 mins at room temperature. The plates were read at 562 nm using a microplate reader (Molecular Devices). Total protein content was then calculated according to a bovine serum albumin standard curve (0-1500 µg/ml). Alkaline phosphatase activity was normalised against total protein content per well and was expressed as pmol 4-MU/µg protein.

2.2.7 Measurement of TGF-β

SAOS-2 cells were seeded in 6 well plates at a density of 2×10^5 cells/well. The cells were incubated in media which was supplemented with 10% FBS and maintained until they were confluent. 24 hrs before adding peptide, media was changed with fresh 0.1% FBS-containing media. On the day of experimentation, media was removed and 1 ml of respective peptides (10^{-12} - 10^{-6} M) was added to each well. Plates were then incubated for 8 hrs. After 8 hrs, media was collected and

TGF-β released in the supernatant was measured using a TGF-β Immunoassay kit (Quantikine, R&D Systems). The concentration of TGF-β was calculated from a standard curve of recombinant human TGF-β ranging from 0 to 2000 pg/ml.

2.2.8 Measurement of IGF-1

SAOS-2 cells were seeded in 6 well plates at a density of 2 $x10^5$ cells/well and were maintained until they were confluent in 10% FBS-containing media. Media was changed with fresh media which was supplemented with 0.1% FBS 24 hrs prior to addition of respective peptides. Then the media was removed, followed by an addition of 1 ml of respective peptides (10^{-12} - 10^{-6} M). Plates were then incubated at 37°C for 8 hrs. After desired incubation, media was collected and IGF-1 released in the supernatant was measured using IGF-1 Immunoassay kit (Quantikine, R&D Systems). The concentrations of IGF-1 in the samples was determined from a standard curve of recombinant human IGF-1 in the range of 0 - 60 ng/ml.

2.2.9 Measurement of cyclic AMP

SAOS-2 cells were seeded at a density of 5 x 10^4 cells in 96-well plates. The cells were cultured in α-MEM 1X media (Invitrogen) which was supplemented with 10% FBS (Lonza), penicillin and streptomycin for 24 hrs so that they attach to the plate. Prior to experimentation, cells were washed with HBSS (Invitrogen). Cells were then incubated with various concentrations (10^{-12}-10^{-6} M) of respective peptides supplemented with 200 µM of 3-isobutyl-1-methylxanthine (IBMX). The plate was left for 40 mins at 37°C and after that, cells were washed 3 times with 150 µl of PBS. Cell lysis buffer (R&D Systems) was then used to lyse the cells and a freeze (-20°C) -thaw (37°C) cycle was carried out. The contents were then collected into 500 µl Eppendorf tubes and centrifugated at 600 g for 10 mins at 4°C. Supernatants

were then collected and cAMP was measured using a cAMP assay kit (R&D Systems). The concentration of cAMP was calculated from a standard curve of cAMP ranging from 0 to 240 pmol/ml.

2.3 ANIMALS

NIH Swiss mice (male, 8 weeks, Envigo Ltd., Blackthorn U.K.) were housed individually in air conditioned room at 22 ± 2^0 C with 12 hour light and 12 hour dark cycle. All animals had free access to standard rodent maintenance or high fat (45% fat, 20% protein, 35% carbohydrate) diets, as appropriate and drinking water. In all experiments calcein (300 µl) was injected 11^{th}, 7^{th} and 4^{th} day before culling, to help determine mineralisation rate. All the animal experiments were performed according to the guidelines given by UK Animals Scientific Procedure Act 1986.

2.3.1 Collection of blood samples

Blood was collected from the tail vein of mice and stored in fluoride coated microvette blood tubes (Sarstedt, Germany). The samples were centrifuged immediately using microcentrifugate (Beckman Instruments, Galway, Ireland) for 5 mins at 13000 g. Plasma was then aliquoted into 500 µl Eppendorf tubes and stored at -20^0C prior to further use.

2.3.2 Intraperitoneal glucose tolerance test

Mice were fasted for 18 hrs before intraperitoneal injection of glucose (18 mmol/kg bw). Blood was collected immediately before (0 mins) giving glucose injection. Blood was then collected at 15, 30, 60 and 105 mins post injection as described in Section 2.3.1, and subsequently processed for measurement of plasma insulin concentrations. Blood glucose was measured immediately using a hand-held glucose monitor (Ascenscia glucose meter, (Bayer Contour).

2.3.3 Intraperitoneal insulin sensitivity test

Bovine insulin (25 U/kg bw in 0.9% saline) was injected intraperitoneally in mice and blood glucose was measured using a hand held glucose monitor at 15, 30, 60 and 105 mins as described in Section 2.3.2.

2.3.4 Plasma insulin determination

Plasma insulin concentration was determined by using modified dextran-coated charcoal radioimmunoassay (RIA) as described in Section 2.2.2.

2.4 MEASUREMENT OF BODY COMPOSITION, BONE MINERAL DENSITY AND BONE MINERAL CONTENT BY DEXA SCANNING

The mice were placed in a glass bell jar; in which the cotton mops were placed at the bottom of the jar. These cotton mops were dipped into isopropanol solution. After placing the mice in the jar, the mice became unconscious. Then the unconscious mice were placed on a specimen tray of the dual energy X-ray absorptiometry (DEXA) scanner and the whole body was scanned. The parameters measured using DEXA scanner (Inside Outside Sales, Wisconsin, USA) were bone mineral density (BMD), bone mineral content (BMC), lean mass, fat mass and percentage of total fat. The mice were exposed to X-rays and a high resolution picture was captured. The whole body was scanned along with regions of interests (femur, tibia and lumbar spine), as shown in Figure 2.2. The calibration of the machine was performed as per the manufacturer's guidelines using a phantom.

Figure 2.2 DEXA scanning images and its region of interest (ROI)

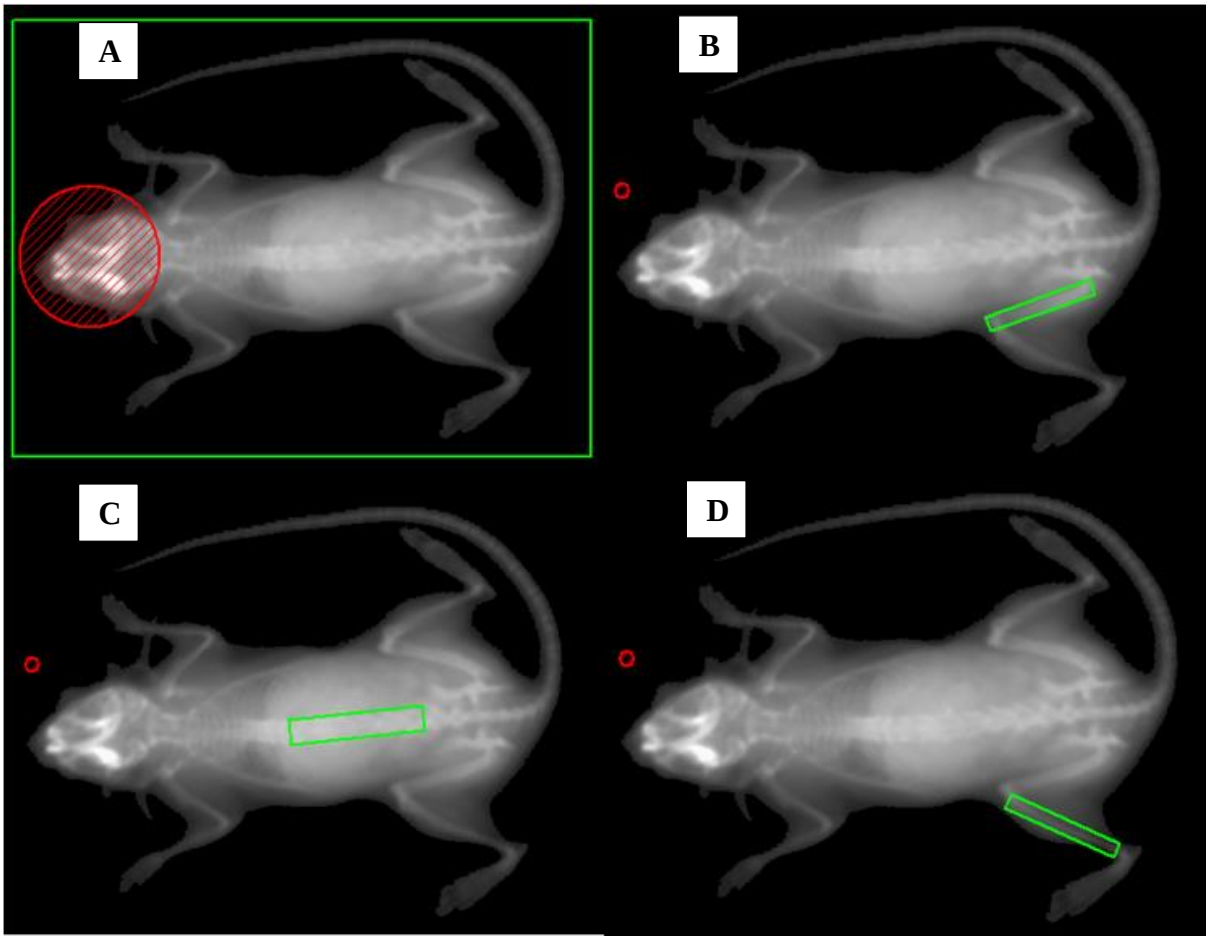

Figure 2.2A shows total region, whole body (in green) excluding the head (in red)
Figure 2.2B shows femoral region
Figure 2.2C shows lumbar or lower spine region
Figure 2.2D shows tibial region

2.5 ASSESSMENT OF BONE STRENGTH AND BONE QUALITY

Tibias and femurs were dissected from the mice and cleaned. The excised tibias and femurs were kept in 70% ethanol, and stored at 4°C until further use. Four techniques that were then employed to assess direct bone properties including; nanoindentation, quantitative back scattered electron imaging, X-ray microcomputed tomography (microCT) and three-point bending. These techniques were performed in bone research lab under the supervision of Dr. Guillaume Mabilleau at University of Angers, France

2.5.1 Nanoindentation

Nanoindentation determines hardness and elastic modulus of the bone. The biggest advantage of nanoindentation is that it can measure mechanical properties of the material on smaller scales (below microns) and therefore provide higher accuracy to investigate material properties of the bone matrix. The main purpose of using nanoindentation is to determine mechanical properties of bone matrix (Mabilleau *et al*. 2013). In order to carry out nanoindentation, blocks of embedded bone were polished with a DiaPro Nap-B diamond particle using Struers Tegramin-30 machine (Struers, Denmark) one day before the assessment and then left in saline solution (NaCl 0.9% (w/v)) overnight. The polished block of the bone was then placed on the Table Top Nanoindentation Tester (TTX-NHT, Figure 2.3) machine platform (CSM instrument, Peseux, Switzerland). An indentation area of 3 mm below growth plate in cortical section of the bone was selected. After selecting the region of indentation the block was passed under the indenter. Up to 12 indentations were positioned in cortical bone using NHT-TTX, which was equipped with a Berkowitch pyramidal diamond probe as an indenter. A force of 40 mN/minute was applied to

the bone and indentations were produced of 900 nm in depth. The load was maintained for total duration of 15 seconds. Maximum force, indentation modulus, hardness and dissipated energy were estimated using nanoindentation as described previously (Olivier & Pharr, 1992).

Hardness was calculated from the following equation;

$$H_{IT} = \frac{F_{\max}}{A_p}$$

Where:

F_{max} is the maximum force

A_p is the projected contact area

Figure 2.3 Nanoindentation (TTX-NHT) apparatus

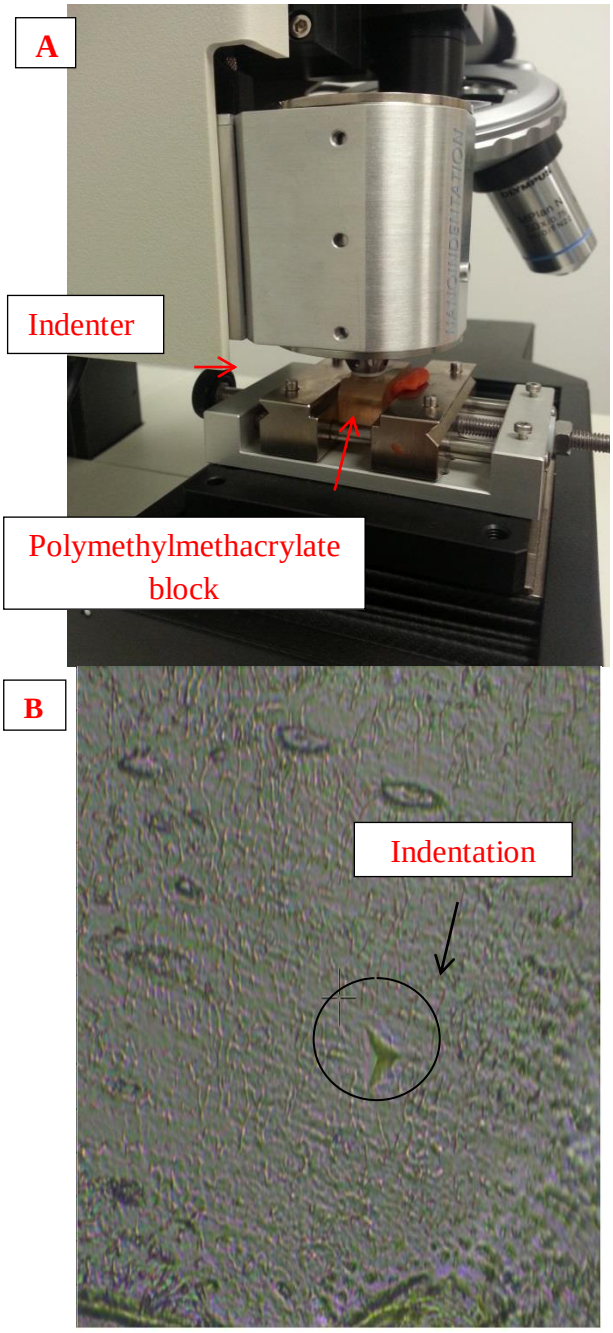

Figure 2.3A shows the position of PMMA block on a stable platform and under the indenter.
Figure 2.3B shows the pyramidal indentation as an impact of Berkowitch diamond probe on cortical bone.

Indentation modulus is the initial slope of the unloading section of the curve and obtained from the equation below;

$$E_{IT} = \frac{1-\nu_s^{\,2}}{\frac{1}{E_r} - \frac{1-\nu_i^{\,2}}{E_i}}$$

Where $E_r = \frac{S.\sqrt{\pi}}{2\beta\sqrt{A_p(h_c)}}$ in Pascal

Where:

E_i = Elastic modulus of the indenter (1141 GPa)

E_r = Reduced modulus of the indentation contact

ν_i = Poisson's ratio of the indenter (0.07)

ν_s = Poisson's ratio of the sample

2.5.2 Quantitative back scattered electron imaging (QBEI)

QBEI was used to determine bone mineral density distribution (BMDD). Polymethylmethacrylate (PMMA) blocks were polished with DiaPro Nap-B diamond particles (Struers, Denmark and then coated with carbon. The blocks were observed under scanning electron microscope (EVO LS10, Carl Zeiss Ltd., Nanterre, France) (Figure 2.4A). The scanning electron microscope was equipped with a five quadrant semi-conductor backscattered electron detector. For every specimen, at least four images were taken from the cortical bone area. The electron microscope was operated at 20 keV with a 250 pA probe current at working distance of 15 mm. The backscattered electron signal was calibrated using pure carbon (Z = 6, mean

grey level = 25), pure aluminium (Z = 13, mean grey level = 225) and pure silicon (Z = 14, mean grey level = 253) as standards (Micro-analysis Consultants Ltd., St. Ives, UK).

Samples were scanned using a focused beam of electrons. This beam of electrons comes in contact with the atoms present in the sample. Based on the composition and topography of sample these electrons produce an image. The signal generated is closely related to atomic number (Z) of the sample. High atomic number atoms will have stronger interaction with the electrons and will appear brighter in the gray level image of microscope.

The advantage of scanning electron microscope is that it provides 200x magnification of region of interest. Images are generated by MATLAB software (Angers University, France), where atomic number (Z) corresponds to y-axis and Backscattered electron (BSE) gray level to x-axis. The BSE gray level histogram was converted to weight percentage of calcium using hydroxyapatite, $Ca_{10}(PO_4)_6(OH)_2$ (Z = 14.06). Bone mineral density distribution (BMDD) was determined from 3 parameters; $Ca_{peak,}$ Ca_{mean} and $Ca_{width.}$ Ca_{peak} represents the most frequent calcium content of the bone area, Ca_{mean} corresponds to mean calcium content of the bone area obtained from area under the curve and Ca_{width} is the heterogeneity of mineralisation measured at 50% of maximum calcium level.

Figure 2.4 Scanning electron microscope (A), PMMA blocks (B) and scanning image of trabecular bone (C)

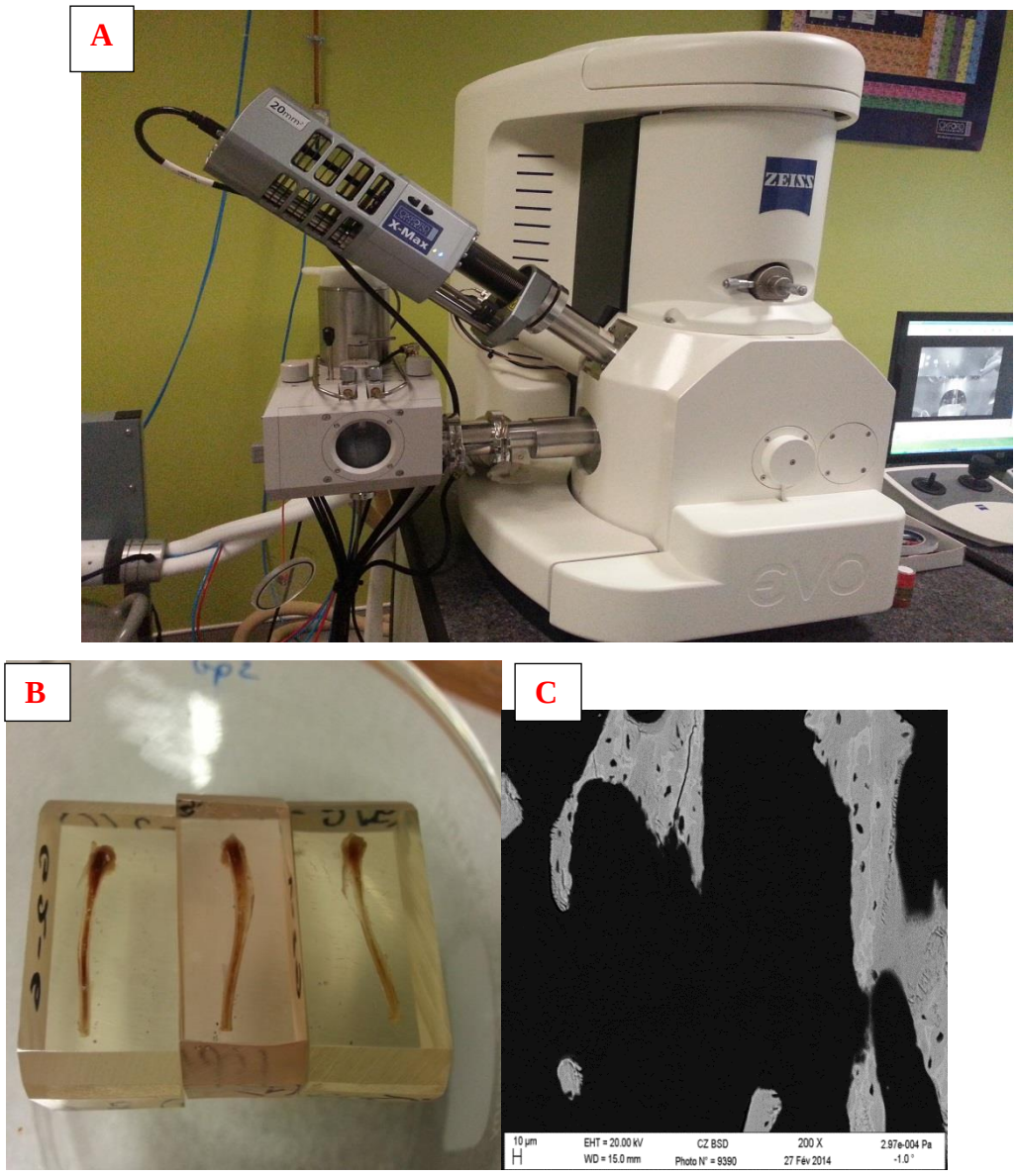

Figure 2.4A shows scanning electron microscope system that was used in quantitative backscattered electron imaging technique

Figure 2.4B shows proximal longitudinal section of embedded bone in PMMA blocks

Figure 2.4C shows microarchitectural image of trabecular bone captured by scanning electron microscope

2.5.3 Micro Computed Tomography (Micro CT)

Micro CT is mainly employed to study bone mass and microstructural morphology of tibia. A high-resolution Skyscan 1172 microtomograph (Bruker-Skyscan, Kontich, Belgium), which was equipped with an X-ray tube working at 50 kV/100 µA, was used to assess the tibia (Figure 2.5). Bones were placed inside an Eppendorf tubes that contained water in order to keep the bones hydrated. A sponge was placed in the tube in order to keep the position of tibia stationary. The Eppendorf tube was kept inside the central scanner along the axis on a carbon bed in the sample's chamber before subjecting the bone to X-rays. The bone is moved 180° step by step, at rotations of 0.3°. Bones were scanned cross-sectionally and distally to produce a series of 2D projection images followed by 3D reconstruction of bones from the stack of images after removing noise background and interactive thresholding using NRecon software (Bruker microCT, Belgium).

Different trabecular variables were measured using CTAn software (release 1.11.4.2, Bruker). These include; BV/TV (bone volume / trabecular volume, %), Tb.Th (trabecular bone thickness, mm), Tb.N (numbers of trabecular bone, 1/mm) and Tb.Sp (trabecular separation, mm). The measurements were in accordance with the guidelines on bone microstructure proposed by the American Society for Bone and Mineral Research (Bouxsein *et al*. 2010).

Along-with trabecular variables, cortical bone thickness (Ct.Th, in µm) and cross-sectional moment of inertia (CSMI, in mm^4) were assessed by measuring the diameter of cortical bone (B.Dm, in mm) and bone marrow (Ma.Dm, in mm) at 3-4 mm below the growth plate using ImageJ software (imajej.nih.gov). The measurements were conducted according to guidelines on

bone histomorphometry proposed by the American Society for Bone and Mineral Research (Dempster *et al*. 2013).

Cortical variables were calculated using the following formula;

$$Ct.Th = \frac{(B.Dm - Ma.Dm)}{2}$$

$$CSMI = \frac{\pi}{64} \bullet \left((B.Dm)^4 - (B.Dm - Ma.Dm)^4\right)$$

Where

B.Dm = the diameter of bone

Ma.Dm = the diameter of bone marrow

Figure 2.5 MicroCT setup apparatus

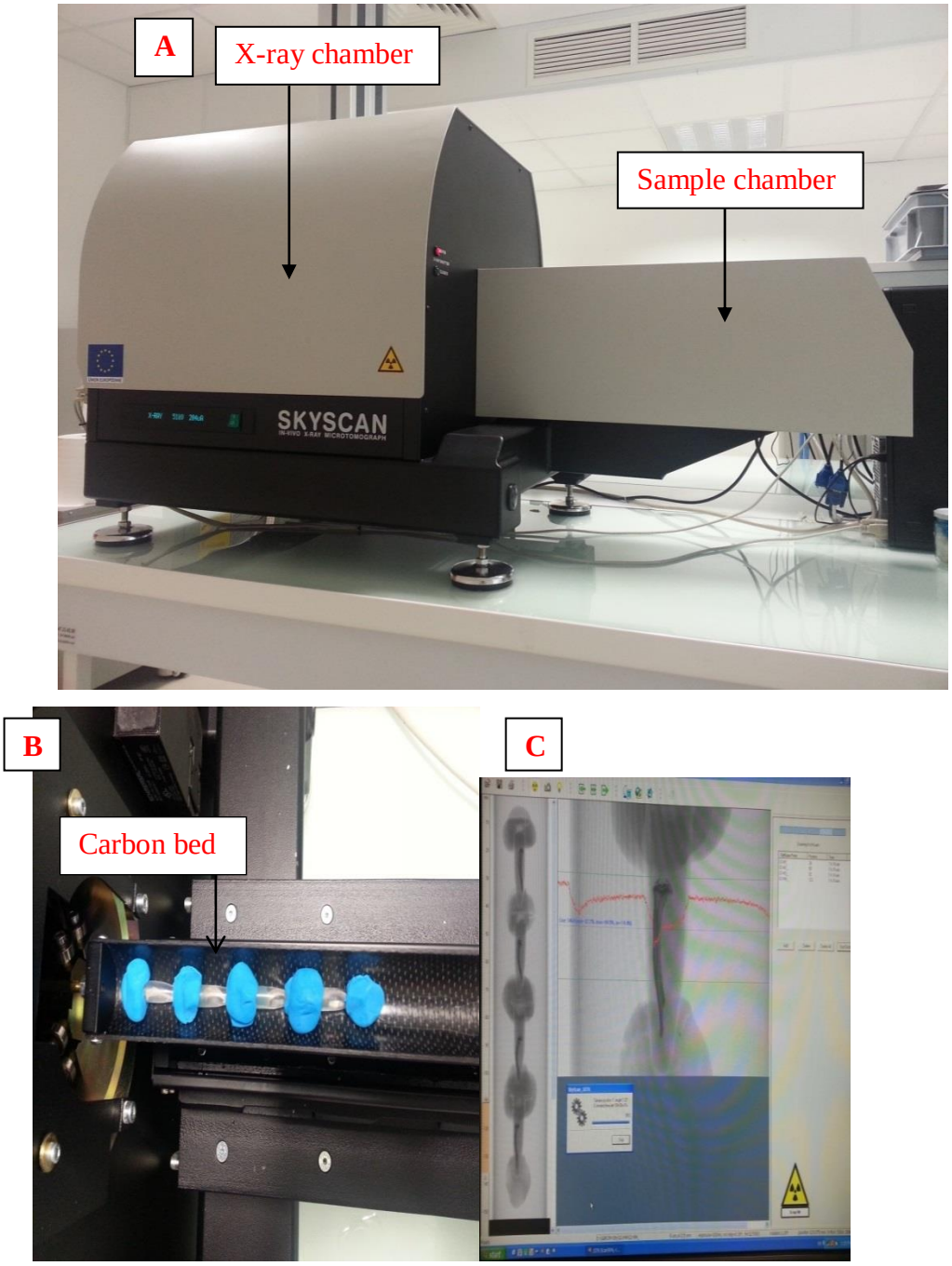

Figure 2.5A shows the microtomography system which consists of sample and x-ray chambers.
Figure 2.5B shows how tubes containing bones aligned on a carbon bed in sample chamber
Figure 2.5C shows the scout view of bones in x-ray chamber

2.5.4 Three- point bending

Three- point bending determines, as assessed using an Instron-5942 3-point bending machine (Instron, U.S.A.), determines the mechanical properties of femoral bones. Before the experiment the bones were kept in saline solution for 24 hrs at room temperature. Femurs were positioned in such a way that their anterior side was facing upward, on top of a pair of rounded grips (10 mm apart) as supports (Figure 2.6). Then using a control panel, a vertically-moving crosshead was slowly brought down to the midshaft of the specimen and a pressing force was applied to the femur until the bone was broken. A loading speed of 2 mm min^{-1} was employed and the load and time taken until bone failure was recorded by the captor. The load-time curve was converted to a force-displacement curve (Figure 2.6), measured by Bluehill 3 software (Instron, France). The variables which were assessed from the curve were ultimate load, ultimate displacement, stiffness and work to failure as published previously (Turner 2006).

2.5.5 Fourier –transformed infrared microscopy (FTIRM)

Femurs were subjected to FTIRM analysis after three-point bending. In order to carry out FTIRM, femurs were cut at the mid-shaft with the help of diamond saw (Accutom, Struers, Champigny sur Marne, France). Further, femurs were embedded in polymethymethacrylate at 4°C. Cross-sections (4 µm thickness) of femur were cut on a microtome equipped with a tungsten carbide blade (Leica Polycut S). Spectral analysis of femurs was obtained on a Bruker Vertex 70 spectrometer interfaced with a Bruken Hyperion 3000 infrared microscope (Bruker Optics Ettlingen, Germany). For every femur, 12 spectra were acquired between the double calcein labelling areas, and analysed with Opus Software (release 6.5, Bruker).

Further, individual spectra were subjected to curve-fitting using G/AI 8.0, Thermofisher scientific commercially available software. Collagen maturity index, collagen glycation index and collagen integrity index was assessed.

Figure 2.6: Setup of the three-point bending machine

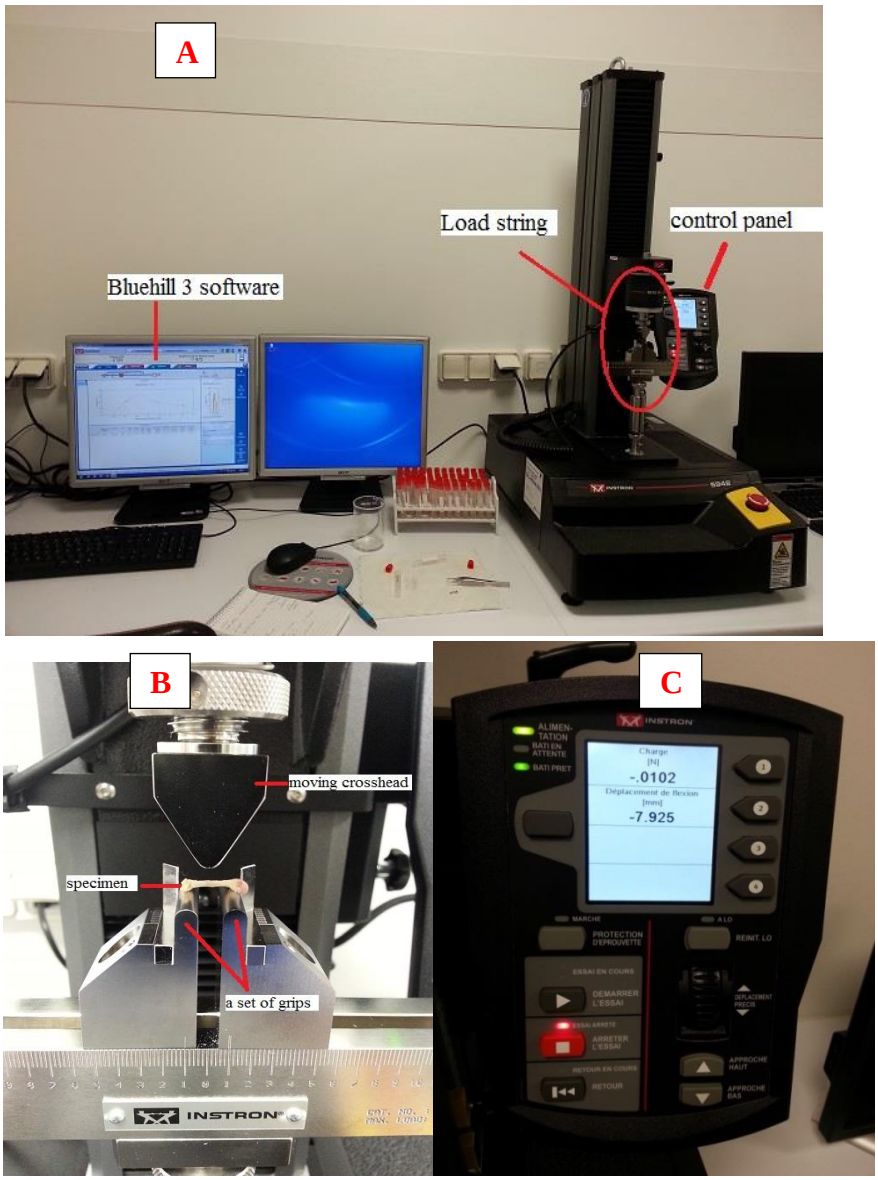

Figure 2.6A shows three-point bending instrument connected to a computer with Bluehill 3 software that is responsible for measuring mechanical properties of bone.
Figure 2.6B shows the position of femur on 10 mm-apart grips and a moving crosshead.
Figure 2.6C shows control panel of the three-point bending instrument that allows vertical movement of load and captor.

Figure 2.7 Representative of force-displacement curve for three-point bending test

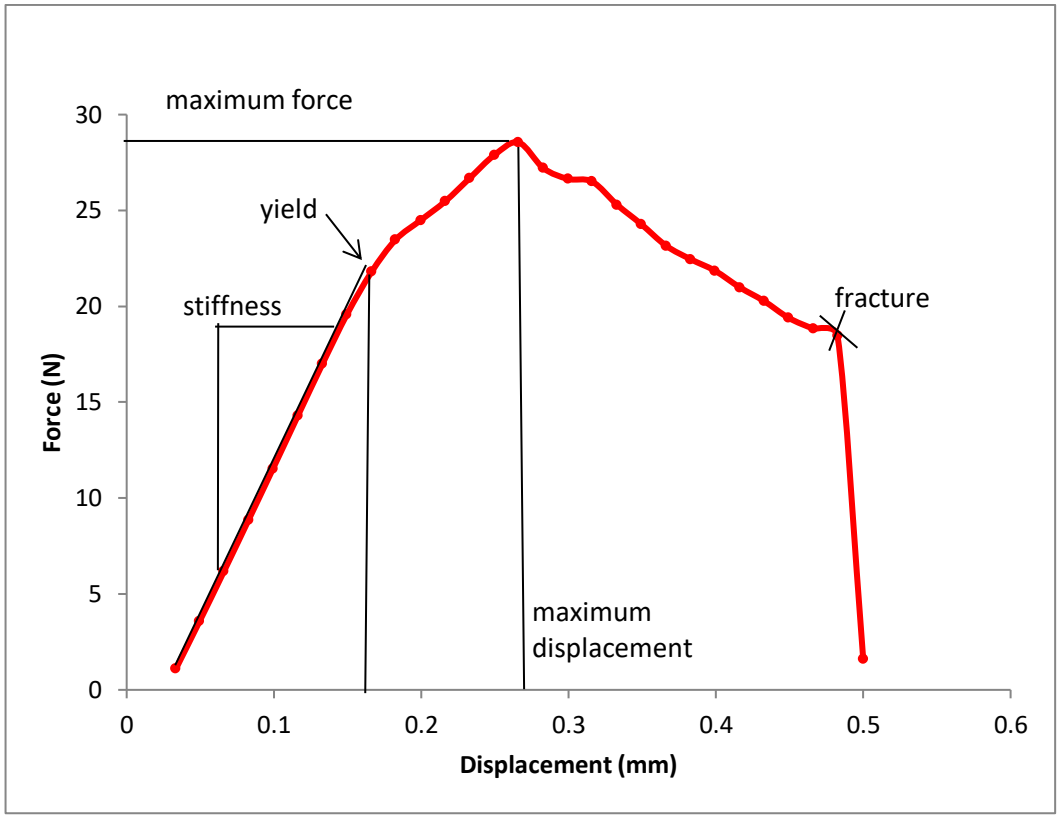

This graph represents mechanical properties determined by three point bending; total absorbed energy (area under curve), stiffness, maximum displacement (displacement at maximum force); yield (a transition point, above which force begins to cause permanent damage to bone) and the post-yield energy (area under the curve after yield point).

2.6 STATISTICAL ANALYSIS

The statistical analysis was carried out using GraphPad Prism-5 software. All results were expressed as mean ± SEM. For the comparative analysis of values student's unpaired t-test, one way ANOVA and Student Newman Kewl's *post hoc* test were used. Groups of data were considered significant if $p<0.05$.

Chapter 3

Effects of GIP, GLP-1, Xenin and Hybrid analogues on SAOS-2 osteoblast cells

3.1 SUMMARY

Incretin hormones such as glucose dependent insulinotropic polypeptide (GIP) and glucagon-like peptide-1 (GLP-1) augment insulin secretion following food ingestion. The bioactivity of GIP and GLP-1 is limited because they are rapidly degraded by dipeptidyl peptidase 4 (DPP-4). In order to prolong their bioactivity several long-acting GIP and GLP-1 analogues have developed which can overcome DPP-4 degradation. It is well known that GIP receptors (GIPR) are present in pancreas, brain, heart, lung, adrenal cortex, and adipose tissue and recently it has been revealed that GIPR are present in the bone as well. With the help of acidic oligopeptide tagging bone-specific GIP, GLP-1, xenin and GIP/Xenin hybrid analogues were designed as they have high affinity towards hydroxyapattite which is a major component of the bone. This study mainly focuses on the effects of bone-specific analogues on bone formation biomarkers- alkaline phosphatase activity, cyclic adenosine monophosphate (cAMP) generation in human osteoblastic SAOS-2 cells as well as role of cytokine factors such as transforming growth factor- beta (TGF-β) and insulin-like growth factor-1 (IGF-1) in bone formation. Bone-specific analogues (D-Ala^2)GIP-Asp and (D-Ala^2)GIP-Glu demonstrated significant ($p<0.01$) insulin secretion as that of (D-Ala^2)GIP. Similar results were obtained regarding xenin-25[Lys^{13}PAL], xenin-25[Lys^{13}PAL]-Asp and GIP/Xenin hybrid analogues. (D-Ala^2)GIP, (D-Ala^2)GIP-Asp were found to have increased ($p<0.01$) alkaline phosphatase activity during 24 and 48 hour incubation at concentrations of 10^{-10} M and above. Alkaline phosphatase activity was enhanced during 72 hour incubation with positive effects observed at 10^{-11} M and above. A similar pattern was observed regarding (D-Ala^2)GLP, (D-Ala^2)GLP-1-Asp and (D-Ala^2)GIP-1-Glu. No activity was observed regarding xenin-25[Lys^{13}PAL] and xenin-25[Lys^{13}PAL]-Asp. GIP/Xenin

and GIP/Xenin-Asp enhanced ($p<0.5$ to $p<0.01$) alkaline phosphatase activity during 24 h incubation period while GIP/Xenin-Glu did not show any effect on alkaline phosphatase activity. Bone specific analogues (D-Ala^2]GIP and (D-Ala^2)GIP-Asp significantly ($p<0.05$ to $p<0.001$) stimulated cAMP production in SAOS-2 cells . Regarding (D-Ala^2)GLP-1, (D-Ala^2)GLP-1-Asp and (D-Ala^2)GLP-1-Glu similar pattern of cAMP production was observed. No cAMP generation was seen regarding xenin-25[Lys^{13}PAL] and xenin-25[Lys^{13}PAL]-Asp. Regardin GIP/Xenin hybrid peptides, GIP/Xenin enhanced cAMP production at 10^{-8} M and above, GIP/Xenin-Asp and GIP/Xenin-Glu increased cAMP production only at 10^{-6} M. For (D-Ala^2)GIP-Asp and (D-Ala^2)GIP-Glu significant ($p<0.05$ to $p<0.01$) augmentation of TGF-β levels were observed at 10^{-8}M and above. Xenin-25[Lys^{13}PAL] and Xenin-25[Lys^{13}PAL]-Asp did not induce any effect in terms of TGF- β release. GIP/Xenin significantly ($p<0.01$ to $p<0.001$) increased TGF-β levels at 10^{-10} M and above. IGF-1 release profile was similar to that of TGF- β.

3.2 INTRODUCTION

Enteroendocrine cells produce different peptides including the incretin hormones glucose dependent insulinotropic polypeptide (GIP) and glucagon-like peptide-1 (GLP-1) as well as xenin, cholecystokinin (CCK) amongst many others (Drucker 2007). In the 1960s a series of experiments were conducted which demonstrated the role of intestinal hormones in post-prandial insulin release (Daniel & Zietek 2015). This effect was described as the 'incretin effect' by Perley& Kipnis in 1967, and relates to the augmentation of insulin release following an oral glucose load mediated exclusively by GIP and GLP-1 (Lindgren *et al*. 2015). GIP is 42 amino acid hormone secreted from enteroendocrine K-cells postprandially (Fujita *et al*. 2016). GIP receptors are present in many tissues including pancreas, lung, testis, kidney, brain and adrenal cortex (Wang *et al*. 2017). Recent evidence has also reported that GIP receptors are present in bone (Holst *et al*. 2016).

Following secretion, GIP is rapidly degraded by ubiquitous enzyme dipeptidyl peptidase-4 (DPP-4) resulting in a very short biological half-life. In humans, it has been reported that the half-life of GIP is around 5-7 mins (Deacon *et al*. 2000, Hanna *et al*. 2014). In rodents, the half- life is GIP is thought to be less than 2 mins (Kieffer *et al*. 1995, Gilor *et al*. 2016). The unique speciality of DPP-4 is that it cleaves GIP at the N-terminal position 2 alanine residue, and converts GIP(1-42) into GIP (3-42), which does not have any biological activity (Irwin *et al*. 2015). In order to overcome this shortcoming several structurally modified DPP-4 resistant GIP analogues have been developed (Irwin *et al*. 2005a).

GLP-1 is secreted from intestinal L-cells in response to food intake (Kim *et al*. 2017). GLP-1 is principally known to stimulate insulin release from pancreatic β cells in a glucose

dependent manner (Pais *et al*. 2016). However, GLP-1 also has positive effects when it comes to weight loss, as it delays gastric emptying and inhibits appetite (Lee & Lee 2017). Like GIP, GLP-1 is also rapidly degraded by ubiquitous enzyme DPP-4, but enzymatically stable forms are also readily available (Mabilleau *et al*. 2017). In terms of effects on bone, GLP-1 administration promotes bone formation and helps normalize the impaired trabecular architecture (Nuche-Berenguer *et al*. 2015). In firm agreement, the GLP-1R agonist, liraglutide, had anabolic bone effects in overiectomized rats (Nan Lu *et al.* 2015).

Xenin is a 25 amino acid peptide hormone and is co-secreted with GIP from the intestinal K-cells in response to food intake (Anlauf *et al*. 2000). The major metabolic actions of xenin include effects on gut motility, stimulating insulin secretion, reducing food intake and promoting satiety (Taylor *et al*. 2010). Unlike GIP and GLP-1, xenin is not degraded by DPP-4 but it rapidly broken down by serine proteases in blood (Taylor *et al.* 2010). Importantly, xenin is known to enhance the biological actions of GIP (Taylor *et al*. 2010). Therefore, xenin may have positive effects on bone that could either be independent or linked to beneficial effects of GIP on bone. Interestingly, the specific receptor that xenin binds to still remains elusive, however interaction with neurotensin receptors has been proposed (Mazella *et al*. 2012).

Several reports highlight the importance of GIP and GLP-1 action on bone. Studies conducted by Gaudin-Audrain and colleagues showed that GIPR knockout (KO) mice exhibited higher trabecular bone volume, but there was a decrease in osteoclasts and increase in osteoblast activity, resulting in increased bone fracture risk (Gaudin-Audrain *et al*. 2013). In addition, collaborative studies at Ulster and Angers have shown that the GLP-1R is essential for maintenance of bone strength and quality (Mabilleau *et al.* 2013). In agreement with these

observations in GIP and GLP-1 receptor KO mice, double-incretin knockout (DIRKO) mice show reduced cortical bone mass and cortical bone strength and exhibit a combination of detrimental effects on bone as seen in GIPR and GLP-1R KO mice (Mieczkowska *et al*. 2015).

Taken together, it is apparent that GIP, GLP-1 and also possibly xenin, could possess beneficial effect on bone. This is especially true for diabetic patients, where fragility bone fractures are a key concern (Mabilleau *et al*. 2017, Hansen *et al*. 2017). However, native GIP, GLP-1 and xenin are rapidly broken down in the circulation immediately upon secretion, making them therapeutically unattractive. To circumvent this problem, numerous well characterised, enzymatically stable, long-acting GIP/GLP-1/xenin analogues have been developed (Irwin & Flatt 2015). However, despite their enhanced pharmacokinetic profile, these analogues show no specificity towards bone. Thus, in 2008, Takahashi-Nishioka *et al*. demonstrated the use of acid olionucleotides tagging (Glu and Asp) which can help deliver peptides to bones, due to preferential peptide deposition in hydroxyapatite (Wang *et al*. 2015). Based in this knowledge, the present study has utilised well established stable GIP, GLP-1, xenin and related hybrid peptides that incorporate oliopeptide tagging to make them more bone specific. Essentially this body of work has investigated the effects of four different families of peptides on metabolic and bone related parameters. The peptide families include GIP, comprising of (D-Ala^2)GIP, (D-Ala^2)GIP-Asp and (D-Ala^2)GIP-Glu; GLP-1 that consists of (D-Ala^2)GLP-1, (D-Ala^2)GLP-1-Asp and (D-Ala^2)GLP-1-Glu; a xenin family including Xenin-25[Lys^{13}PAL], Xenin-25[Lys^{13}PAL]-Asp and finally a GIP/xenin family of peptides that incorporates GIP/Xenin, GIP/Xenin-Asp, GIP/Xenin-Glu. As such, following peptide characterisation, the potential beneficial effects of these peptides on the release of TGF-β and IGF-1, cAMP production

and alkaline phosphatase activity in human osteoblastic-derived SaOS-2 cells was examined. In addition, in a screening exercise to confirm bioactivity, relating to the insulinotropic action of all peptides was conducted in pancreatic clonal BRIN BD11 beta-cells.

3.3 MATERIALS AND METHODS

3.3.1 Peptides

All the peptides namely, (D-Ala^2)GIP, (D-Ala^2)GIP-Asp, (D-Ala^2)GIP-Glu, (D-Ala^2)GLP-1, (D-Ala^2)GLP-1-Asp, (D-Ala^2)GLP-1-Glu, Xenin-25[Lys^{13}PAL], Xenin-25[Lys^{13}PAL]-Asp, GIP/Xenin, GIP/Xenin-Asp and GIP/Xenin-Glu were purchased from EZ Biolabs Ltd. (Carmel, United States of America) and were characterised by mass spectrometry as described in section 2.1.1.

3.3.2 Maintenance of BRIN-BD11 cells

BRIN-BD11cells were maintained as described in Section 2.2.1. Culture medium was changed every 3 days and the cells were utilised at 80% confluency.

3.3.3 Maintenance of SAOS-2 cells

SAOS-2 cells were maintained as described in Section 2.2.3. Culture medium was changed every 3 days and the cells were utilised at 80% confluency. MEM alpha medium supplemented with 10% of foetal bovine serum (FBS) and 1% of penicillin/streptomycin was used to culture the cells. The cells were maintained in a controlled atmosphere at 37°C, 5% CO_2.

3.3.4 Measurement of plasma insulin

An insulin RIA was carried out as described in Section 2.2.2 to determine plasma insulin concentrations.

3.3.5 Measurement of TGF-β

TGF-β was measured using a TGF-β Immunoassay kit (Quantikine, R&D Systems) as described in Section 2.2.7. Briefly, SAOS-2 cells were incubated in media which was supplemented with 10% FBS and maintained until the cells were confluent. Before adding the peptides the media was changed with 0.1% FBS-containing media. 1 ml of respective peptides (10^{-12} - 10^{-6} M) was added to each well and plates were then incubated for 8 hrs. After 8 hrs, TGF-β released in the supernatant was measured using a TGF-β Immunoassay kit (Quantikine, R&D Systems).

3.3.6 Measurement of IGF-1

IGF-1 was measured using IGF-1 Immunoassay kit (Quantikine, R&D Systems) as described in Section 2.2.8. In order to carry out IGF-1 assay, SAOS-2 cells were seeded at a density of 2 $x10^5$ cells/well and cells were maintained until they were confluent in 10% FBS-containing media. Afterwards, media was changed with fresh media (supplemented with 0.1% FBS) 24 hrs prior to addition of respective peptides. Then the media was removed and 1 ml of respective peptides (10^{-12} - 10^{-6} M) was added. Plates were then incubated for 8 hrs. After desired incubation, IGF-1 released in the supernatant was measured using IGF-1 Immunoassay kit (Quantikine, R&D Systems).

3.3.7 Measurement of cyclic AMP

cAMP was measured using a cAMP assay kit (R&D Systems) as described in Section 2.2.9. For cAMP assay, SAOS-2 cells were cultured in α-MEM 1X media which was supplemented with

10% FBS, penicillin and streptomycin for 24 hrs so that the cells could attach to the plate. Cells were then incubated with various concentrations (10^{-12}-10^{-6} M) of respective peptides supplemented with 200 µM of 3-isobutyl-1-methylxanthine (IBMX). The plate was left for 40 mins at 37ºC. Following this, the cells were washed 3 times with 150 µl of PBS. Cell lysis buffer (R&D Systems) was then used to lyse the cells and a freeze (-20ºC) -thaw (37˚C) cycle was carried out. The contents were then collected into 500 µl Eppendorf tubes and centrifugated at 600 g for 10 mins at 4˚C. Supernatant was collected and cAMP was measured using a cAMP assay kit (R&D Systems).

3.3.8 Measurement of alkaline phosphatase activity

Alkaline phosphatase activity was determined as described in Section 2.2.4. Samples (50 µl) were added to 96-well plates in duplicate and alkaline phosphatase activity was indirectly measured using 4-methyl umbelliferyl phosphate (Sigma) as the substrate. The reaction was stopped after 30 mins incubation at 37ºC, addition of 100 µl of 0.6 M Na_2CO_3 (Sigma-Aldrich). FlexStation 3 (Molecular Devices) was used to measure the fluorescence at excitation wavelength of 360 nm and an emission wavelength of 450 nm. The cut off was kept at 435 nm. Alkaline phosphatase activity was calculated from a standard curve (0-1000 pmol) of 4-methyl umbelliferone.

3.3.9 Statistical analysis

Data were analyzed using one-way and two-way ANOVA with Newman-Keuls post hoc tests and two-tailed t-tests using PRISM 5.0. Data are expressed as mean ± S.E.M and a P value < 0.05 was considered statistically significant.

3.4 RESULTS

3.4.1 Reverse-phase HPLC purification HPLC Traces of pure peptides

The reverse-phase HPLC of the synthetic peptides, performed using a C-18 analytical column, showed homogenous well resolved peaks indicating a high degree of purity (Figure 1, A; Figure 2, A; Figure 3 A; Figure 4, A; Figure 5, A; Figure 6, A; Figure 7, A; Figure 8, A; Figure 9, A; Figure 10, A and Figure 11, A). Furthermore, this in-house HPLC analysis confirmed the peptide purity information supplied by the manufacturer.

3.4.2 Mass spectrometry analysis

The molecular mass of each peptide was determined using mass spectrometry (Figure 1, B; Figure 2, B; Figure 3 B; Figure 4, B; Figure 5, B; Figure 6, B; Figure 7, B; Figure 8, B; Figure 9, B; Figure 10, B and Figure 11, B). Mass spectrometry data confirmed the peptides were synthesised successfully, as all *m/z* ratios corresponded well to theoretical masses (Table 1).

3.4.3 Dose dependent effects of GIP, GLP-1, Xenin and Hybrid peptides on *in-vitro* insulin secretion from BRIN-BD11 cells

Figure 12 (A) demonstrates the effect of a range of concentrations (10^{-12} to 10^{-6} M) of (D-Ala^2)GIP, (D-Ala^2)GIP-Asp and (D-Ala^2)GIP-Glu on insulin secretion from the clonal pancreatic beta cell line, BRIN-BD11 at 5.6 and 16.7 mM glucose. As expected, (D-Ala^2)GIP demonstrated significant ($p<0.001$) dose-dependent increases in insulin secretion at both glucose concentrations (Figure 12A,B). (D-Ala^2)GIP-Asp and (D-Ala^2)GIP-Glu also evoked similar significant ($p<0.01$) increases of insulin secretion, but were marginally less effective than (D-Ala^2)GIP at 10^{-12} M when incubated at 16.7 mM glucose (Figure 12A,B). For (D-Ala^2)GLP-1, (D-Ala^2)GLP-1-Asp and (D-Ala^2)GLP-1-Glu there was a comparable augmentation ($p<0.001$) of insulin secretion at

both 5.6 and 16.7 mM glucose, with (D-Ala^2)GLP-1-Glu being somewhat less efficacious at lower concentrations (Figure 13A,B). The significant ($p<0.001$) insulinoptropic actions of xenin-25[Lys^{13}PAL] and xenin-25[Lys^{13}PAL]-Asp were also comparable, with xenin-25[Lys^{13}PAL]-Asp being less effective at 10^{-11} and 10^{-12} M when incubated with 5.6 and 16.7 mM glucose, respectively (Figure 14A,B). In case of the hybrid peptides, namely GIP/Xenin, GIP/Xenin-Asp and GIP/Xenin-Glu, again there was a cleat dose-dependent increase ($p<0.001$) of insulin secretion at both 5.6 and 16.7 mM glucose (Figure 15A, B). Similar to the other peptide families, at lower concentrations (10^{-12} and 10^{-11} M) there was a marginal reduction in efficacy with both GIP/Xenin-Asp and GIP/Xenin-Glu (Figure 15A,B). Taken together, these data confirm that C-terminal extension of stable GIP, GLP-1, xenin or GIP/xenin hybrid peptides did not dramatically impede biological activity.

3.4.4 Dose- and time-dependent effects of GIP, GLP-1, xenin and hybrid peptides on alkaline phosphatase activity

(D-Ala^2)GIP, (D-Ala^2)GIP-Asp and (D-Ala^2)GIP-Glu enhanced ($p<0.05$ to $p<0.001$) alkaline phosphatise activity during 24, 48 and 72 hour incubation periods (Figure 16A,B & 17). During 24 and 48 hour incubations, (D-Ala^2)GIP, (D-Ala^2)GIP-Asp were found to have increased ($p<0.01$) alkaline phosphatase activity at concentrations of 10^{-10} M and above (Figure 16A,B), with positive effects observed at 10^{-11} M and above during 72 hour incubations (Figure 17). Interestingly, (D-Ala^2)GIP-Asp appeared to be more effective than (D-Ala^2)GIP-Glu (Figure 16A,B & 17). A similar pattern was observed for (D-Ala^2)GLP-1, (D-Ala^2)GLP-1-Asp and (D-Ala^2)GIP-Glu (Figure 18 A,B & 19). As such, alkaline phosphatase activity increased as the incubation time was increased from 24 to 72 hrs in a dose-dependent manner for each peptide (Figure 18 A,B & 19). (D-Ala^2)GLP-1 possessed

significant activity at concentrations 10^{-9} M (p<) and above during 24 hour incubations (Figure 18A) and 10^{-10} M (p<0.001) and above during 48 and 72 hrs time periods (Figure 18B & 19). As with the GIP family of peptides, the (D-Ala^2)GLP-1-Asp analogue seemed to be more effective than the (D-Ala^2)GIP-Glu peptide (Figure 18 A,B & 19). In terms of alkaline phosphatase an activity of xenin-25[Lys13PAL] and xenin-25[Lys13PAL]-Asp, no activity was observed at any of the time points or doses employed (Figure 20A, B & 21). In terms of GIP/Xenin, GIP/Xenin-Asp and GIP/Xenin-Glu, during 24 hour incubations only GIP/Xenin and GIP/Xenin-Asp caused elevations (p<0.5 to p<0.01) in alkaline phosphatase activity, with GIP/Xenin-Glu being ineffective (Figure 22A). However, all three GIP/Xenin peptides evoked increases (p<0.05 to p<0.001) in alkaline phosphatase activity during 48 and 72 hour incubation periods (Figure 22B & 23). Similar to observations with the GIP and GLP-1 families of peptides, GIP/Xenin-Asp was more effective than GIP/Xenin-Glu (Figure 22A,B & 23)

3.4.5 Dose-dependent effects of GIP, GLP-1, Xenin and hybrid peptides on cAMP production in SAOS-2 cells

As shown in Figure 24, (D-Ala^2]GIP and (D-Ala^2)GIP-Asp significantly (p<0.05 to p<0.001) stimulated cAMP production in SAOS-2 cells compared to controls at 10^{-10} M and above (Figure 24A). The only effective (p<0.05) concentration of (D-Ala^2)GIP-Glu was 10^{-6} M (Figure 24A). A fairly similar pattern of cAMP production was observed for (D-Ala^2)GLP-1, (D-Ala^2)GLP-1-Asp and (D-Ala^2)GLP-1-Glu (Figure 24B), with (D-Ala^2)GLP-1 and (D-Ala^2)GLP-1-Asp being effective (p<0.01) at 10^{-8} M and (D-Ala^2)GLP-1-Glu (p<0.01) only at 10^{-6} M (Figure 24B). No cAMP generation was observed with xenin-25[Lys^{13}PAL] and xenin-25[Lys^{13}PAL]-Asp (Figure 25A). In terms of the GIP/xenin hybrid peptides, there was enhanced (p<0.05 to p<0.01) cAMP

production for GIP/Xenin at 10^{-8} M and above, but only at 10^{-6} M for GIP/Xenin-Asp and GIP/Xenin-Glu (Figure 25B).

3.4.6 Dose-dependent effects of GIP, GLP-1, xenin and hybrid peptides on TGF-β and IGF-1 release from SAOS-2 cells

After exposure of SAOS-2 cells for 8 hrs, TGF-β levels were increased significantly ($p<0.01$ to $p<0.001$) by (D-Ala^2)GIP at all concentrations employed (Figure 26A). Significant ($p<0.05$ to $p<0.01$) augmentation of TGF-β levels were recorded for (D-Ala^2)GIP-Asp and (D-Ala^2)GIP-Glu at 10^{-8} M and above (Figure 26A). Furthermore, (D-Ala^2)GLP-1 significantly ($p<-0.01$ to $p<0.001$) increased TGF–β levels in SAOS-2 cells at 10^{-10} M and above (Figure 26B). For (D-Ala^2)GLP-1-Asp, increased ($p<0.01$ to $p<0.001$) levels were observed at 10^{-6} and 10^{-8} M, whereas (D-Ala^2)GLP-1-Glu was only effective ($p<0.01$) at the highest dose, 10^{-6} M, employed (Figure 26B). No effect of xenin-25[Lys^{13}PAL] and xenin 25[Lys^{13}PAL]-Asp was seen in terms of TGF-β release (Figure 27A). However, GIP/Xenin produced significant ($p<0.01$ to $p<0.001$) increases TGF-β concentrations at 10^{-10} M and above (Figure 27B). GIP/Xenin-Asp generated significant ($p<0.01$ to $p<0.001$) levels of TGF-β at both 10^{-6} to 10^{-8} M, whilst this was only observed at 10^{-6} M for GIP/Xenin-Glu (Figure 27B). The impact of the peptides of IGF-1 release was remarkably similar to that observed with TGF-B release (Figures 28&29). As such, all GIP-related (Figure 28A), GLP-1-related (Figure 28B) and GIP/xenin-related (Figure 29B) peptides evoked significant increases of IGF-1 release from SAOS-2 cells, whereas the xenin family of peptides were ineffective in this regard (Figure 29A).

3.5 DISCUSSION

Bone is highly complex dynamic organ and is constantly remodeled throughout life by the sequential activity of osteoblasts

and osteoclasts (Murugananda & Sinal 2014). This activity is controlled by various autocrine and paracrine factors (Matsuo & Ire 2008). Gastrointestinal hormones such as GIP and GLP-1 are known to play important role in remodelling of bone (Henrikson *et al*. 2003). GIP, secreted by intestinal K-cells, has specific receptors present on bone cells (Bollag *et al*.2000, Zhong *et al* 2007). Thus, GIP has direct positive beneficial effects on the bones (Gilbert & Pratley 2015, Palmero *et al*. 2016). Interestingly, xenin is a hormone co-released with GIP from K-cells (Hasib *et al*. 2017). To date there is no real knowledge in relation to the potential effects of xenin on bone, but since xenin is known to augment the biological actions of GIP (Martin *et al*. 2016); an effect on bone would not be unsurprising. Intriguingly, there has been a recent report of a GIP/xenin hybrid molecule that combines the activity of GIP and xenin into a single compound (Hasib *et al*. 2017). Given the aforementioned actions, it would be interesting to examine the effects of this hybrid peptide on bone. Another important gastrointestinal hormone is GLP-1, secreted by ileal L-cells (Grneier & Backhed 2016). There are numerous reports which suggest that GLP-1 can be considered as a potential option for treatment of bone fractures (Lepsen *et al*. 2015, Wolverton & Blair 2017). In addition, there are numerous GLP-1 receptor knock out studies in mice that suggest that GLP-1R is essential for maintenance of bone strength and quality (Lu *et al*. 2015, Mabilleau *et al*. 2015, Mieczkowska *et al*. 2015, Meng *et al*. 2016).

There are many obstacles in considering the use GIP, GLP-1, xenin or related peptides as a therapeutic option against bone fractures. Firstly, the native peptides are not enzymatically stable, and have an extremely short half-life (Gilor *et al*. 2016, Hanna *et al*. 2014). Fortunately however, numerous well characterised stable long-acting forms of GIP, GLP-1 and xenin analogues have been described (Uccellatore *et al*. 2015, Minamnres & Perez

2017). The second main obstacle revolves around specificity of these peptide analogues for bone. Bone is composed of mainly three main components, fibrous protein collagen, calcium phosphate hydroxyapatite and water (Ferreira *et al*. 2012). Thus, through oligopeptide tagging, involving addition of six C-terminal acidic L-Asp or L-Glu amino acid residues to encourage binding to hydroxyapatite (Takahashi-Nishioka *et al*. 2008), we can increase specificity of these peptides towards bone. Initially, all peptides were characterised by HPLC and mass spectrometry before progressing to investigating effects within each experimental system.

In order to confirm bioactivity of the novel C-terminally extended peptides, effects on insulin secretion from clonal BRIN BD11 cells was examined. Notably, (D-Ala^2)GIP, (D-Ala^2)GLP-1, xenin-25[Lys^{13}PAL] and the GIP/xenin hybrid peptide have all been shown to stimulate insulin secretion from this cell line (Parthsarthy *et al*. 2016, Martin *et al*. 2016, Hasib *et al*. 2017). In addition, since the GIP receptor on pancreatic beta-cells is identical to that found on bone (Faienza *et al*. 2015, Holst *et al*. 2016, Hansen *et al*. 2017), we can be confident that effects can be translated to bone. Interestingly, all peptides dose-dependently stimulated insulin secretion, suggesting retention of bioactivity. It did appear the C-terminal extensions (Takahashi-Nishioka *et al*. 2008) slightly impaired bioactivity, and that the L-Asp extension was less detrimental than the L-Glu extension in this regard. Further studies would be required to examine why this difference occurred. Nonetheless, given the potential for increased deposition within bone of the novel peptides, bioactivity data generated here was still very encouraging. This paved the way for investigating the effects of all peptides on bone cells.

There are various osteoblastic cell lines available, namely SAOS-2 and MG-63 which have shown the presence of GIP receptors (Mabilleau *et al*. 2016). With this in mind, the SAOS-2 cell line

was chosen for this study. TGF-β is a product of osteoblasts and it is abundantly found in bone matrix (Florencio-Silva *et al*. 2015). The main function of TGF-β is stimulating proliferation and differentiation of osteoblasts (Robey *et al*. 1987, Lee at al. 2002, Janssens *et al*. 2005, Tang *et al*. 2009). In the current study, TGF-β concentrations were significantly increased in presence of (D-Ala^2)GIP and related C-terminally extended analogues, which was expected (Budi *et al*. 2015). In harmony with this, (D-Ala^2)GLP-1 analogues also evoked increased concentrations of TGF-β, suggesting a direct effect of GLP-1 on these osteoblast cells. However, the xenin family of peptides was unable to modulate TGF-β concentrations. This would suggest that xenin has no direct effect on osteoblast cells. Although, since the exact xenin receptor has not yet been characterised (Irwin & Flatt 2015), it is difficult to relate this effect to a specific receptor. In case of the GIP/Xenin hybrid peptide, this peptide enhanced concentrations of TGF-β, suggesting that the acute effects of this peptide are mediated largely by the GIP component, as observed perviosuly (Hasib *et al*. 2017). IGF-1 is considered as important growth factor because of its dual action in both proliferation and differentiation of bone cells, and through positive effects on bone mineralization (Zhang *et al*. 2002, Xian *et al*. 2012). Interestingly, effects of the peptides on IGF-1 release almost mirrored actions on TGF-β release. This could suggest similar effects of gut-derived peptides on the secretion of both IGF-1 and TGF-β from osteoblasts. However, further investigation of the cell signalling pathways involved in these actions would be required to confirm this.

Alkaline phosphatase is considered as an important biomarker for bone formation (Kuo & Chen 2017). In the current study, as would be anticipated alkaline phosphatase activity increased as incubation time was increased from 24 to 72 h, confirming suitability of the experimental system. As expected (Lee *et al*.

2016, Pujari-Palmer *et al*. 2016) all GIP peptide forms augmented alkaline phosphatase activity, again confirming a direct effect on osteoblasts. Similar observations were made for all GLP-1 and GIP/xenin hybrid peptides. In addition, no activity was seen with the xenin group of peptides. These effects are virtually identical to those observed with IGF-1 and TGF-β release. This is interesting and again suggests similar effects of gut-derived hormones on bone. Moreover, activation of the GIP and GLP-1 receptors is known to modulate very similar pathways within various cell types (Campbell & Drucker 2013, Lee & Jun 2014, Athauda & Foltynie 2016), so the current observations may not be completely unexpected. Further research into lack of direct effects of xenin on SAOS-2 cells is required, although it may be that indirect effects are key, as has been observed with xenin actions on pancreatic beta cells. Nonetheless, alkaline phosphatase is a protein involved in bone mineralisation, with the main principle that it reduces extracellular inorganic pyrophosphate which is considered as a suppressor of hydroxyapatite crystals (Orimo 2010, Penido & Alon 2012). Therefore, the GIP, GLP-1 and GIP/Xenin peptides examined within the current study could play an important role in bone mineralisation.

In terms of cell signalling effects of peptides within SAOS-2 cells, effects on intracellular cAMP levels were assessed (Baggio & Drucker 2007). It was found that in presence of the GIP and GLP-1 peptides, cAMP generation was enhanced. Xenin had no impact on cAMP levels, but this has also been observed in pancreatic beta-cells (Taylor *et al*. 2010). In terms of the GIP/Xenin hybrid, enhanced cAMP production was also seen, likely related to activation of GIP receptors (Hasib *et al*. 2016). The results from cAMP assay further highlight the direct effect of GIP and GLP-1 on osteoblast cells.

In conclusion, the present work has confirmed that biologically active, C-terminally extended, versions of stable gut-derived

peptides were generated. These novel peptides exhibited good bioactivity both in pancreatic beta-cells and bone derived osteoblast cells. It is clear that L-Asp extensions were superior to L-Glu extensions in terms of retention of biological activity. Given that these novel peptides are likely to accumulate in hydroxylapatite within bone, they may have potential as therapeutic options for bone fractures. In addition, since GIP, GLP-1 and xenin already have established benefits in the treatment of diabetes (Irwin & Flatt 2015, Pais *et al*. 2016, Hasib *et al*. 2017) it would seem most logical to assess the impact of these novel peptides on bone fragility that is often reported in diabetes.

Table 1 Mass spectroscopy analysis of the peptides

Name	Amino acid sequence	Theoretical Mol. Wt (Da)	Expected Mol. Wt (Da)	Difference
(D-Ala^2)GIP	Y-(d-Ala)-EGTFISDYSIAMDKIHQQDFVNWLLAQK-HN2	3533.02	3534.02	1.26
(D-Ala^2)GIP-Asp	Y-(d-Ala)EGTFISDYSIAMDKIHQQDFVNWLLAQKGAADDDDDD-NH2	4421.77	4423.48	1.71
(D-Ala^2)GIP-Glu	Y-(d-Ala)-EGTFISDYSIAMDKIHQQDFVNWLLAQKGAAEEEEEEE-NH2	4506.93	4507.16	1.23
(D-Ala^2)GLP-1	H-(d-Ala)-EGTFTSDVSSYLEGQAAKEFIAWLVKGRG-NH2	3355.76	3353.77	0.99
(D-Ala^2)GLP-1-Asp	H-(d-Ala)-EGTFTSDVSSYLEGQAAKEFIAWLVKGRGGAADDDDDD-NH2	4245.50	4244.49	0.21
(D-Ala^2)GLP-1-Glu	H-(d-Ala)-EGTFTSDVSSYLEGQAAKEFIAWLVKGRGGAAEEEEEEE-NH2	4329.67	4326.20	3.47
Xenin-25[Lys^{13}PAL]	MLTKFETKSARVK(gamma glutamyl PAL)GLSFHPKRPWIL-OH	3336.13	3333.17	2.96
Xenin-25[Lys^{13}PAL]-Asp	MLTKFETKSARVK(gammaglutamylPAL)GLSFHPKRPWILGAADDDDDD-NH2	4219.54	4216.29	3.25
GIP/Xenin	H-Y-(d-Ala)-EGTFISDYS-IAMHPQQPWIL-OH	2562.59	2558.02	4.47
GIP/Xenin-Asp	H-Y-(d-Ala)-GTFISDTSIAMHPQQPQILGAADDDDDD-NH2	3454.69	3451.26	3.43
GIP/Xenin-Glu	H-Y-(d-Ala)-EGTFISDTSIAMH PQQPWILGAAGLUEEEEE-NH2	3531.65	3528.49	3.16

Details of the peptides along with mass spectroscopy analysis

Figure 3.1 (A) RP-HPLC of (D-Ala^2)GIP and (B) Mass Spec of (DAla^2)GIP

A

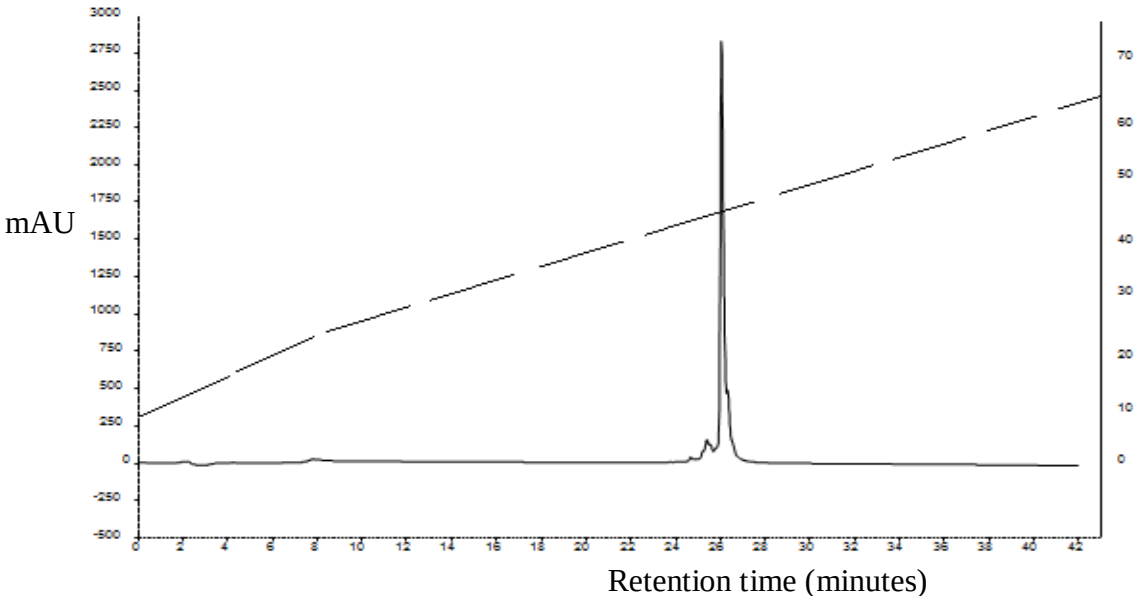

B

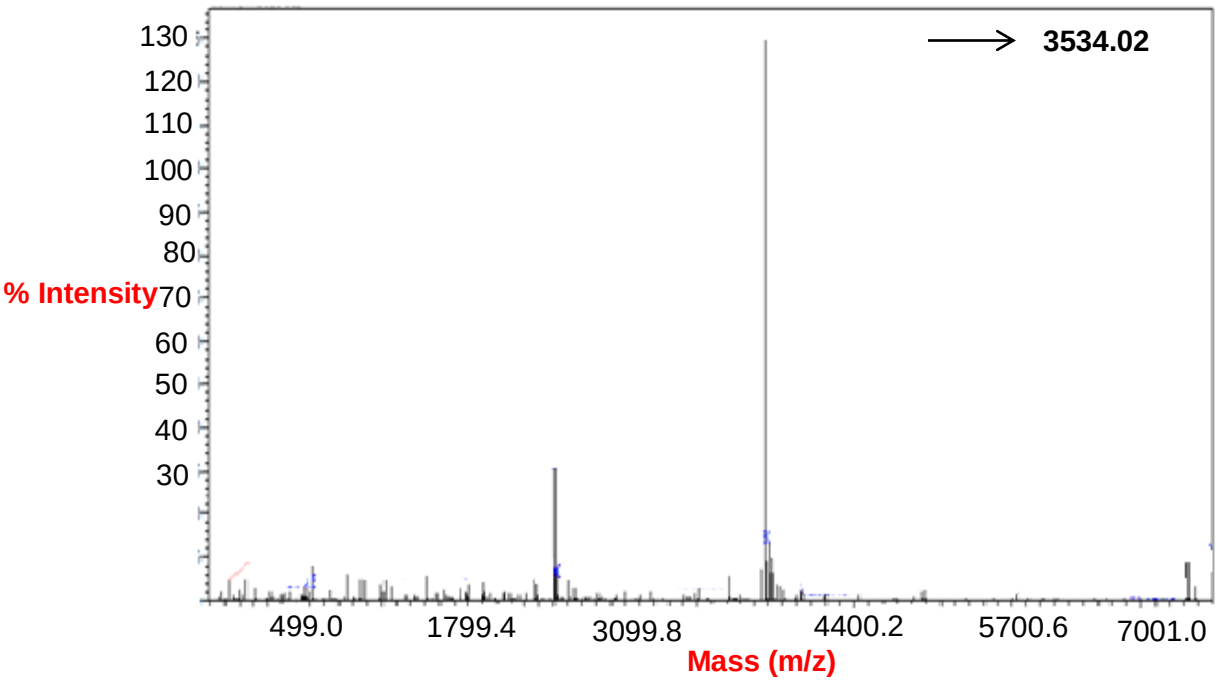

RP-HPLC trace and Mass Spec trace of (D-Ala^2)GIP

Figure 3.2 (A) RP-HPLC of (D-Ala^2)GIP-Asp and (B) Mass Spec of (D-Ala^2)GIP-Asp

A

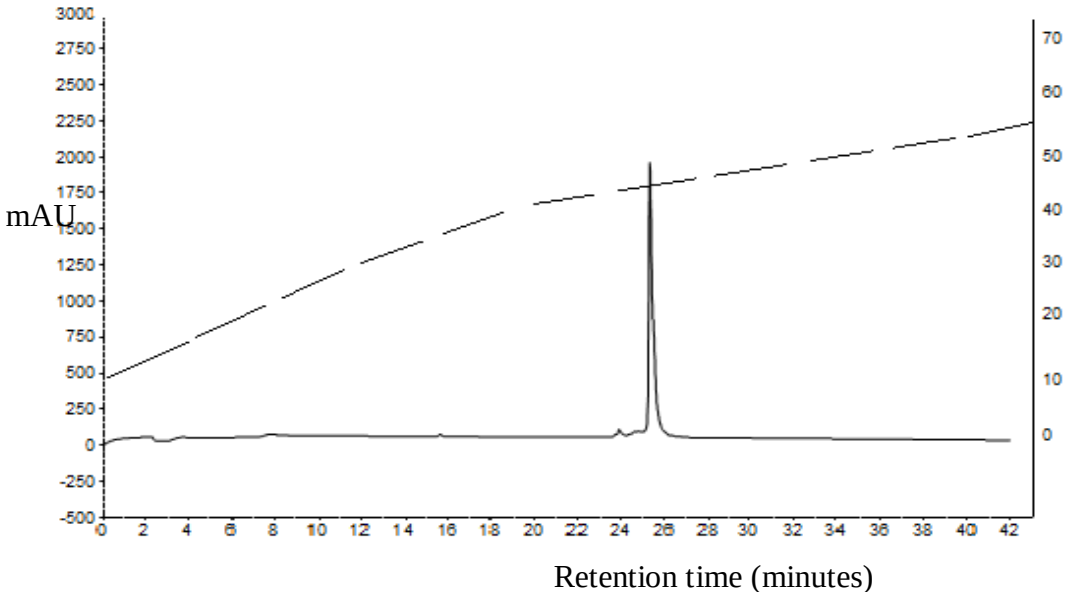

B

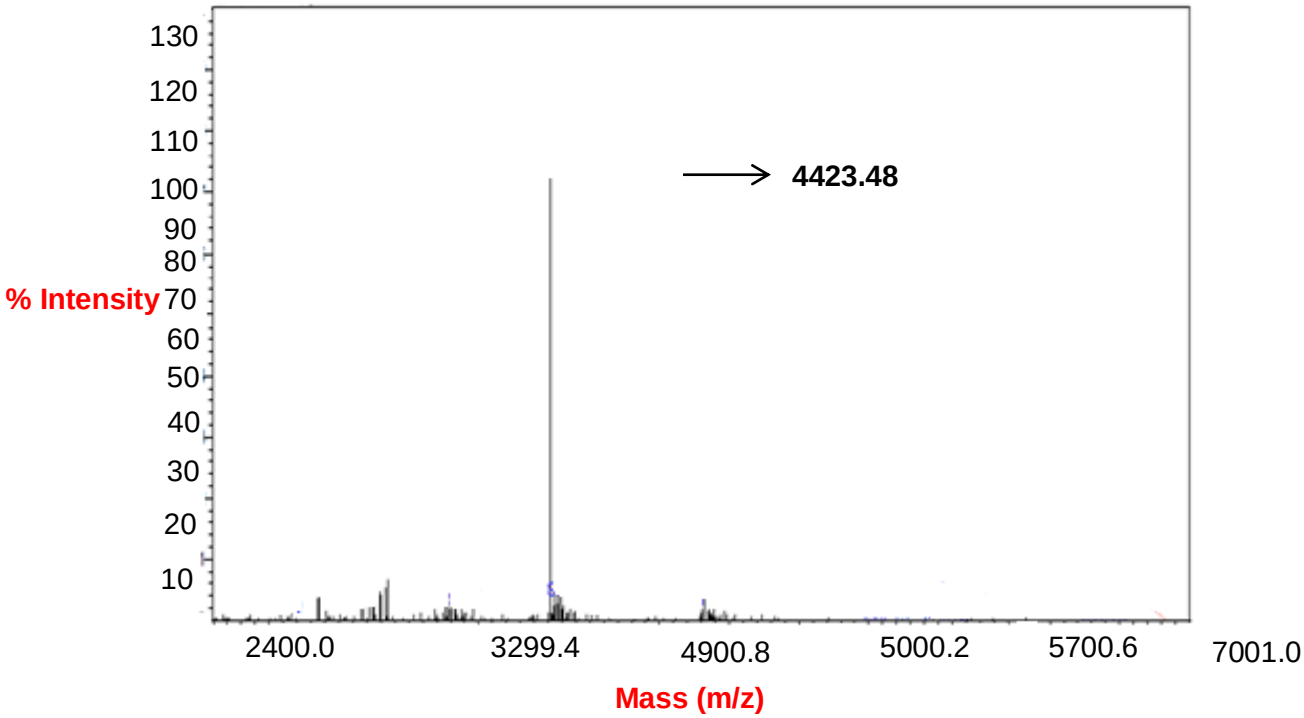

RP-HPLC and Mass Spec trace of (D-Ala^2)GIP-Asp

Figure 3.3 (A) RP-HPLC of (D-Ala^2)GIP-Glu and (B) Mass Spec of (DAla^2)GIP-Glu

A

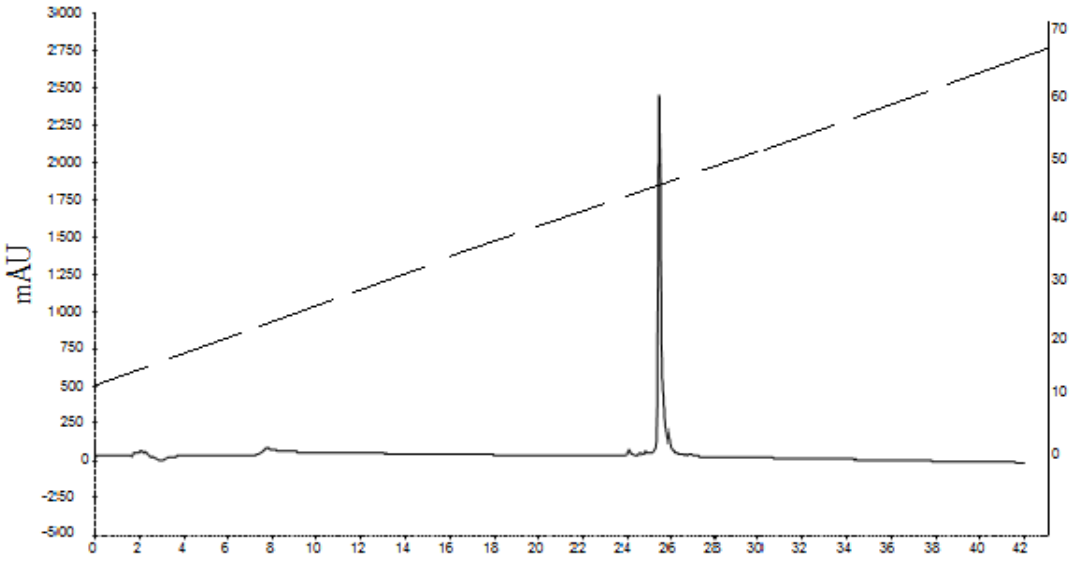

B

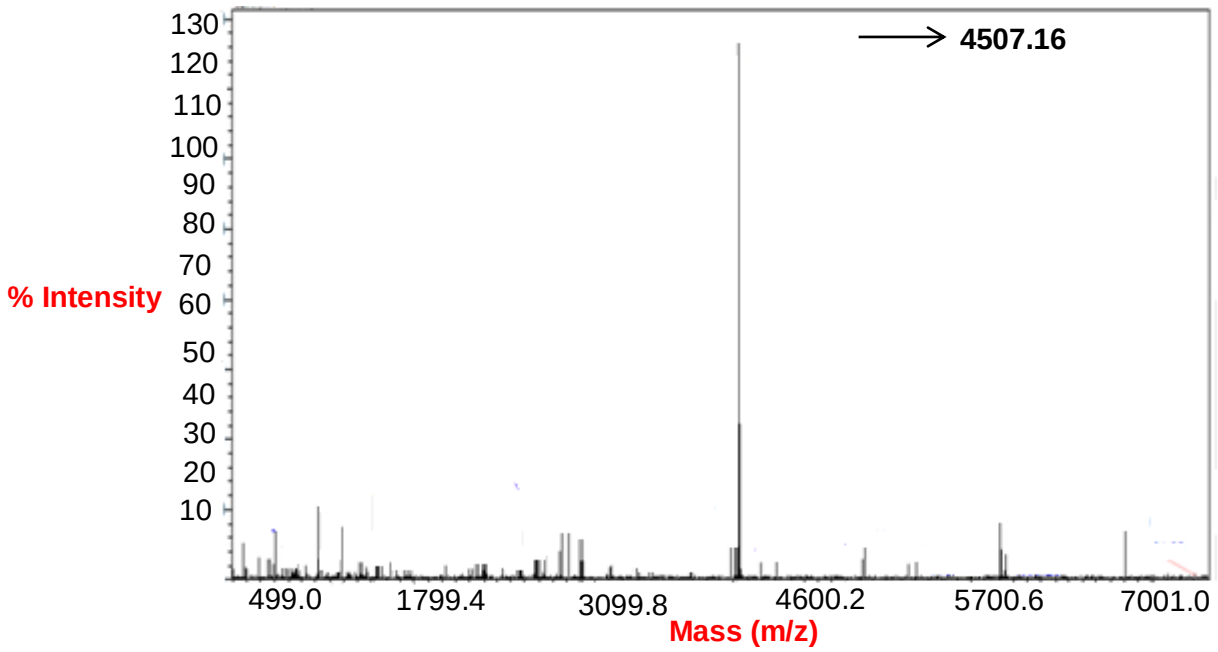

RP-HPLC and Mass Spec trace of (D-Ala^2)GIP-Glu

Figure 3.4 (A) RP-HPLC of (D-Ala^2)GLP-1 and (B) Mass Spec of (DAla^2)GLP-1

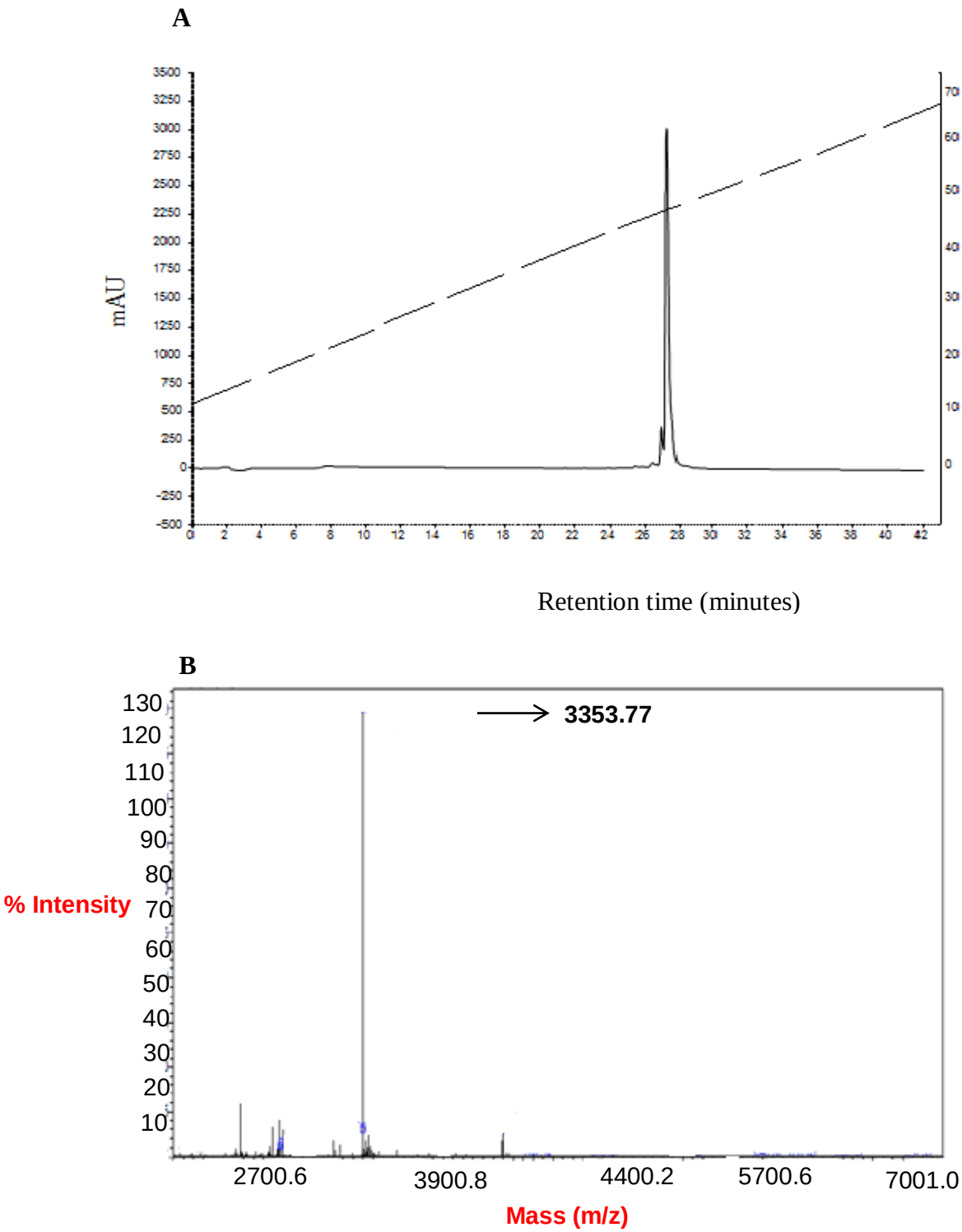

RP-HPLC and Mass Spec trace of (D-Ala^2)GLP-1

Figure 3.5 (A) RP-HPLC of (D-Ala^2)GLP-1-Asp and (B) Mass Spec of (DAla^2)GLP-1-Asp

A

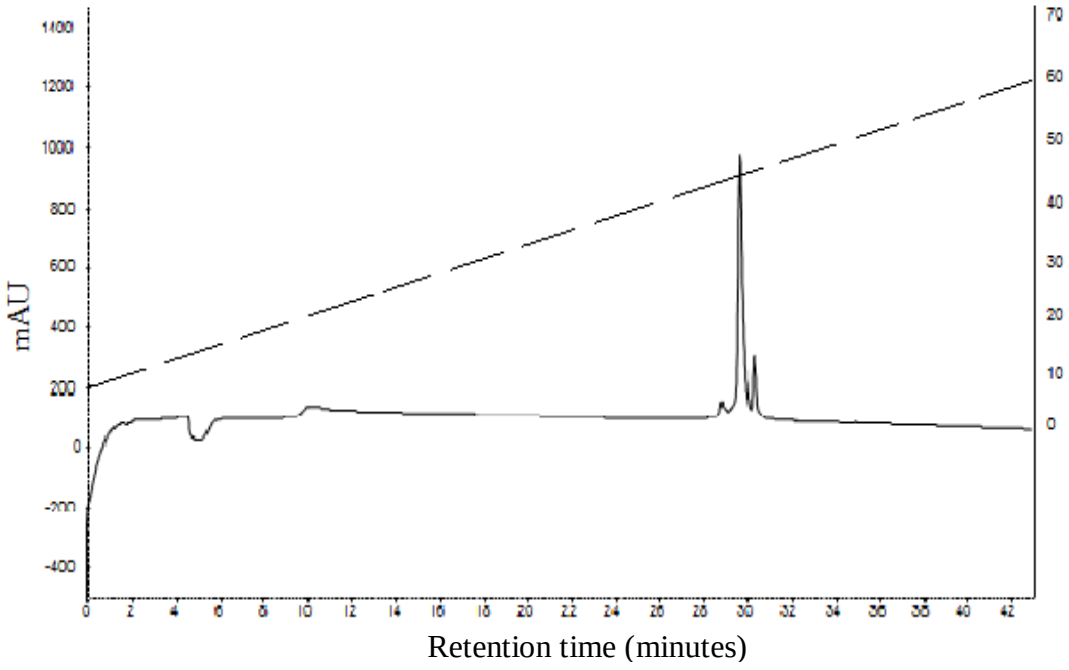

B

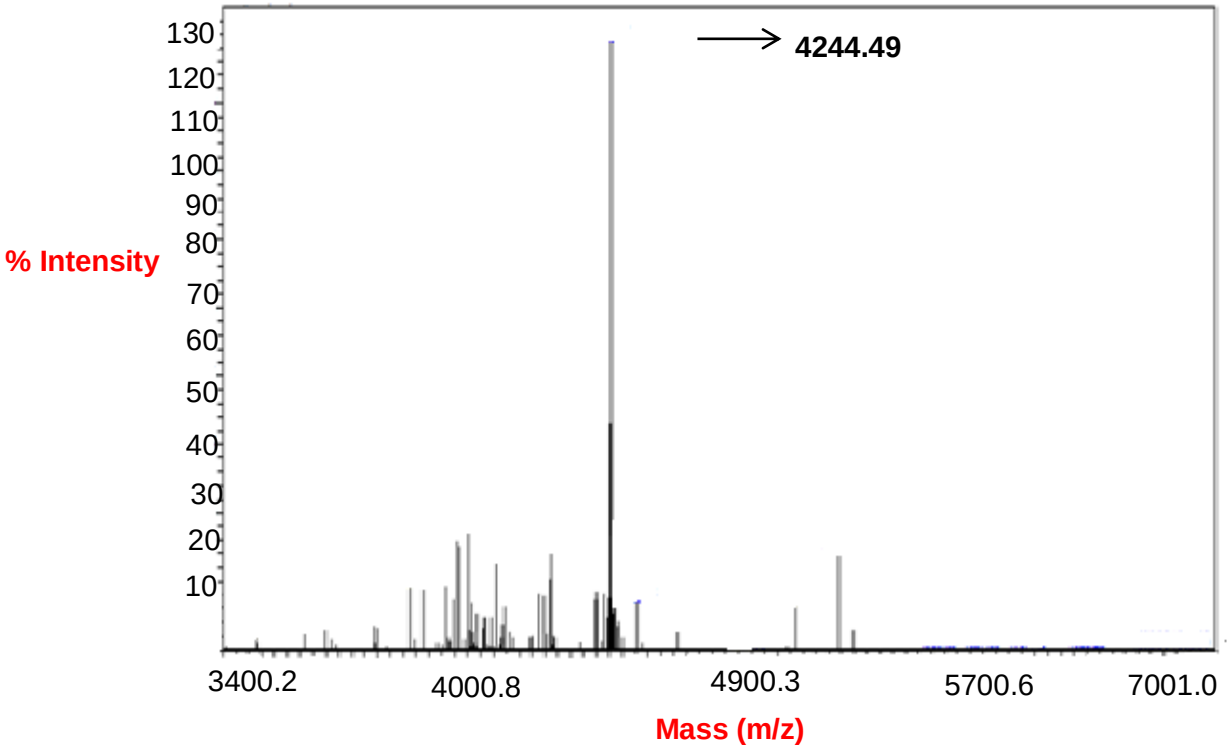

RP-HPLC and Mass Spec trace of (D-Ala^2)GLP-1-Asp

Figure 3.6 (A) RP-HPLC of (D-Ala^2)GLP-1-Glu and (B) Mass Spec of (DAla^2)GLP-1-Glu

A

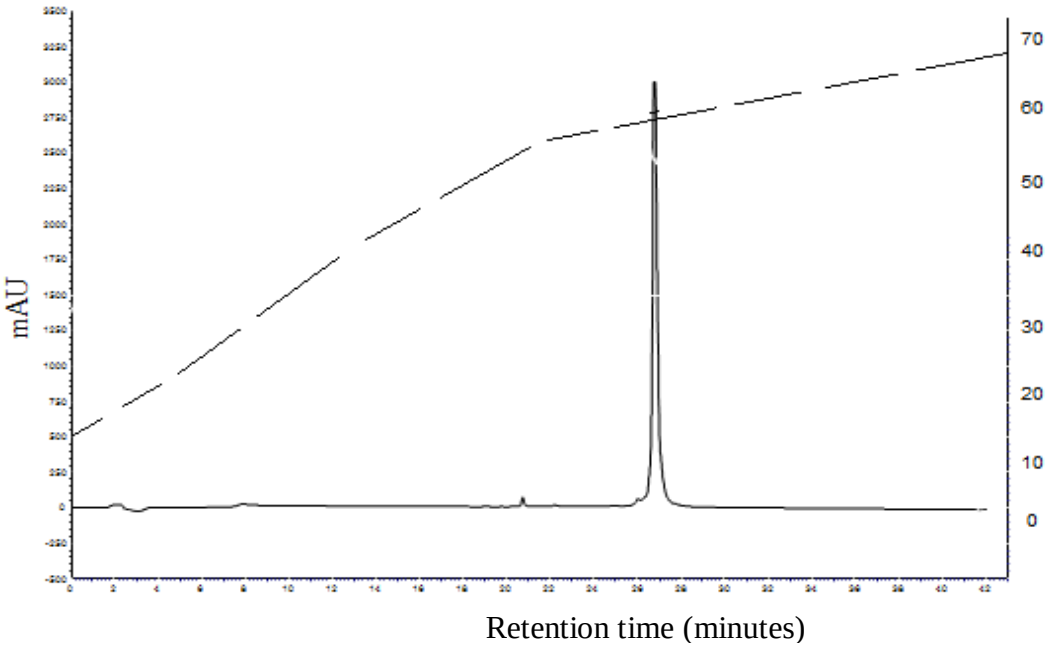

B

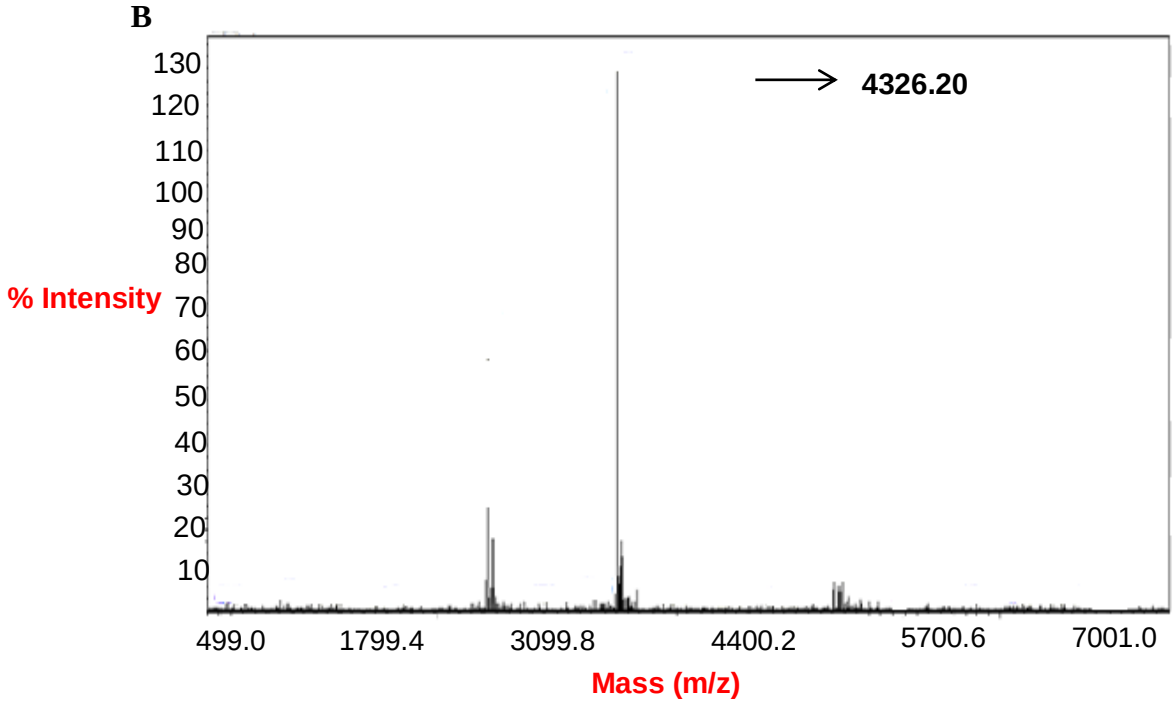

RP-HPLC and Mass Spec trace of (D-Ala^2)GLP-1Glu

Figure 3.7 (A) RP-HPLC of Xenin-25[Lys^{13}PAL] and (B) Mass Spec of Xenin 25[Lys^{13}PAL]

A

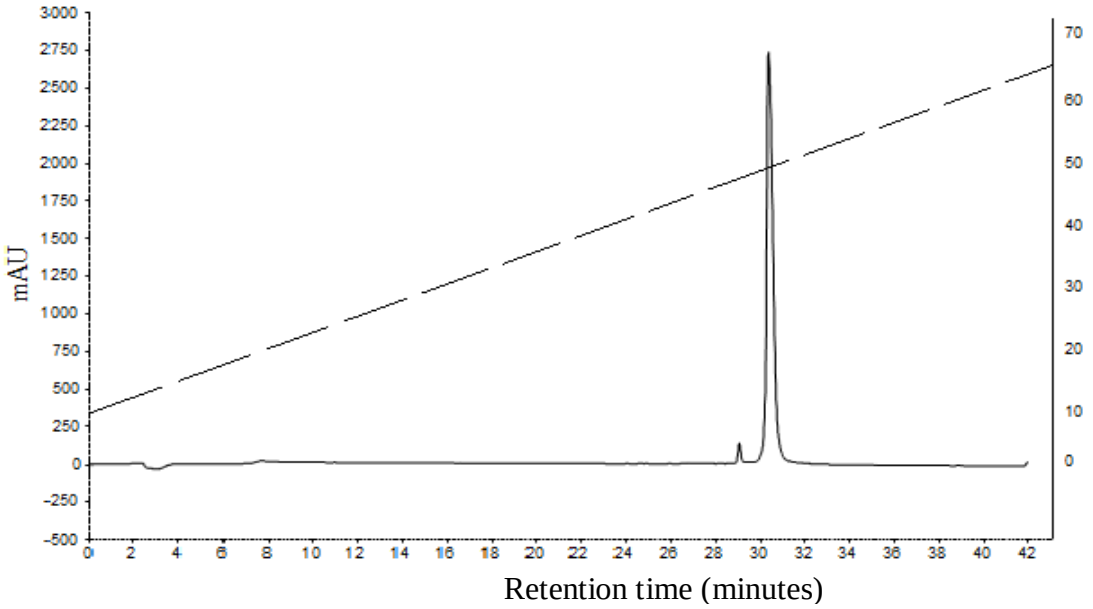

B

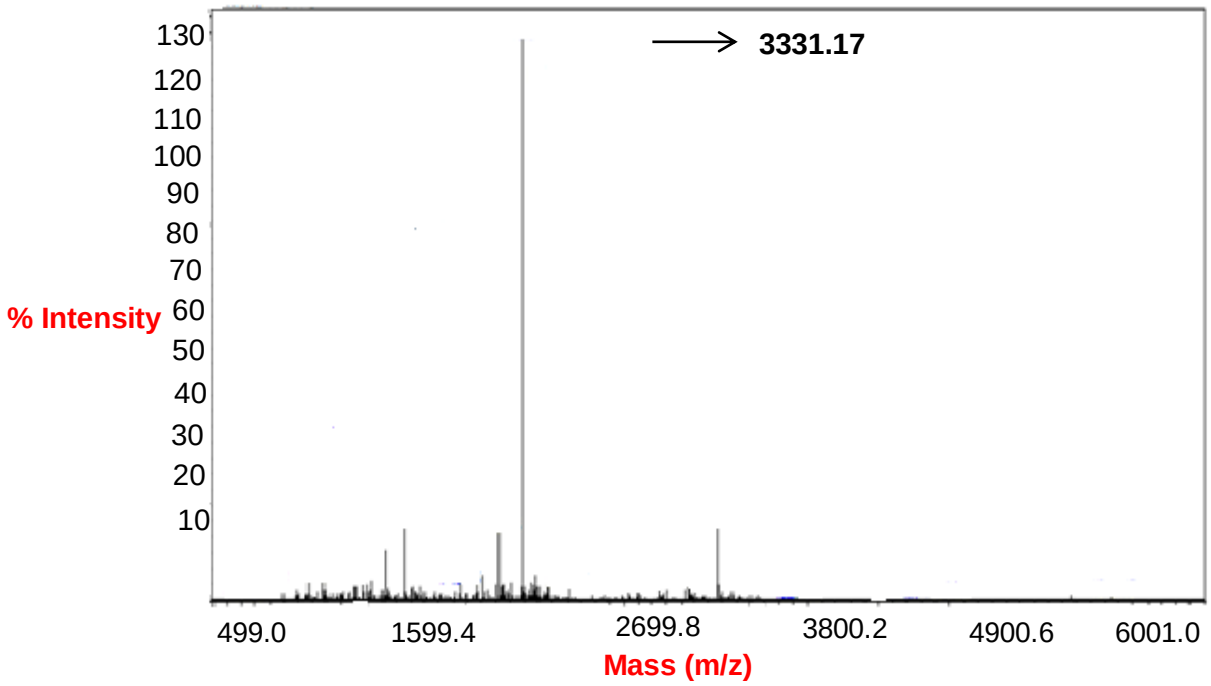

RP-HPLC and Mass Spec trace of Xenin-25[Lys^{13}PAL]

Figure 3.8 (A) RP-HPLC of Xenin-25[Lys^{13}PAL]-Asp and (B) Mass Spec of Xenin-25[Lys^{13}PAL]-Asp

A

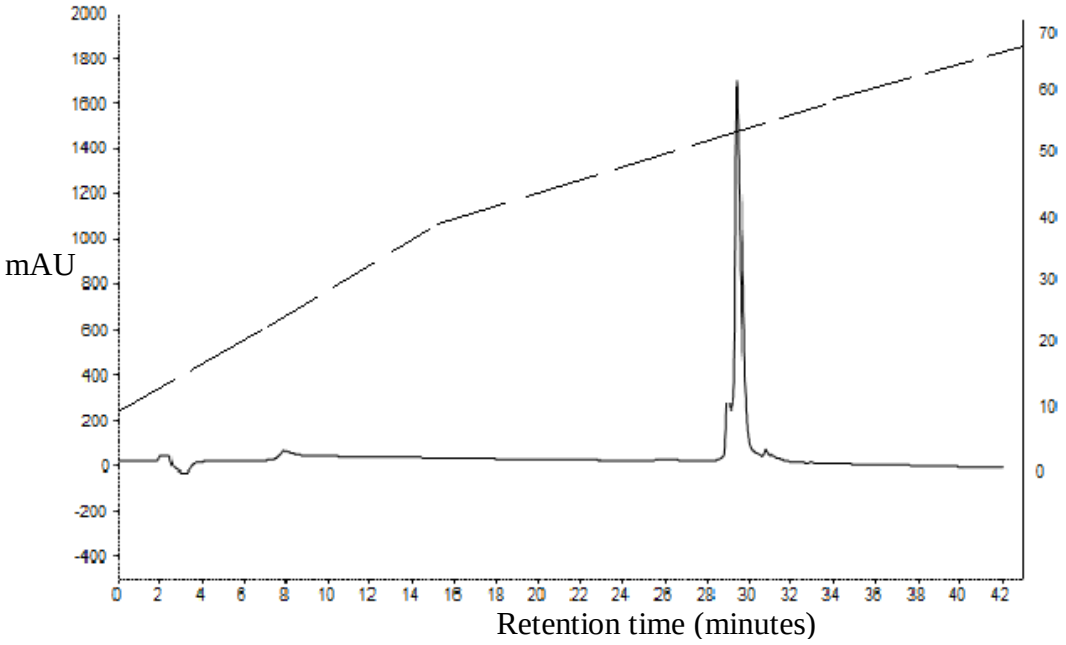

B

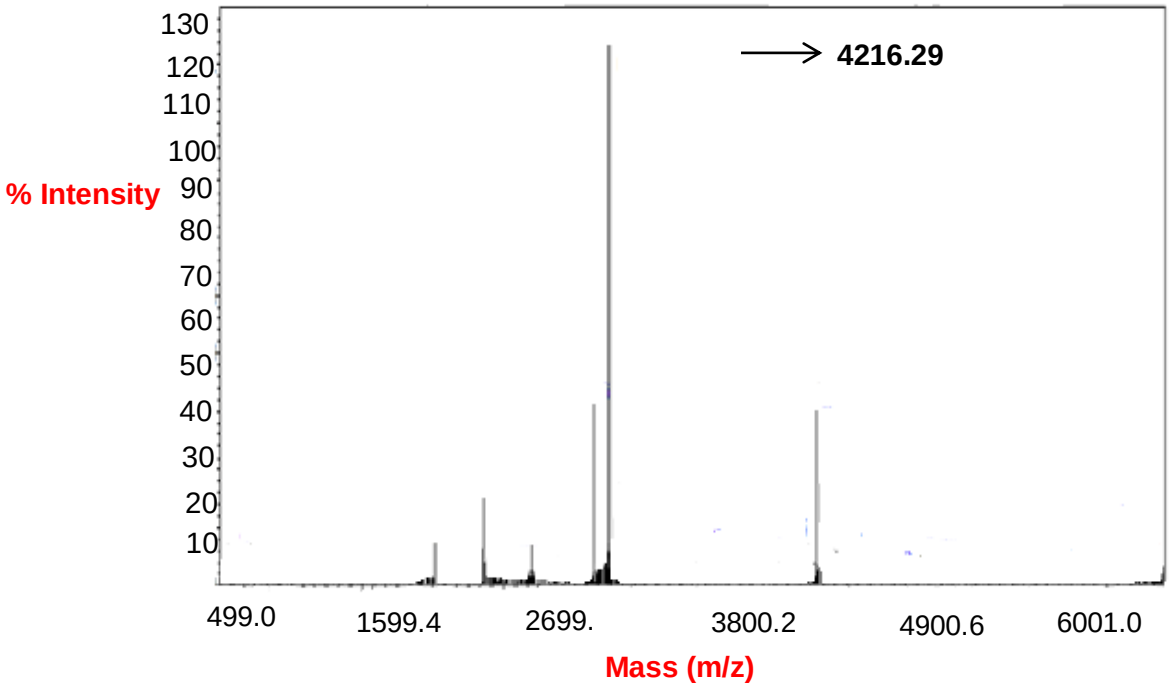

RP-HPLC and Mass Spec trace of Xenin-25[Lys^{13}PAL]-Asp

Figure 3.9 (A) RP-HPLC of GIP/Xenin and (B) Mass Spec of GIP/Xenin

A

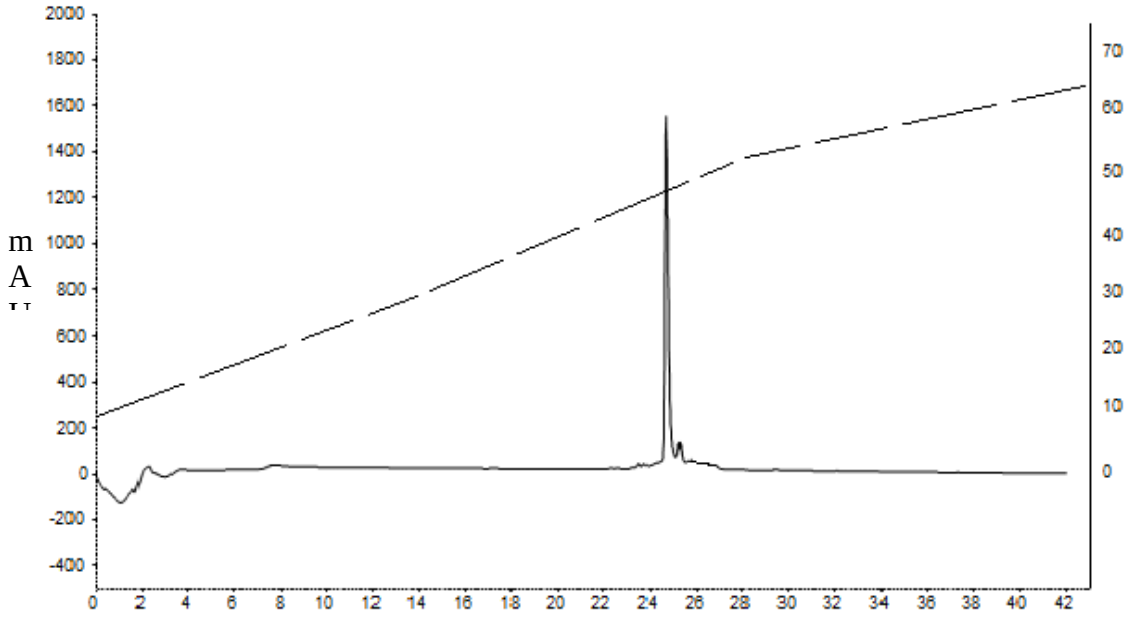

B

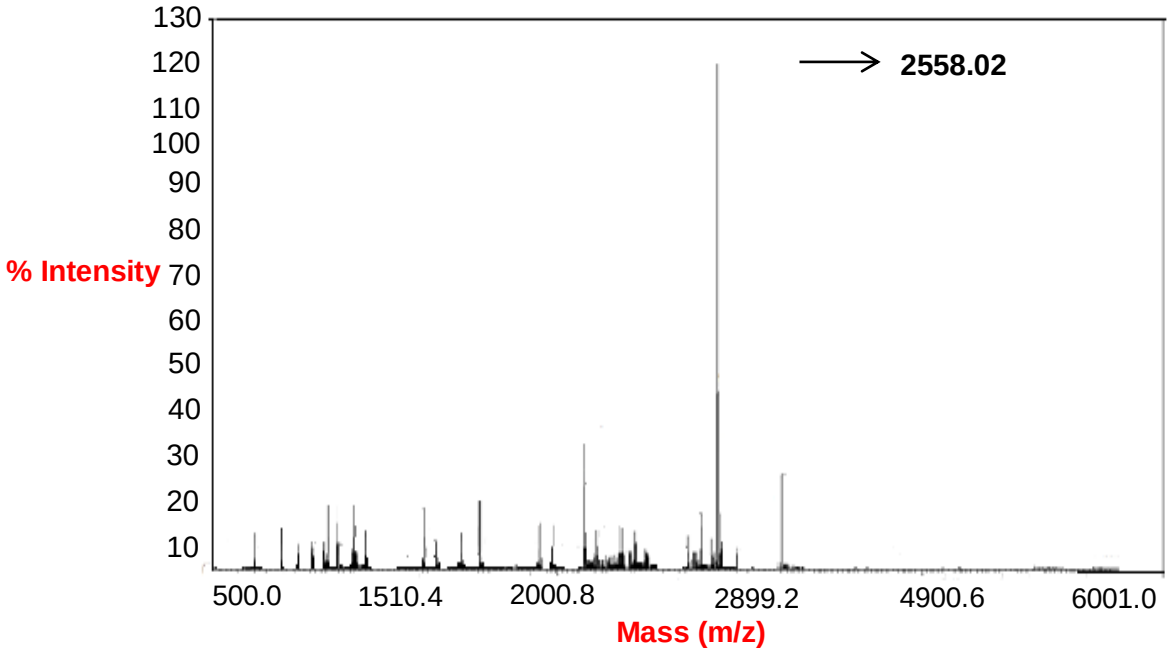

RP-HPLC and Mass Spec trace of GIP/Xenin

Figure 3.10 (A) RP-HPLC of GIP/Xenin-Asp and (B) Mass Spec of GIP/Xenin-Asp

A

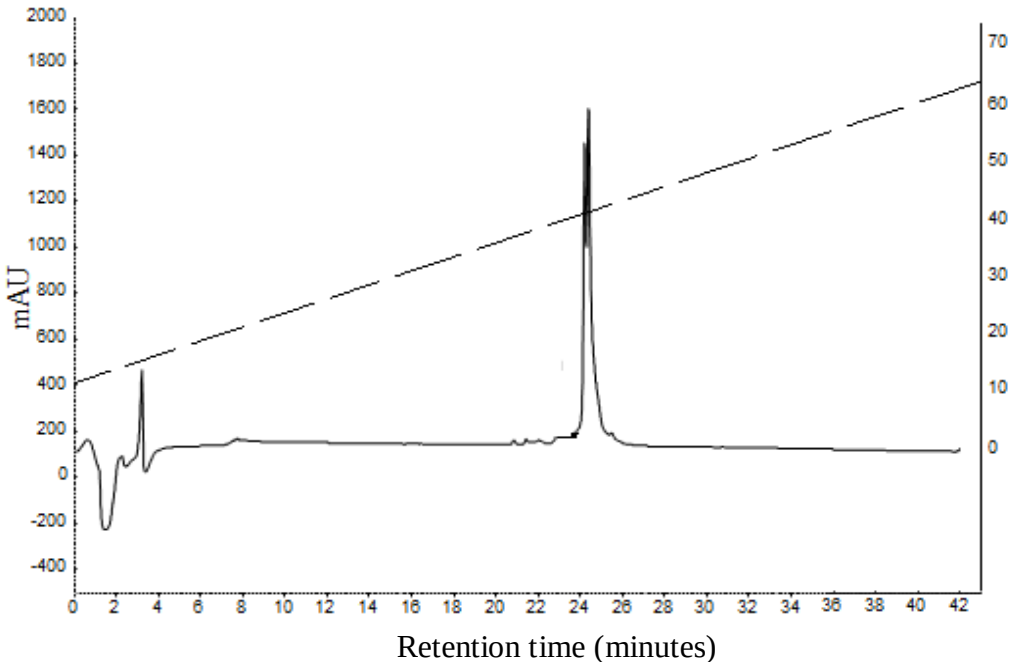

B

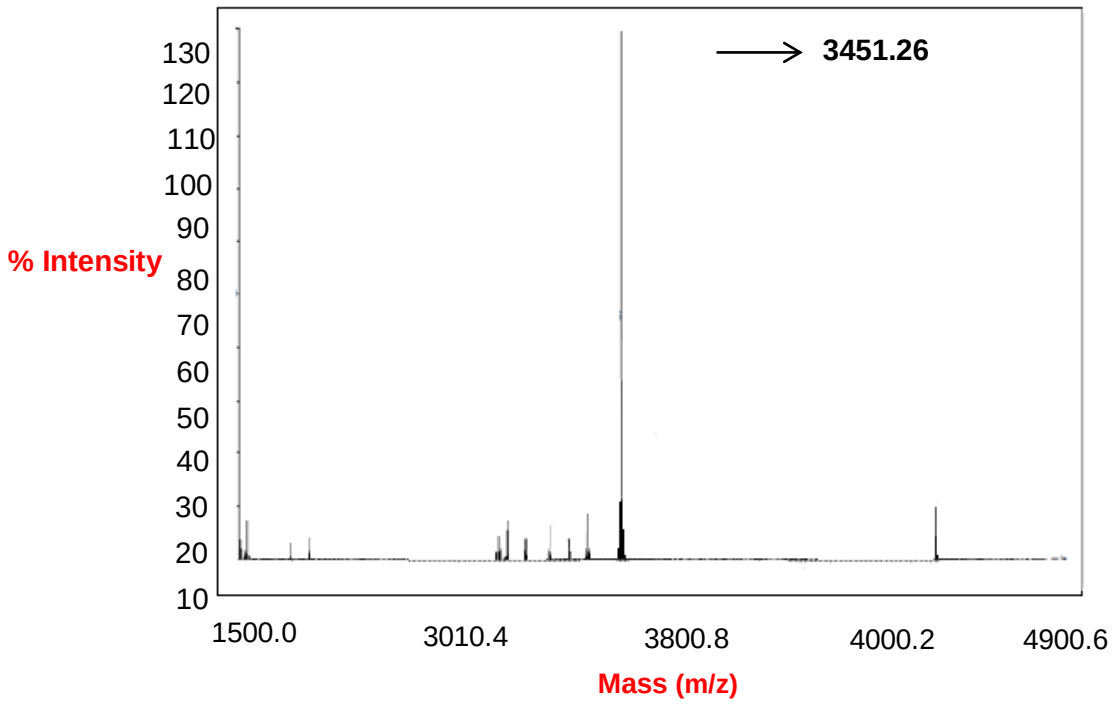

RP-HPLC and Mass Spec trace of GIP/Xenin-Asp

Figure 3.11 (A) RP-HPLC of GIP/Xenin-Glu and (B) Mass Spec of GIP/Xenin-Glu

A

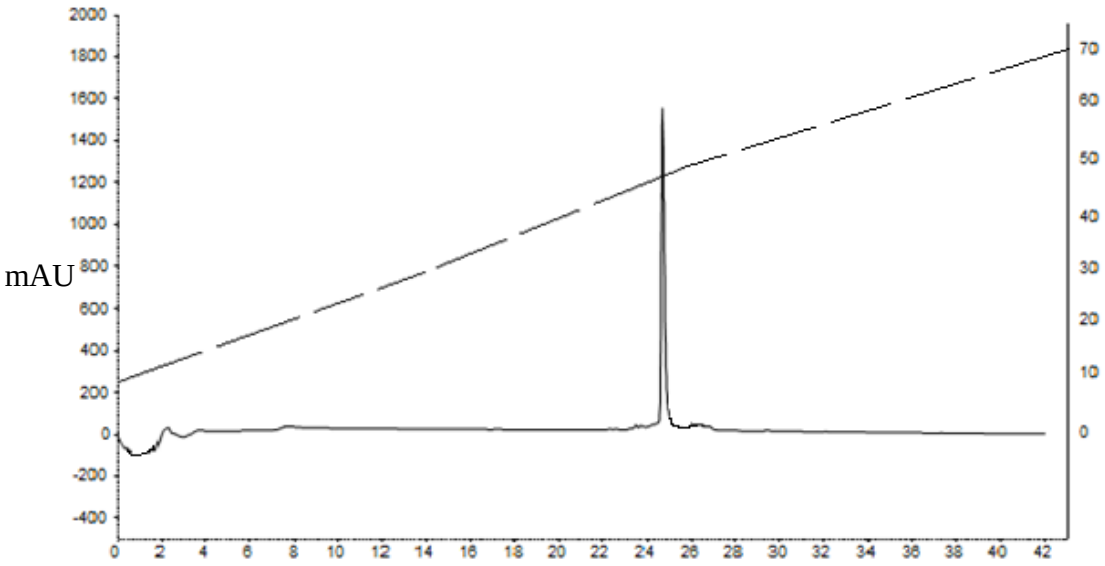

B

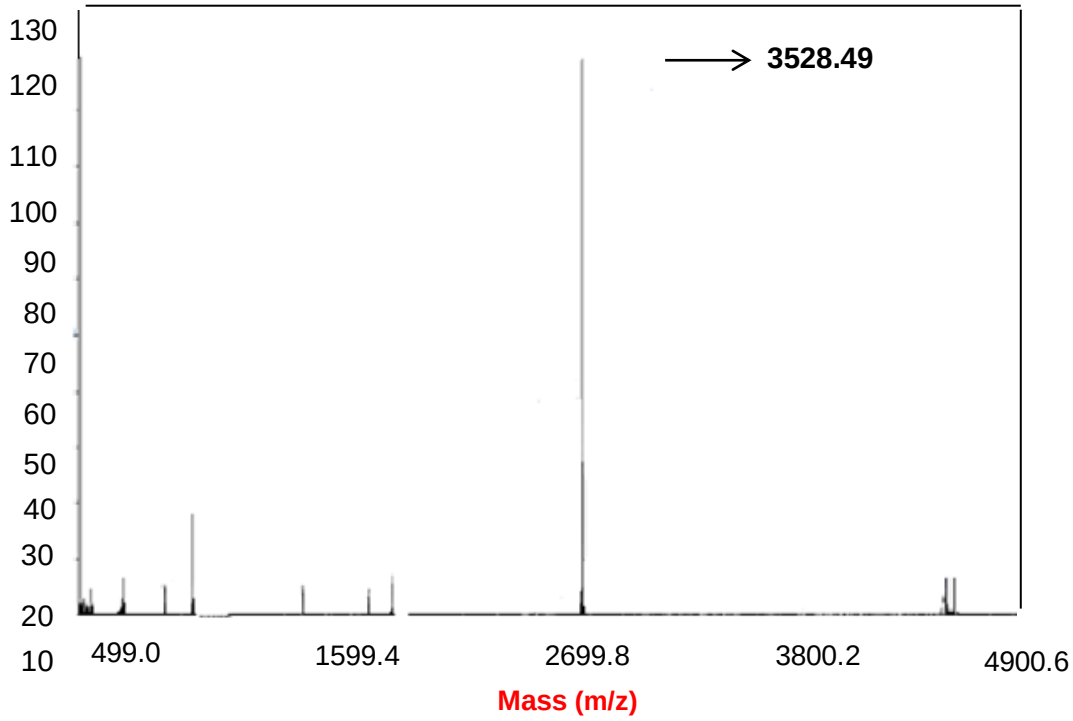

RP-HPLC and Mass Spec trace of GIP/Xenin-Glu

Figure 3.12 Dose dependent effects of (D-Ala^2)GIP,(D-Ala^2)GIP-Asp and (D-Ala^2)GIP-Glu on insulin secretion from BRINBD-11 cells.

A

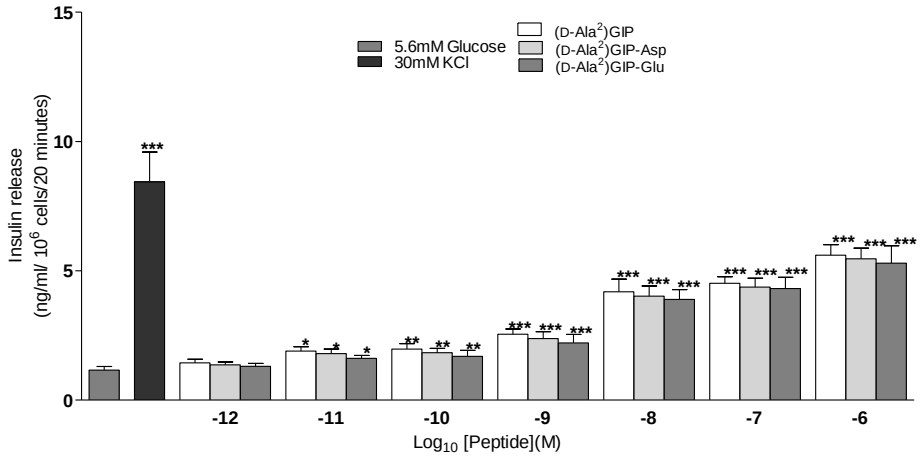

B

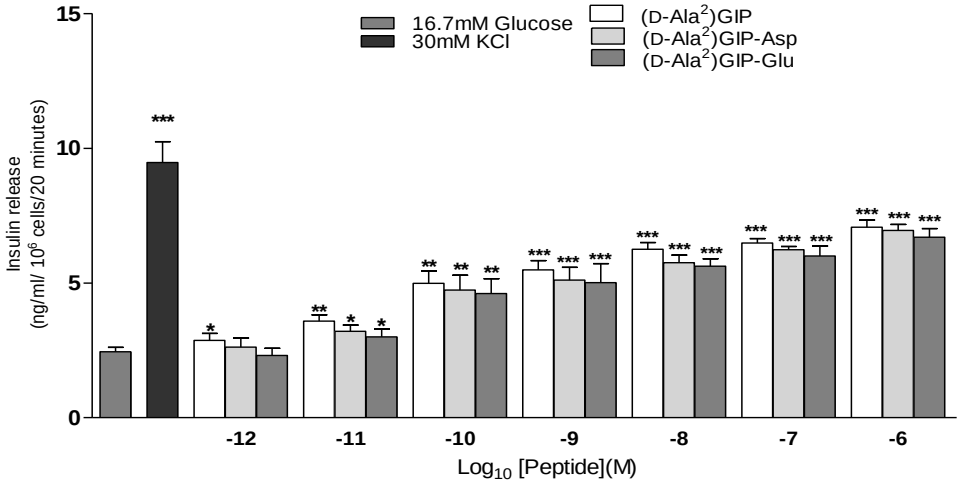

Insulinotropic responses of (D-Ala^2)GIP,(D-Ala^2)GIP-Asp and (D-Ala^2)GIP-Glu at A) 5.6mM, B) 16.7mM glucose from BRIN BD11 cells. Values are mean ± SEM with n=8 for insulin release. *p<0.05, **p<0.01, ***p<0.001 compared with respective control.

Figure 3.13 Dose dependent effects of (D-Ala^2)GLP-1,(D-Ala^2)GLP-1-Asp and (D-Ala^2)GLP-1-Glu on insulin secretion from BRINBD-11 cells.

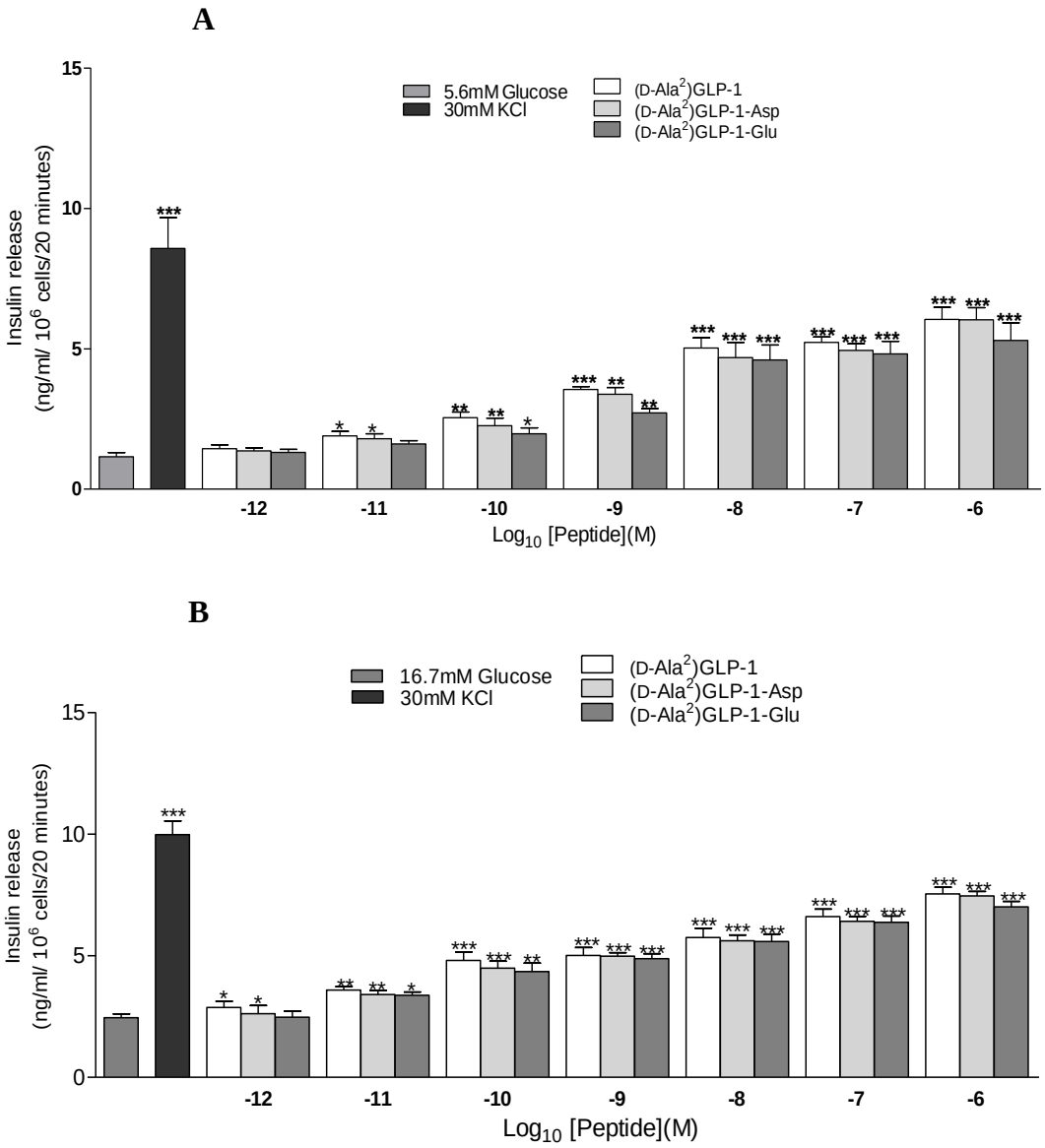

Insulinotropic responses of (D-Ala^2)GLP-1,(D-Ala^2)GLP-1-Asp and (D-Ala^2)GLP-1-Glu at A) 5.6mM, B) 16.7mM glucose from BRIN BD11 cells. Values are mean ± SEM with n=8 for insulin release. *<0.05, **p<0.01, ***p<0.001 compared with respective control.

Figure 3.14 Dose dependents effect of Xenin-25[Lys^{13}PAL] and Xenin-25[Lys^{13}PAL]-Asp on insulin secretion from BRINBD-11 cells.

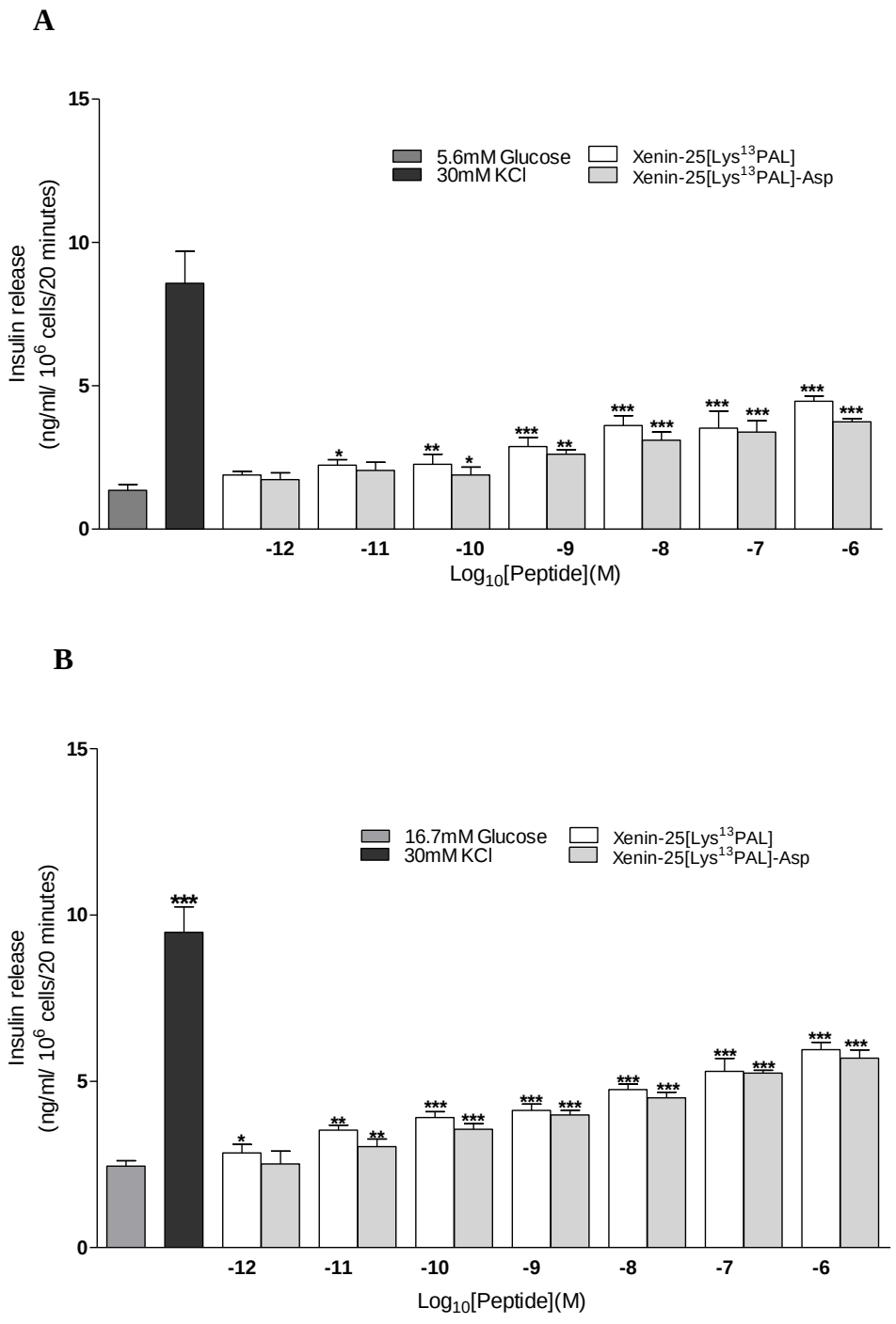

Insulinotropic responses of Xenin-25[Lys^{13}PAL] and Xenin-25[Lys^{13}PAL]-Asp at at A) 5.6mM glucose and B) 16.7mM glucose from BRIN BD11 cells. Values are mean ± SEM with n=8 for insulin release. *p<0.05, **p<0.01, ***p<0.001 compared with respective control.

Figure 3.15 Dose dependent effects of GIP/Xenin, GIP/Xenin-Asp and GIP/Xenin-Glu on insulin secretion from BRIN BD11 cells.

A

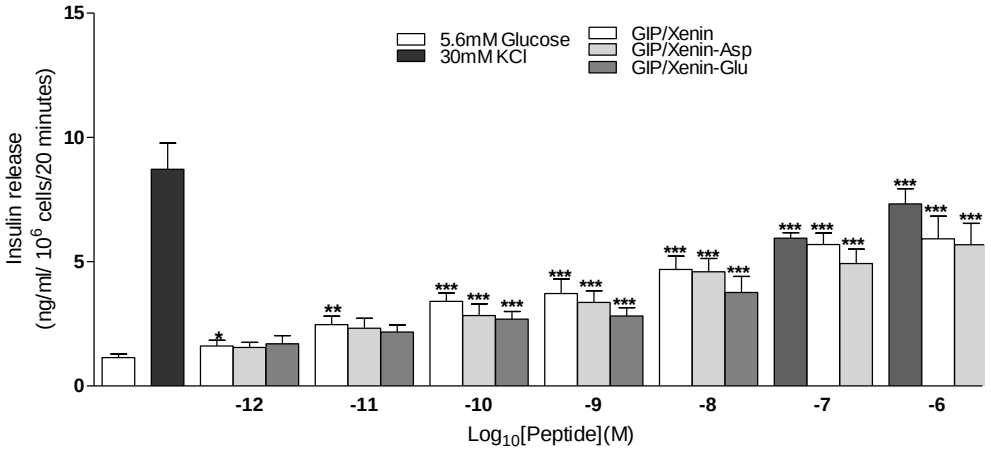

B

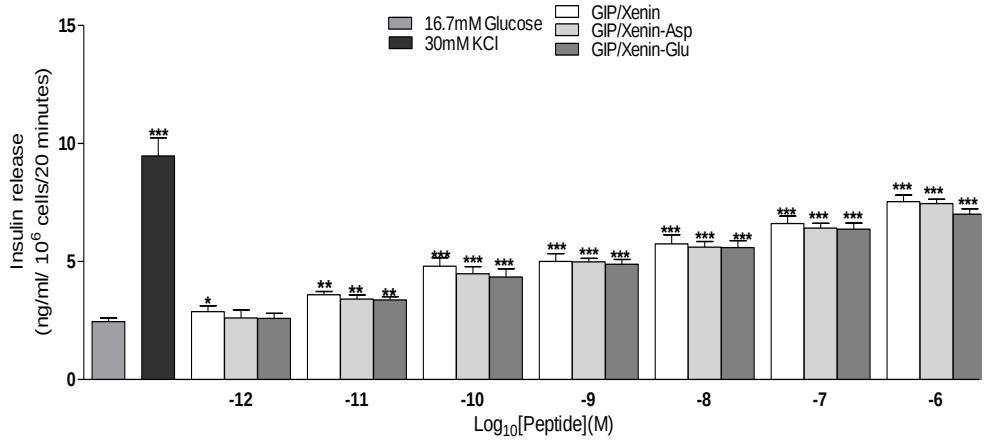

Insulinotropic responses of GIP/Xenin, GIP/Xenin-Asp and GIP/Xenin-Glu at A) 5.6mM, B) 16.7mM glucose from BRIN BD11 cells. Values are mean ± SEM with n=8 for insulin release. *p<0.05, **p<0.01, ***<0.001 compared with respective control.

Figure 3.16 Dose dependent effects of (D-Ala^2)GIP, (D-Ala^2)GIP-Asp and (D-Ala^2)GIP-Glu on alkaline phosphatase activity after (A) 24 hrs and (B) 48 hrs in human osteoblast SAOS-2 cells.

A

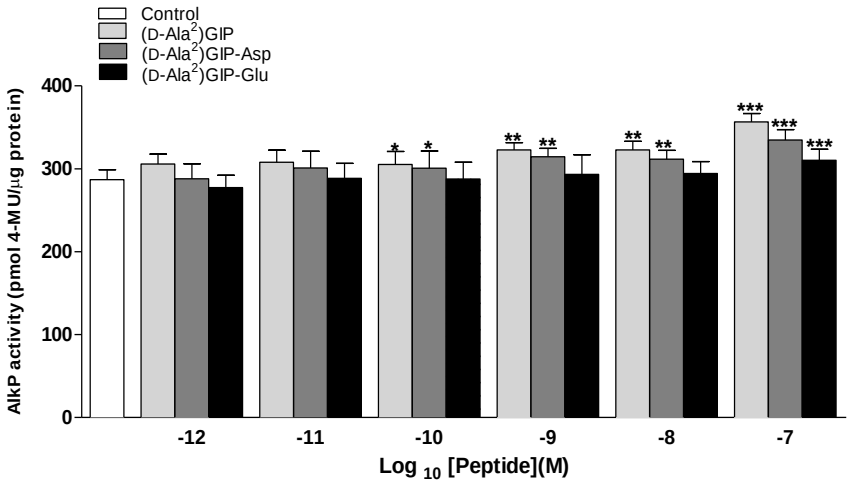

B

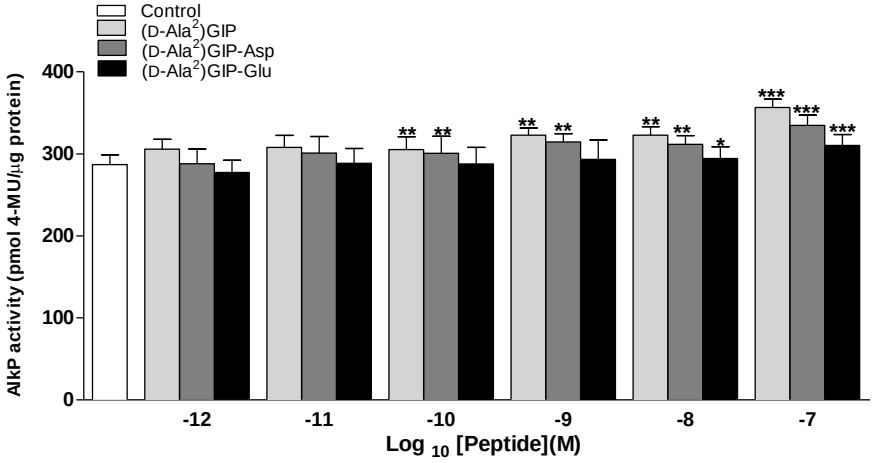

SAOS-2 cells were grown in 6-well plates and stimulated with indicated concentrations of peptides. After (A) 24 h and (B) 48 h, the reaction was stopped and AlkP production was indirectly measured using 4-methyl umbelliferyl phosphate as substrate. The values were normalised against total amount of protein/well using BCA protein kit. Values are mean ± SEM of n=6. *p<0.05, **<0.01, ***p<0.001 vs control.

Figure 3.17 Dose dependent effects of (D-Ala^2)GIP, (D-Ala^2)GIP-Asp and (D-Ala^2)GIP-Glu on alkaline phosphatase activity after 72 hrs in human osteoblast SAOS-2 cells.

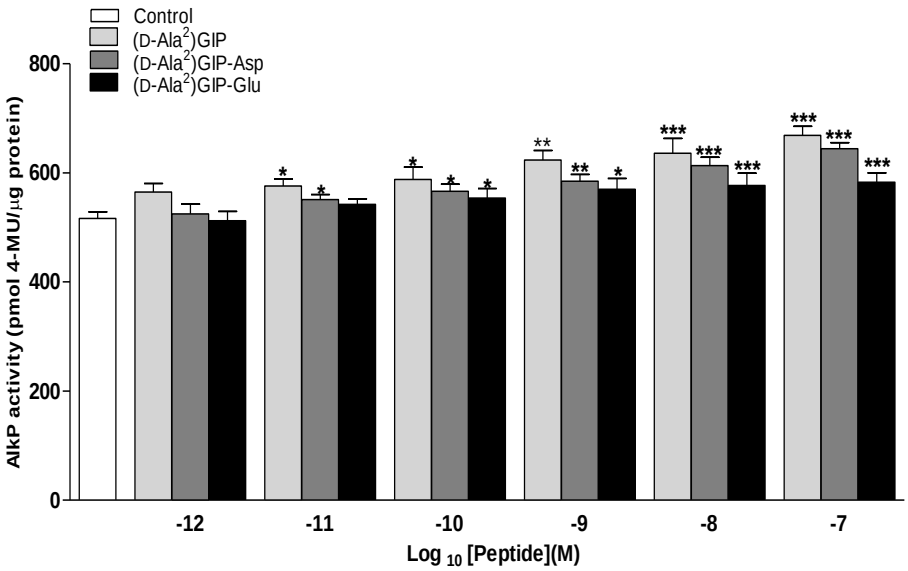

SAOS-2 cells were grown in 6-well plates and stimulated with indicated concentrations of peptides. After 72 h, the reaction was stopped and AlkP production was indirectly measured using 4-methyl umbelliferyl phosphate as substrate. The values were normalised against total amount of protein/well using BCA protein kit. Values are mean ± SEM of n=6. *p<0.05, **p<0.01, ***p<0.001 vs control.

Figure 3.18 Dose dependent effects of (D-Ala^2)GLP-1, (D-Ala^2)GLP-1-Asp and (D-Ala^2)GLP-1-Glu on alkaline phosphatase activity after (A) 24 hrs and (B) 48 hrs in human osteoblast SAOS-2 cells.

A

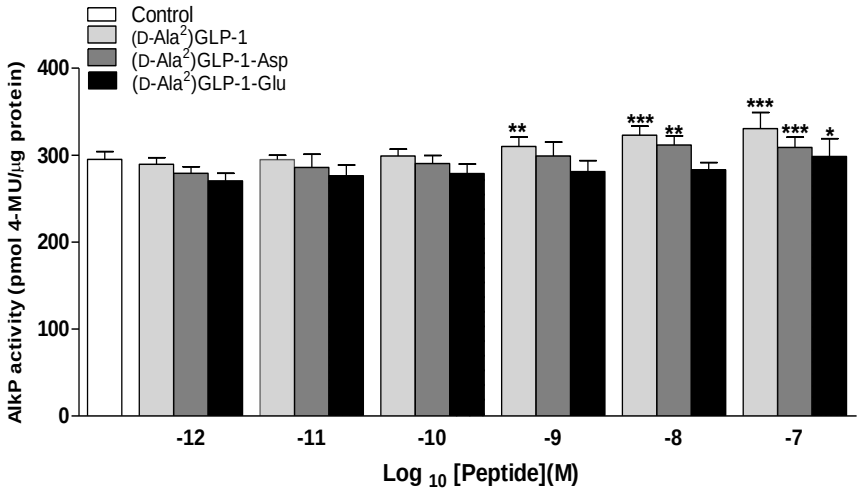

B

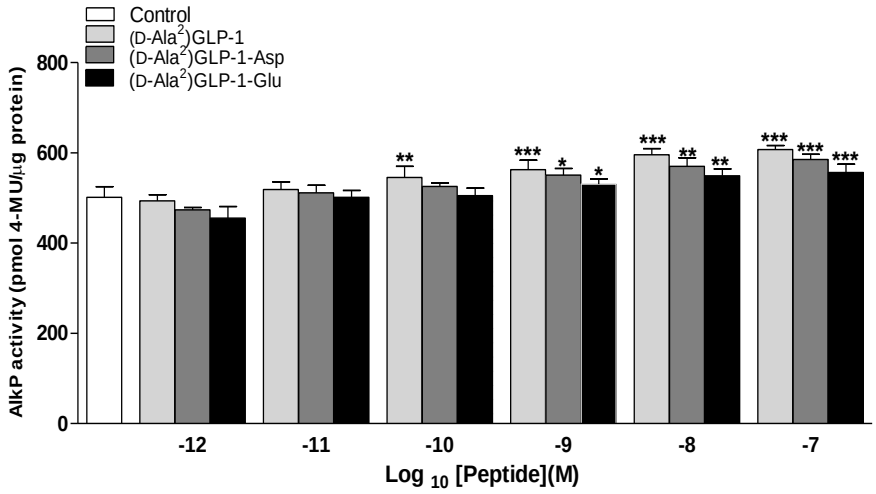

SAOS-2 cells were grown in 6-well plates and stimulated with indicated concentrations of peptides. After (A) 24 h and (B) 48 h the reaction was stopped and AlkP production was indirectly measured using 4-methyl umbelliferyl phosphate as substrate. The values were normalised against total amount of protein/well using BCA protein kit. Values are mean ± SEM of n=6. *p<0.05, **p<0.01, ***p<0.001 vs control.

Figure 3.19 Dose dependent effects of (D-Ala^2)GLP-1,(D-Ala^2)GLP-1-Asp and (D-Ala^2)GLP-1-Glu on alkaline phosphatase activity after 72 hrs in human osteoblast SAOS-2 cells.

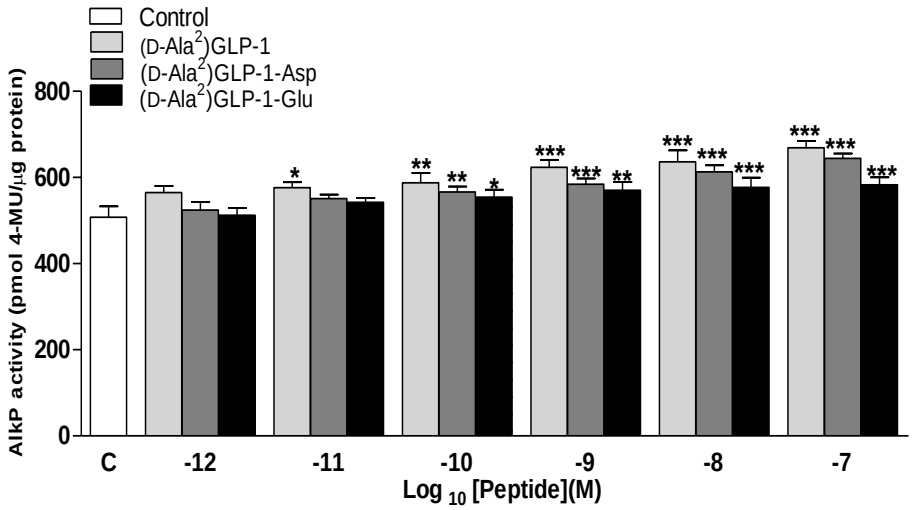

SAOS-2 cells were grown in 6-well plates and stimulated with indicated concentrations of peptides. After 72 h, the reaction was stopped and AlkP production was indirectly measured using 4-methyl umbelliferyl phosphate as substrate. The values were normalised against total amount of protein/well using BCA protein kit. Values are mean ± SEM of n=6. *p<0.05, **p<0.01, ***p<0.001 vs control.

Figure 3.20 Dose dependent effects of Xenin-25[Lys^{13}PAL] and Xenin25[Lys^{13}PAL]-Asp on alkaline phosphatase activity after (A) 24 hrs and (B) 48 hrs in human osteoblast SAOS-2 cells.

A

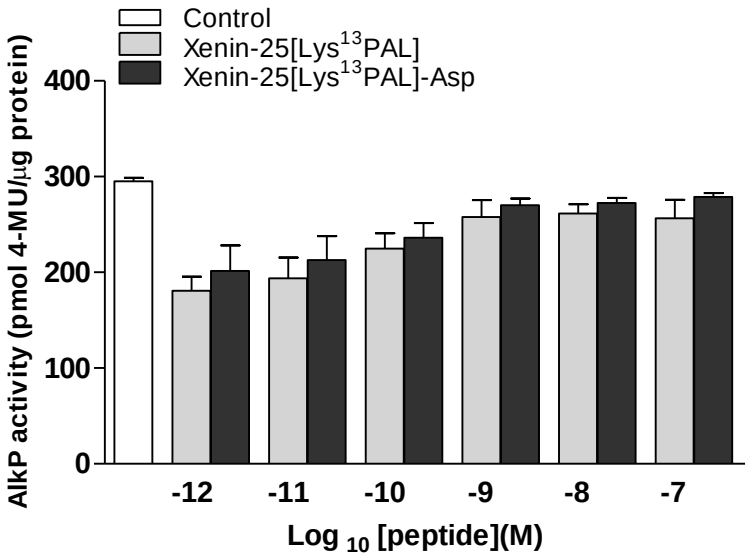

B

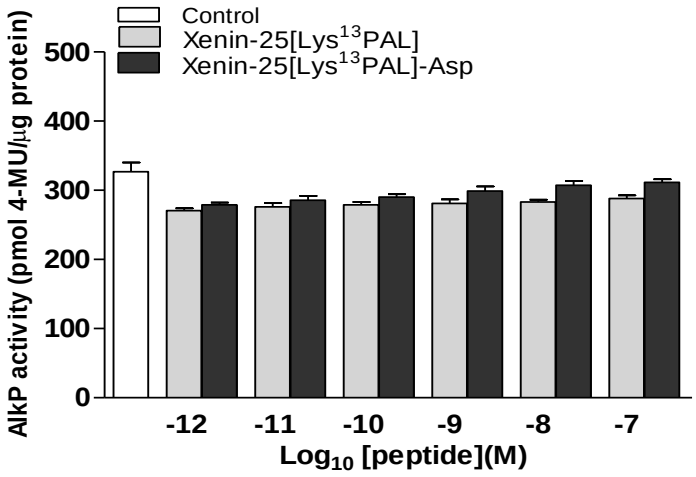

SAOS-2 cells were grown in 6-well plates and stimulated with indicated concentrations of peptides. After (A) 24 hrs and (B) 48 hrs the reaction was stopped and AlkP production was indirectly measured using 4-methyl umbelliferyl phosphate as substrate. The values were normalised against total amount of protein/well using BCA protein kit. Values are mean ± SEM of n=6.

Figure 3.21 Dose dependent effects of Xenin-25[Lys^{13}PAL] and Xenin25[Lys^{13}PAL] Asp on alkaline phosphatase activity after 72 hrs in human osteoblast SAOS-2 cells.

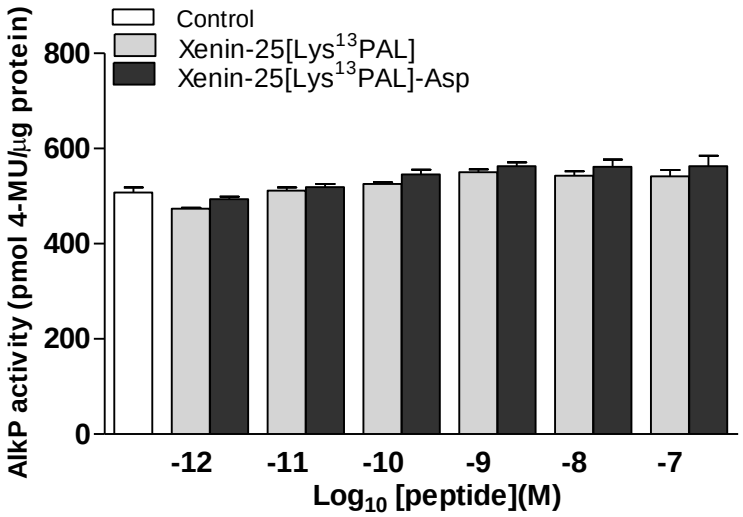

SAOS-2 cells were grown in 6-well plates and stimulated with indicated concentrations of peptides. After 72 h, the reaction was stopped and AlkP production was indirectly measured using 4-methyl umbelliferyl phosphate as substrate. The values were normalised against total amount of protein/well using BCA protein kit. Values are mean ± SEM of n=6.

Figure 3.22 Dose dependent effects of GIP/Xenin, GIP/Xenin-Asp andGIP/Xenin-Glu on alkaline phosphatase activity after (A) 24 hrs and (B) 48 hrs in human osteoblast SAOS-2 cells.

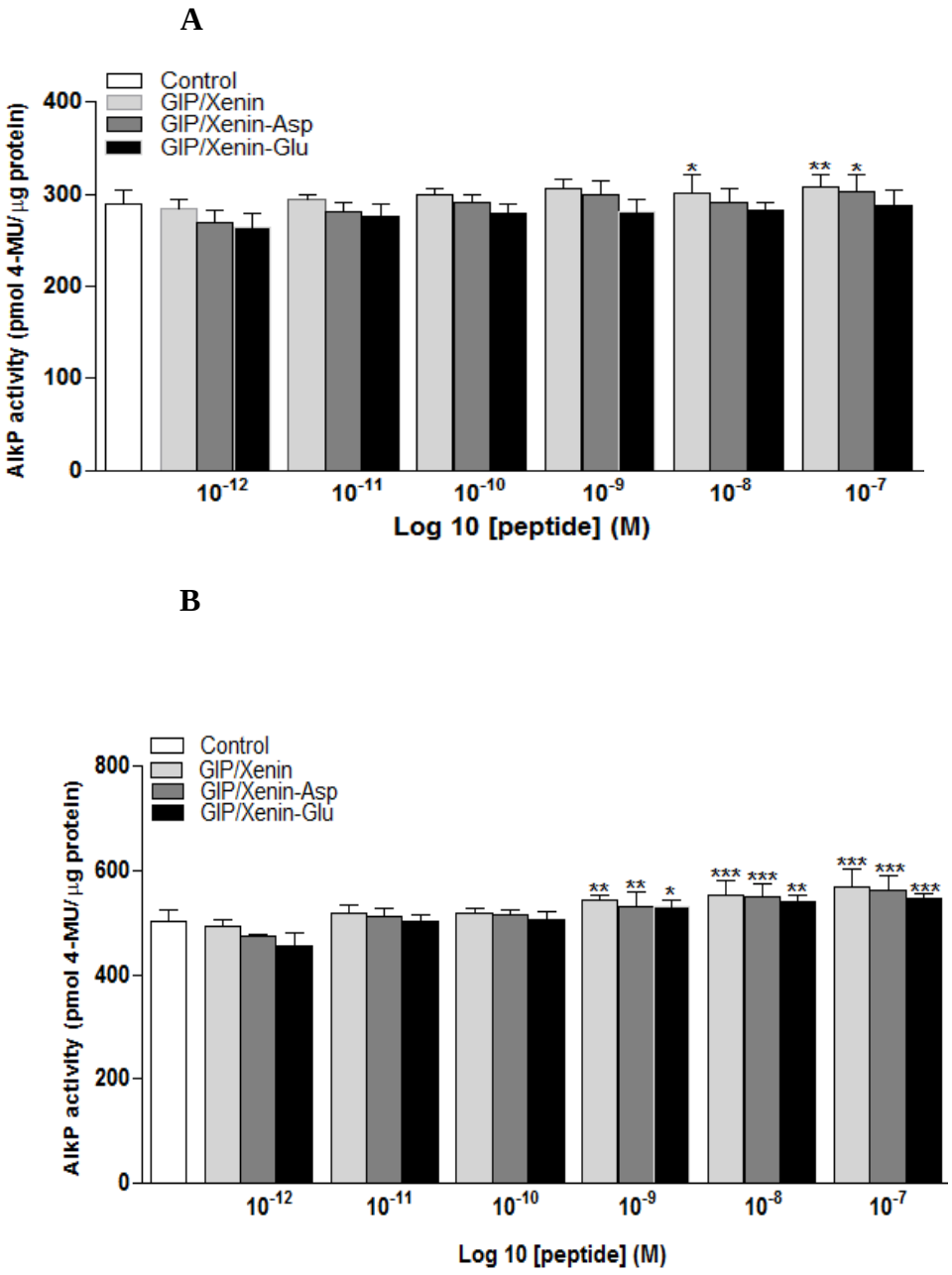

SAOS-2 cells were grown in 6-well plates and stimulated with indicated concentrations of peptides. After (A) 24 h and (B) 48 h, the reaction was stopped and AlkP production was indirectly measured using 4-methyl umbelliferyl phosphate as substrate. The values were normalised against total amount of protein/well using BCA protein kit. Values are mean ± SEM of n=6. *p<0.05, **p<0.01, ***p<0.001 vs control.

Figure 3.23 Dose dependent effects of GIP/Xenin, GIP/Xenin-Asp and GIP/Xenin Glu on alkaline phosphatase activity after 72 hrs in human osteoblast SAOS-2 cells.

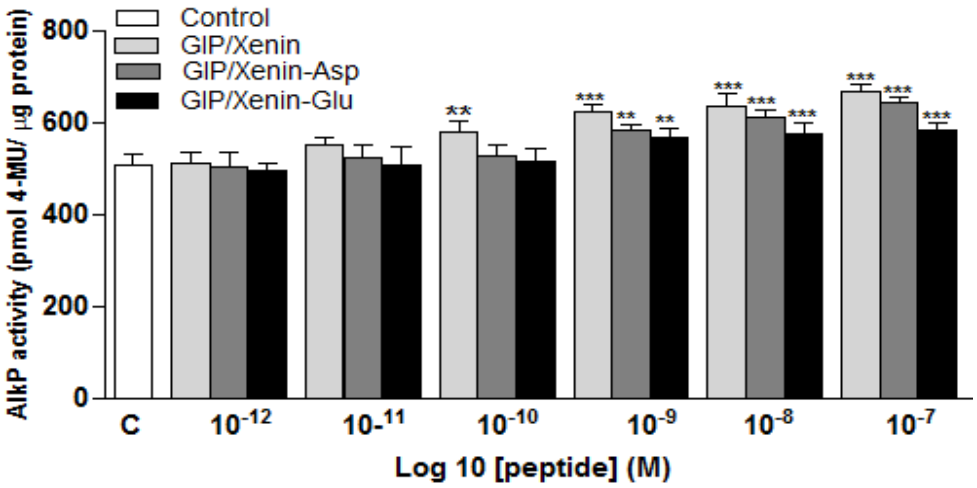

SAOS-2 cells were grown in 6-well plates and stimulated with indicated concentrations of peptides. After 24 h, the reaction was stopped and AlkP production was indirectly measured using 4-methyl umbelliferyl phosphate as substrate. The values were normalised against total amount of protein/well using BCA protein kit. Values are mean ± SEM of n=6. *p<0.05, **p<0.01, ***p<0.001 vs control.

Figure 3.24 Effects of (A) (D-Ala^2)GIP, (D-Ala^2)GIP-Asp, (D-Ala^2)GIP-Glu and (B) (D-Ala^2)GLP-1, (D-Ala^2)GLP-1-Asp and (D-Ala^2)GLP-1-Glu on cAMP generation in human osteoblast SAOS-2 cells.

A

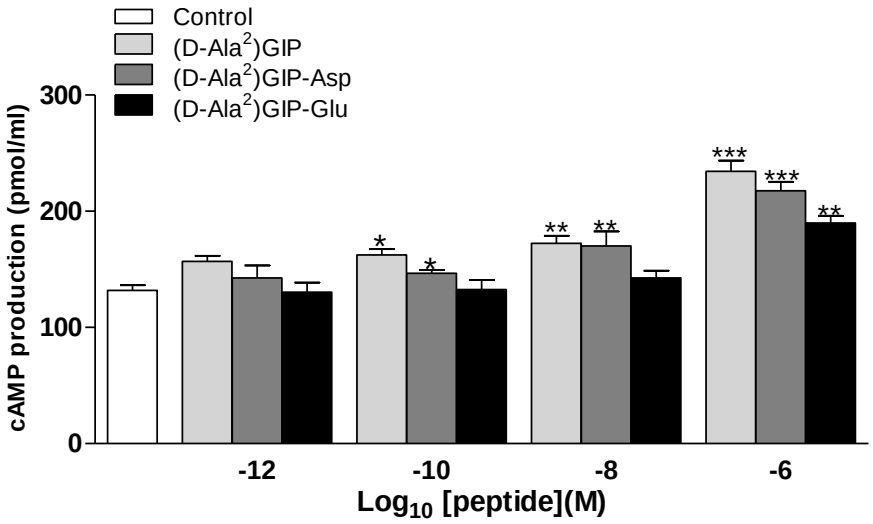

B

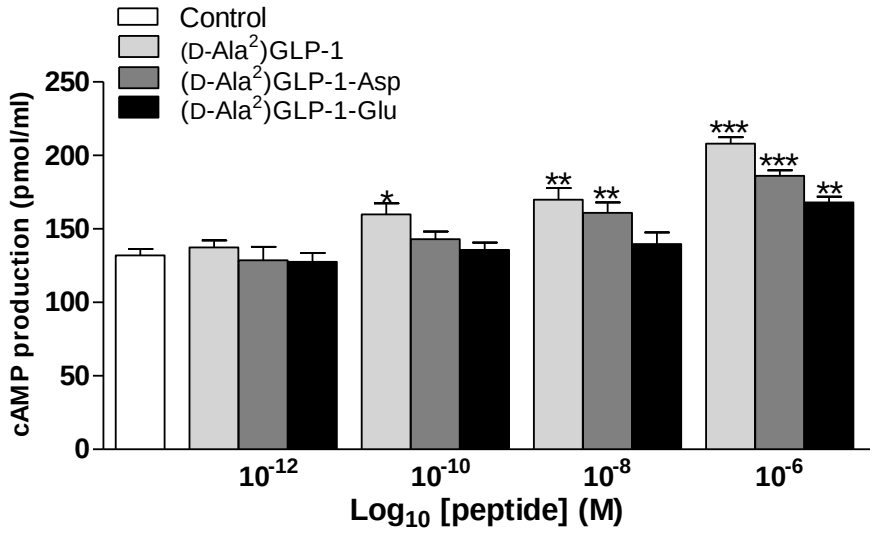

Human osteoblast SAOS-2 cells were exposed to different concentrations (10^{-12} – 10^{-6} M) of test peptides for 60 mins. cAMP release was then measured using a commercially available cAMP assay kit. Values are mean ± SEM for n=4-5. *p<0.05, **p<0.01, ***p<0.0001 vs. control.

Figure 3.25 Effects of (A) Xenin-25[Lys^{13}PAL], Xenin-25[Lys^{13}PAL]-Asp and (B) GIP/Xenin, GIP/Xenin-Asp and GIP/Xenin-Glu on cAMP generation in human osteoblast SAOS-2 cells.

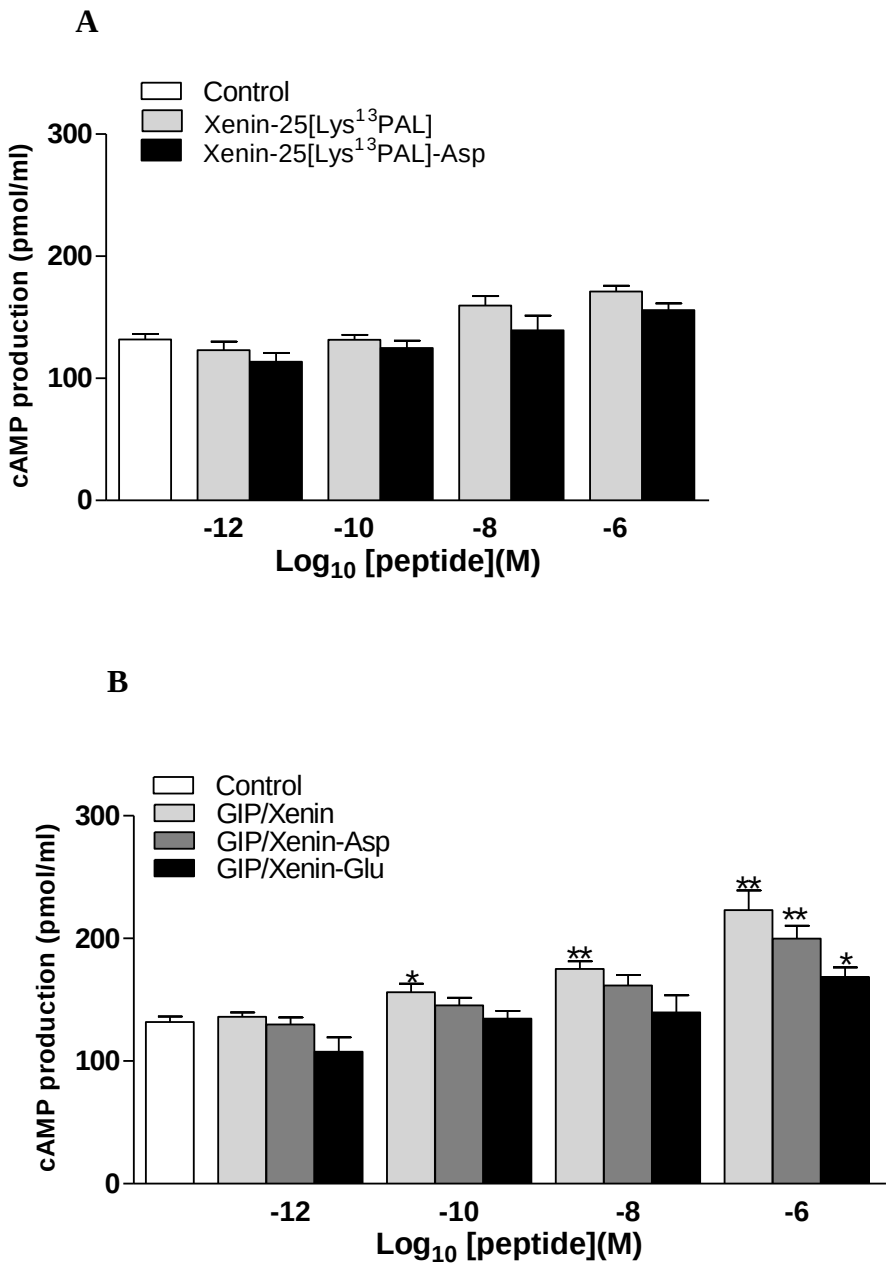

Human osteoblast SAOS-2 cells were exposed to different concentrations of GIP/Xenin, GIP/Xenin-Asp and GIP/Xenin-Glu for 60 mins. cAMP release was then measured using a commercially available cAMP assay kit. Values are mean ± SEM for n=4-5. *$p<0.05$, **$p<0.01$ vs control.

Figure 3.26 Effects of (A) (D-Ala^2)GIP, (D-Ala^2)GIP-Asp, (D-Ala^2)GIP-Glu and (B) (D-Ala^2)GLP-1, (D-Ala^2)GLP-1-Asp and (D-Ala^2)GLP-1-Glu on TGF-β re1ease from human osteoblast SAOS-2 cells.

A

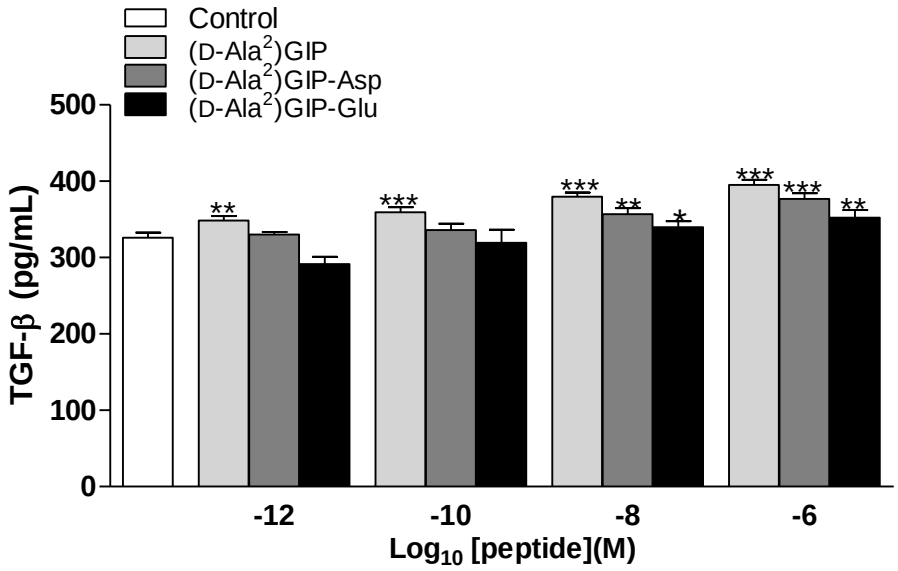

B

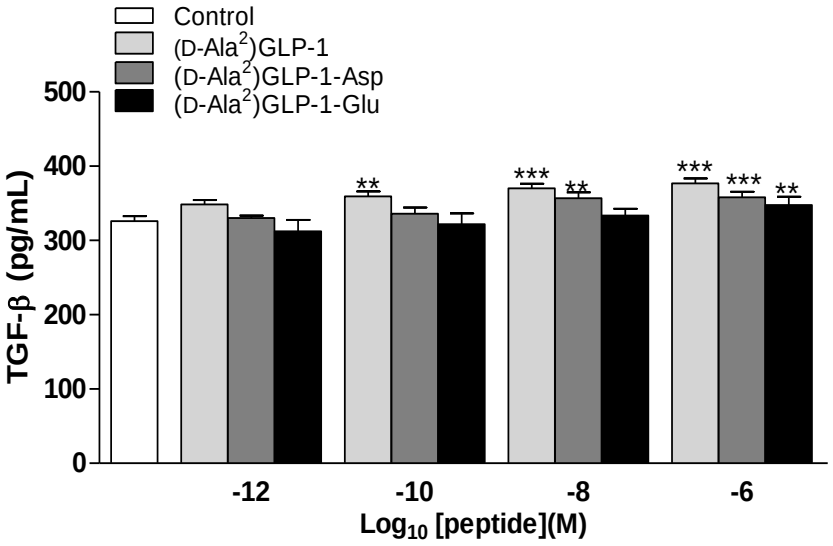

Human osteoblast SAOS-2 cells were exposed to different concentrations of (D-Ala^2)GLP-1, (D-Ala^2)GLP-1-Asp and (D-Ala^2)GLP-1-Glu for 8 h and TGF-β levels were measured using recombinant human TGF-β Immunoassay kit. Values are mean ± SEM for n=4. **p< 0.01, ***p< 0.001 vs control.

Figure 3.27 Effects of (A) Xenin-25[Lys^{13}PAL], Xenin-25[Lys^{13}PAL]-Asp and (B) GIP/Xenin, GIP/Xenin-Asp and GIP/Xenin-Glu on TGF-β release from human osteoblast SAOS-2 cells.

A

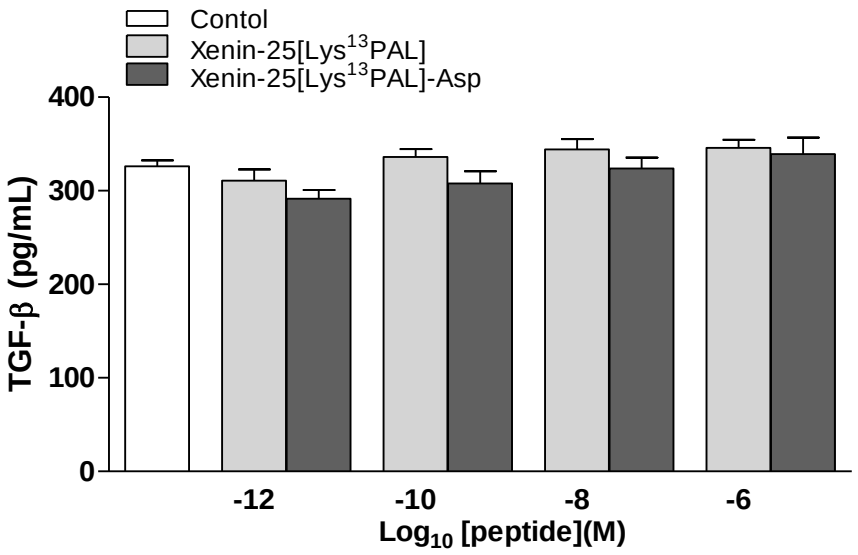

B

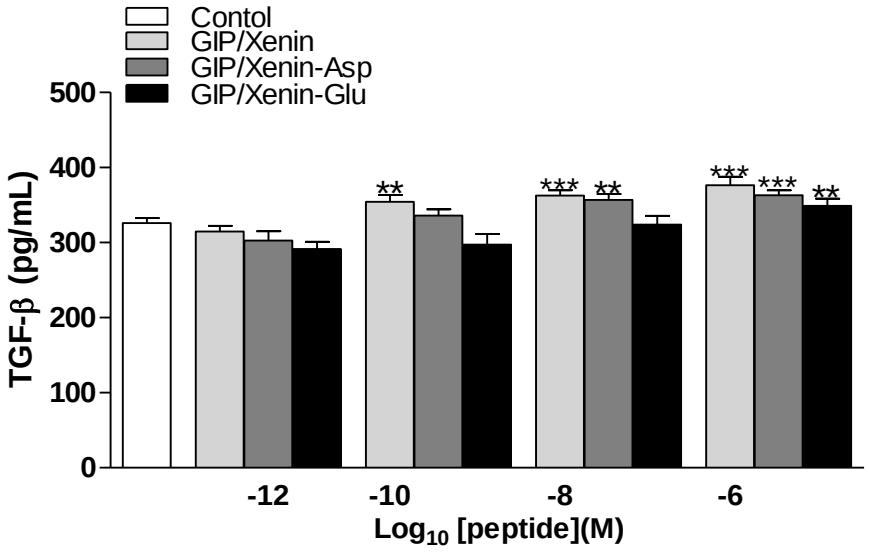

Human osteoblast SAOS-2 cells were exposed to different concentrations of GIP/Xenin, GIP/Xenin-Asp and GIP/Xenin-Glu for 8 h and TGF-β levels were measured using recombinant human TGF-β Immunoassay kit. Values are mean ± SEM for n=4. **p< 0.01, ***p< 0.001 vs control.

Figure 3.28 Effects of (A) (D-Ala^2)GIP, (D-Ala^2)GIP-Asp, (D-Ala^2)GIP-Glu and (B) (D-Ala^2)GLP-1, (D-Ala^2)GLP-1-Asp and (D-Ala^2) GLP-1-Glu on IGF-1 release from human osteoblast SAOS-2 cells.

A

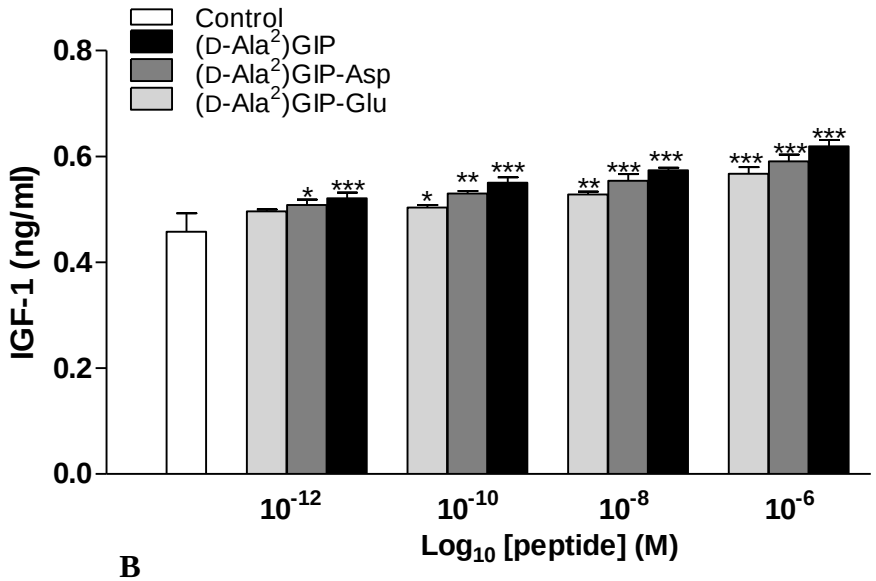

B

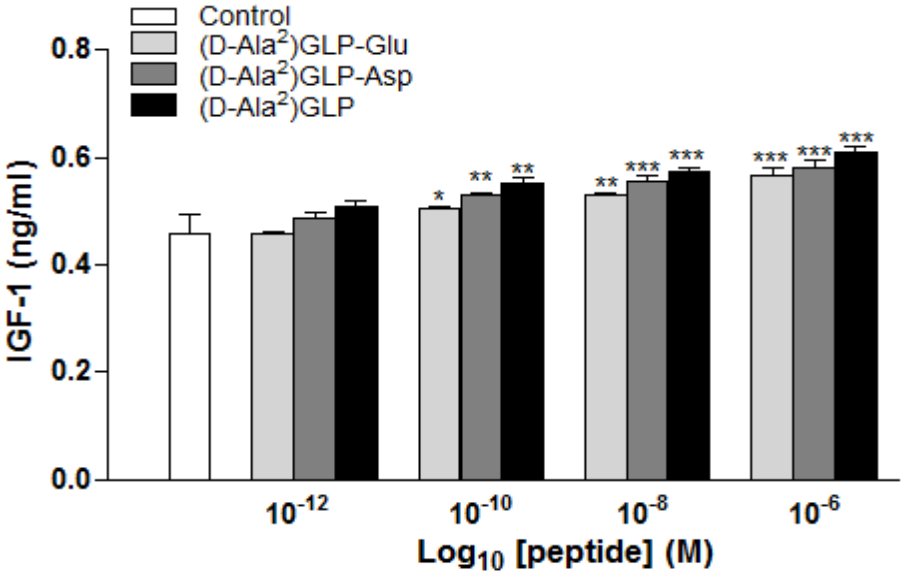

Human osteoblast SAOS-2 cells were exposed to different concentrations of (D-Ala^2)GLP-1, (D-Ala^2)GLP-1-Asp and (D-Ala^2)GLP-1-Glu for 8 h and IGF-1 levels were measured using recombinant human IGF-1 Immunoassay kit. Values are mean ± SEM for n=4. *p< 0.05, **p< 0.01 ***p< 0.001 vs control.

Figure 3.29 Effects of (A) Xenin-25[Lys^{13}PAL], Xenin-25[Lys^{13}PAL]-Asp and (B) GIP/Xenin, GIP/Xenin-Asp and GIP/Xenin-Glu on IGF-1 release from human osteoblast SAOS-2 cells.

A

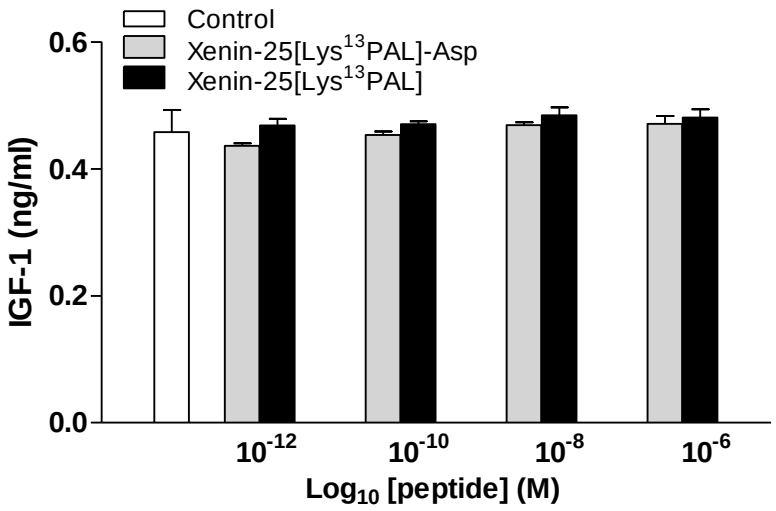

B

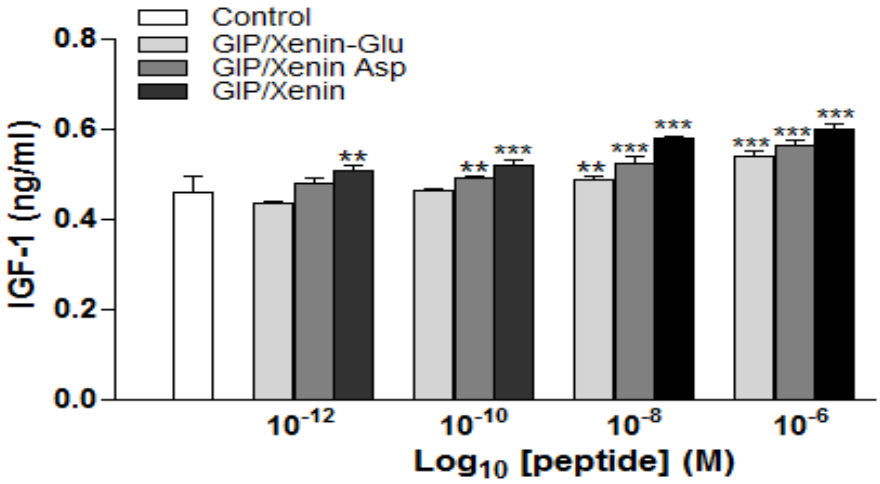

Human osteoblast SAOS-2 cells were exposed to different concentrations of GIP/Xenin, GIP/Xenin-Asp and GIP/Xenin-Glu for 8 h and IGF-1 levels were measured using recombinant human IGF-1 Immunoassay kit. Values are mean ± SEM for n=4. **p< 0.01, ***p< 0.001 vs control.

Chapter 4

Impact of bone-specific GIP peptides on metabolic control as well as bone quality and strength in high-fat fed mice

4.1 SUMMARY

Glucose-dependent insulinotropic polypeptide (GIP) is a 42-amino acid gastrointestinal hormone that regulates blood glucose levels by stimulating insulin secretion following food intake. GIP receptors (GIPRs) are found in pancreas, brain, and liver. However recently, the presence of functional GIPRs has been reported on bone cells, and been shown to have direct positive effects on bone strength and quality. GIP is rapidly degraded by dipeptidyl peptidase 4 (DPP-4). In order to circumvent DPP-4 activity, stable GIP peptides have been developed. The bone-specific action of GIP could be further exploited by generating bone-targeting GIP forms, through oligopeptide tagging by addition of six C-terminal acidic L-Asp amino acid residues that encourage binding to hydroxyapatite, the major component of the bone. The present study has investigated the effects of once-daily administration of (D-Ala^2)GIP and (D-Ala^2)GIP-Asp (25 nmol/kg bw) for 42 days on bone mineral density (BMD) and content (BMC), bone geomertry and bone tissue specific properties, as well as metabolic control in high-fat fed mice. Once daily injection of the peptides had no effect on body weight and food intake, but circulating glucose was significantly ($p<0.001$) decreased by day 42. Glucose tolerance was enhanced by (D-Ala^2)GIP, but not by (D-Ala^2)GIP-Asp. DEXA analysis revealed that there was no difference in overall, femoral and lumbar BMD and BMC between groups of mice. However, tibial BMC was enhanced, revealing marked ($p<0.01$) benefits of [D-Ala^2]GIP-Asp. Total trabecular area was enhanced ($p<0.01$) in the mice treated with (D-Ala^2)GIP-Asp. In (D-Ala^2)GIP treated mice cortical thickness was reduced ($p<0.01$) but not in (D-Ala^2)GIP-Asp mice. Infrared spectroscopy analysis revealed enhancement of collagen cross-linking by (D-Ala^2)GIP and (D-Ala^2)GIP-Asp. In conclusion, this study has shown that biologically active, bone-targeting,

forms of stable GIP analogues can be produced which requires further investigation for the treatment of bone-related diseases.

4.2 INTRODUCTION

Glucose-dependent insulinotropic polypeptide (GIP) is released in response to food ingestion (Christensen MB 2016). The primary effect of GIP is to enhance the secretion of insulin in a glucose-dependent manner and therefore, control postprandial glucose concentrations (Seino *et al*. 2016). However, previously it has been reported that functional GIP receptors are present on bone (Bollag *et al*. 2000, Zhong *et al*.2007), indicating a direct action of GIP on bone. GIP has only short half-life of around 2 to 4 mins in rodents and humans (Kieffer *et al*. 1995, Deacon *et al*. 2000). GIP is rapidly degraded by dipeptidyl peptidase 4 (DPP-4) upon secretion into the bloodstream (Godinho *et al*. 2015). To overcome this, DPP-4-resistant GIP molecules with prolonged bioactivity have been developed (Irwin *et al*. 2005a). The insulin secretory activity of GIP is well documented, but less attention has been given to the fact that GIP has positive effect on bone.

Bone remodeling is a complex and continuous process which occurs via communication between osteoblasts and osteoclasts, where old bone is constantly removed by osteoclasts, and is replaced by new bone formed by osteoblasts (Matsuo & Irie 2008). Bone is mainly comprised of collagen, hydroxyapaptite and water (Bolesky 2013). Through oligopeptide tagging, by addition of six C-terminal acidic L-Asp amino acid residues to GIP, binding of peptides to hydroxyapaptite can be increased (Takahashi-Nishioka *et al*. 2008) making these types of GIP analogues potential treatment option for fragility bone fractures. Thus, (D-Ala^2)GIP-Asp represents one such analogue (Chapter 3), that will be further characterised in this chapter.

Different types of mice models have been developed to investigate detrimental effects of type 2 diabetes on bone quality. Some of these models include obese Zucker (*fa/fa*) rats, obese diabetic (*ob/ob*) mice and diabetic (*db/db)* mice (Fajardo *et al*. 2014). In 2004, studies carried out by Hamrick and co-workers reported that homozygous mutation of the leptin gene in *ob/ob* mice or defective leptin receptor in *db/db* mice, severely and detrimentally affected bone microarchitecture and strength (Hamrick *et al*. 2004). Similar findings were reported by Matsunuma *et al*., as they also found there were severe alterations in bone microarchitecture (Matsunuma *et al*. 2004). Regarding *ob/ob* mice, histomorphometry analysis revealed reduced bone mass, shorter femoral length and reduced cortical thickness (Stephen *et al*. 2000). In *db/db* mice, it has been reported that bone mineral content (BMC) and bone mineral density (BMD); are both significantly reduced leading to alterations on bone biomechanical properties (Ealey *et al*. 2006). Another important model which allows studying the effects of type 2 diabetes on bone skeleton is high-fat fed mice model. The high-fat diet is more or less similar to the Westernised diet that can lead to obesity, insulin resistance and type 2 diabetes (Zhang *et al*. 2009). Several studies have been carried on high-fat fed mouse models, and report detrimental effects on bone mass and bone volume (Patsch *et al*. 2011), as well as reduction in bone biomechanical strength and alterations in bone microstructure (Halade *et al*. 2010). This suggests that the high-fat diet has adverse effects on bone. The present study was therefore undertaken to assess the effects of (D-Ala^2)GIP, and (D-Ala^2)GIP-Asp on metabolic control, BMD, BMC and specific bone tissue parameters in high fat fed mice.

4.3 MATERIALS AND METHODS

4.3.1 Synthesis of peptides

The (D-Ala^2)GIP, (D-Ala^2)GIP-Asp peptides used in this study were purchased from EZ Biolabs Ltd. (Carmel, IN, USA). The peptides were characterised by mass spectrometry as described in Section 2.1.2. Identity of the peptides was confirmed by comparing values for experimental mass obtained from mass spectroscopy and theoretical masses.

4.3.2 Animals and study design

Young male NIH Swiss mice (n=5, 8 weeks old) were maintained on high-fat diet for three months. All the mice were housed separately in air conditioned room with 12 hour light and 12 hour dark cycle. Mice were grouped (n=5) according to body weight and blood glucose. Initially mice were injected with saline solution (0.9% NaCl) for 3 days so that they could get accustomed to the injection regimen. Group 1 received high-fat diet and saline injection (0.9% NaCl). Group 2 mice received high fat diet and (D-Ala^2)GIP injection (25 nmol/kg bw) once a day. Group 3 received high-fat diet and (D-Ala^2)GIP-Asp (25 nmol/kg bw) injection once a day. The injecton schedule was followed for 42 days. Body weight, food consumption, non-fasting and blood glucose concentrations were measured at regular intervals. Intraperitoneal glucose tolerance test (18 mmol/kg bw, 18 hour fast) and non-fasting insulin sensitivity (25 U/kg bw) tests were performed at the end of the study as described in Sections 2.3.2 and 2.3.3, respectively. All experiments were carried out according to UK Home Office Regulations (UK Animals Scientific Procedures Act 1986).

4.3.3 Measurement of plasma insulin

An insulin RIA was carried out as described in Section 2.4.2 to determine plasma insulin concentrations.

4.3.4 Measurement of body composition, bone density and mineral content by DEXA scanning

Mice were anaesthetised with isoflurane and then they were placed on a specimen tray of DEXA scanner and the whole body was scanned. BMD, BMC, lean mass and fat mass were determined as explained in Section 2.4.

4.3.5. X-ray microcomputed tomography (µCT)

Microcomputed tomography was carried out to assess trabecular bone mass, trabecular bone thickness, number of trabeculae, cortical bone diameter, cortical thickness, diameter of bone marrow and cross-sectional moment of inertia as described in Section 2.5.3.

4.3.6 Fourier transformed infrared (FT-IR) imaging and micro spectroscopy

FT-IR was performed as per described in section 2.5.5. In short, polymethylacrylate sections (4 µm) of bones were prepared using micrtome equipped with tungsten carbide knife. Further, spectral analysis was carried out using a Bruker Vertex 70 spectrometer interfaced with Bruker Hyperion 3000 infrared microscope equipped with mercury cadmium telluride detector. The spectra were recorded in the same location (region of interest on the bone). On an average 32 spectra were recorded.

4.3.7 Statistical analysis

Data were analysed using repeated measures one-way or two-way ANOVA with Tukey post hoc tests or two-tailed t-tests using PRISM 5.0. Data are expressed as mean ± S.E.M and a P value < 0.05 was considered statistically significant.

4.4 RESULTS

4.4.1 Effects of (D-Ala^2)GIP and (D-Ala^2)GIP-Asp on body weight, food intake, blood glucose and plasma insulin in high-fat fed mice

Daily administration of (D-Ala^2)GIP and (D-Ala^2)GIP-Asp did not cause any significant changes in terms of body weight, fat mass, lean mass (Figure 4.1A-C) or food intake (Figure 4.2). Circualting blood glucose was decreased by both treatment interventions, with both (D-Ala^2)GIP and (D-Ala^2)GIP-Asp treated mice having significantly ($p<0.05$ to $p<0.001$) reduced glucose concentrations compared to saline controls on day 42 (Figure 4.3 A). Insulin levels were reduced in the mice treated with (D-Ala^2)GIP-Asp (Figure 4.3 B)

4.4.2 Effects of (D-Ala^2)GIP and (D-Ala^2)GIP-Asp on glucose tolerance and insulin sensitivity in high-fat fed mice

Glucose tolerance tests were carried out on day 42 and blood glucose and plasma insulin measured at 0, 15, 30, 60 and 105 mins post glucose challenge. Blood glucose levels were reduced ($p<0.01$) in both treatment groups at 105 min (Figure 4.4A), but AUC values were not different from saline controls (Figure 4.4B). Corresponding insulin levels were reduced by the treatments, and signficaintly ($p<0.05$ to $p<0,001$) so by (D-Ala^2)GIP-Asp (Figure 4.4C), but again AUC values were similar in all groups (Figure 4.4D). Accordignly, insulin sensitivity was imporved by (D-Ala^2)GIP and (D-Ala^2)GIP-Asp comapared to controls, but only significantly by (D-Ala^2)GIP-Asp (Figure 5A,B).

4.4.3 DEXA analysis of femur, tibia and lumbar spine in high-fat fed mice

DEXA analysis revealed that there was no difference in wholw body (Figure 4.6), femoral (Figure 4.7) and lumbar (Figure 4.8)

BMD and BMC between groups of mice. However, tibial BMC was increased ($p<0.01$) by (D-Ala^2)GIP-Asp (Figure 4.9), indicating the potential benefits of (D-Ala^2)GIP-Asp.

4.4.4 Effects of (D-Ala^2)GIP and (D-Ala^2)GIP-Asp on trabecular bone morphology and cortical bone geometry in high-fat fed mice

Microcomputed tomography (MicroCT) was performed on bones to analyse parameters such as trabecular bone volume, cortical thickness, trabecular separation and number of trabeculae (Figure 4.10). Interestingly, total trabecular area was augmented ($p<0.01$) in the mice treated with (D-Ala^2)GIP-Asp, but not by (D-Ala^2)GIP (Figure 4.11A). Cortical area, bone mineralisation and moment of inertia were unaffected after treatment with (D-Ala^2)GIP and (D-Ala^2)GIP-Asp (Figure 4.11B-D). Cortical thickness was reduced ($p<0.01$) in the mice treated with (D-Ala^2)GIP, but not in (D-Ala^2)GIP-Asp mice (Figure 4.10E). Cross-sectional moment of inertia was similar in all groups (Figure 4.10F).

4.4.5 Effects of (D-Ala^2)GIP and (D-Ala^2)GIP-Asp on bone tissue level parameters in high-fat fed mice

Five different parameters were analysed using infrared spectroscopy. These parameters included collagen cross-linking, crystallinity of hydroxyapaptite, degree of mineralisation, degree of carbonate substitution and content of acid phosphate (Figure 4.11A-O). From these measurements, the only treatment-indcued changes were an enhancement of collagen cross-linking by both by (D-Ala^2)GIP, and especially (D-Ala^2)GIP-Asp (Figure 4.11B,C). The rest of the parameters were not affected.

4.5 DISCUSSION

Bone turnover is controlled by sequential activity of osteoblasts and osteoclasts which is controlled by various autocrine and paracrine factors (Matsuo & Ire 2008). After food ingestion bone resorption biomarkers undergo rapid change (Henrikson *et al*. 2003), suggesting that gastrointestinal hormones do play a role in bone remodelling. GIP is released by entero-endocrine K cells and it has been reported that GIP receptors are present on bone cells (Bollag *et al*.2000, Zhong *et al* 2007). Less attention has been given to the fact that there are direct positive beneficial effects of GIP on bone. A small number of studies have been carried out to suggest use GIP as a therapeutic option for treatment of fragility fractures. For example, in 2013, Gaudin-Audrain and colleagues reported that GIPR KO mice exhibited higher trabecular bone volume, but had decreased osteoclasts and increased osteoblast activity, resulting in increased bone formation (Gaudin-Audrain *et al*. 2013). In a similar study carried out study in double incretin receptor knockout mice (DIRKO), it was found that cortical bone mass and cortical bone strength was reduced and exhibited detrimental effects on bone (Mieczkowska *et al*. in 2015). However, most importantly, administration of a long acting GIPR agonist had positive effects on bone in normal and diabetic rodents (Mabilleau *et al*. 2015).

The present study assessed the effects of once-daily administration of (D-Ala^2)GIP and (D-Ala^2)GIP-Asp for 42 days on bone parameters in high-fat fed mice. (D-Ala^2)GIP is a well characterised long-acting GIP agonist (Tatarkiewicz *et al*. 2014) whereas (D-Ala^2)GIP-Asp is a bone-targetting stable GIP form charatersied within Chapter 3 of this thesis. The findings of this study revealed that there was no effect on body weight and food intake, but that circulating non-fasting glucose levels were reduced by both treatments. These observations are consistent with other studies employing stable GIP agonists in diabetic

mouse models (Shimazu-Kuwahara *et al*. 2017). Interestingly, (D-Ala^2)GIP-Asp enhanced glucose tolerance and insulin sensitivity to an equal, or even superior degree than (D-Ala^2)GIP. This is interesting and merits further study, and might suggest that (D-Ala^2)GIP-Asp has potential important antidiabetic actions. DEXA analysis revealed that there was no difference in overall, femoral and lumbar BMD and BMC. However, BMC assessment of tibia revelaed clear benefits of (D-Ala^2)GIP-Asp over (D-Ala^2), highlighting the benefit afforded by directing the peptide towards bone by acidic oligopeptide tagging (Wang *et al*. 2016, Zhu *et al*. 2017).

Microcomputed tomography was performed to assess cortical area, bone mineralisation, cortical thickness, moment of inertia and total area. MicorCT analysis revealed that cortical area, bone mineralisation and moment of inertia remain unaffected in the mice treated with (D-Ala^2)GIP and (D-Ala^2)GIP-Asp. Cortical thickness was increased in the mice treated with (D-Ala2)GIP-Asp. These findings are in harmony with the previous studies suggesting positive effects of GIP on bone (Mansur *et al*. 2015, Mabilleau 2017). Similarly, total area was also increased in the mice treated with (D-Ala^2)GIP-Asp. This again suggests key bone-specific benefits of the additional six aspartic acid residues added to the molecule (Carbone *et al*. 2017, Smith & Samadfam 2017). The abnormalities in cortical bone geometry in the high fat fed mice are due to overt hyperglycaemia, as hyperglycaemia leads to alterations and modifications in bone collagen which further causes alterations in bone matrix eventually leading to bone fragility (Palmero *et al*. 2017).

The analysis of bone at the tissue level was performed by infrared spectroscopy. Collagen cross-linking, crystallinity of hydroxyapaptite, degree of mineralisation, degree of carbonate substitution and content of acid phosphate were determined with the help of infrared spectroscopy. Collagen cross-linking was

augmented significantly in the mice treated with (D-Ala^2)GIP and (D-Ala^2)GIP-Asp. Indeeed, as observed before this bone effect was enhanced by acidic oligopeptide tagging (Castro *et al*. 2017, Schimdt *et al*. 2017). An increase in collagen cross-linking demonstrates enhanced collagen maturity and integrity (Kimura-Suda & Ito 2017). These findins can be backed up by previous studies where hybrid peptides, that contained a significant GIP component, have shown to improve bone strength at organ and tissule levels (Mansur *et al*. 2016). The degree of mineralisation, degree of carcarbonate substitution, crystallinity of hydroxyapaptite and acid phosphate content remain unaffected by the treatment interventions. The contradictory findings with increased collagen cross linking on the one hand, but no effects on rest of the parameters, point out the fact that dynamics of bone biology are dependent on many factors including bone integrity, mineralisation, morphology, bone mass and microstructure. Further analysis by three-point bending and nanoindentation would therefore be required to assess biomechanical properties of cortical bone, and confirm this viewpoint (Peacock *et al*. 2017, Arnold *et al*. 2018).

Based on the findings from this chapter, it is clear that generation of biologically active, bone-targeting, forms of stable GIP analogues is possible. Further investigation still needs to be done for the treatment of bone-related diseases.

FIGURES

Figure 4.1 Effects of once daily administration of (D-Ala^2)GIP and (DAla^2)GIP-Asp for 42 days on (A) body weight (B) % fat mass and (C) total lean mass in high fat fed mice

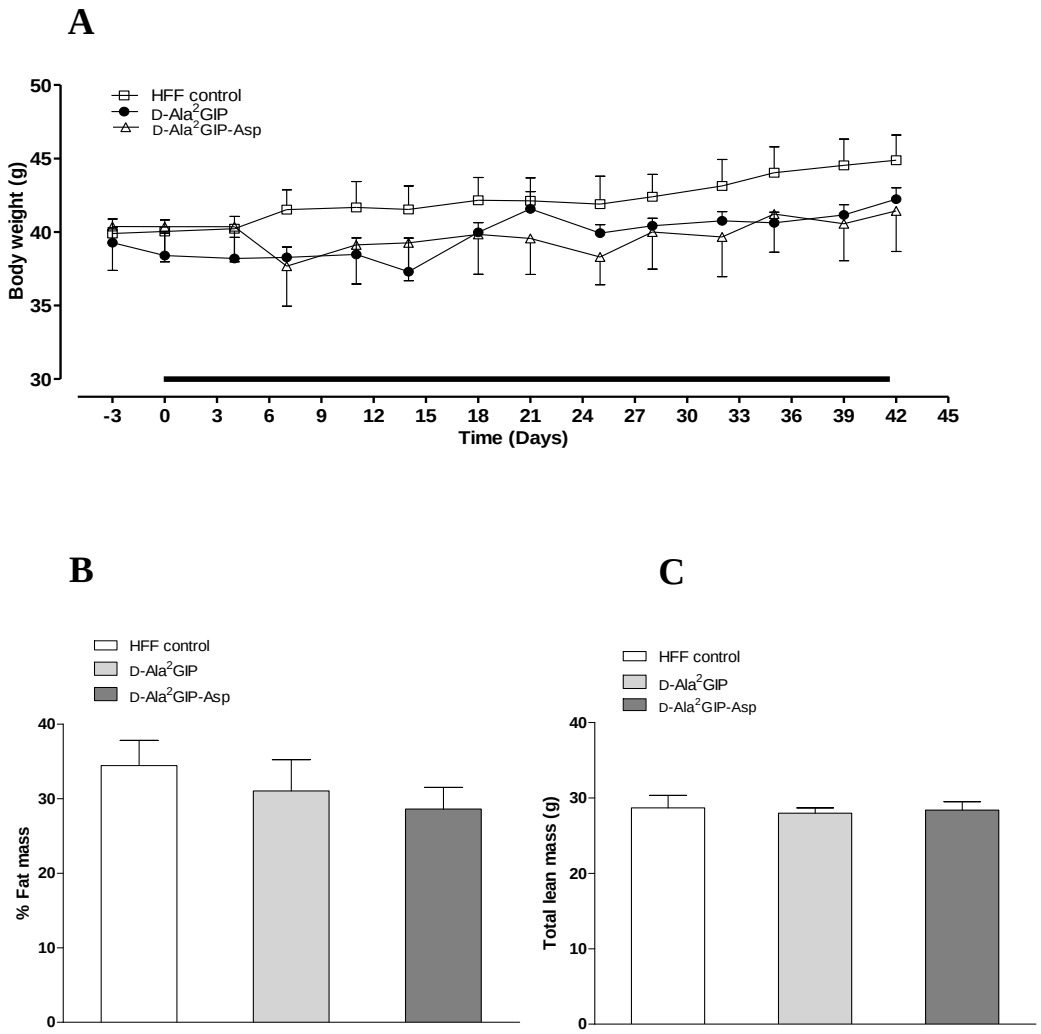

(A) Body weight was measured for 3 days before and 42 days during (indicated by blackhorizontal bar) once daily treatment with saline vehicle (0.9% w/v NaCl), (D-Ala^2)GIP and (D-Ala^2)GIP-Asp (each peptide at 25 nmol/kg bw). Values represent means ± SEM for 5 mice. (B) % fat mass and (C) lean mass as measured by DEXA scanning in high fat fed mice following 42 days treatment with (D-Ala^2)GIP and (D-Ala^2)GIP-Asp. Values represent means ± SEM for 5 mice.

Figure 4.2 Effects of once daily administration of (D-Ala^2)GIP and (D-Ala^2)GIP-Asp for 42 days on cumulative energy intake in high fat fed mice

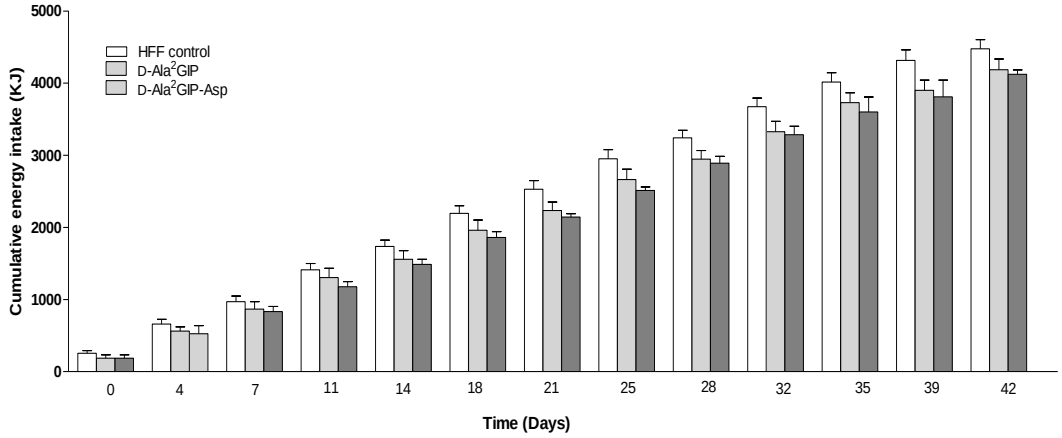

Cumulative energy intake was measured for 3 days before and 42 days during (indicated by black horizontal bar) once daily treatment with saline vehicle (0.9% w/v NaCl), (D-Ala^2)GIP and (D-Ala^2)GIP-Asp (each peptide at 25 nmol/kg bw). Values represent means ± SEM for 5 mice.

Figure 4.3 Effects of once daily administration of (D-Ala^2)GIP and (D-Ala^2)GIP-Asp for 42 days on non fasting (A) blood glucose and (B) plasma insulin in high fat fed mice.

A

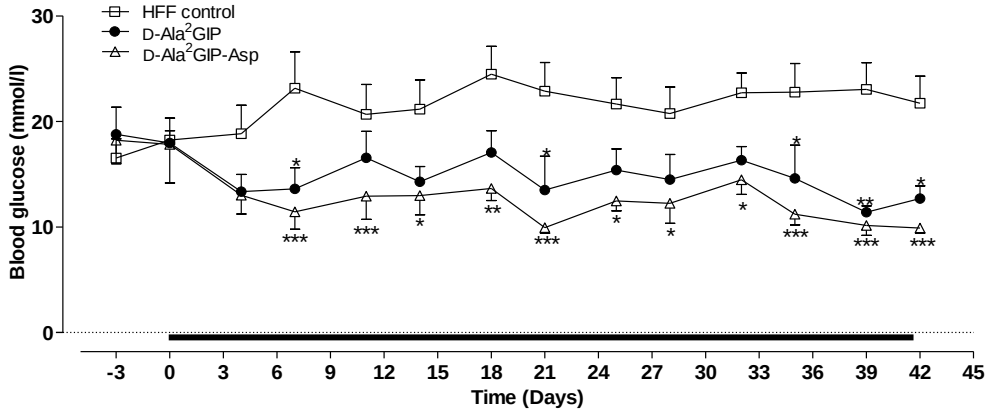

B

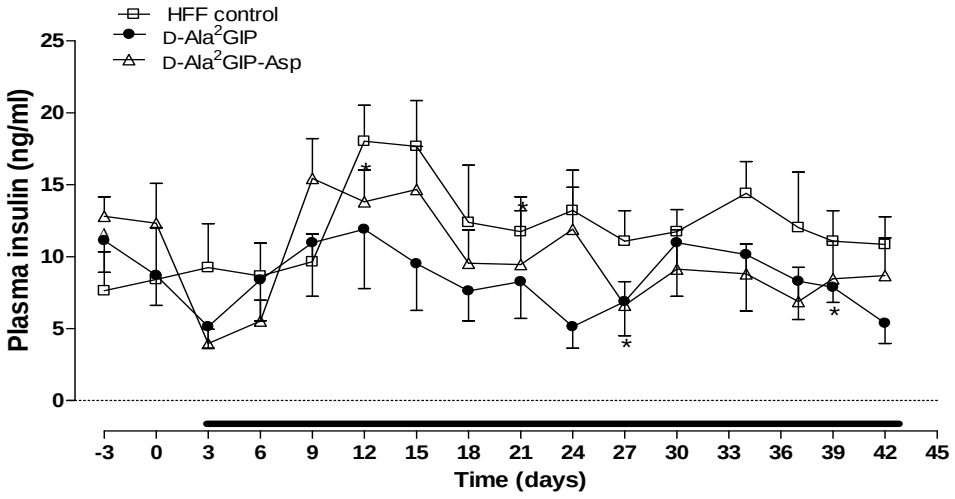

(A) Non fasting blood glucose and (B) plasma insulin levels were measured for 3 days before and 42 days during (indicated by black horizontal bar) once daily treatment with saline vehicle (0.9% w/v NaCl), (D-Ala^2)GIP and (D-Ala^2)GIP-Asp (each peptide at 25 nmol/kg bw). (B) Mice were injected once daily with saline vehicle (0.9%, w/v, NaCl), (D-Ala^2)GIP and (D-Ala^2)GIP-Asp (each at 25 nmol/kg b.w) for 42 days. Blood was collected 3 days before and 42 days and every 4 days thereafter. Values are expressed as mean ± S.E.M for 5 mice. *p<0.05, **p<0.01, ***p<0.001 compared with high-fat fed control.

Figure 4.4 Effects of once daily administration of (D-Ala^2)GIP and (D-Ala^2)GIP-Asp for 42 days on (A) glucose tolerance and (B) plasma insulin response in high fat fed mice

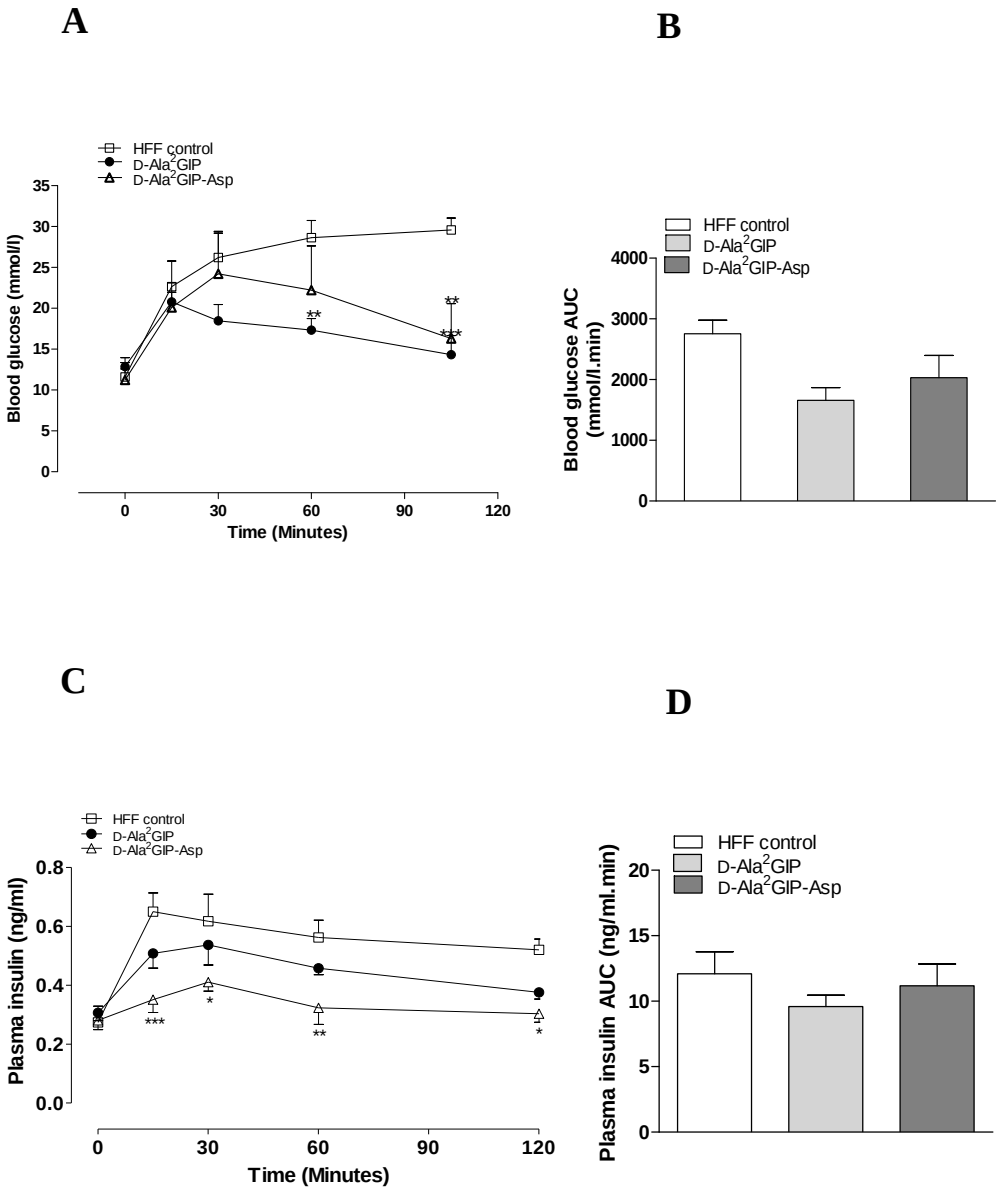

Tests were conducted after once daily treatment with saline, (D-Ala^2)GIP and (D-Ala^2)GIP-Asp for 42 days. (A) Blood glucose before and after i.p injection of glucose (18 mmol/kg bw) alone in 18 hrs fasted mice. (B) AUC values for blood glucose for 0-105 min are shown in insets. (C) Glucose alone (18 mmol/kg b.w) was administered at time 0 in 18 hrs fasted mice and plasma insulin concentrations prior to, and 15, 30 and 60 min after glucose administration were recorded. (D) Plasma insulin AUC values are also shown. Values are mean ± S.E.M for 5 mice per group. *$p<0.05$, **$p<0.01$ compared with high-fat fed control.

Figure 4.5 Effects of once daily administration of (D-Ala^2)GIP and (D-Ala^2)GIP-Asp for 42 days on insulin sensitivity in high fat fed mice

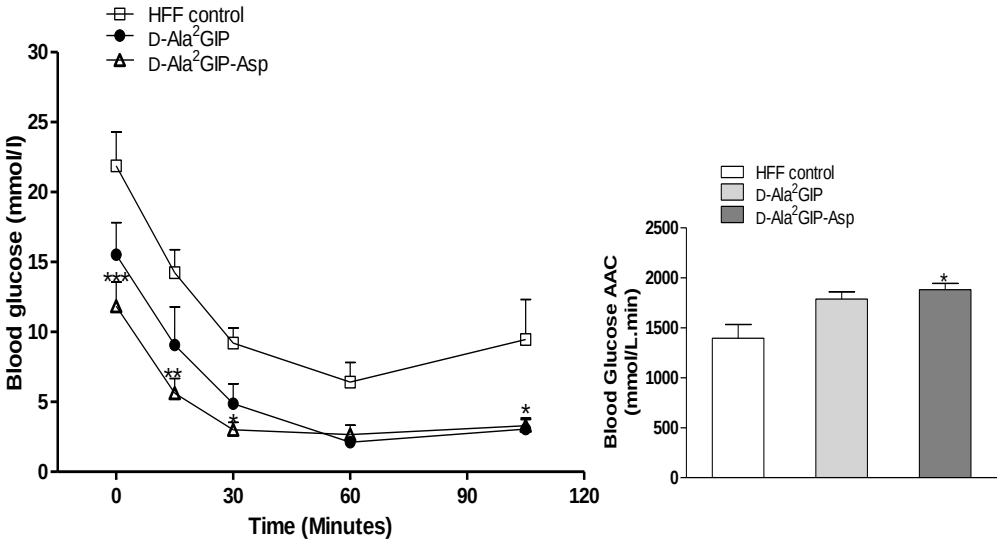

Following 42 days treatment with saline, (D-Ala^2)GIP and (D-Ala^2)GIP-Asp (each peptide at 25 nmol/kg bw), insulin (25 U/kg bw) was injected intraperitoneally (at t=0) in non-fasted mice to assess insulin sensitivity. Blood glucose and blood glucose AAC values for 0-105 min are shown in inset. Values represent means ± SEM for 5 mice. *p< 0.05, **p < 0.01 and ***p< 0.001 compared to high-fat fed control.

Figure 4.6 Effects of once daily administration of (D-Ala^2)GIP and (D-Ala^2)GIP-Asp for 42 days on whole body (A) BMD and (B) BMC in high fat fed mice

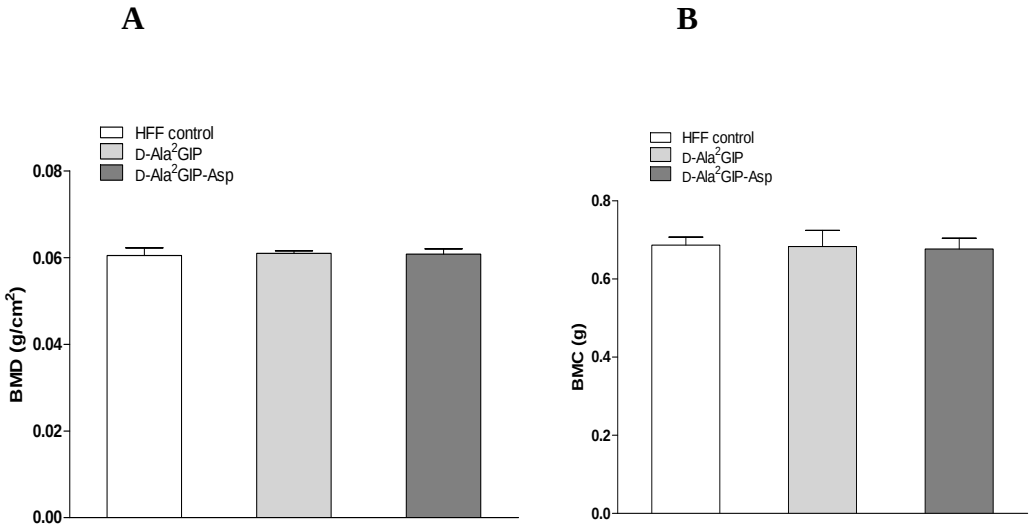

(A)Bone mineral density (BMD) and (B) Bone mineral content (BMC) as measured by DEXA scanning in high fat fed mice following 42 days treatment with (D-Ala^2)GIP and (D-Ala^2)GIP-Asp. Values represent means ± SEM for 5 mice.

Figure 4.7 Effects of once daily administration of (D-Ala^2)GIP and (D-Ala^2)GIP-Asp for 42 days on femur (A) BMD and (B) BMC in high fat fed mice

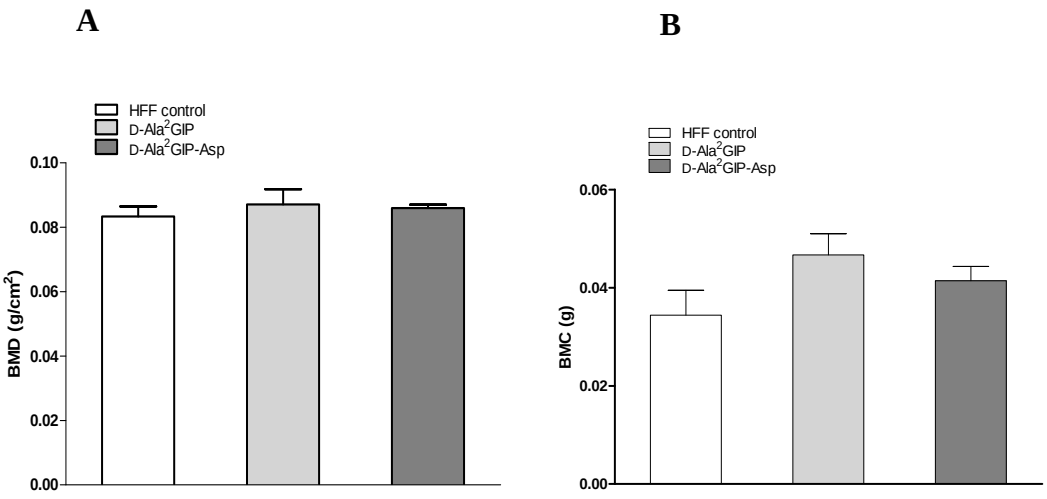

(A) Bone mineral density (BMD) and (B) Bone mineral content (BMC) as measured by DEXA scanning in high fat fed mice following 42 days treatment with (D-Ala^2)GIP and (D-Ala^2)GIP-Asp. Values represent means ± SEM for 5 mice.

Figure 4.8 Effects of once daily administration of (D-Ala^2)GIP and (D-Ala^2)GIP-Asp for 42 days on lumbar spine (A) BMD and (B) BMC in high fat fed mice

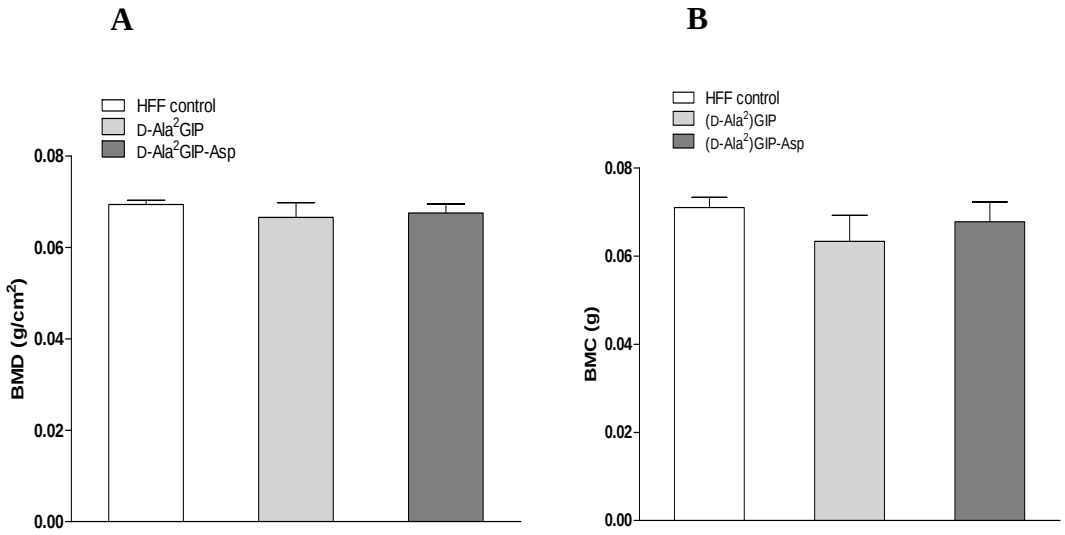

(A) Bone mineral density (BMD) and (B) Bone mineral content (BMC) as measured by DEXA scanning in high fat fed mice following 42 days treatment with (D-Ala^2)GIP and (D-Ala^2)GIP-Asp.

Figure 4.9 Effects of once daily administration of (D-Ala^2)GIP and (D-Ala^2)GIP-Asp for 42 days on tibia (A) BMD and (B) BMC in high fat fed mice

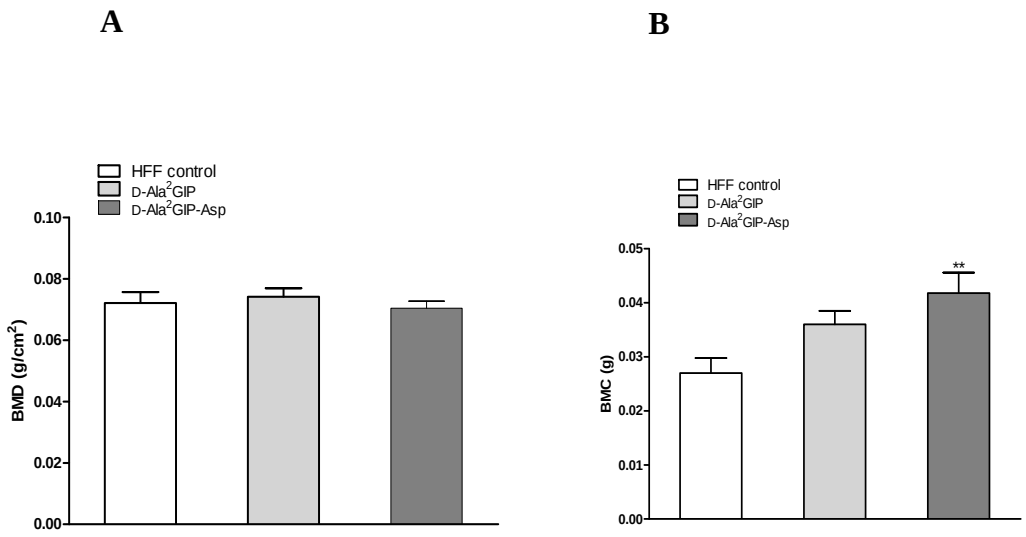

(A) Bone mineral density (BMD) and (B) Bone mineral content (BMC) mass as measured by DEXA scanning in high fat fed mice following 42 days treatment with (D-Ala^2)GIP and (D-Ala^2)GIP-Asp. Values represent means ± SEM for 5 mice. **p<0.01 compared to high- fat fed control.

Figure 4.10 Effects of once daily administration of (D-Ala^2)GIP and (D-Ala^2)GIP-Asp on cortical bone geometry in high fat fed mice

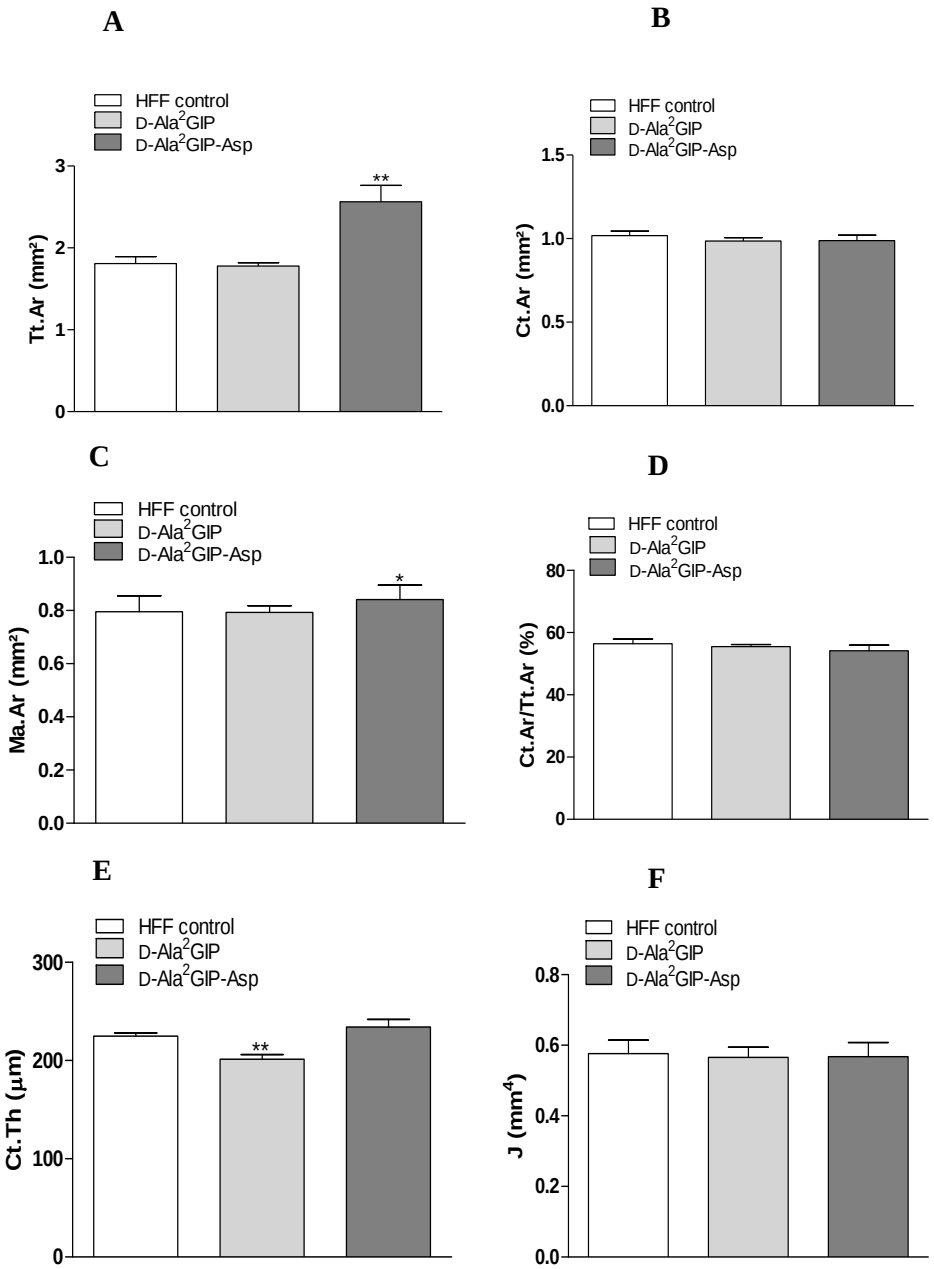

Images of cortical bone were obtained from a microtomography scan of tibia following 42 days once daily administration of saline (0.9%, w/v, NaCl), (D-Ala^2)GIP or (D-Ala^2)GIP-Asp (each at 25 nmol/kg b.w). Cortical bone was located 3 mm below growth plate and total area (A), cortical area (B), bone marrow diameter (C) cortical thickness (D), bone mineralisation (E) and moment of inertia (F) were measured. Values are mean ± S.E.M for 5 mice. *$p < 0.05$, **$p < 0.01$ compared to high-fat fed control.

Figure 4.11 Effects of once daily administration of (D-Ala^2)GIP and (D-Ala^2)GIP-Asp on bone tissue parameters in high-fat fed mice

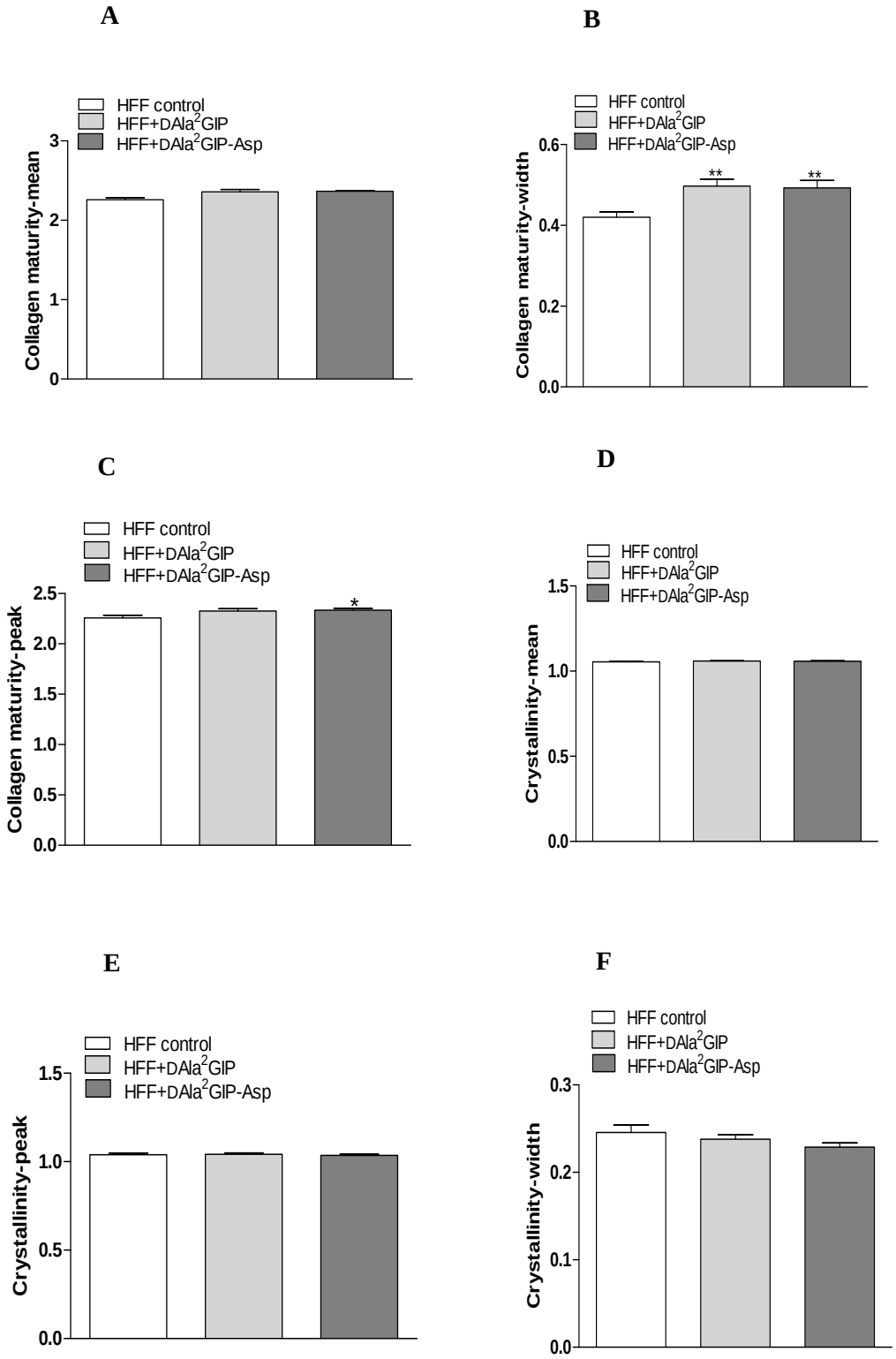

G

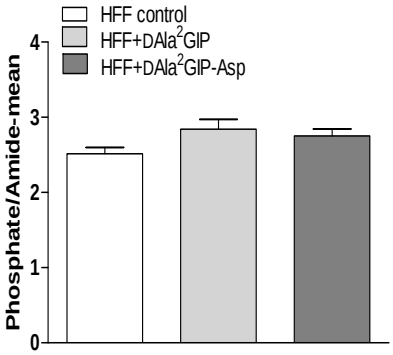
HFF control
HFF+DAla2GIP
HFF+DAla2GIP-Asp
Phosphate/Amide-mean
0
1
2
3
4

H

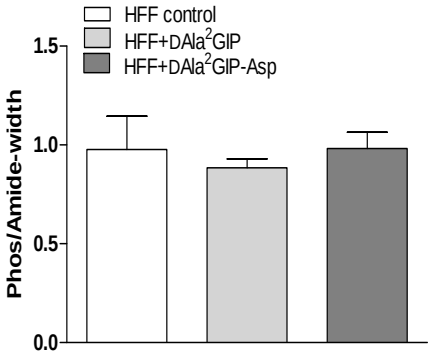
HFF control
HFF+DAla2GIP
HFF+DAla2GIP-Asp
Phos/Amide-width
0.0
0.5
1.0
1.5

I

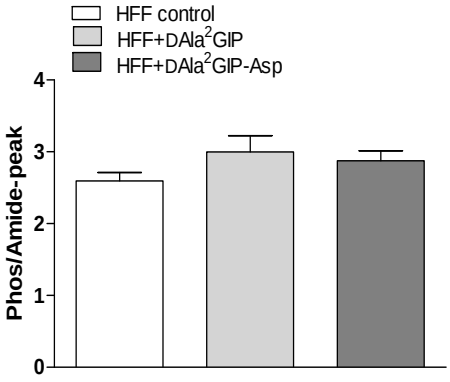
HFF control
HFF+DAla2GIP
HFF+DAla2GIP-Asp
Phos/Amide-peak
0
1
2
3
4

J

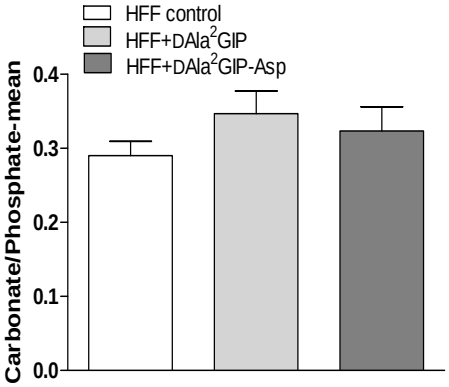
HFF control
HFF+DAla2GIP
HFF+DAla2GIP-Asp
Carbonate/Phosphate-mean
0.0
0.1
0.2
0.3
0.4

K

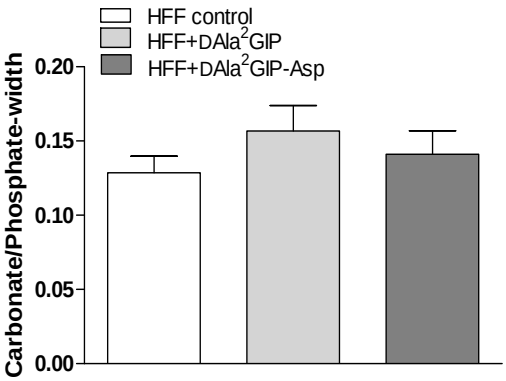
HFF control
HFF+DAla2GIP
HFF+DAla2GIP-Asp
Carbonate/Phosphate-width
0.00
0.05
0.10
0.15
0.20

L

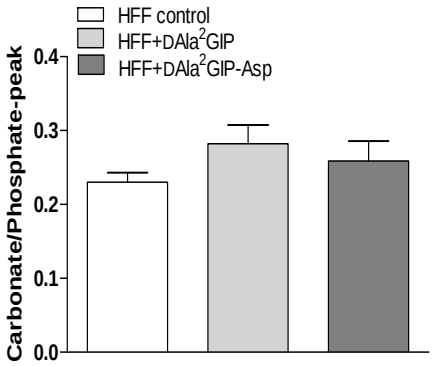
HFF control
HFF+DAla2GIP
HFF+DAla2GIP-Asp
Carbonate/Phosphate-peak
0.0
0.1
0.2
0.3
0.4

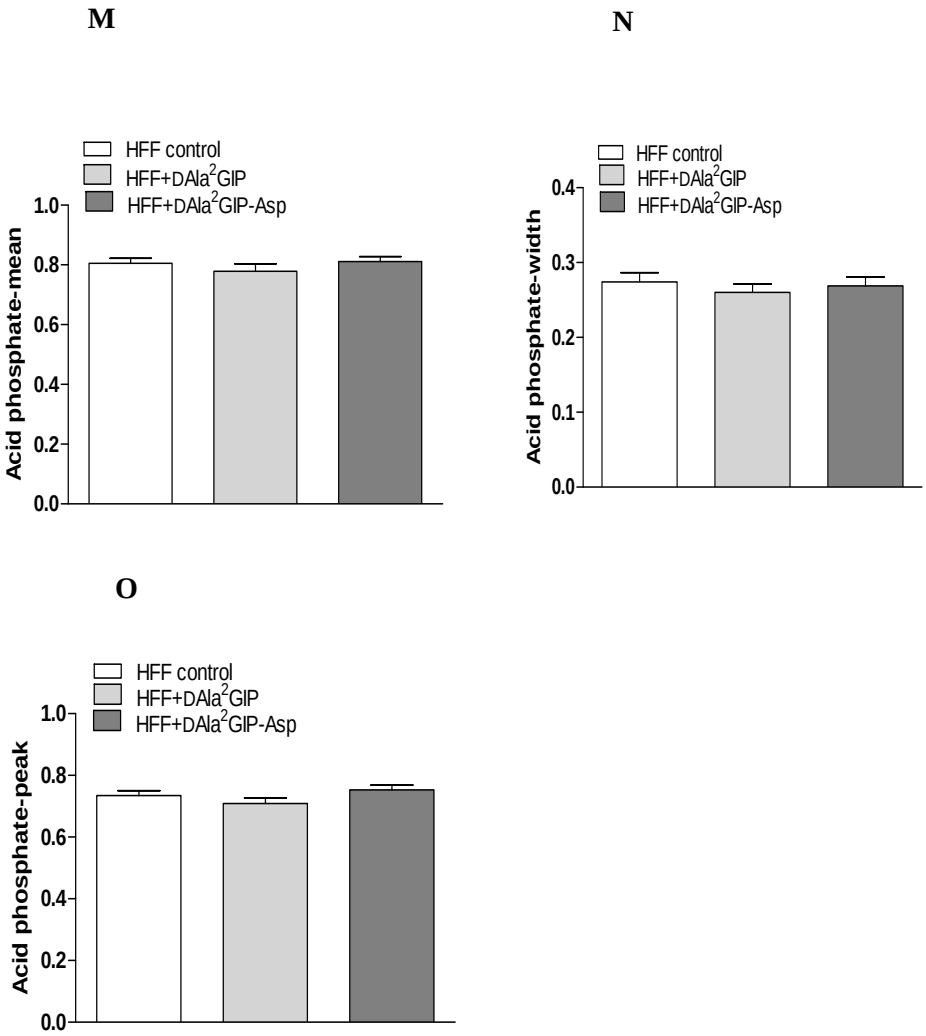

(A) Collagen maturity-mean, (B) collagen maturity width, (C) collagen maturity-peak, (D) crystallinity-mean, (E) crystallinity-width, (F) crystallinity-peak, (G) phosphate/amide-mean, (H) phosphate/amide-width, (I) phosphate/amide peak, (J) carbonate/phosphate-mean, (K) carbonate/phosphate-width, (L) carbonate/phosphate-peak, (M) acid/phosphate-mean, (N) acid/phosphate-width, and (O) acid/phosphate-peak were measured by infrared spectroscopy following 42 days once daily administration of saline (0.9%, w/v, NaCl), (D-Ala^2)GIP and (D-Ala^2)GIP-Asp (each at 25 nmol/kg b.w). Values are mean ± S.E.M for 5 mice. *$p<0.05$, **$p<0.01$ compared with high-fat fed control.

Chapter 5

Impact of bone-specific, enzymatically stable xenin peptides on metabolic control as well as bone quality and strength in lean control and high-fat fed mice

5.1 SUMMARY

Peptide based therapies are often restricted by number of factors, including rapid enzymatic degradation and renal clearance. Hence, in the current chapter, the effects of modified, long-acting and enzyme-resistant bone-specific peptides on metabolism, bone quality and bone strength was examined in lean and high fat fed mice. Once daily administration of xenin-25[Lys^{13}PAL] did not cause any significant changes in any of the body weight, food intake or any of metabolic parameters assessed in lean mice. However, Xenin-25[Lys^{13}PAL] increased ($p<0.05$) lumbar BMD and tibial BMC in lean mice. Interestingly, three-point bending analysis revealed a reduction ($p<0.01$) in ultimate load bearing capacity of femoral cortical bone following 42 days treatment with Xenin-25[Lys^{13}PAL] in lean mice. Xenin-25[Lys^{13}PAL] treated lean mice also had reduced ($p<0.05$) trabecular bone volume and number. In addition, Xenin-25[Lys^{13}PAL] induced significant ($p<0.05$ to $p<0.01$) increases in hardness, indentation modulus and force, with no change in dissipated energy, of cortical bone matrix in lean mice. However, collagen maturity, carbonate phosphate ratio and carbonate substitution were reduced ($p<0.01$) following once daily treatment of Xenin-25[Lys^{13}PAL] in lean mice. In high-fat fed mice, Xenin-25[Lys^{13}PAL], and its related bone-targeting form Xenin-25[Lys^{13}PAL]-Asp, did not cause any significant changes in body weight, fat mass, lean mass or food intake. Xenin-25[Lys^{13}PAL] and xenin-25[Lys^{13}PAL]-Asp reduced ($p<0.05$) circulating blood glucose but there was no change in plasma insulin concentrations in high-fat fed mice. Both Xenin-25[Lys^{13}PAL] and Xenin-25[Lys^{13}PAL]-Asp improved glucose tolerance, despite decreased glucose-stimulated insulin concentrations in high fat fed mice. This suggested improved insulin sensitivity, which was corroborated by injection of exogenous insulin into these high fat fed mice.

DEXA analysis revealed that both peptides increased ($p<0.05$ to $p<0.001$) lumbar spine BMC, with Xenin-25[Lys^{13}PAL] also increasing ($p<0.05$) whole body as well as tibial BMC in high fat mice. No changes were observed on nanomechanical properties of cortical bone matrix or cortical bone mineral density distribution in Xenin-25[Lys^{13}PAL] and Xenin-25[Lys^{13}PAL]-Asp treated high fat mice. However, Xenin-25[Lys^{13}PAL] increased ($p<0.05$ to $p<0.01$) crystallinity, phosphate/amide ratio, acid/phosphate ratio and carbon content of bone in high fat fed mice. No effect of Xenin-25[Lys^{13}PAL] and Xenin-25[Lys^{13}PAL]-Asp was seen on trabecular thickness. However, numbers of trabeculae were reduced in mice treated with Xenin-25[Lys^{13}PAL] and Xenin-25[Lys^{13}PAL]-Asp. Cortical microarchitecture parameters of the bone such as total area, cortical area, bone marrow diameter, cortical thickness, bone mineralization and moment of inertia remain unaffected in the mice treated with Xenin-25[Lys^{13}PAL] and Xenin-25[Lys^{13}PAL]-Asp. In conclusion, activation of xenin pathways appeared to improve overall metabolic control in lean and high fat fed mice, but had variable effects on the specific bone parameters assessed.

5.2 INTRODUCTION

Bone is highly complex, living mineralized material and undergoes constant remodeling (Elnenaei *et al*. 2010). Bone remodelling is under complex regulation from various autocrine and paracrine factors. In this regard, recent evidence suggests a role for gastrointestinal (GIT) hormones in bone remodelling (Guadin-Adrian *et al*. 2012). In addition, altered secretion and action of these GIT hormones has been implicated in the pathogenesis of diabetes (Adamska *et al*. 2014, Choudhury *et al*. 2016). Thus, there has been growing interest to understand the mechanisms involved in diabetic related bone loss, and to

develop new therapies to tackle bone fragility fractures in diabetes, where GIT hormones could be key (Moseley 2012). A variable increase in fracture risk has been reported in diabetes of around 20%, but this appears to be highly dependent on skeletal site and diabetes duration (Moayeri *et al*. 2017, Russo *et al*. 2016). Indeed, the detrimental effects of chronically elevated glucose levels on bone should be added to the more well-known complications of diabetes (Oie el al. 2015). As such, the longer the disease duration, presence of diabetic complications, inadequate glycemic control, insulin use and increased risk of falls are all reported to increase fracture risk in diabetes (Moayeri *et al* 2017).

Xenin, a 25 amino acid peptide hormone co-secreted with GIP from the intestinal K-cells in response to food intake (Anlauf *et al*., 2000), is known to enhance the insulin secretory action of GIP (Taylor *et al*. 2010, Wice *et al* 2010, Chowdhury *et al*. 2014). This has resulted in a recent upsurge in interest in the therapeutic capacity of xenin for type 2 diabetes (Hasib *et al*. 2017), since reduced biological activity of GIP is known to be an important characteristic of type 2 diabetic patients (McIntosh 2017, Wang *et al*. 2017). However, native xenin is rapidly broken by serine proteases in blood (Taylor *et al*., 2010), but like other gut-derived peptide hormones, stable xenin derivatives have been generated (Gault *et al*. 2015, Parthsarthy *et al*. 2016, Hasib *et al*. 2017). In addition, there is no specific receptor reported for xenin to date, but there is some evidence to suggest that the actions of xenin could be linked to modulation of neurotensin receptors (Clemens *et al*. 1997; Nustede *et al*. 1999; Kim and Mizuno, 2010a). It has been also reported that xenin potentiates GIP-mediated insulin secretion by activating non-ganglionic cholinergic neurons (Wice *et al*. 2010). Given the GIP potentiating effect of xenin, and the notable action of GIP on bone (Holst *et al*. 2016, Hansen *et al*. 2017) the

possibility that xenin might have positive direct or indirect effects on the bone requires further investigation.

Bone is unique tissue because it is mostly composed of the inorganic compound hydroxyapatite (Florencio-Silva *et al*. 2015, Wu *et al*. 2017). Therefore, targeting a drug to hydroxyapatetite would appear to be the most promising approach for selective drug delivery to bone (Takahashi-Nishioka *et al*. 2008). There has been increased interest in use of amino acid oligopeptide tagging (Glu and Asp) that can help deliver the peptides to bones, due to preferential peptide deposition in hydroxyapatite (Takahashi-Nishioka *et al*. 2008). Acidic oligopeptides tagging is a new approach where repetitive L-Asp and L-Glu acidic amino acid sequences will rapidly bind to hydroxyapaptite in bone (Lips 2001 and Teitelbaum & Ross 2003). With this idea in mind, in the present study, the well characterised stable xenin analogue, xenin-25[Lys^{13}PAL] (Martin *et al*. 2014, Gault *et al*. 2015, Hasib *et al*. 2017), and its oligopeptide tagged counterpart, namely xenin-25[Lys^{13}PAL]-Asp with six C-terminal aspartic acid amino acid residues extensions, were synthesised and characterised.

These peptides were then taken forward to experiments in lean control and high fat fed mice, using a once daily injection regimen. Thus, xenin-25[Lys^{13}PAL] has previously been shown to exert prominent antidiabetic effects following once daily dosing in mice (Irwin & Flatt 2015, Gault *et al*. 2015, Hasib *et al*. 2017). The aim was to investigate the effects of xenin-25[Lys^{13}PAL] on metabolic control and bone related parameters under normal physiological conditions, and similarly under the pathophysiology of diet-induced diabetes whilst also employing oligopeptide tagging of the test peptide. Highly advanced imaging techniques were used to assess bone quality and strength following 42 days administration of the respective peptides in each mouse model. These techniques included bone

three-point bending, nanoindentation, quantitative backscattered electron imaging (QBEI) and fourier transformed infrared microscopy (FTIR) imaging. The findings of this study reveal that xenin-25[Lys^{13}PAL] and xenin-25[Lys^{13}PAL]-Asp possesses positive effects on diabetes control and bone health in high fat fed mice.

5.3 MATERIALS AND METHODS

5.3.1 Synthesis of peptides

Xenin-25[Lys^{13}PAL] and xenin-25[Lys^{13}PAL]-Asp were purchased from EZ Biolabs Ltd. (Carmel, IN, USA). The peptides were characterised in-house by mass spectrometry as described in Section 2.1.2.

5.3.2 Animal study design

Two separate *in-vivo* studies were carried out as part of these studies. In the first study, high fat fed mice were used, and in the second study the effects of test peptides lean mice was examined. All studies used male NIH Swiss male mice (12-14 week old), and for high fat studies mice (8 week old) were maintained on high-fat diet for three months. All mice were housed separately in air conditioned room with 12 hour light and 12 hour dark cycle. All mice were grouped (n=5-6) according body weight and blood glucose. Prior to commencing the experiment, all mice were injected with saline vehicle (0.9% NaCl) for 3 days to acclimatise to the injection regimen. Lean control mice received saline injection (0.9%NaCl) and Xenin-25[Lys^{13}PAL]. Groups of high fat fed mice then received saline injection (0.9% NaCl), xenin-25[Lys^{13}PAL] or xenin-25[Lys^{13}PAL]-Asp (each at 25 nmol/kg bw) once daily for 42 days. Body weight, food intake, non-fasting glucose and insulin concentrations were measured at regular intervals.

Intraperitoneal glucose tolerance (18 mmol/kg bw, 18 hour fast) and non-fasting insulin sensitivity test (25 U/kg bw) tests were performed at the end of the study as described in Section 2.3.2 and 2.3.3 respectively. Bones were then collected and processed to assess bone mass and bone quality. All experiments were carried out according to UK Home Office Regulations (UK Animals Scientific Procedures Act 1986).

5.3.3 Measurement of plasma insulin

An insulin RIA was carried out as described in Section 2.4.2 to determine plasma insulin concentrations.

5.3.4 Measurement of body composition, bone density and mineral content by DEXA scanning

Mice were anesthetised using isoflurane before being placed on a specimen tray of the DEXA scanner. Bone mineral density (BMD), bone mineral content (BMC), lean mass, fat and lean masses were determined as explained in Section 2.4.

5.3.5 Three-point bending test

Mechanical properties of the femur were measured using three-point bending. The properties determined were ultimate load, ultimate displacement, stiffness and work to failure ratio. Before carrying out studies, femurs were kept in vials containing saline (NaCl, 0.9%) so that they remained hydrated. Three-point bending was carried out as described in Section 2.5.4.

5.3.6 X-ray microcomputed tomography (µCT)

Microcomputed tomography was used to process the tibias of all the mice. Tibias were further scanned to assess trabecular bone mass, trabecular bone thickness, number of trabeculae, cortical bone diameter, cortical thickness, diameter of bone marrow and cross-sectional moment of inertia as described in Section 2.5.3.

5.3.7 Nanoindentation

Nanoindentation was performed on all the bones as described in the Section 2.5.1 and following parameters were assessed: maximum force, hardness, indentation modulus and dissipated energy. Briefly, polymethylacrylate blocks of bone were polished three times with diamond particles to obtain a smooth surface. Afterwards, blocks were left in saline (NaCl, 0.9%) solution overnight and processed next morning.

5.3.8 Quantitative backscattered electron imaging (qBEI)

Polymethylmethacrylate blocks were again polished three times with diamond particles, and were then subjected to carbon coating for 4 hrs. After carbon coating, the polymethylacrylate blocks were observed under a scanning electron microscope as described in Section 2.5.2 to assess bone mineral density distribution.

5.3.9 Fourier transformed infrared (FT-IR) imaging and micro spectroscopy

FT-IR was carried out as per described in section 2.5.5. Briefly, polymethylacrylate sections (4 µm) of bones were prepared using micrtome equipped with tungsten carbide knife. Spectral analysis was conducted using a Bruker Vertex 70 spectrometer interfaced with Bruker Hyperion 3000 infrared microscope equipped with mercury cadmium telluride detector. Infrared spectra were recorded with an average of 32 scans in transmission mode in the same locations (region of interest on the bone) as for qBEI and nanoindentation.

5.3.10 Statistical analysis

Data were analysed using one-way or two-way ANOVA with two-tailed t-tests using PRISM 5.0. Data are expressed as mean ± S.E.M and a P value < 0.05 was considered statistically significant.

5.4 RESULTS

5.4.1 Effects of Xenin-25[Lys^{13}PAL] on body weight, fat mass, total lean mass and food intake in lean mice

Once daily administration of Xenin-25[Lys^{13}PAL] did not cause any significant changes in body weight (Figure 5.1A), fat mass (Figure 5.1B), lean mass (Figure 5.1C) or food intake (Figure 5.2) in lean mice.

5.4.2 Effects of Xenin-25[Lys^{13}PAL] on circulating blood glucose and plasma insulin in lean mice

There was no significant difference between groups of lean mice in terms of circulating blood glucose (Figure 5.3A) or plasma insulin (Figure 5.3B) concentrations.

5.4.3 Effects of Xenin-25[Lys^{13}PAL] on glucose tolerance and insulin sensitivity in lean mice

After injecting glucose intraperitoneally (18 mmol/kg bw) on day 42, blood glucose levels were not affected by Xenin-25[Lys^{13}PAL] treatment (Figure 5.4A, B). Similarly, glucose-induced insulin concentrations were not significantly different between control and treated mice (Figure 5.4C, D). In addition, no change in the action of peripherally injected insulin was observed (Figure 5.5).

5.4.4 DEXA analysis of whole body, femur, tibia and lumbar spine in lean mice

DEXA analysis revealed that there was no significant difference in femoral BMD and BMC but the whole body BMC was increased ($p<0.05$) in Xenin-25[Lys^{13}PAL] treated lean mice (Figure 5.6A-D). No differences were observed in lumbar BMC (Figure 5.7B) however, xenin-25[Lys^{13}PAL] decreased ($p<0.05$) lumbar BMD compared to saline controls (Figure 5.7A). In addition, tibial BMD was no different between groups (Figure 5.8A), but tibial BMC was increased ($p<0.05$) by xenin-25[Lys^{13}PAL] treatment in lean mice (Figure 5.8B).

5.4.5 Effects of Xenin-25[Lys^{13}PAL] on trabecular bone morphology and cortical bone geometry in lean mice

Microcomputed tomography (MicroCT) was carried out to analyse different parameters of the bone including trabecular bone volume, thickness, separation and number of trabeculae. Xenin-25[Lys^{13}PAL] treated lean mice showed a reduction ($p<0.05$) in both bone volume and number of trabeculae (Figure 5.9A, C). In addition, Xenin-25[Lys^{13}PAL] did not affect trabecular thickness (Figure 5.9D), but increased ($p<0.05$) trabecular separation (Figure 5.9D). Cortical bone geometry parameters including total area, cortical area, bone marrow diameter, cortical thickness, bone mineralisation and moment of inertia were not affected by Xenin-25[Lys^{13}PAL] treatment for 42 days in lean mice (Figure 5.10A-F).

5.4.6 Effects of Xenin-25[Lys^{13}PAL] on whole-bone mechanical properties in lean mice

Three-point bending analysis revealed a reduction ($p<0.05$) in ultimate load bearing capacity of femoral cortical bone following 42 days treatment with Xenin-25[Lys^{13}PAL] (Figure 5.11A). However, no significant changes in ultimate

displacement were observed (Figure 5.11.B). Xenin-25[Lys^{13}PAL] treated mice also had reduced ($p<0.01$) femoral cortical bone stiffness (Figure 5.11C). Work-to-failure ratio was similar between the two groups of lean mice (Figure 5.11D).

5.4.7 Effects of Xenin-25[Lys^{13}PAL] on nanomechanical properties of cortical bone matrix in lean mice

Xenin-25[Lys^{13}PAL] induced significant ($p<0.05$ to $p<0.01$) increases in hardness (Figure 5.12A), indentation modulus (Figure 5.12B), and force (Figure 5.12C), with no change in dissipated energy (Figure 5.12D), of cortical bone matrix in lean mice.

5.4.8 Effects of Xenin-25[Lys^{13}PAL] on bone mineral density distribution in lean mice

All the three variables analysed relating to bone mineral density distribution includi ng Ca_{peak}, Ca_{mean} and Ca_{width} at cortical parts of the tibial bone were similar in both groups of lean mice (Figure 5.13A-C).

5.4.9 Effects of Xenin-25[Lys^{13}PAL] on bone at tissue level in lean mice

Different parameters relating directly to the bone tissue were analysed using infrared spectroscopy. These parameters included collagen maturity, crystallinity, acid phosphate ratio, mineral to matrix ratio, carbonate phosphate ratio and carbonate substitution (Figure 5.14A-G). Among these, collagen maturity, carbonate phosphate ratio and carbonate substitution were reduced ($p<0.05$ to $p<0.01$) following once daily treatment with Xenin-25[Lys^{13}PAL] in lean mice.

5.4.10 Effects of Xenin-25[Lys^{13}PAL] and Xenin-25[Lys^{13}PAL]-Asp on body weight, fat mass, total lean mass and food intake in high-fat fed mice

Once daily administration of Xenin-25[Lys^{13}PAL] or Xenin-25[Lys^{13}PAL]-Asp did not cause any significant changes in body weight (Figure 5.15A), fat mass (Figure 5.15B), lean mass (Figure5.15C) or food intake (Figure 5.16) in high fat fed mice.

5.4.11 Effects of Xenin-25[Lys^{13}PAL] and Xenin-25[Lys^{13}PAL]-Asp on circulating blood glucose and plasma insulin in high-fat fed mice

In terms of blood glucose, Xenin-25[Lys^{13}PAL] and Xenin-25[Lys^{13}PAL]-Asp reduced ($p<0.05$) blood glucose by day 42 (Figure 5.17A), but there was no significant difference in plasma insulin concentrations between groups (Figure 5.17B).

5.4.12 Effects of Xenin-25[Lys^{13}PAL] and Xenin-25[Lys^{13}PAL]-Asp on glucose tolerance and insulin sensitivity in high-fat fed mice

After injecting glucose intraperitoneally (18 mmol/kg bw) on day 42, blood glucose was significantly ($p<0.05$ to $p<0.01$) reduced in all treatment groups when compared to saline controls at 30 and 60 mins post-injection (Figure 5.18 A). This corresponded to significantly ($p<0.001$) decreased AUC values in these mice when compared to saline controls (Figure 5.18B). No significant effect of the treatments was seen on individual plasma insulin concentrations at the time points examined (Figure 5.18C), however both Xenin-25[Lys^{13}PAL] and Xenin-25[Lys^{13}PAL]-Asp treated mice had significantly reduced ($p<0.05$ and $p<0.01$, respectively) overall insulin secretory response (Figure 5.18D). This effect was accompanied by significantly ($p<0.05$ to $p<0.01$) reduced individual and overall blood glucose values following injection of exogenous insulin in

both peptide treated groups when compared to high fat controls (Figure 5.19A).

5.4.13 DEXA analysis of whole body, femur, tibia and lumbar spine in high-fat fed mice

DEXA analysis revealed that there was no significant overall difference in whole body or femoral BMD between all groups of high fat fed mice (Figure 5.20A, C). However, whole body BMC was increased ($p<0.05$) by Xenin-25[Lys^{13}PAL] treatment (Figure 5.20B). In addition, no difference was observed in lumbar BMD (Figure 5.21A), but both treatment groups had elevated ($p<0.05$ to $p<0.01$) lumbar BMC compared to saline controls (Figure 5.21B). Similarly, tibial BMD was consistent among all groups of high fat mice (Figure 5.22.A), however tibial BMC was increased by Xenin-25[Lys^{13}PAL] treatment for 42 days (Figure 5.22.B).

5.4.14 Effects of Xenin-25[Lys^{13}PAL] and Xenin-25[Lys^{13}PAL]-Asp on trabecular bone morphology and cortical bone geometry in high-fat fed mice

Microcomputed tomography (MicroCT) was performed to analyse various parameters of the bone such as trabecular bone volume, thickness, trabecular separation and number of trabeculae. Xenin-25[Lys^{13}PAL] treated high fat fed mice showed reduction in bone volume ($p<0.01$) as well as number of trabeculae. Xenin-25[Lys^{13}PAL]-Asp treated high fat fed mice showed almost the same results as both bone volume ($p<0.05$) and number of trabeculae ($p<0.01$) were reduced (Figure 5.23A, C). Xenin-25[Lys^{13}PAL] and Xenin-25[Lys^{13}PAL]-Asp did not affect trabecular thickness (Figure 5.23B), but increased ($p<0.01$) trabecular separation (Figure 5.23D). Cortical bone geometry parameters such as total area, cortical area, bone marrow diameter, cortical thickness, bone mineralisation and moment of inertia remain unchanged by Xenin-25[Lys^{13}PAL]

and Xenin-25[Lys^{13}PAL]-Asp treatment for 42 days in high fat fed mice (Figure 5.24A-F).

5.4.15 Effects of Xenin-25[Lys^{13}PAL] and Xenin-25[Lys^{13}PAL]-Asp on whole-bone mechanical properties in high-fat fed mice

Three-point bending analysis was carried out to analyse ultimate load, stiffness, ultimate displacement and work-to-failure ratio. However, no significant changes were observed in any of these parameters (Figure 5.25A-D).

5.4.16 Effects of Xenin-25[Lys^{13}PAL] and Xenin-25[Lys^{13}PAL]-Asp on nanomechanical properties of cortical bone matrix in high-fat fed mice

No changes were detected in terms of hardness, indentation modulus, force and dissipated energy of cortical bone matrix in Xenin-25[Lys^{13}PAL] and Xenin-25[Lys^{13}PAL]-Asp treated high fat fed mice (Figure 5.26A-D).

5.4.17 Effects of Xenin-25[Lys^{13}PAL] and Xenin-25[Lys^{13}PAL]-Asp on bone mineral density distribution in high-fat fed mice

All the three variables analysed relating to cortical bone mineral density distribution including Ca_{peak}, Ca_{mean} and Ca_{width} in high-fat fed mice were unaffected in both treatment groups when compared to saline controls (Figure 5.27A-C).

5.4.18 Effects of Xenin-25[Lys^{13}PAL] and Xenin-25[Lys^{13}PAL]-Asp on bone at tissue level in high-fat fed mice

Infrared spectroscopy was used to analyse different parameters related directly to the bone tissue. These parameters included collagen maturity, crystallinity, phosphate amide ratio and acid phosphate ratio (Figure 5.28A-J). Crystallinity, phosphate/amide ratio, acid/phosphate ratio, carbon content and acid phosphate

were increased ($p<0.05$ to $p<0.01$) in the mice treated with Xenin-25[Lys^{13}PAL] (Figure5.28D, F, G, I). Interestingly, Xenin-25[Lys^{13}PAL]-Asp decreased ($p<0.05$) collagen maturity (Figure 5.28B), but had no effect on any of the other variables assessed.

5.5 DISCUSSION

Xenin is a hormone co-secreted with GIP from a subset of enteroendocrine K cells (Althage *et al*. 2008, Hasib *et al*. 2017), and enhances the biological activity of GIP (Martin *et al*. 2016). As such, numerous previous studies confirm the GIP-potentiating effects of xenin in normal and type 2 diabetes conditions (Taylor *et al*. 2010, Wice *et al*. 2010, Martin *et al*. 2014 and Choudhary *et al*. 2016). There is also evidence to suggest that xenin acts as an independent satiety hormone in animals (Cline *et al*. 2007, Cooke *et al*. 2009, Taylor *et al*. 2010 and Kim *et al*. 2016) and humans (Schiavo-Cadozo *et al*. 2013). Given this, it is plausible that xenin could affect bone metabolism in its own right, or as a consequence of its GIP enhancing actions. To date, there has been absolutely no investigation into the effects of xenin on bone.

It is already reported that, with the help of amino acid acidic oligopeptide tagging, peptides can be preferentially delivered to the bone because of the affinity of the acidic oligopeptides towards hydroxyapetite (Lips 2001, Teitelbaum & Ross 2003, Takahashi-Nishioka *et al*. 2008). With this idea, the present study was undertaken to assess the impact of enzymatically stable xenin peptide, Xenin-25[Lys^{13}PAL], on metabolic control as well as bone quality and strength in lean mice. In addition, acidic oligopeptide tagging of Xenin-25[Lys^{13}PAL] was employed and the impact of this on high fat fed mice examined.

The xenin peptides had no impact on body weight or food intake in lean and high fat fed mice following 42 days daily administration of 25 nmol/kg body weight. Thus, xenin has been shown to induce appetite suppression, but only at much higher doses than those employed for this study (Kaji *et al*. 2017). Interestingly, Xenin-25[Lys^{13}PAL] had no effect on glucose or insulin levels in lean mice, but significantly reduced circulating glucose in high fat fed mice. As such, the suggestion that xenin does not possess important biological actions in type 2 diabetes, appears to be unfounded. Furthermore, glucose tolerance and insulin sensitivity were substantially improved by Xenin-25[Lys^{13}PAL] in high fat fed mice, in full agreement with previous observations (Gault *et al*. 2015, Martin *et al*. 2016 and Hasib *et al*. 2017). Xenin-25[Lys^{13}PAL] had no real impact on metabolic control in lean mice, likely because no pathologies are apparent here.

DEXA analysis of lean mice on day 42 revealed no difference in whole body and femoral BMC and BMD. However, lumbar BMD was decreased and tibial BMC were increased by Xenin-25[Lys^{13}PAL]. These inconsistencies in terms of BMC indicate the need for further detailed study, or the possibility that xenin differentially affects bone regions. In terms of high fat fed mice, DEXA analyses revealed that no significant difference in whole body and femoral BMD; however, whole body BMC was increased by Xenin-25[Lys^{13}PAL], but not by Xenin-25[Lys^{13}PAL]-Asp. However, lumbar BMC was augmented by Xenin-25[Lys^{13}PAL] and Xenin-25[Lys^{13}PAL]-Asp, whereas Tibial BMC was increased only by Xenin-25[Lys^{13}PAL] treatment. In type-2 diabetic patients, BMD is believed to be higher than the normal (Janghorbani *et al*. 2007, Vestergaard, 2007) and fracture risk is often misjudged in this population, which could also be true for the high-fat fed mice used in this study. Thus, the observed effects on BMD, and especially BMC,

need to be considered in this context. As such, bone quality does not depend only on BMD and BMC as there are many other factors such as microarchitecture, bone matrix composition, biomechanical strength that play an important role in overall bone quality and integrity (Hernandez & Keaveny 2006, Seeman & Delmas 2006, Mieczkowska *et al*. 2013). This may also help explain the differences observed between treatment with Xenin-25[Lys^{13}PAL] and Xenin-25[Lys^{13}PAL]-Asp in high fat fed mice. In order to gain a deeper insight of bone quality at tissue level, more detailed bone-specific investigations were undertaken.

MicroCT was performed to assess trabecular bone volume, thickness, separation and number of trabeculae in the bone. Interestingly, in normal lean mice it was found that the number of trabeculae and trabecular bone volume were reduced by Xenin-25[Lys^{13}PAL], and trabecular separation increased. This might suggest a negative impact of xenin signalling on bone under normal physiological conditions. In high fat fed mice, micocomputed tomography results revealed reduction in bone volume and number of trabeculae. However, trabecular separation was increased in the mice after treatment with Xenin-25[Lys^{13}PAL] and Xenin-25[Lys^{13}PAL]-Asp. Cortical bone parameters were assessed to further understand the possible differential actions of Xenin-25[Lys^{13}PAL] and Xenin-25[Lys^{13}PAL]-Asp on bone in diabetes (Pickle *et al*. 2016, Shanbhogue *et al*. 2016, Samelson *et al*. 2017). None of the cortical bone parameters showed any changes after treatment with both Xenin-25[Lys^{13}PAL] and Xenin-25[Lys^{13}PAL]-Asp. However, treatment of high-fat fed mice with Xenin-25[Lys^{13}PAL] or Xenin-25[Lys^{13}PAL]-Asp had no effect on the nanomechanical properties of cortical bone and bone mineral density distribution. On the other hand, Xenin-25[Lys^{13}PAL] induced significant benefits on the nanomechanical properties of

cortical bone including increase in hardness, indentation modulus and force. Interestingly, this mirrors with similar observations in GIP receptor KO mice (Meiczkowska *et al*. 2013, Gaudin-Audrain *et al*. 2013), and rodents treated with stable GIP receptor mimetics (Mansur *et al*. 2016, Ramsey *et al*. 2017, Hansen *et al*. 2017). Thus, in contrast to effects on trabecular bone, this would suggest benefits of xenin signalling in bone. Again, the idea that xenin may have differential effects on bone is strongly suggested here, and requires further detailed study. Indeed, the impact of xenin in combination with GIP merits investigation, given their biological interplay (Parthsarthy *et al*. 2016).

Infrared spectroscopy was performed in to analyse collagen maturity, crystallinity, phosphate amide ratio, acid phosphate ratio and carbon content (Schimdt *et al*. 2017). This analysis revealed contrasting effects of Xenin-25[Lys^{13}PAL] in lean control and high fat fed mice. Thus, in lean mice there were reductions in crystallinity, carbonate/phosphate ratio and carbonate substitutions, all of which imply reduced bone quality (Gourion-Arsiquaud *et al*. 2012, Wang *et al*. 2016). Whereas in high fat fed mice, Xenin-25[Lys^{13}PAL] actually increased crystallinity of the bone tissue, phosphate/amide ratio and carbon content. Thus, as noted previously, and although not fully consistent with all data collected here, there is a suggestion that xenin has altered biological effects under diabetic conditions (Khan *et al*. 2017, Sterl *et al*. 2016). This could be one reasonable explanation for the very contrasting data on bone tissue properties in lean control and high fat fed mice. Further to this, Xenin-25[Lys^{13}PAL]-Asp was generated in an effort to enhance xenin-induced actions on bone. In contrast, Xenin-25[Lys^{13}PAL]-Asp lacked any positive effects on bone tissue properties and actually decreased collagen maturity in high fat fed mice. This is extremely hard to comprehend, and

sophisticated imaging studies would be required to establish the fate of Xenin-25[Lys^{13}PAL]-Asp after injection. Indeed, fatty acid derivation may in some way impede the actions of acidic oligopeptide tagging to deposit the peptide in bone, likely through stearic hindrance (Narayana *et al*. 2015).

In conclusion, Xenin-25[Lys^{13}PAL] and Xenin-25[Lys^{13}PAL]-Asp possessed beneficial metabolic effects in high fat fed mice. Xenin-25[Lys^{13}PAL] appeared to have a positive impact on bone health in diabetes, but inconsistent effects on bone under normal physiological conditions. Engineering of a bone-specific xenin analogue, namely Xenin-25[Lys^{13}PAL]-Asp, did not appear to further enhance the benefits of xenin on diabetic bone. Further detailed studies are needed to fully assess whether the current peptides, Xenin-25[Lys^{13}PAL] and Xenin-25[Lys^{13}PAL]-Asp, can be used as potential therapeutic candidates for individuals affected with diabetes and bone disorders.

Figure 5.1 Effects of once daily administration of Xenin-25[Lys^{13}PAL] for 42 days on (A) body weight (B) % fat and (C) total lean mass in lean mice

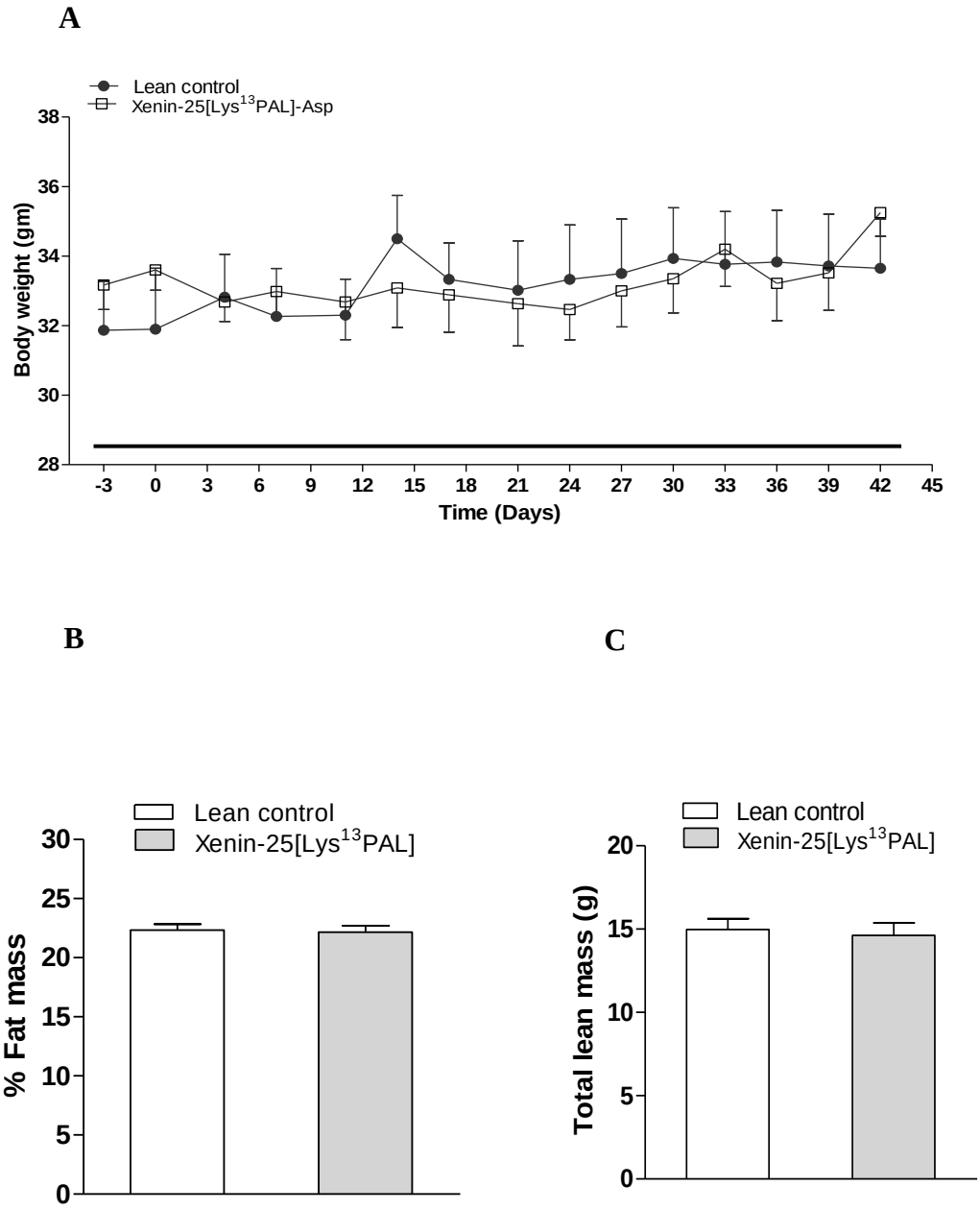

(A) Body weight was measured for 3 days before and 42 days during (indicated by black horizontal bar) once daily treatment with saline vehicle (0.9%w/v NaCl) or Xenin-25[Lys^{13}PAL] (peptide at 25 nmol/kg bw). (B) %Fat mass and (C) lean mass as measured by DEXA scanning in lean mice on day 42 Values represent means ± SEM for 6 mice.

Figure 5.2 Effects of once daily administration of Xenin-25[Lys^{13}PAL] for 42 days on cumulative energy intake in lean mice

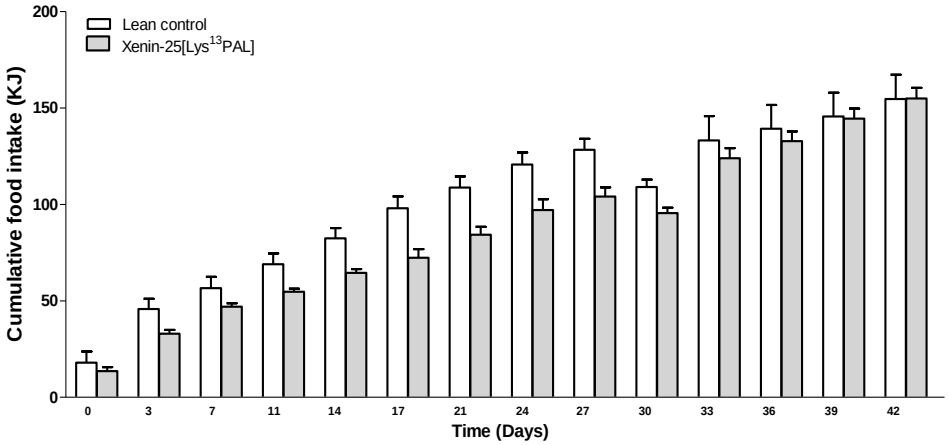

Cumulative energy intake was measured for 3 days before and 42 days during once daily treatment with saline vehicle (0.9% w/v NaCl) or Xenin-25[Lys^{13}PAL] (peptide at 25 nmol/kg bw). Values represent means ± SEM for 6 mice.

Figure 5.3 Effects of once daily administration of Xenin-25[Lys^{13}PAL] for 42 days on non-fasting (A) glucose and (B) insulin concentrations in lean mice

A

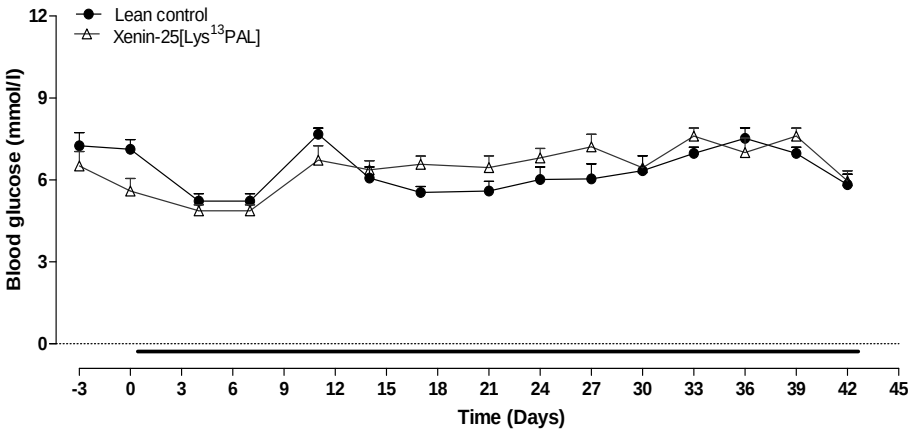

B

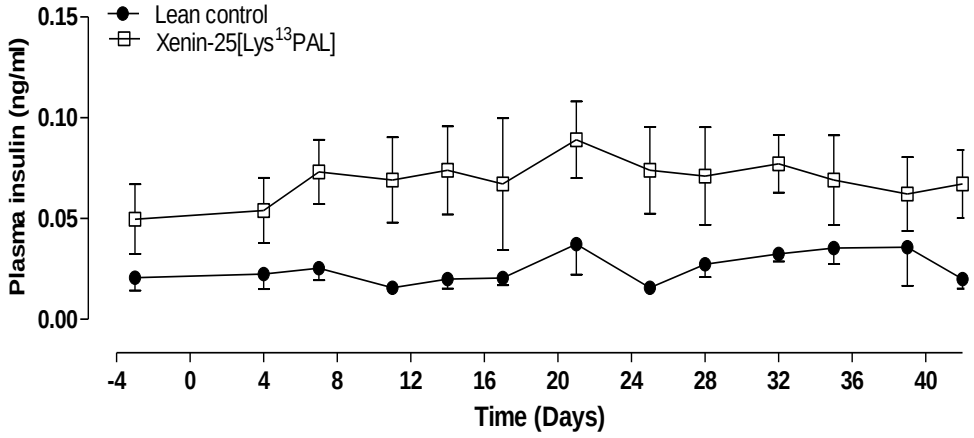

(A) Blood glucose and (B) plasma insulin were measured for 3 days before and 42 days during once daily treatment with saline vehicle (0.9%w/v NaCl) or Xenin-25[Lys^{13}PAL] (peptide at 25 nmol/kg bw). Values represent means ± SEM for 7 mice.

Figure 5.4 Effects of once daily administration of Xenin-25[Lys^{13}PAL] for 42 days on (A) glucose tolerance and (B) plasma insulin response to glucose in lean mice

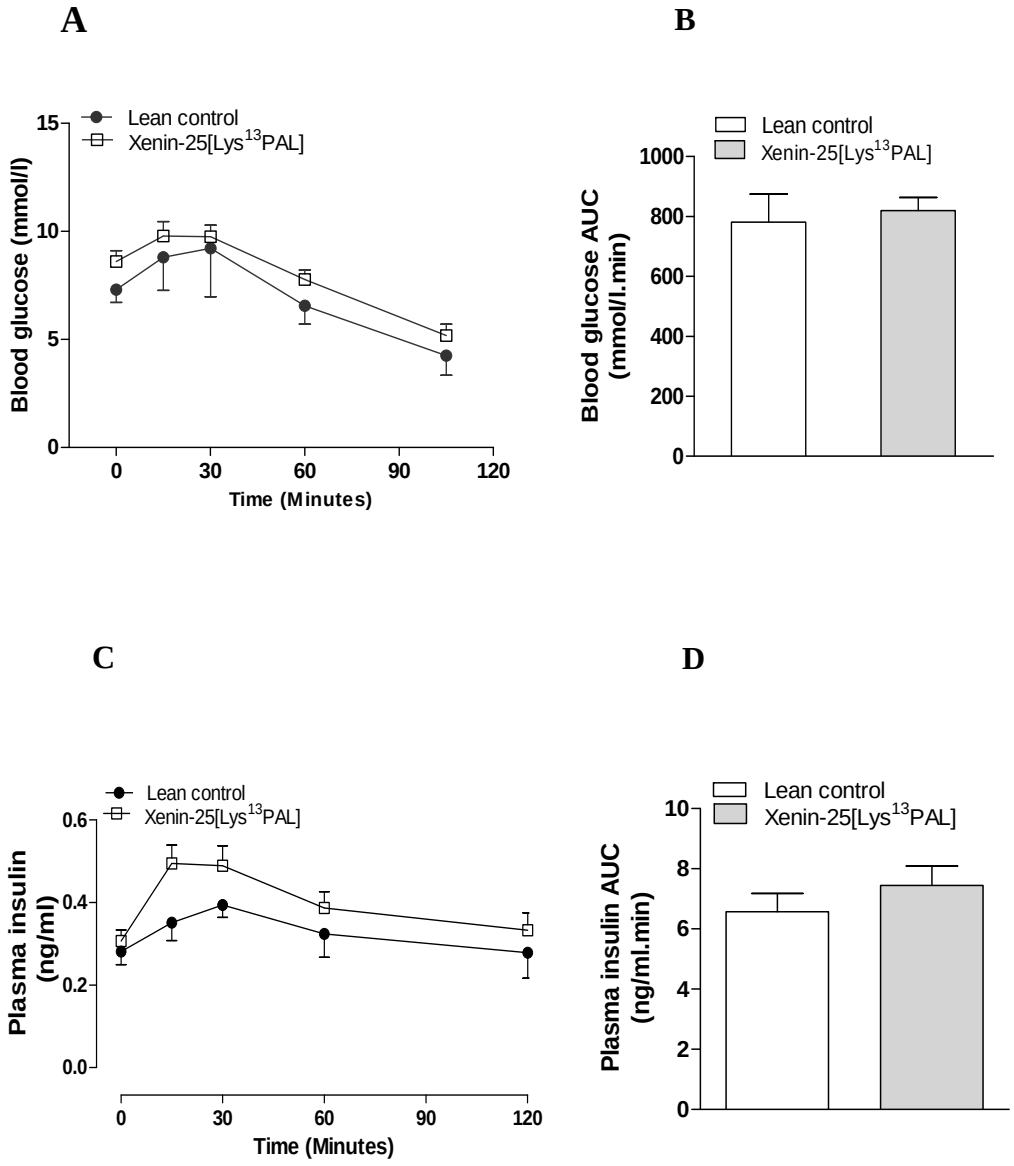

Tests were conducted after once daily treatment with saline or Xenin-25[Lys^{13}PAL] for 42 days. (A) Blood glucose before and after i.p injection of glucose (18 mmol/kg bw) alone in 18 hrs fasted mice. (B) AUC values for blood glucose for 0-120 min are shown. (C) Glucose alone (18 mmol/kg b.w) was administered at time 0 in 18 hrs fasted mice and plasma insulin concentrations prior to, and 15, 30, 60 and 120 min after glucose administration were recorded. (D) Plasma insulin AUC values are also shown. Values are mean ± S.E.M for 6 mice.

Figure 5.5 Effects of once daily administration of Xenin-25[Lys^{13}PAL] for 42 days on insulin sensitivity lean mice

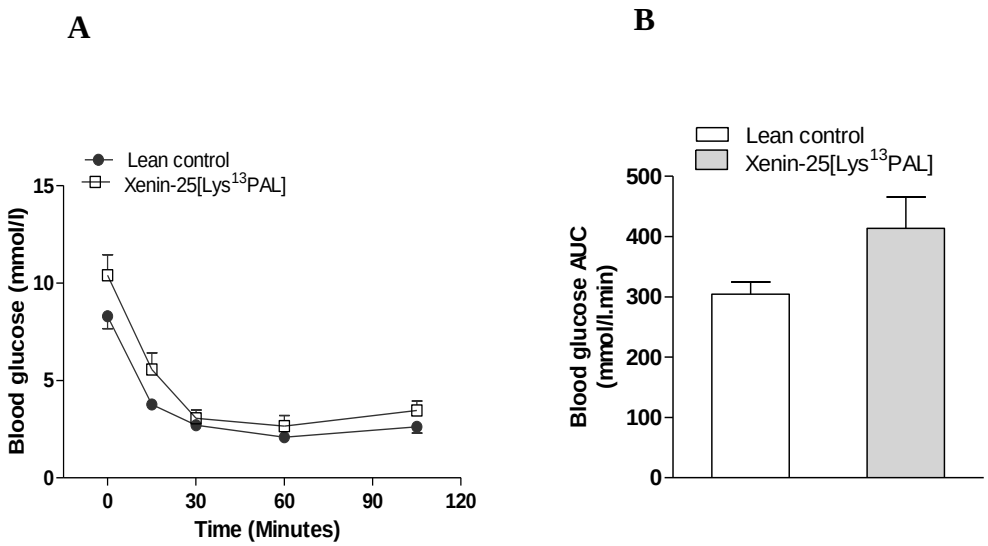

(A) Insulin (25 U/kg bw) was injected intraperitoneally (at t=0) in non-fasted mice following 42 days treatment with saline or Xenin-25[Lys^{13}PAL] (peptide at 25 nmol/kg bw). (B) Blood glucose AUC values for 0-120 min are shown. Values represent means ± SEM for 6 mice.

Figure 5.6 Effects of once daily administration of Xenin-25[Lys^{13}PAL] for 42 days on (A) whole body bone mineral density (BMD), (B) whole body bone mineral content (BMC), femur (A) bone mineral density (BMD) and (B) bone mineral content (BMC) in lean mice

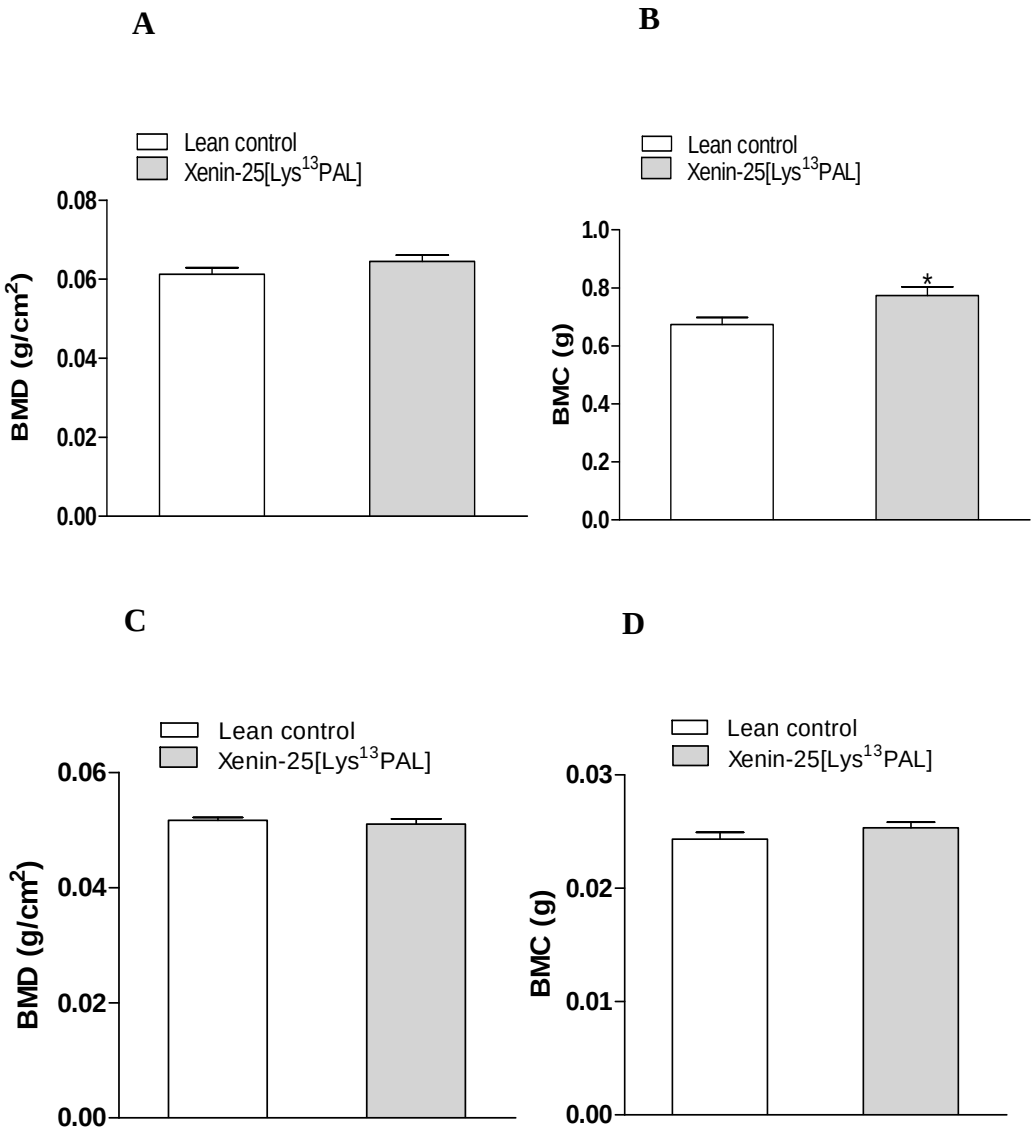

(A) Whole body bone mineral density (BMD) and (B) whole body bone mineral content (BMC) as measured by DEXA scanning in lean mice following 42 days treatment with Xenin-25[Lys^{13}PAL]. (C) Femur BMD and (D) femur BMC as measured by DEXA scanning in lean mice following 42 days treatment with Xenin-25[Lys^{13}PAL] (peptide at 25 nmol/kg bw). Values represent means ± SEM for 6 mice. $^{*}p < 0.05$ compared to lean control.

Figure 5.7 Effects of once daily administration of Xenin-25[Lys^{13}PAL] for 42 days on lumbar spine (A) bone mineral density (BMD) and (B) bone mineral content (BMC) in lean mice

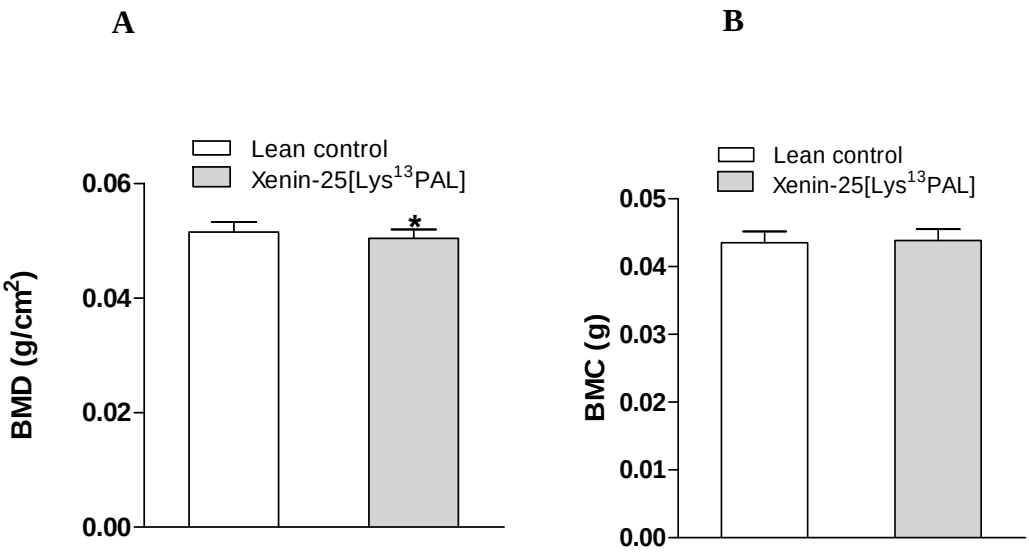

(A) Bone mineral density (BMD) and (B) Bone mineral content (BMC) of lumbar spine as measured by DEXA scanning in high fat fed mice following 42 days treatment with Xenin-25[Lys^{13}PAL]. Values represent means ± SEM for 6 mice. $^{*}p < 0.05$ compared to lean control.

Figure 5.8 Effects of once daily administration of Xenin-25[Lys^{13}PAL] for 42 days on tibia (A) bone mineral density (BMD) and (B) bone mineral content (BMC) in lean mice

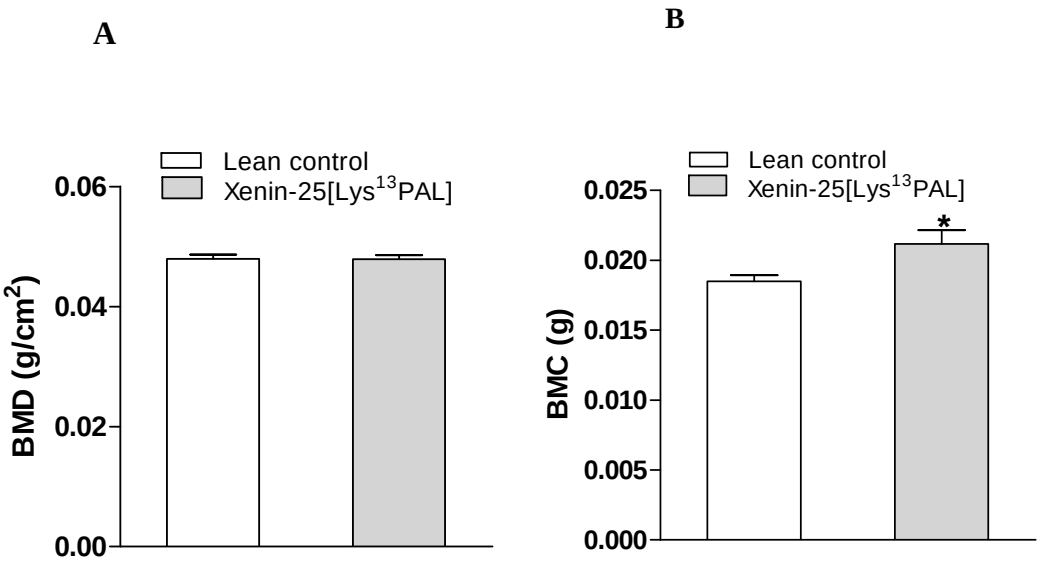

(A) Bone mineral density (BMD) and (B) Bone mineral content (BMC) mass of tibia as measured by DEXA scanning in lean mice following 42 days treatment with Xenin-25[Lys^{13}PAL]. Values represent means ± SEM for 6 mice. *$p < 0.05$ compared to lean control.

Figure 5.9 Effects of once daily administration of Xenin-25[Lys^{13}PAL] on trabecular bone mass and microarchitecture in lean mice

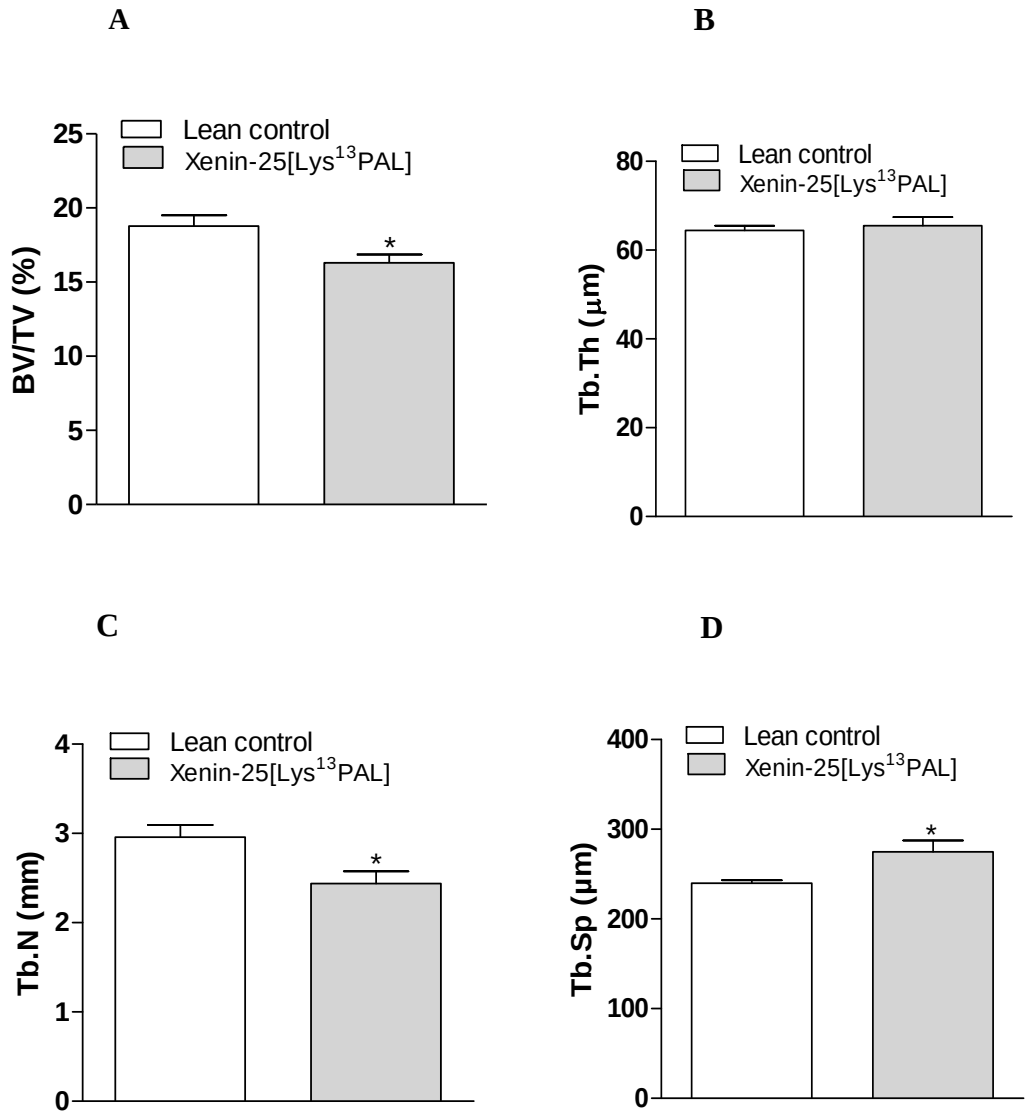

Parameters were obtained from a microtomography scan of tibia following 42 days once daily administration of saline (0.9%, w/v, NaCl), Xenin-25[Lys^{13}PAL] (peptide at 25 nmol/kg bw). Values are means ± SEM for 6 mice. *$p<0.05$ compared with lean control.

Figure 5.10 Effects of once daily administration of Xenin-25[Lys^{13}PAL] on cortical bone geometry in lean mice

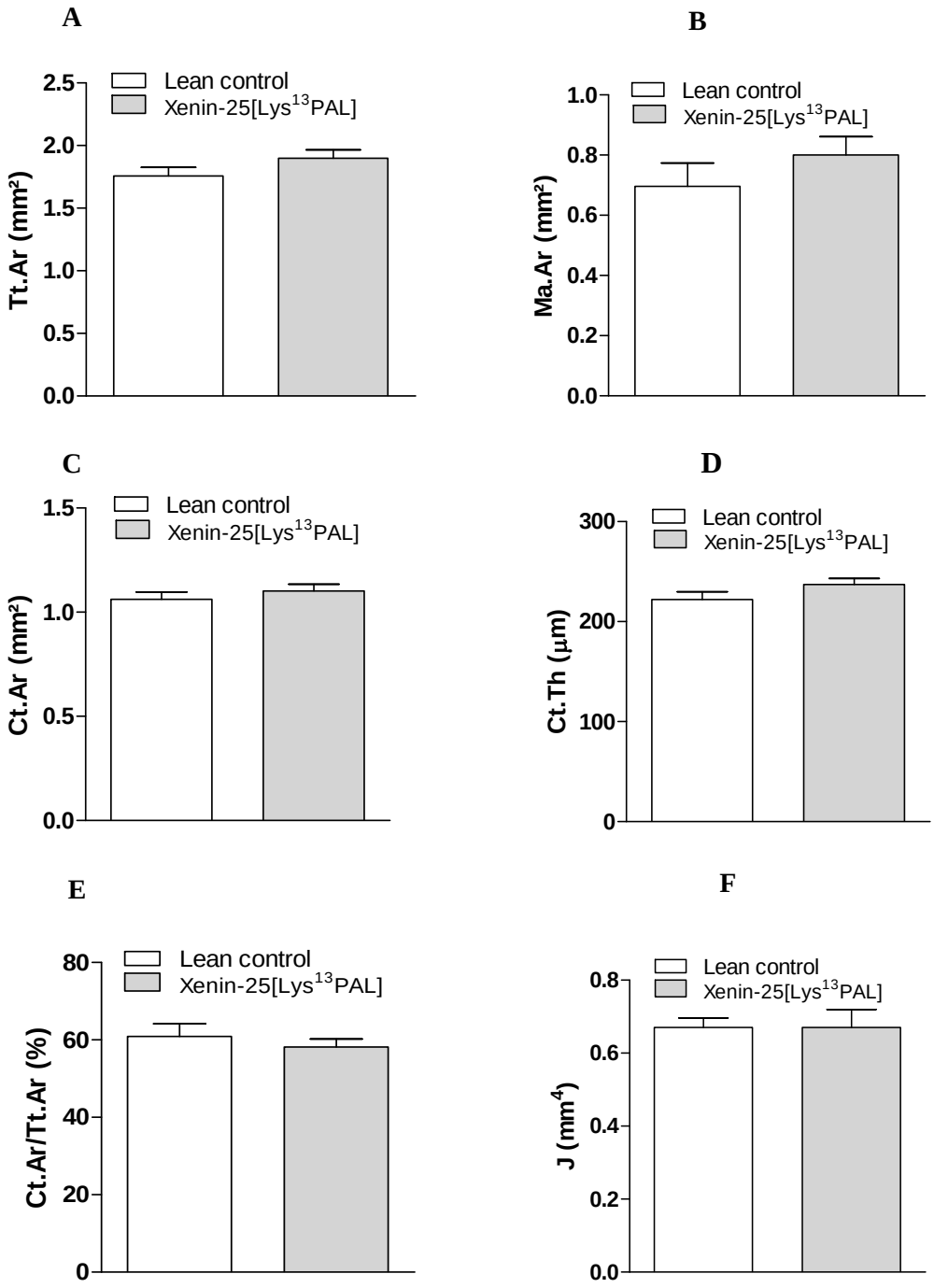

Images of cortical bone were obtained from a microtomography scan of tibia following 42 days once daily administration of saline (0.9%, w/v, NaCl) or Xenin-25[Lys^{13}PAL] (each at 25 nmol/kg b.w). Cortical bone was located 3 mm below growth plate and total area (A), cortical area (B), bone marrow diameter (C) cortical thickness (D), bone mineralisation (E) and moment

of inertia (F) were measured. Values are mean ± S.E.M for 6 mice.

Figure 5.11 Effects of once daily administration of Xenin-25[Lys^{13}PAL] for 42 days on whole-bone mechanical properties of femoral cortical bone in lean mice

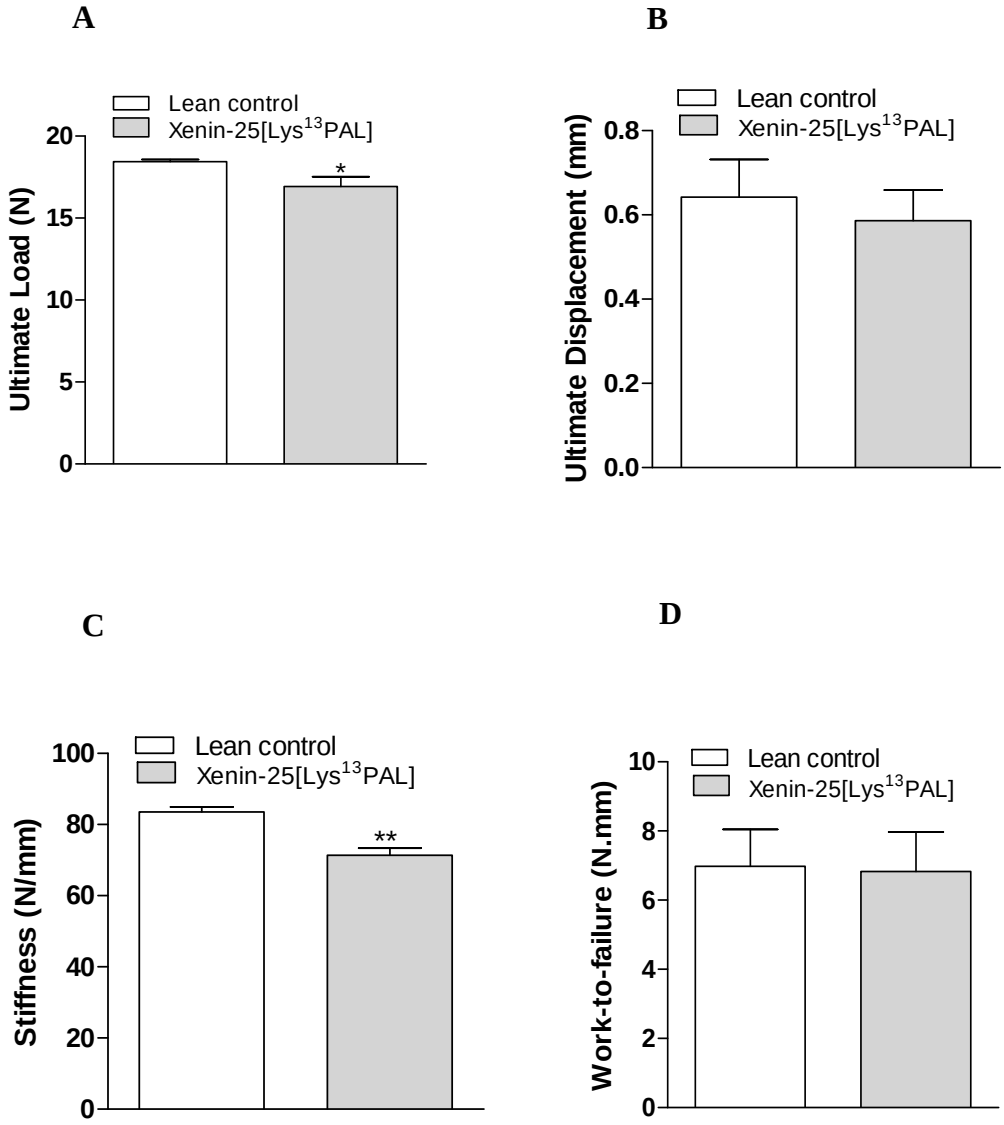

Parameters were obtained following 3-point bending tests after 42 days once daily administration of Xenin-25[Lys^{13}PAL] (25 nmol/kg b.w) in high fat fed mice. Values are mean ± S.E.M for 6 mice. *$p < 0.05$, **$p < 0.01$ compared to lean control mice.

Figure 5.12 Effects of once daily administration of Xenin-25[Lys^{13}PAL] on nanomechanical properties of cortical bone matrix in lean mice

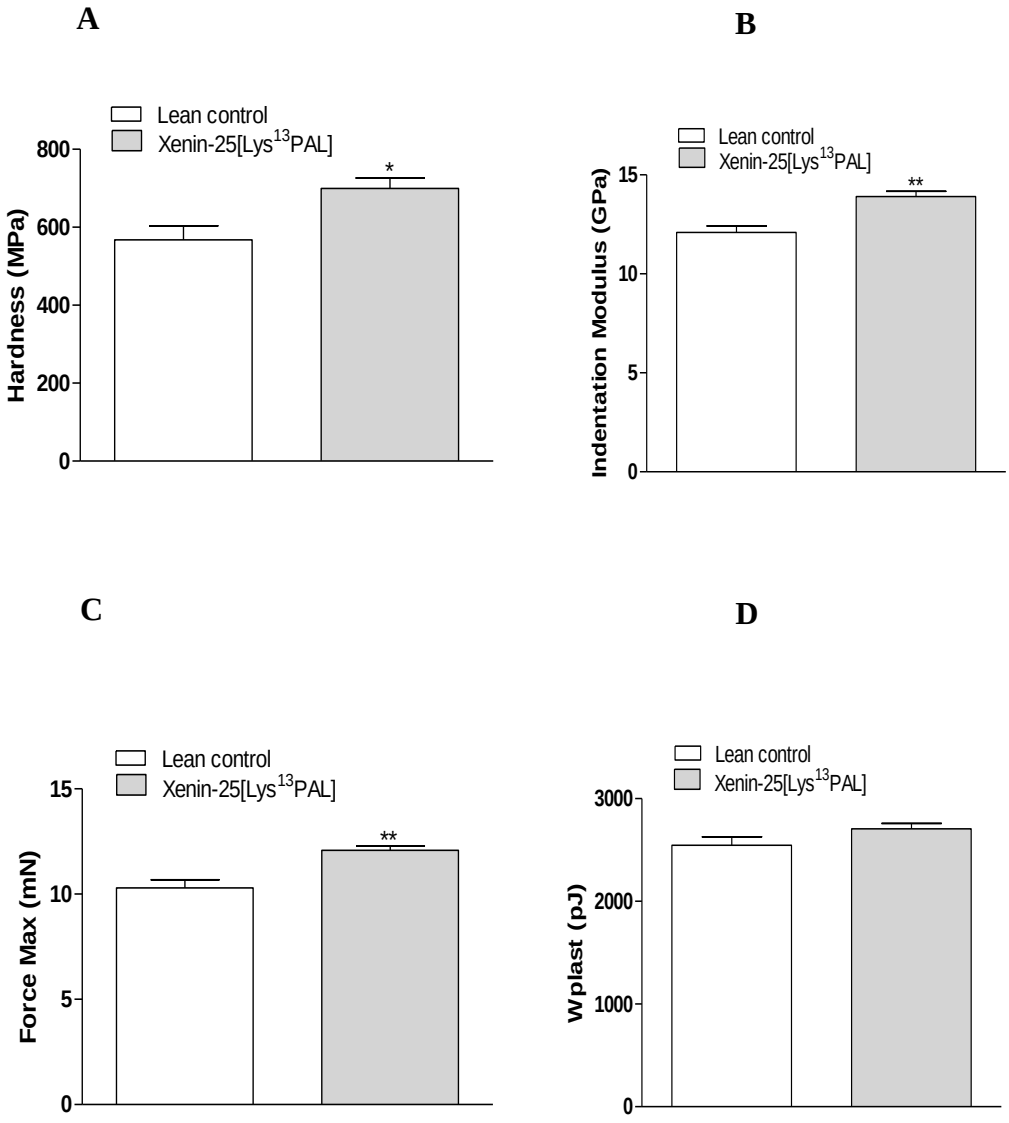

Parameters were measured by nanoindentation following 42 days once daily administration of saline (0.9%, w/v, NaCl) or Xenin-25[Lys^{13}PAL] (each at 25 nmol/kg b.w). Values are mean ± S.E.M for 6 mice. *$p < 0.05$, **$p < 0.01$ compared to lean control.

Figure 5.13 Effects of once daily administration of Xenin-25[Lys^{13}PAL] on cortical bone mineral density distribution (BMDD) in lean mice

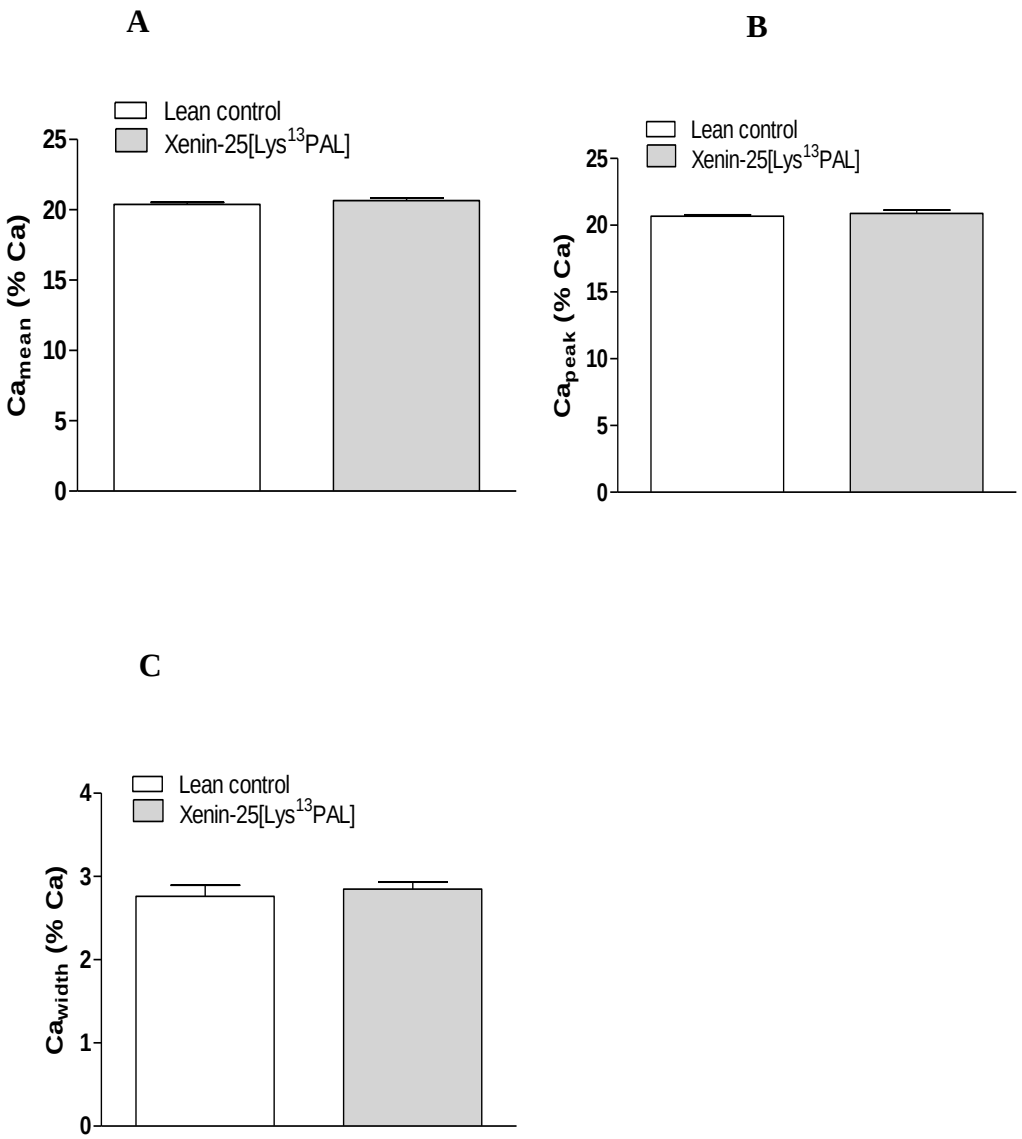

Bone mineralisation at cortical bone was measured by quantitative backscattered electron imaging following 42 days once daily administration of saline (0.9%, w/v, NaCl) or Xenin-25[Lys^{13}PAL] (each at 25 nmol/kg b.w). Values are mean ± S.E.M for 6 mice.

Figure 5.14 Effects of once daily administration of Xenin-25[Lys^{13}PAL] on bone tissue in lean mice

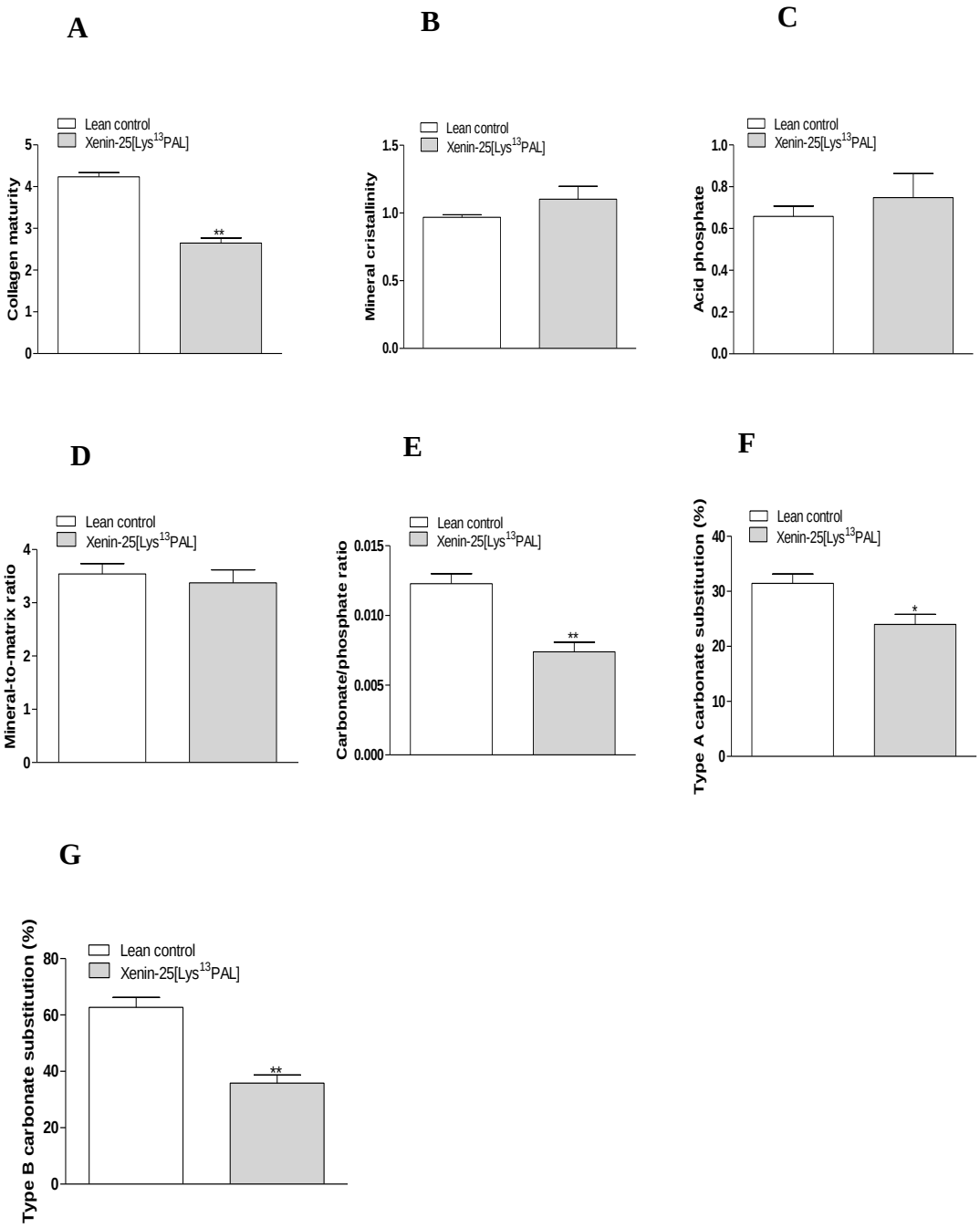

(A)Collagen maturity, (B) mineral crystallinity, (C) acid phosphate, (D) mineral-to-matrix, (E) carbonate/phosphate ratio, (F) type-A carbonate substitution and (G) type-B carbonate substitution were measured by infrared spectroscopy following 42 days once daily administration of saline (0.9%, w/v, NaCl) or Xenin-25[Lys^{13}PAL] (each at 25 nmol/kg b.w) in lean mice. Values are mean ± S.E.M for 6 mice. *p< 0.05, **p< 0.01 compared to lean control.

Figure 5.15 Effects of once daily administration of Xenin-25[Lys^{13}PAL] and Xenin-25[Lys^{13}PAL]-Asp for 42 days on (A) body weight (B) % fat mass and (C) total lean mass in high fat fed mice.

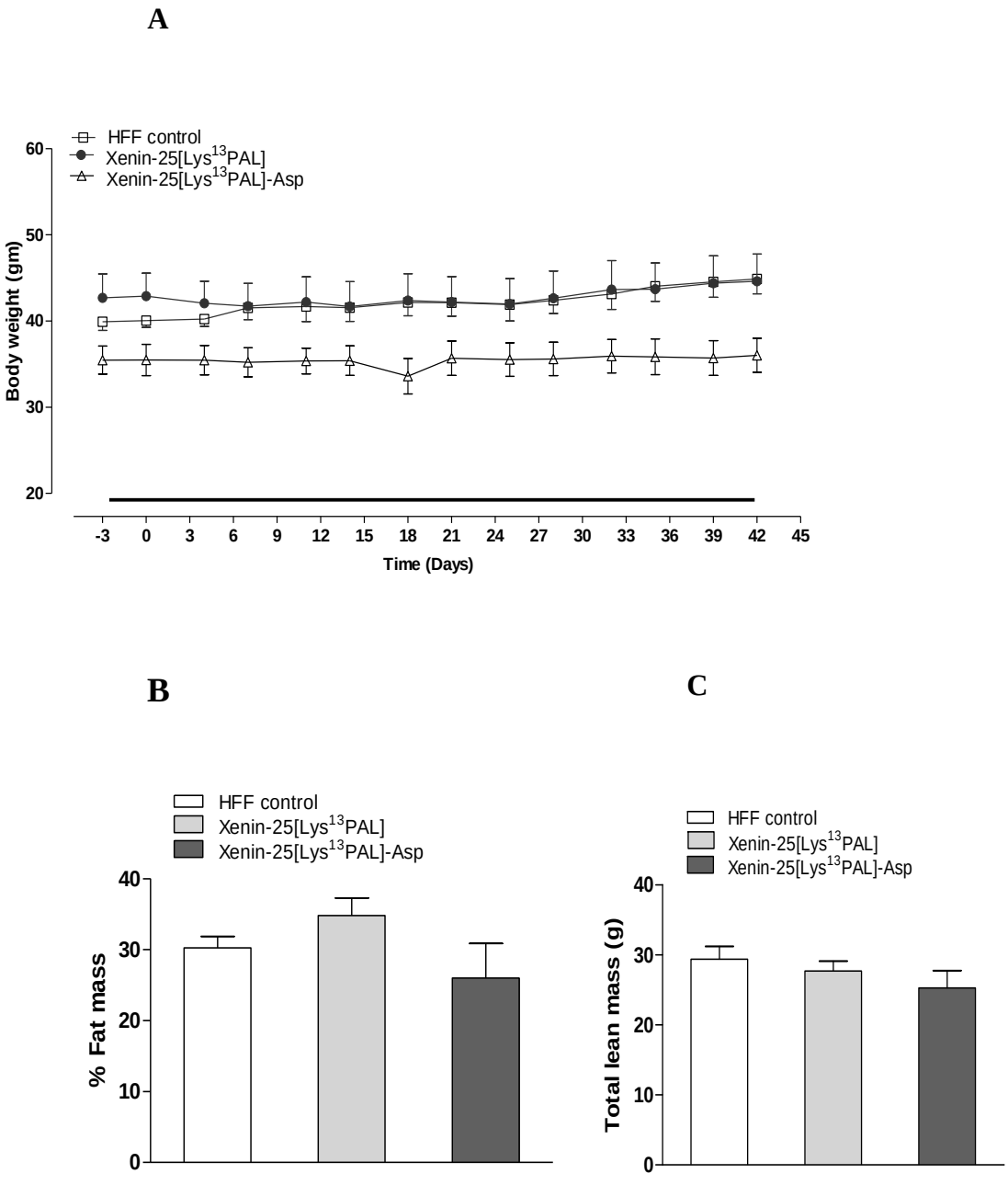

(A) Body weight was measured for 3 days before and 42 days during (indicated by black horizontal bar) once daily treatment with saline vehicle (0.9% w/v NaCl), Xenin-25[Lys^{13}PAL] and Xenin-25[Lys^{13}PAL]-Asp (each peptide at 25 nmol/kg bw). (B) % fat mass and (C) lean mass as measured by DEXA scanning in high fat fed mice on day 42. Values represent means ± SEM for 5 mice.

Figure 5.16 Effects of once daily administration of Xenin-25[Lys^{13}PAL] and Xenin-25[Lys^{13}PAL]-Asp for 42 days on cumulative energy intake in high fat fed mice

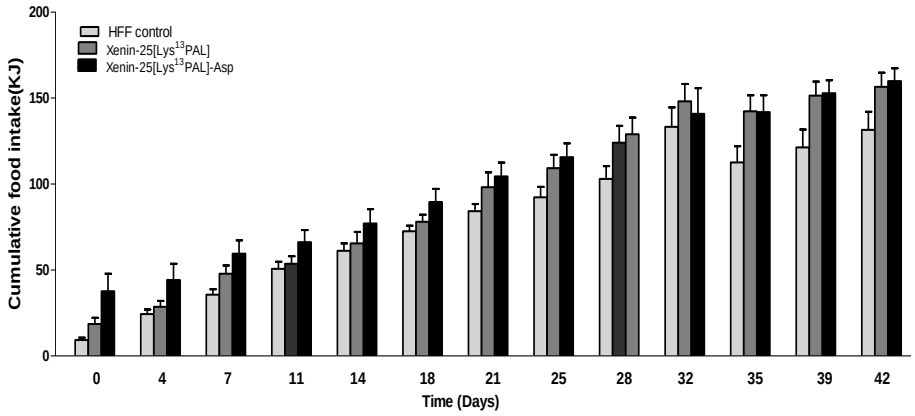

Cumulative energy intake was measured for 3 days before and 42 days during once daily treatment with saline vehicle (0.9%w/v NaCl), Xenin-25[Lys^{13}PAL] and Xenin-25[Lys^{13}PAL]-Asp (each peptide at 25 nmol/kg bw). Values represent means ± SEM for 5 mice.

Figure 5.17 Effects of once daily administration of Xenin-25[Lys^{13}PAL] and Xenin-25[Lys^{13}PAL]-Asp for 42 days on non fasting (A) blood glucose and (B) plasma insulin in high fat fed mice

A

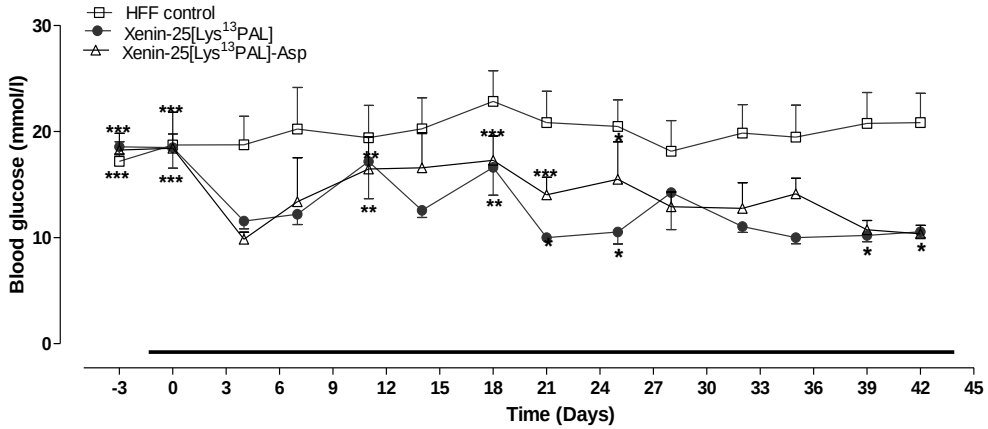

B

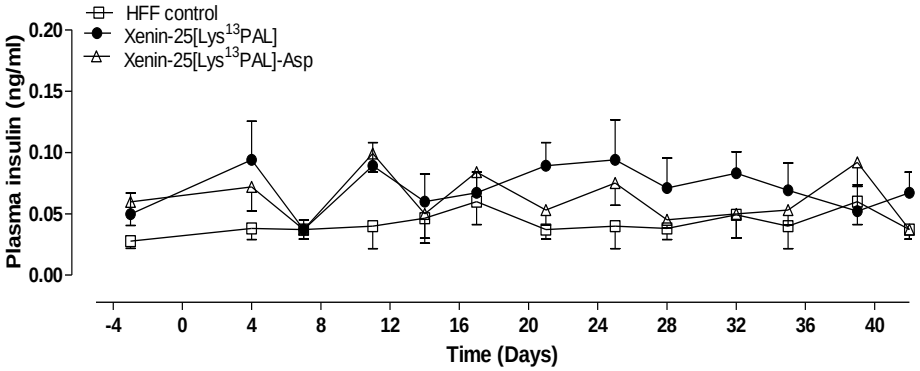

(A) Blood glucose and (B) plasma insulin were measured for 3 days before and 42 days during once daily treatment with saline vehicle (0.9%w/v NaCl), Xenin-25[Lys^{13}PAL] and Xenin-25[Lys^{13}PAL]-Asp (each peptide at 25 nmol/kg bw). Values represent means ± SEM for 5 mice. *p < 0.05, **p < 0.01, ***p< 0.001 compared with high fat fed control.

Figure 5.18 Effects of once daily administration of Xenin-25[Lys^{13}PAL] and Xenin-25[Lys^{13}PAL]-Asp for 42 days on (A) glucose tolerance and (B) plasma insulin response in high fat fed mice

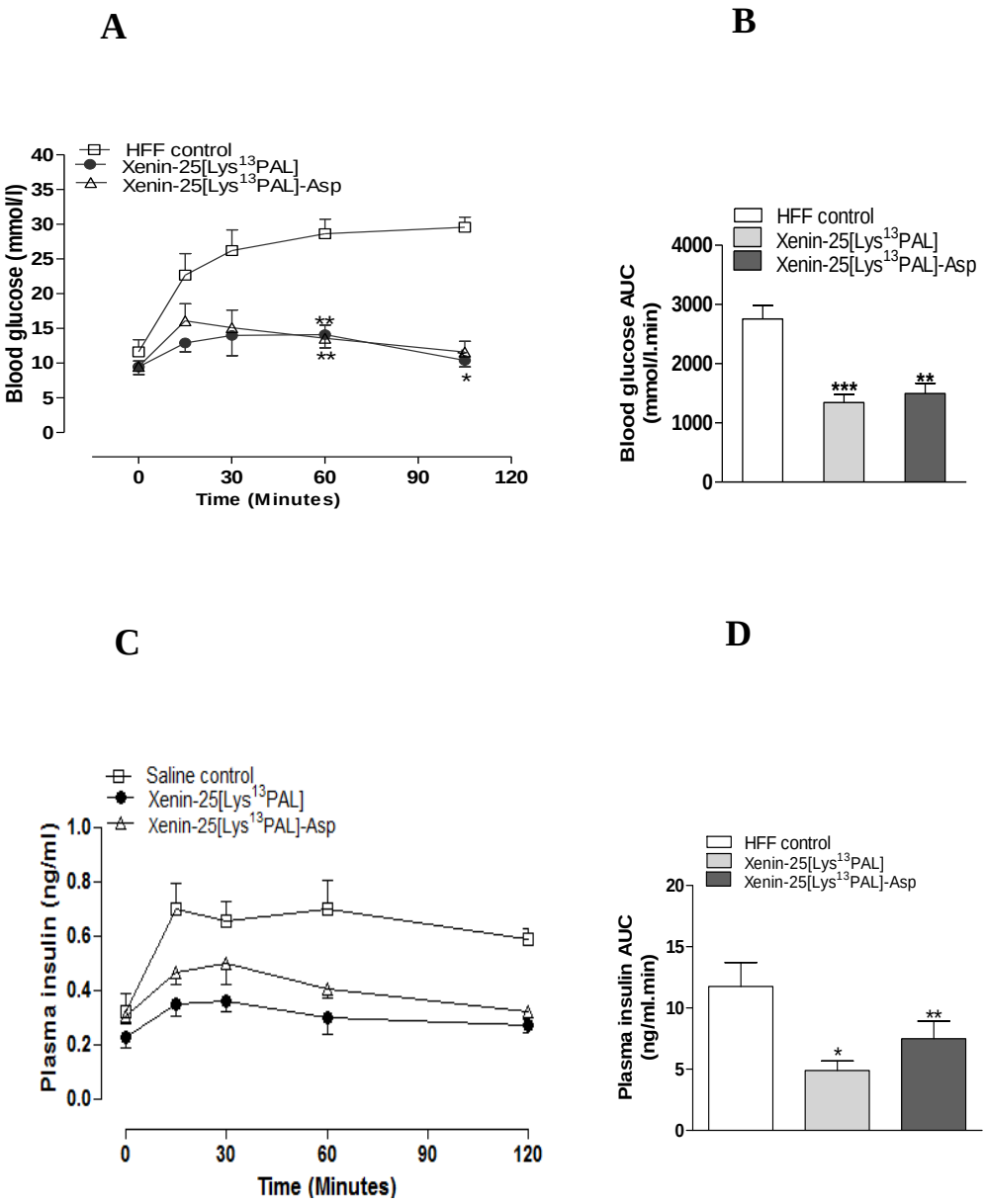

Tests were conducted after once daily treatment with saline, Xenin-25[Lys^{13}PAL] and Xenin-25[Lys^{13}PAL]-Asp (each peptide at 25 nmol/kg bw) for 42 days. (A) Blood glucose (C) plasma before and after i.p injection of glucose (18 mmol/kg bw) alone in 18 hour fasted mice. (B, D) AUC values for 0-120 min are shown. Values are mean ± S.E.M for 5 mice per group. *p< 0.05, **p< 0.01, ***p < 0.001 compared with high fat fed control.

Figure 5.19 Effects of once daily administration of Xenin-25[Lys^{13}PAL] and Xenin-25[Lys^{13}PAL]-Asp for 42 days on insulin sensitivity in high fat fed mice.

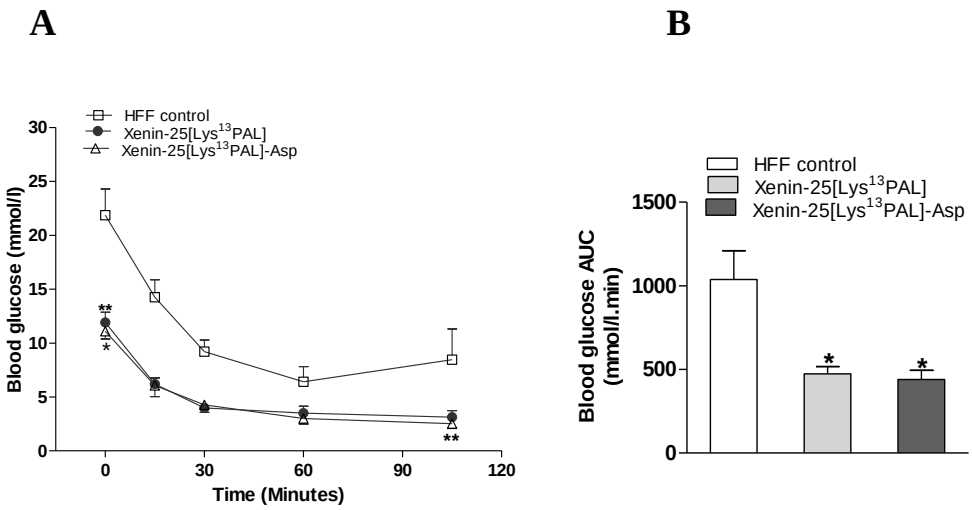

(A) Insulin (25 U/kg bw) was injected intraperitoneally (at t=0) in non-fasted mice following 42 days treatment with saline, Xenin-25[Lys^{13}PAL] and Xenin-25[Lys^{13}PAL]-Asp (each peptide at 25 nmol/kg bw). (B) Blood glucose and blood glucose AUC values for 0-120 min are shown in inset. Values represent means ± SEM for 5 mice. *$p < 0.05$, **$p < 0.01$ compared to high fat fed control.

Figure 5.20 Effects of once daily administration of Xenin-25[Lys^{13}PAL] and Xenin-25[Lys^{13}PAL]-Asp for 42 days on (A) whole body bone mineral density (BMD), (B) whole body bone mineral content (BMC), (C) femur BMD and (D) femur BMC in high fat fed mice

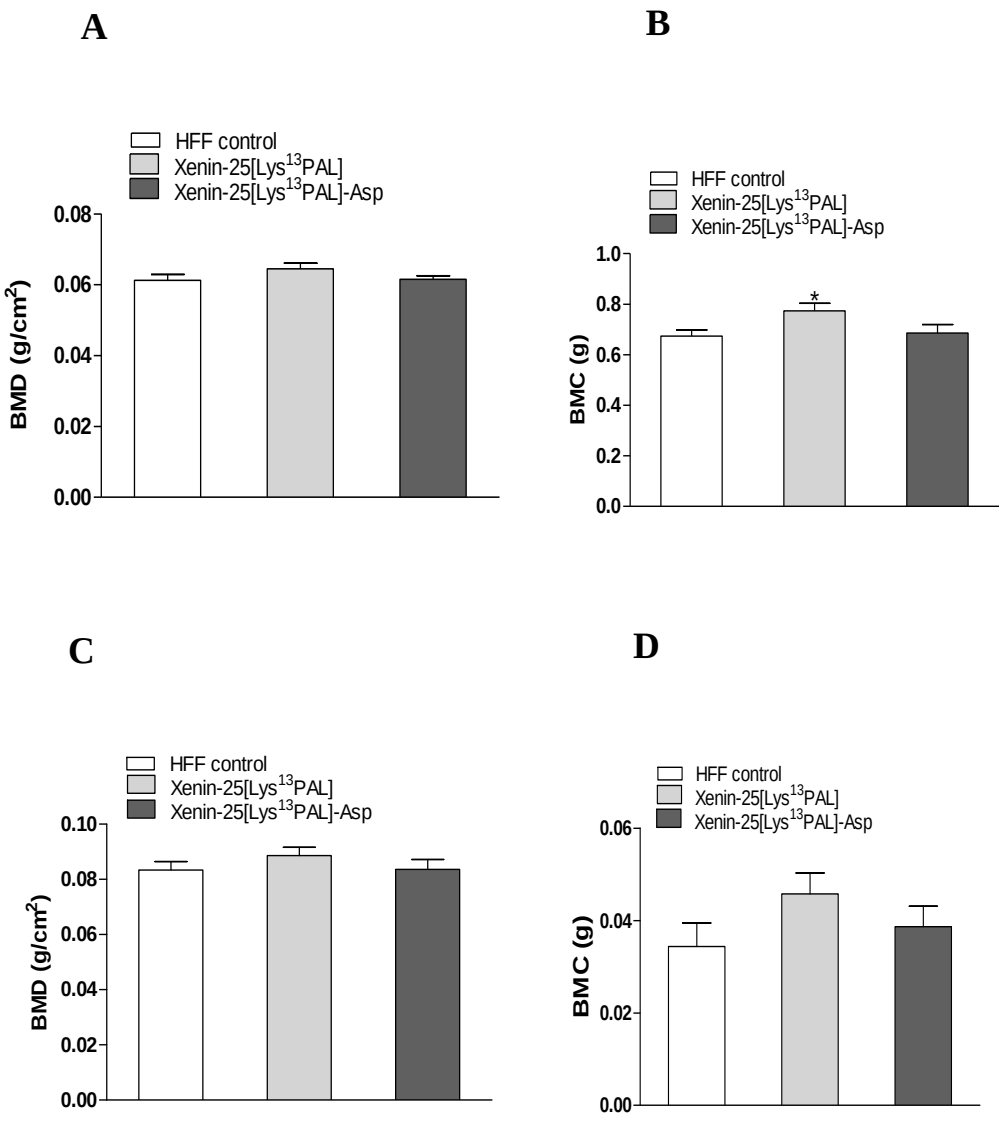

(A) Whole body bone mineral density (BMD) and (B) whole body bone mineral content (BMC) as measured by DEXA scanning in high fat fed mice following 42 days treatment with Xenin-25[Lys^{13}PAL] and Xenin-25[Lys^{13}PAL]-Asp. (C) Femur BMD and (D) femur BMC as measured by DEXA scanning in high fat fed mice following 42 days treatment with Xenin-25[Lys^{13}PAL] and Xenin-25[Lys^{13}PAL]-Asp (each peptide at 25 nmol/kg bw). Values represent means ± SEM for 5 mice. $^{*}p < 0.05$ compared to high fat fed control.

Figure 5.21 Effects of once daily administration of Xenin-25[Lys^{13}PAL] and Xenin-25[Lys^{13}PAL]-Asp for 42 days on lumbar spine (A) bone mineral density (BMD) and (B) bone mineral content (BMC) in high fat fed mice

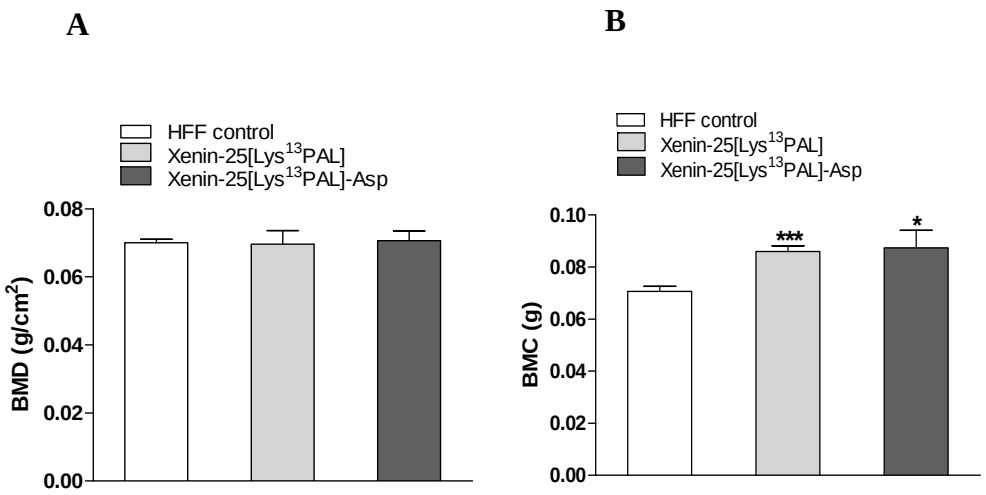

(A) Bone mineral density (BMD) and (B) Bone mineral content (BMC) of lumbar spine as measured by DEXA scanning in high fat fed mice following 42 days treatment with Xenin-25[Lys^{13}PAL] and Xenin-25[Lys^{13}PAL]-Asp (each peptide at 25 nmol/kg bw). Values represent means ± SEM for 5 mice. $^{*}p< 0.05$, $^{***}p< 0.01$ compared to high fat fed control.

Figure 5.22 Effects of once daily administration of Xenin-25[Lys^{13}PAL] and Xenin-25[Lys^{13}PAL]-Asp for 42 days on tibia (A) bone mineral density (BMD) and (B) bone mineral content (BMC) in high fat fed mice

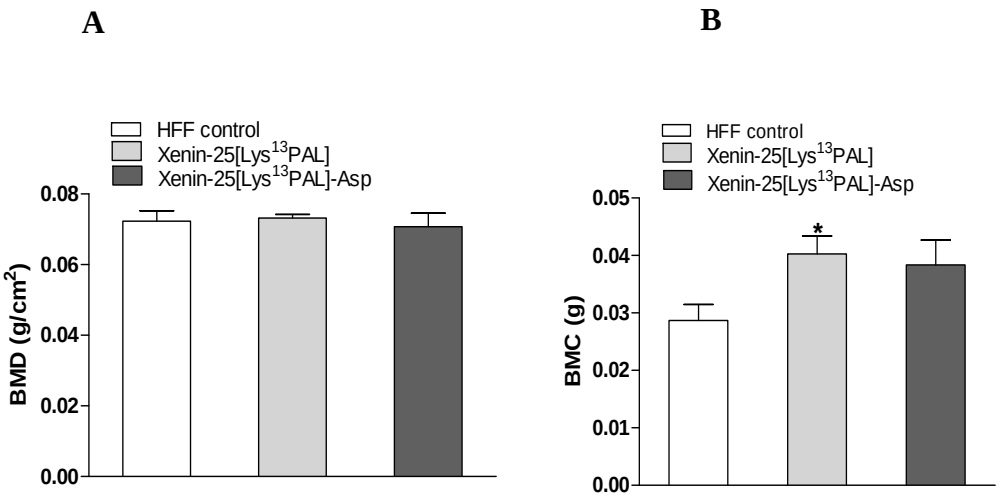

(A) Bone mineral density (BMD) and (B) Bone mineral content (BMC) of tibia as measured by DEXA scanning in high fat fed mice following 42 days treatment with Xenin-25[Lys^{13}PAL] and Xenin-25[Lys^{13}PAL]-Asp (each peptide at 25 nmol/kg bw). Values represent means ± SEM for 5 mice. *$p < 0.05$ compared to high fat fed control.

Figure 5.23 Effects of once daily administration of Xenin-25[Lys^{13}PAL] and Xenin-25[Lys^{13}PAL]-Asp on trabecular bone mass and micro architecture in high fat fed mice

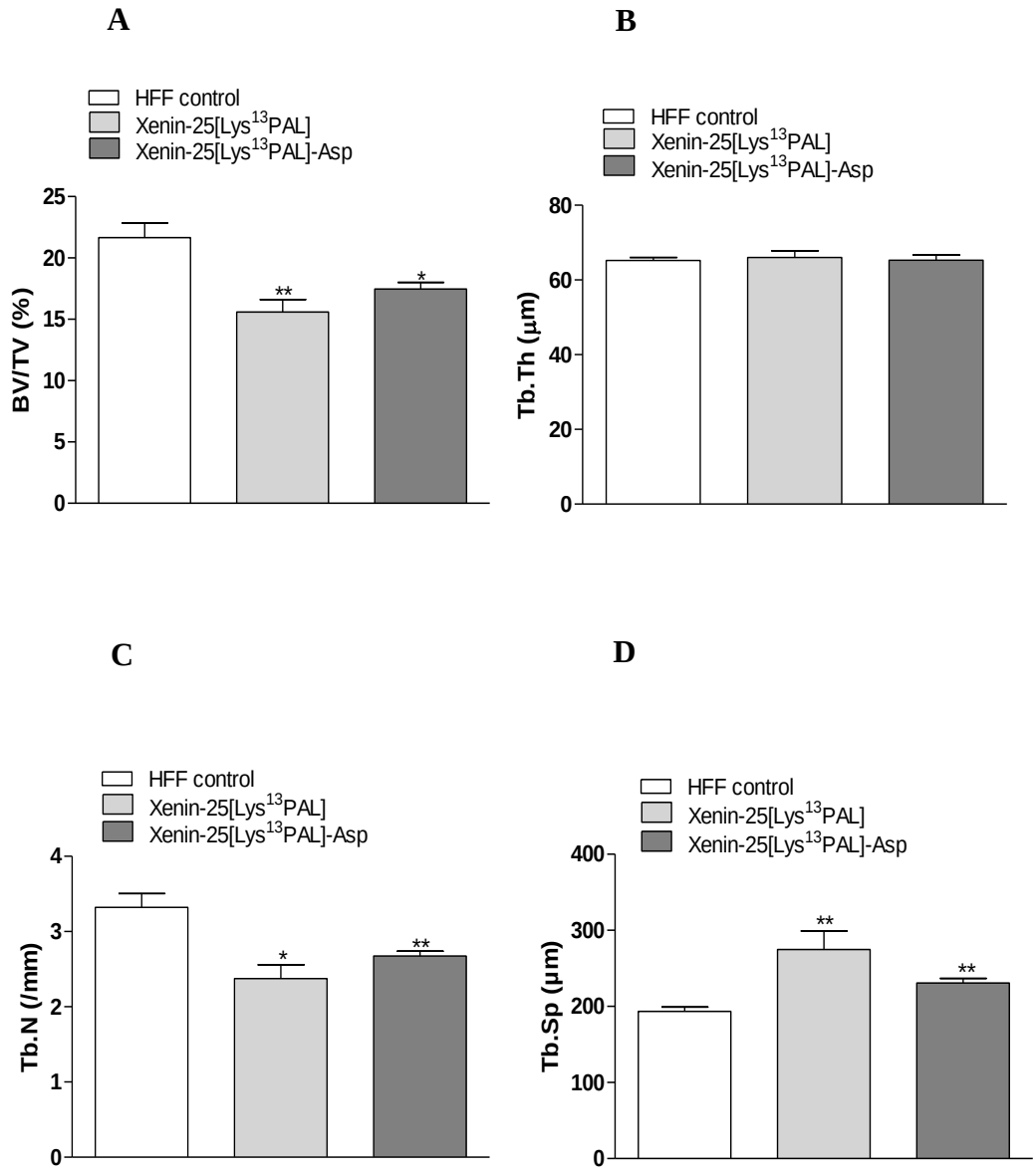

Parameters were obtained from a microtomography scan of tibia following 42 days once daily administration of saline (0.9%, w/v, NaCl), Xenin-25[Lys^{13}PAL] and Xenin-25[Lys^{13}PAL]-Asp (each peptide at 25 nmol/kg bw). Values are means ± SEM for 5 mice. *p< 0.05, **p< 0.01 compared with high fat fed control.

Figure 5.24 Effects of once daily administration of Xenin-25[Lys^{13}PAL] and Xenin-25[Lys^{13}PAL]-Asp on cortical micro architecture in high fat fed mice

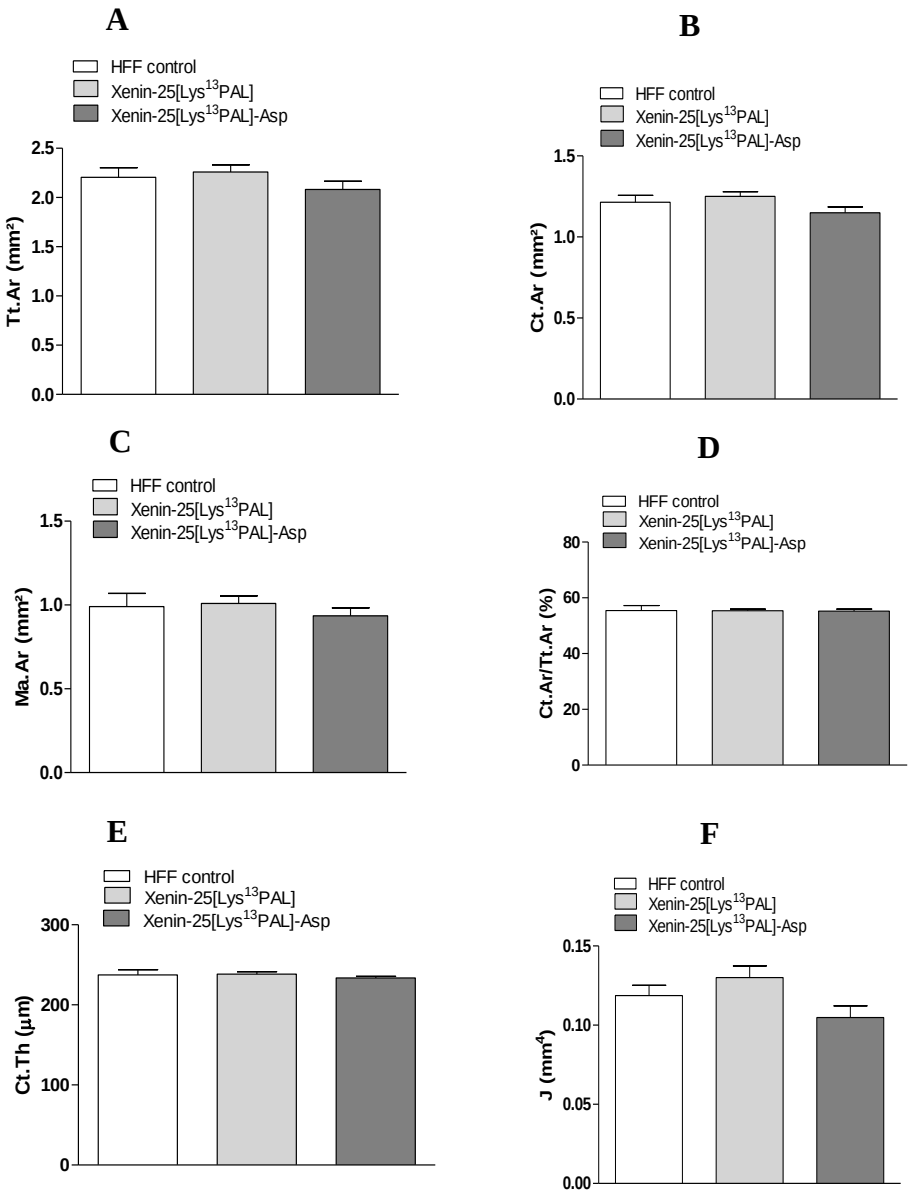

Images of cortical bone were obtained from a microtomography scan of tibia following 42 days once daily administration of saline (0.9%, w/v, NaCl), Xenin-25[Lys^{13}PAL] and Xenin-25[Lys^{13}PAL]-Asp (each at 25 nmol/kg b.w). Cortical bone was located 3 mm below growth plate and total area (A), cortical area (B), bone marrow diameter (C) cortical thickness (D), bone mineralisation (E) and moment of inertia (F) were measured. Values are mean ± S.E.M for 5 mice.

Figure 5.25 Effects of once daily administration of Xenin-25[Lys^{13}PAL] and Xenin-25[Lys^{13}PAL]-Asp for 42 days on whole-bone mechanical properties of femoral cortical bone in high fat fed mice

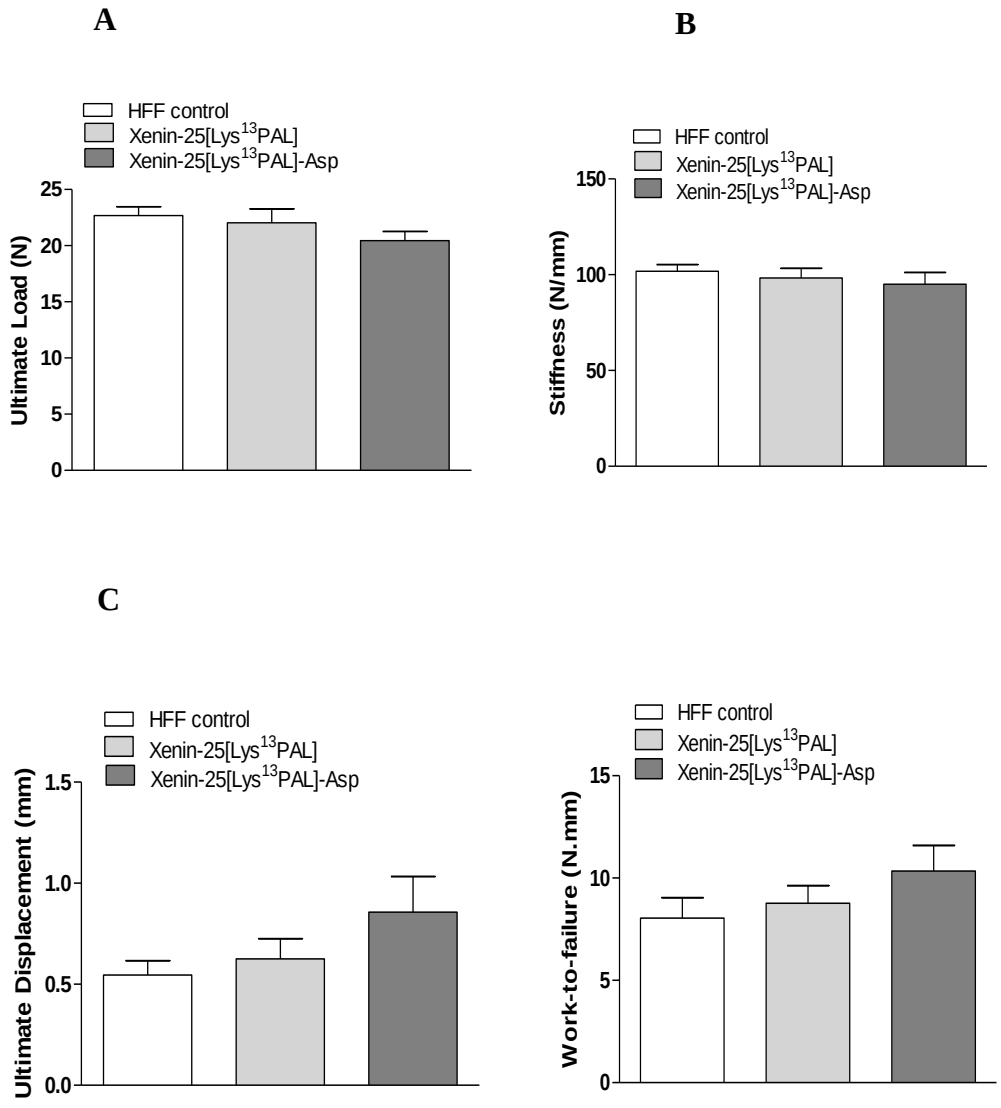

Parameters were obtained following 3-point bending tests after 42 days once daily administration of Xenin-25[Lys^{13}PAL] and Xenin-25[Lys^{13}PAL]-Asp (each peptide at 25 nmol/kg b.w) in high fat fed control. Values are mean ± S.E.M for 5 mice.

Figure 5.26 Effects of Xenin-25[Lys^{13}PAL] and Xenin-25[Lys^{13}PAL]-Asp on nanomechanical properties of cortical bone matrix in high-fat fed mice

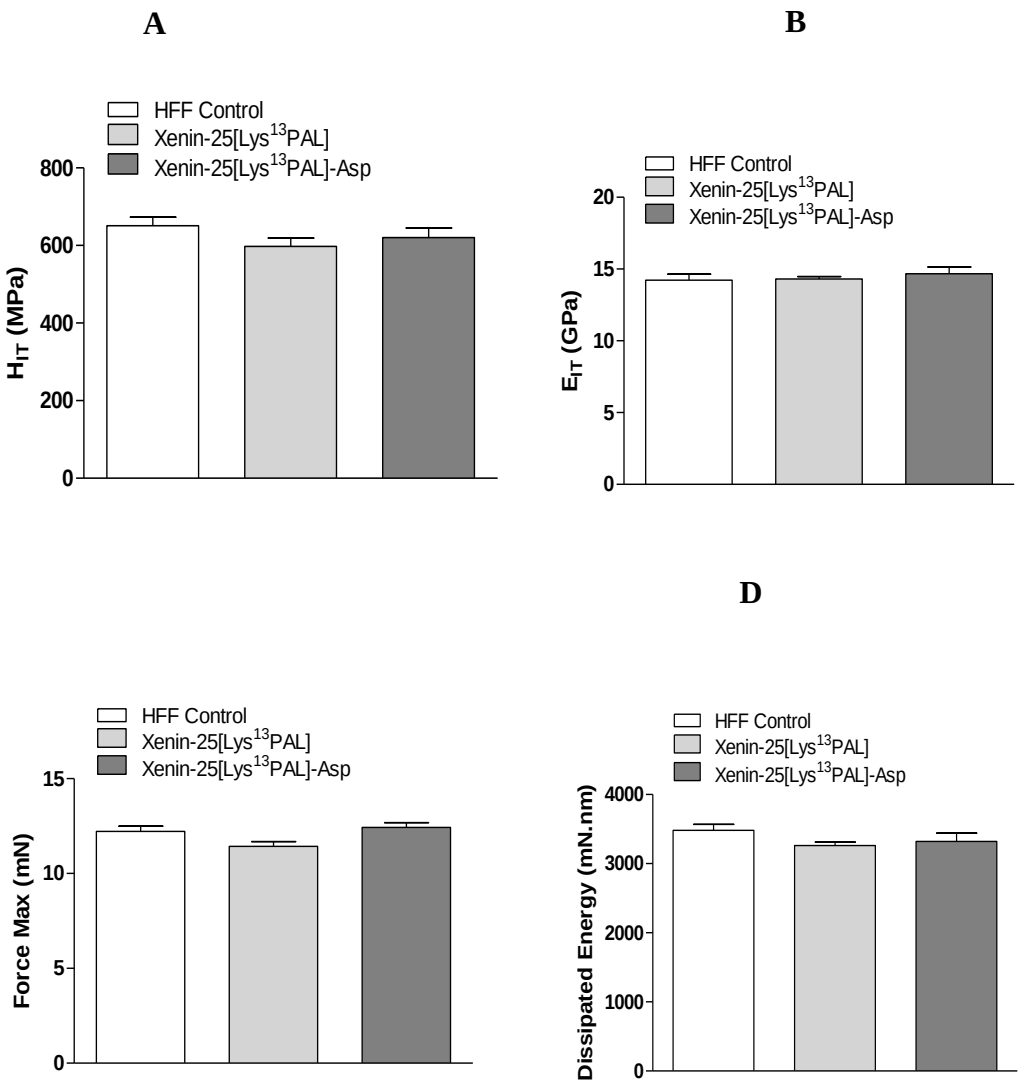

Parameters were measured by nanoindentation following 42 days once daily administration of saline (0.9%, w/v, NaCl), Xenin-25[Lys^{13}PAL] and Xenin-25[Lys^{13}PAL]-Asp (each at 25 nmol/kg b.w). Values are mean ± S.E.M for 5 mice.

Figure 5.27 Effects of once daily administration of Xenin-25[Lys^{13}PAL] and Xenin-25[Lys^{13}PAL]-Asp on cortical bone mineral density distribution (BMDD) in high-fat fed mice

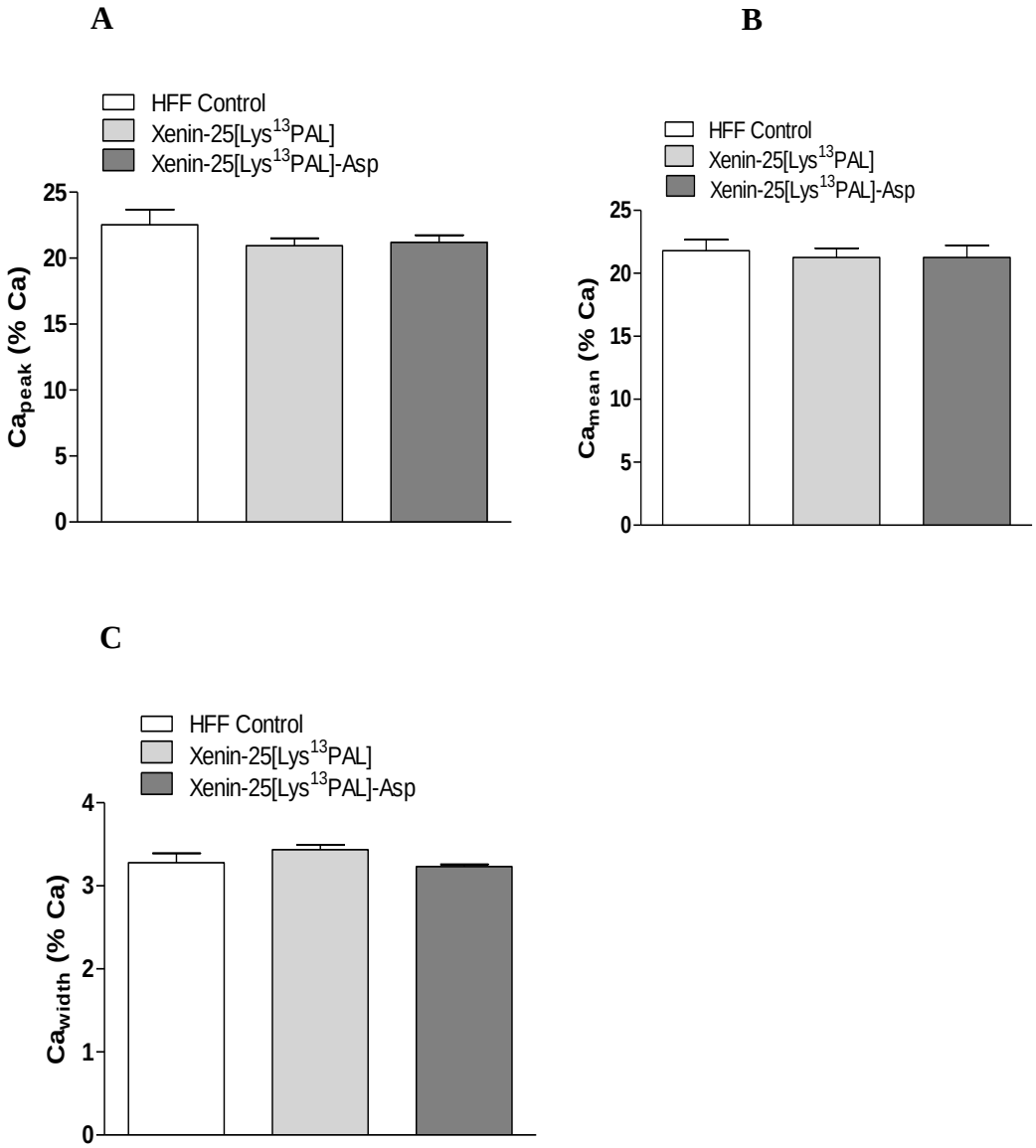

Bone mineralisation at cortical bone was measured by quantitative backscattered electron imaging following 42 days once daily administration of saline (0.9%, w/v, NaCl), Xenin-25[Lys^{13}PAL] and Xenin-25[Lys^{13}PAL]-Asp (each at 25 nmol/kg b.w). Values are mean ± S.E.M for 5 mice.

Figure 5.28 Effects of once daily administration of Xenin-25[Lys^{13}PAL] and Xenin-25[Lys^{13}PAL]-Asp on bone tissue in high fat fed mice

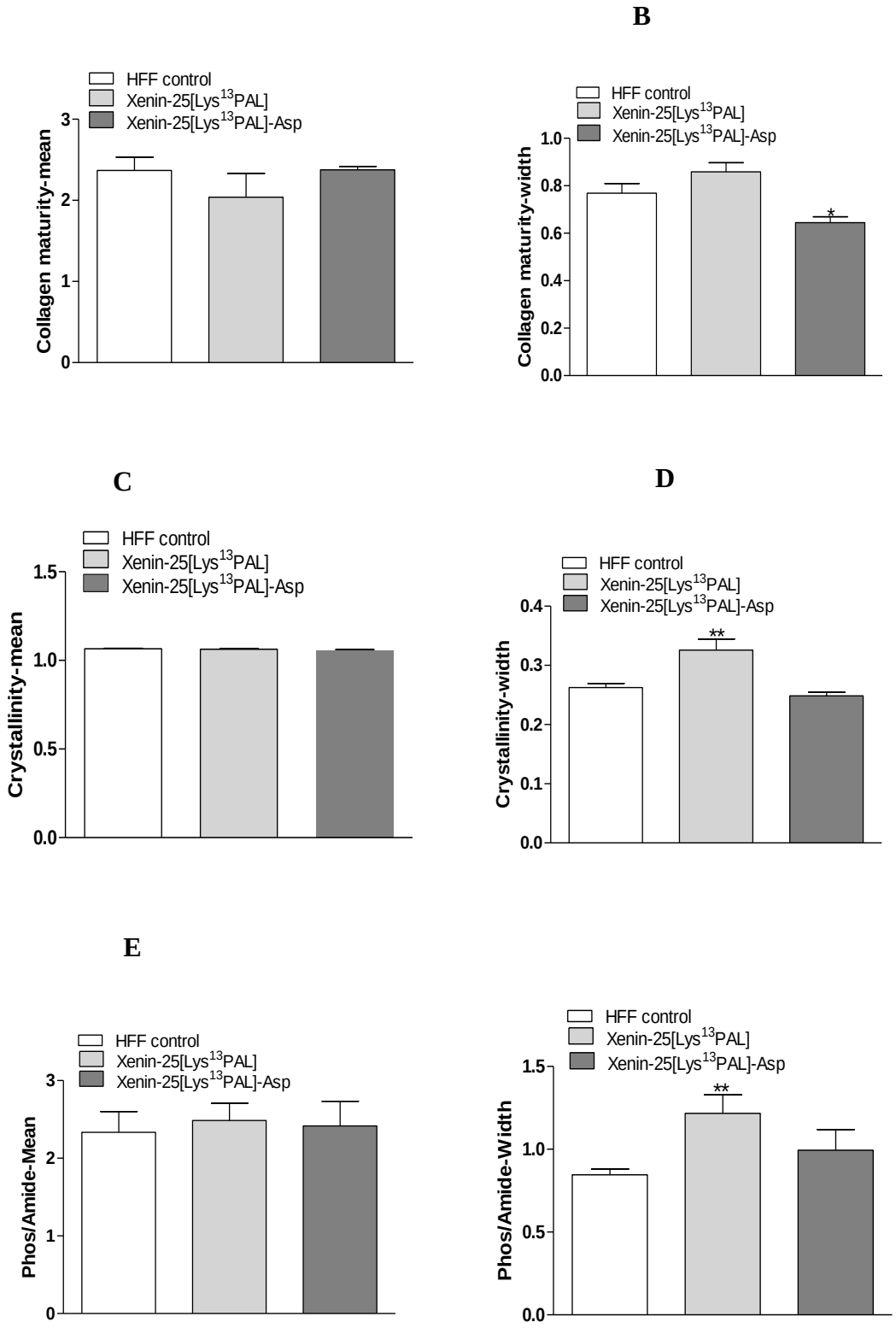

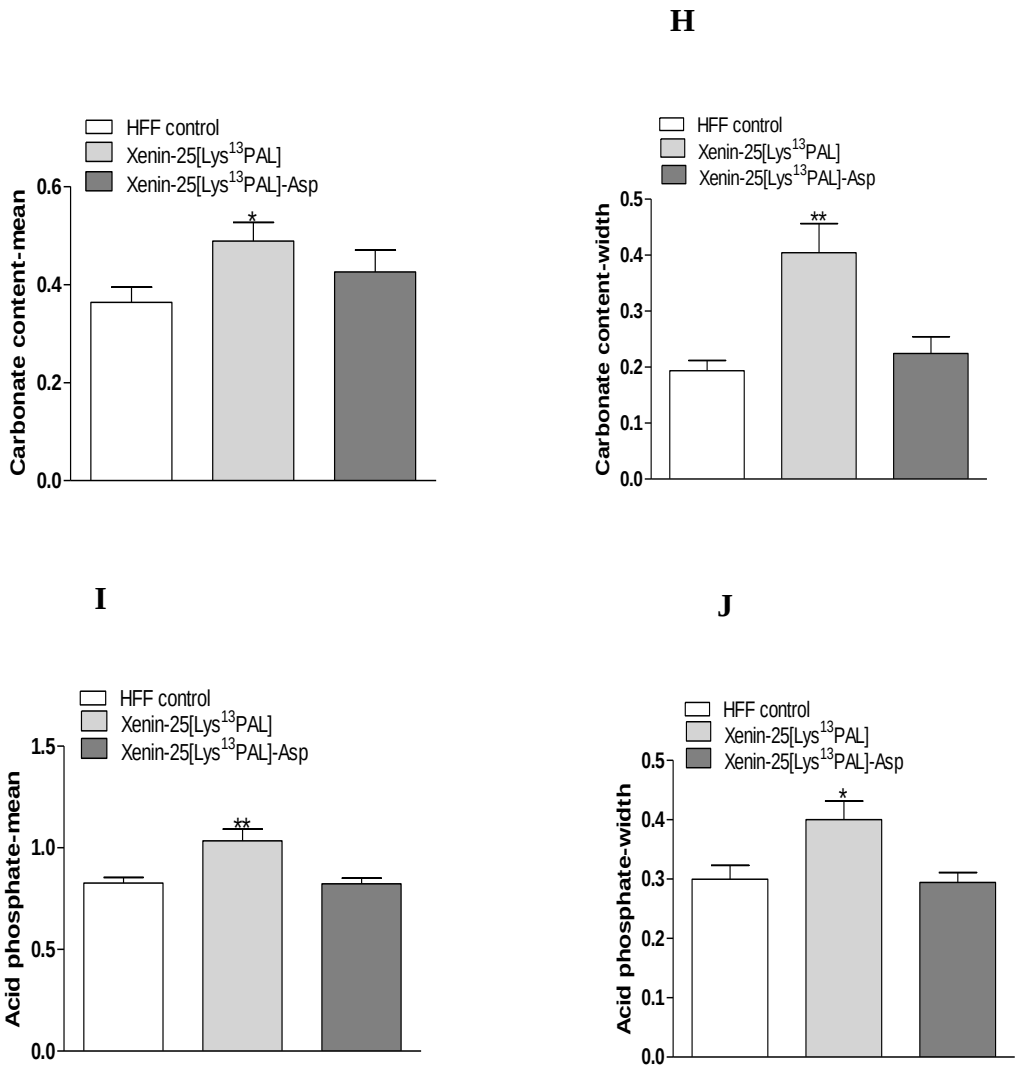

(A) Collagen maturity-mean, (B) collagen maturity width, (C) crystallinity-mean, (D) crystallinity-width, (E) phosphate/amide ratio mean, (F) phosphate/amide ratio-width, (G) carbon/phosphate ratio-mean, (H) carbon/phosphate ratio-width (I) acid phosphate mean and (J) acid phosphate with were measured by infrared spectroscopy following 42 days once daily administration of saline (0.9%, w/v, NaCl), Xenin-25[Lys^{13}PAL] and Xenin-25[Lys^{13}PAL]-Asp (each at 25 nmol/kg b.w). Values are mean ± S.E.M for 5 mice. *p< 0.05, **p< 0.01 compared to high fat fed control.

Chapter 6

Impact of bone-specific GIP/Xenin hybrid peptides on metabolic control as well as bone quality and strength in high-fat fed mice

6.1 SUMMARY

There is now compelling evidence indicating that the gut hormones, such as glucose-dependent insulinotropic polypeptide (GIP) and glucagon-like peptide-1 (GLP-1), play important role in the maintenance of bone strength and quality in addition to their more recognised benefits on metabolic control. Xenin is chiefly considered as a gut peptide that potentiates the biological action of GIP. Therefore, the possibility that xenin might have important effects on the bone is likely. This study was undertaken to assess the effect of bone-specific GIP/Xenin hybrid analogues on metabolism and bone health in high-fat fed mice model. High-fat fed mice received once-daily i.p injections of saline (0.9% w/v NaCl), GIP/Xenin and the bone-specific GIP/xenin hybrids, namely GIP/Xenin-Asp and GIP/Xenin-Glu (each at 25 mmol/kg bw) for 42 days. GIP/Xenin, GIP/Xenin-Asp and GIP/Xenin-Glu had no significant effect on body weight or composition, food intake or circulating glucose and insulin. Glucose tolerance was improved ($p<0.001$) in all treatment mice on day 42, and this was accompanied by enhanced insulin secretion in GIP/Xenin-Asp and GIP/Xenin-Glu treated mice. Insulin sensitivity was similar in all groups, but GIP/Xenin-Glu did induce a significant ($p<0.05$) enhancement compared to controls. DEXA analysis at the end of the study revealed no significant difference in whole body or femoral bone mineral density (BMD) and content (BMC). However, lumbar BMC was enhanced ($p<0.05$) by GIP/Xenin, and tibial BMD increased ($p<0.05$ and $p<0.01$, respectively) by GIP/Xenin-Asp and GIP/Xenin-Glu treatment. More detailed bone analyses revealed that GIP/Xenin-Glu reduced femoral cortical bone ultimate load ($p<0.01$) and stiffness ($p<0.05$). However, the number of trabeculae and trabecular bone volume was increased ($p<0.05$) following GIP/Xenin treatment for 42 days in high fat fed mice. Interestingly, cortical bone thickness

was reduced ($p<0.05$) by GIP/Xenin-Glu. None of the treatments impacted upon cortical bone matrix, bone mineral density distribution and bone tissue material properties. In conclusion, administration of GIP/Xenin, GIP/Xenin-Asp and GIP/Glu to high fat fed mice improved metabolic control but had variable effects on bone health.

6.2 INTRODUCTION

Bone is highly sophisticated mineralised material consisting of mineral phase (hydroxyapetite), collagen, non-collagenous proteins, lipids and water (Boskey 2001). These constituents are variable depending on age, tissue type, diet and health status (Boskey *et al*. 2006). Bone is continuously remodelled in mass and architecture and undergoes constant deterioration due to number of factors such as growth, aging and mechanical stress. Bone remodelling occurs through spatio-temporal coupling between osteoclasts and osteoblasts and is a complex process regulated by local, hormonal and neuronal factors (Ikeda & Takeshita 2014, Sims & Martin 2015, Florencio-Silvia *et al*. 2015). In this regard, gut hormones play an important role in bone remodelling (Elneanaei *et al*. 2010, Quach & Britton 2017, Collins *et al*. 2017, Yan & Charles 2017).

Glucose-dependent insulinotropic polypeptide (GIP), a 42-amino-acid incretin hormone secreted by enteroendocrine K cells, plays an important role in regulation of glucose homeostasis as well as enhancing glucose stimulated insulin secretion (Jonvall *et al*. 1981). Unlike its sister incretin, glucagon-like peptide-1 (GLP-1), GIP has received much less attention in terms of physiological and therapeutic importance. However, GIP receptors are found in adipose tissue, small intestine, adrenal cortex, lung, pancreas, heart, testis, bone and brain (Usdin *et al*. 1993). As such, there is substantial evidence indicating GIP plays dual role in bone formation and inhibiting

bone resorption making it potential candidate for treatment of bone fractures (Zhong *et al*. 2007). However, native GIP is rapidly degraded by the ubiquitous enzyme DPP-4 and is subject to efficient renal clearance (Mentlein *et al*. 1993).

Recently, it has been shown that xenin, a hormone co-secreted with GIP from enteroendocrine K cells, potentiates the insulin-secretory action of GIP (Althage *et al*. 2008, Taylor *et al*. 2010, Wice *et al* 2010, Chowdhury *et al*. 2014). The major metabolic actions of xenin include effects on gut motility, glucose homeostasis, insulin secretion, reducing food intake and promoting satiety (Cline *et al*. 2007, Cooke *et al*. 2016). Therefore, combination of biological actions of GIP and xenin to treat metabolic diseases and potentially combat bone fractures is a real possibility.

In this regard, there has been increased interest in designing hybrid peptides that can target multiple regulatory pathways (Gault *et al* 2013, Irwin *et al* 2015). Previous reports suggest that it is possible to design hybrid peptides through addition of key bioactive amino acid sequences (Yan *et al*. 2016, Fan *et al*. 2017,). Indeed, a GIP/xenin hybrid peptide has recently been described and characterised (Hasib *et al* 2017). Moreover, it is already reported that use of amino acid oligopeptide tagging (Glu and Asp) can help deliver peptides to bones, due to preferential peptide deposition in hydroxyapatite (Takahashi-Nishioka *et al*. 2008). This would enhances therapeutic applicability of peptides, such as the GIP/xenin hybrid (Hasib *et al*. 2017), for bone related disorders. Use of acidic oligopepties tagging is an innovative approach where repetitive L-Asp and L-Glu acidic amino acid sequences will rapidly bind to hydroxyapaptite in bone (Teitelbaum & Ross 2003 and Lips 2001). With this in mind, the present project has created GIP/xenin hybrids with either six C-terminal aspartic acid and

glutamic acid amino acid residues extensions, potentially making the peptide highly specific and selective to bone.

Studies were conducted in high fat fed mice that have recognised bone defects associated with poor metabolic control (Kerckhofs *et al*. 2016, Koks *et al*. 2016, Yan *et al*. 2016). As well as assessing metabolic control, highly advanced imaging techniques were employed for assessment of bone quality and strength following 42 days administration of each peptide. These techniques included bone three-point bending, nanoindentation, quantitative backscattered electron imaging (QBEI) and fourier transformed infrared microscopy (FTIR) imaging. The findings of this study reveal that GIP/xenin hybrid peptides with C-terminal L-Asp and L-Glu extensions have retained biological activity and possess distinct effects on diabetes control and bone health in high fat fed mice.

6.3 MATERIALS AND METHODS

6.3.1 Synthesis of peptides

GIP/Xenin, GIP/Xenin-Asp and GIP/Xenin-Glu were purchased from EZ Biolabs Ltd. (Carmel, IN, USA). The peptides were identified and characterised by mass spectrometry as described in Section 2.1.2.

6.3.2 Animals and study design

Young male NIH Swiss mice (8 weeks old) were maintained on high-fat diet for three months. All the mice were housed separately in air conditioned room with 12 hour light and 12 hour dark cycle. Mice were grouped (n=7) according body weight and blood glucose. Prior to commencing the experiment, all mice were injected with saline solution (0.9% NaCl) for 3 days to acclimatise to the injection regimen. Group of high fat fed mice then received saline injection (0.9% NaCl), GIP/Xenin,

GIP/Xenin-Asp or GIP/Xenin-Glu (each at 25 nmol/kg bw) once daily for 42 days. Body weight, food consumption, non-fasting glucose and insulin concentrations were measured at regular intervals. Intraperitoneal glucose tolerance test (18 mmol/kg bw, 18 hour fast) and non-fasting insulin sensitivity test (25 U/kg bw) were performed at the end of the study as described in Section 2.3.2 and 2.3.3 respectively. Bones were then collected and processed as noted in Sections 2.5.1 to 2.5.5, and described below. All experiments were carried out according to UK Home Office Regulations (UK Animals Scientific Procedures Act 1986).

6.3.3 Measurement of plasma insulin

An insulin RIA was carried out as described in Section 2.4.2 to determine plasma insulin concentrations.

6.3.4 Measurement of body composition, bone density and mineral content by DEXA scanning

Isoflurane was used to anesthetize the mice before being placed on a specimen tray of the DEXA scanner. Bone mineral density (BMD), bone mineral content (BMC), lean mass, fat mass were determined as explained in Section 2.4.

6.3.5 Three-point bending test

Mechanical properties of the femur were assessed using three-point bending. The properties examined were ultimate load, ultimate displacement, stiffness and work to failure ratio. Femurs were kept in vials containing saline (NaCl, 0.9%) so that they remained hydrated. Three- point bending was carried out as described in Section 2.5.4.

6.3.6 X-ray microcomputed tomography (µCT)

Tibias were also processed for microcomputed tomography. Scanning of the tibias was carried out to assess trabecular bone mass, trabecular bone thickness, number of trabeculae, cortical bone diameter, cortical thickness, diameter of bone marrow and cross-sectional moment of inertia as described in Section 2.5.3.

6.3.7 Nanoindentation

Nanoindentation was performed on bone as described in the Section 2.5.1 and following parameters were assessed: maximum force, hardness, indentation modulus and dissipated energy. Polymethylacrylate blocks were polished with three times with diamond particles to obtain smooth surface. Following this, blocks were left in saline (NaCl, 0.9%) solution for overnight and processed next morning.

6.3.8 Quantitative backscattered electron imaging (qBEI)

The polymethylmethacrylate blocks were polished three times, as above, and then subjected to carbon coating for 4 hrs. After carbon coating, the polymethylacrylate blocks were observed under scanning electron microscope as described in Section 2.5.2 to assess bone mineral density distribution.

6.3.9 Fourier transformed infrared (FT-IR) imaging and micro spectroscopy

Following embedding of bone, as described in Section 2.x.x, sections (4 µm) were cut using a micrtome equipped with tungsten carbide knife and sandwiched between BaF_2 optical windows. Spectral analysis was performed using Bruker Vertex 70 spectrometer interfaced with Bruker Hyperion 3000 infrared microscope equipped with mercury cadmium telluride detector. Infrared spectra were recorded with an average of 32 scans in

transmission mode in the same locations as for qBEI and nanoindentation.

6.3.10 Statistical analysis

Data were analysed using one-way or two-way ANOVA with two-tailed t-tests using PRISM 5.0. Data are expressed as mean ± S.E.M and a P value < 0.05 was considered statistically significant.

6.4 RESULTS

6.4.1 Effects of GIP/Xenin, GIP/Xenin-Asp and GIP/Xenin-Glu on body weight, fat mass, lean mass and food intake in high-fat fed mice

Once daily administration of GIP/Xenin, GIP/Xenin-Asp and GIP/Xenin-Glu did not cause any significant changes in body weight (Figure 6.1 A), fat mass (Figure 6.1 B), lean mass (Figure 6.1 C) or food intake (Figure 6.2) in high fat fed mice.

6.4.2 Effects of GIP/Xenin, GIP/Xenin-Asp and GIP/Xenin-Glu on circulating blood glucose and plasma insulin in high-fat fed mice

There was no significant differences between groups of high at fed mice in terms of blood glucose (Figure 6.3 A) or plasma insulin (Figure 6.3 B) concentrations.

6.4.3 Effects of GIP/Xenin, GIP/Xenin-Asp and GIP/Xenin-Glu on glucose tolerance and insulin sensitivity in high-fat fed mice

After injecting glucose intraperitoneally (18 mmol/kg bw) on day 42, blood glucose was significantly ($p<0.001$) reduced in all treatment groups when compared to saline controls at 60 mins post-injection (Figure 6.4A). In addition, GIP/Xenin-Asp treated

mice had lowered blood glucose levels at the 15 and 30 minute observation points, which corresponded with significantly ($p<0.05$) decreased AUC values in these mice (Figure 6.4B). No effect of the treatments was seen on plasma insulin concentrations at the time points examined (Figure 6.4C), however both GIP/Xenin-Glu and GIP/Xenin-Asp treated mice had a reduced ($p<0.05$) overall insulin secretory response (Figure 6.4D). Mice treated with GIP/Xenin, GIP/Xenin-Asp or GIP/Xenin-Glu had significantly ($p<0.05$ to $p<0.001$) deceased blood glucose values following injection of insulin at 15, 30, 60 and 120 min when compared to saline controls (Figure 6.5A). In addition, GIP/Xenin-Glu mice had a reduced ($p<0.05$) overall glycaemic excursion (Figure 6.5B).

6.4.4 DEXA analysis of whole body, femur, tibia and lumbar spine in in high-fat fed mice

DEXA analysis on day 42 revealed that there was no difference in whole body or femoral BMD and BMC between all groups of high fat fed mice (Figure 6.6A-D). However, whilst lumbar BMD was also not different (Figure 6.7A) GIP/Xenin enhanced ($p<0.01$) lumbar BMC compared to saline controls (Figure 6.7B). In addition, tibial BMD assessment (Figure 6.8.A) revealed that GIP/Xenin-Asp and GIP/Xenin-Glu both increased ($p<0.01$ and $p<0.05$, respectively) this parameter in high fat fed mice, BMC was similar in all groups (Figure 6.8.B).

6.4.5 Effects of GIP/Xenin, GIP/Xenin-Asp and GIP/Xenin-Glu on whole-bone mechanical properties in high-fat fed mice

Three-point bending analysis revealed a reduction ($p<0.01$) in ultimate load bearing of femoral cortical bone following 42 days treatment with GIP/Xenin-Glu (Figure 6.9A). However, no significant changes in ultimate displacement were observed with

any of the treatment regimens (Figure 6.9B). Despite this, GIP/Xenin-Glu mice also presented with reduced ($p<0.05$) femoral cortical bone stiffness (Figure 6.9C). Interestingly, work-to-failure ratio was not significantly different within the groups of high fat fed mice (Figure 6.9D).

6.4.6 Effects of GIP/Xenin, GIP/Xenin-Asp and GIP/Xenin-Glu on trabecular bone morphology and cortical bone geometry in high-fat fed mice

Microcomputed tomography (MicroCT) was performed to analyse trabecular bone volume, thickness, separation and number of trabeculae. Notably, none of the bone-specific GIP/Xenin hybrids affected these parameters (Figure 6.10A-C). However, GIP/Xenin treatment for 42 days increased ($p<0.05$) trabecular bone volume and the number of trabeculae (Figure 6.10A,B). Cortical bone geometry was similar in all high fat fed mice, apart from those treated with GIP/Xenin-Glu (Figure 6.11A-F). As such, cortical area ($p<0.01$), thickness ($p<0.01$) and moment of inertia ($p<0.05$) were reduced by GIP/Xenin-Glu treatment (Figure 6.11B, D,F). No changes in tibial overall area, bone marrow diameter and mineralisation were noted (Figure 6.11A, C, and E).

6.4.7 Effects of GIP/Xenin, GIP/Xenin-Asp and GIP/Xenin-Glu on nanomechanical properties of cortical bone matrix in high-fat fed mice

GIP/Xenin, GIP/Xenin-Asp and GIP/Xenin-Glu did not induce any significant changes in hardness (Figure 6.12A), indentation modulus (Figure 6.12B), force (Figure 6.12C) and dissipated energy (Figure 6.12D) of cortical bone matrix.

6.4.8 Effects of GIP/Xenin, GIP/Xenin-Asp and GIP/Xenin-Glu on bone mineral density distribution in high-fat fed mice

All the three variables analysed relating to bone mineral density distribution including Ca_{peak}, Ca_{mean} and Ca_{width} at cortical parts of the tibia in high-fat fed mice were similar in all treatment groups when compared to high-fat fed controls (Figure 6.13A-C)

6.4.9 Effects of GIP/Xenin, GIP/Xenin-Asp and GIP/Xenin-Glu on bone at tissue level in high-fat fed mice

Different parameters relating directly to the bone tissue were analysed using infrared spectroscopy. These parameters included collagen maturity, crystallinity, phosphate amide ratio and acid phosphate ratio (Figure 6.14A-J). However, none of these factors were affected by 42 days once daily treatment with GIP/Xenin, GIP/Xenin-Asp or GIP/Xenin-Glu in high-fat fed mice.

6.5 DISCUSSION

Bone resorption biomarkers have been shown to undergo a rapid change following food ingestion (Henrikson *et al*. 2003, Cross *et al*. 2017, Chandran 2017, Kline *et al*. 2017). This suggests that gastrointestinal hormones play a role in bone remodelling. Glucose dependent insulinotrpic polypeptide (GIP) is released by entero-endocrine K cells and GIP receptors are present on bone cells (Bollag *et al*.2000, Zhong *et al* 2007). Whilst there are many GIP-related studies focusing on diabetes and glucose dependent insulin secretion (Ramsey *et al*. 2017, Seino & Yabe 2013, Li *et al*. 2016) less attention has been given to the fact that GIP has direct positive beneficial effects on bone. It has also been well established recently that xenin, co-secreted with GIP from K-cells, can potentiate the action of GIP (Martin *et al*. 2016, Gault *et al*. 2015). Therefore, recently a GIP/xenin hybrid peptide has been characterised, that incorporates the benefits of

combined GIP and xenin activity into one single molecule (Hasib *et al*. 2017). Although highly effective, this hybrid peptide would have no specificity for bone tissue. Therefore, in this study bone-targeting GIP/xenin hybrid forms were created, through addition of six C-terminal acidic L-Asp and L-Glu amino acid residues by using acid oligopeptide tagging that encourages binding to mainly hydroxyapatite (Ulbrich *et al*. 2016).

Once daily administration of GIP/Xenin, GIP/Xenin-Asp and GIP/Xenin-Glu for 42 days had no effect on body weight or food intake in high-fat fed mice. Thus, any potential effect of the peptides on bone would not be linked to altered body weight, that can affect bone physiology (Harper *et al*. 2016, Meier *et al*. 2016, MacDonell *et al*. 2016, Shanbhogue *et al*. 2016). In addition, we did not see any changes in non-fasted plasma glucose and insulin levels in high-fat fed mice. This is in contrast to previous studies with GIP/Xenin (Hasib *et al*. 2017), but could be due to frequency of peptide administered and type of diabetic model employed here. However, insulin is a known anabolic hormone in bone (Krishnan & Muthusami 2016, Bortolin *et al*. 2016, Anderson *et al*. 2017) and therefore changes in bone properties by each of the peptides can be viewed independently of altered insulin levels. In agreement with previous studies (Hasib *et al*. 2017), administration of GIP/Xenin and related bone-specific analogues improved glucose tolerance and enhance insulin sensitivity. This is encouraging, as it suggests that the C-terminal additions in GIP/Xenin-Asp and GIP/Xenin-Glu do not adversely affect biological activity.

In terms on bone related analyses, DEXA analysis revealed that no difference in whole body and femoral BMD and BMC. However, lumbar BMC was enhanced by GIP/Xenin and tibial

BMD by GIP/Xenin-Asp and GIP/Xenin-Glu. This differential effect of the peptides on bone BMD and BMC is interesting and merits further detailed study. However, type 2 diabetic patients are noted to have increased or unchanged BMD (Vestergaard, 2007), which may also be true for the high fat fed mice used in this study. Nonetheless, bone quality does not merely depend on BMD and BMC, and there are many other factors such as microarchitecture, bone matrix composition, biomechanical strength that play an important role in overall bone quality and integrity (Mieczkowska *et al*. 2013). Therefore, the current study assessed these parameters in more detail, in an attempt to separate the effects of GIP/Xenin, GIP/Xenin-Asp and GIP/Xenin-Glu on bone health in high fat fed mice.

MicroCT was carried out to analyse trabecular bone volume, thickness, separation and number of trabeculae in the bone. It was found that the number of trabeculae and trabecular bone volume was increased in GIP/Xenin treated mice. In harmony with this, Gaudin-Audrain and colleagues reported that GIP receptor deficiency leads to modification of trabecular bone volume and reduction in number of trabeculae (Gaudin-Audrain *et al*. 2013). The reason behind the lack of significant effect of GIP/Xenin-Asp and GIP/Xenin-Glu is intriguing, and perhaps more deposition in bone and reduced circulating peptide levels may explain this, although detailed studies would be required to confirm this. However, cortical bone geometry seemed to be detrimentally altered by GIP/Xenin-Glu that could possibly be linked to the observed decrease in overall cortical bone strength noted from three-point bending studies. The reason why GIP/Xenin-Glu, but not GIP/Xenin-Asp, should induce such effects is intriguing and suggests altered biological action and/or pharmacokinetics of these modified GIP/xenin hybrid molecules. Further studies would certainly be required, and of major interest, to resolve this

conundrum. Interestingly, Mieczkowska *et al*. in 2015 carried out study in double incretin receptor knock-out mice, where both GIP and GLP-1 receptors have been removed, and demonstrated reduced cortical bone mass and cortical bone strength. In our study, we found that cortical thickness was reduced by GIP/Xenin-Glu indicating that it might have deleterious effects on the cortex.

Further assessment of cortical bone parameters was also conducted, in an attempt to further ascertain possible differential actions of GIP/Xenin, GIP/Xenin-Asp and GIP/Xenin-Glu on bone. However, treatment of high fat fed mice for 42 days with each of the peptides had no obvious effect the nanochemical properties or cortical bone or mineral density distribution. Infrared spectroscopy was performed to analyse collagen maturity, crystallinity, phosphate amide ratio and acid phosphate ratio. This analysis revealed that collagen maturity, crystallinity of the bone tissue, phosphate/amide ratio, carbon/phosphate ratio and acid phosphate was not significantly affected by any of the treatment regimens. Lack of clear effects could be due to the timing of injections, length of the study, age of mice at onset and the strain of mice employed. Indeed, it is worth bearing in mind that bone quality and strength determines overall bone integrity (Miller *et al*. 2017). As such, the strength of bone and its ability to resist fracture is not only dependent on bone geometry and bone mass but also on intrinsic material properties of the bone, microstructure, morphology, mineralisation and bone mass (Vennin *et al*. 2017). This is a complex process, and dependent upon many interlining variables. However, it seems clear that GIP/Xenin-Glu imparted detrimental effects on bone strength and quality in the current study.

In conclusion, GIP/xenin, GIP/Xenin-Asp and GIP/Xenin-Glu all possessed beneficial metabolic effects in high fat fed mice.

Both GIP/xenin and GIP/Xenin-Asp appeared to have a positive impact on bone health. Considering that diabetes is linked to increased bone fractures and lower quality bone (Sosa & Eriksen 2017, Sheu *et al*. 2017, Nilsson *et al*. 2017) these hybrid peptides may merit further study as potential therapeutic candidates for diabetes, and particularly diabetic patients who present with related bone disorders.

Figure 6.1 Effects of once daily administration of GIP/Xenin, GIP/Xenin-Asp and GIP/Xenin-Glu for 42 days on (A) body weight (B) fat mass and (B) total lean mass in high fat fed mass

A

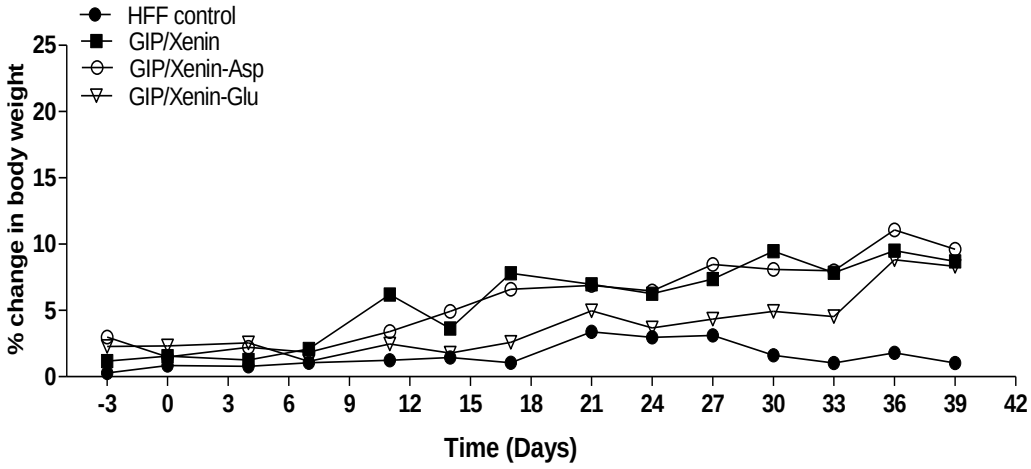

B

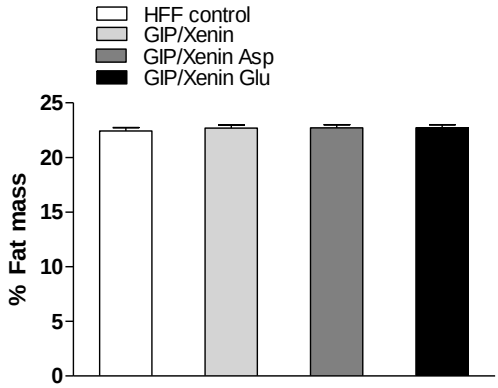

C

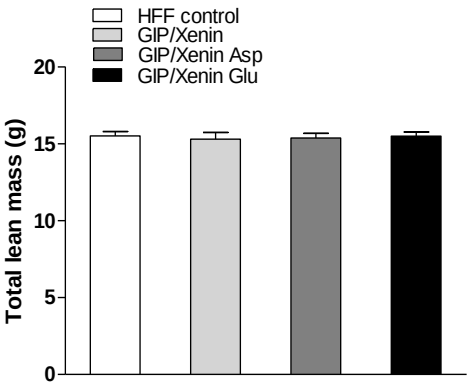

(A) Body weight was measured for 3 days before and 42 days during (indicated by black horizontal bar) once daily treatment with saline vehicle (0.9%w/v NaCl), GIP/Xenin, GIP/Xenin-Asp and GIP/Xenin-Glu (each peptide at 25 nmol/kg bw). (B) %Fat mass and (C) Lean mass as measured by DEXA scanning in high fat fed mice on day 42 Values represent means ± SEM for 7 mice.

Figure 6.2 Effects of once daily administration of GIP/Xenin, GIP/Xenin-Asp and GIP/Xenin-Glu for 42 days on cumulative energy intake in high fat fed mice

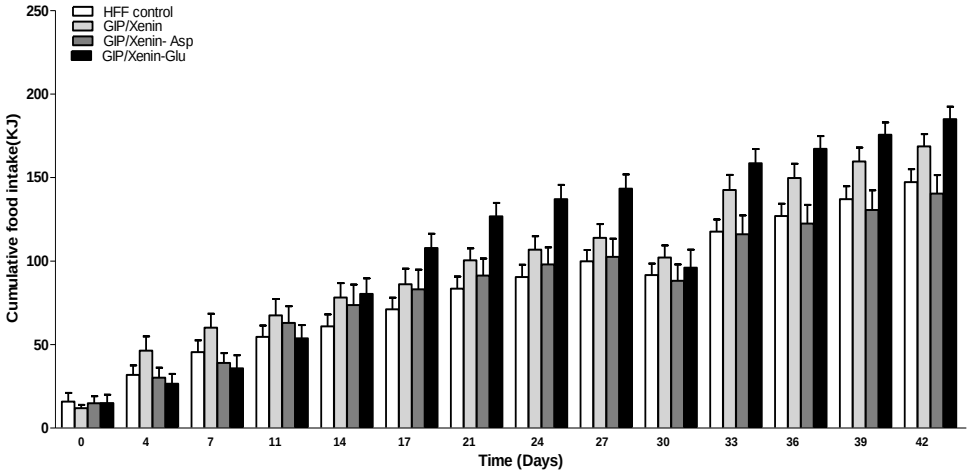

Cumulative energy intake was measured for 3 days before and 42 days during (indicated by black horizontal bar) once daily treatment with saline vehicle (0.9% w/v NaCl), GIP/Xenin, GIP/Xenin-Asp and GIP/Xenin-Glu (each peptide at 25 nmol/kg bw). Values represent means ± SEM for 7 mice.

Figure 6.3 E**ffects of once daily administration of GIP/Xenin, GIP/Xenin-Asp and GIP/Xenin-Glu for 42 days on non fasting (A) blood glucose and (B) plasma insulin in high fat fed mice**

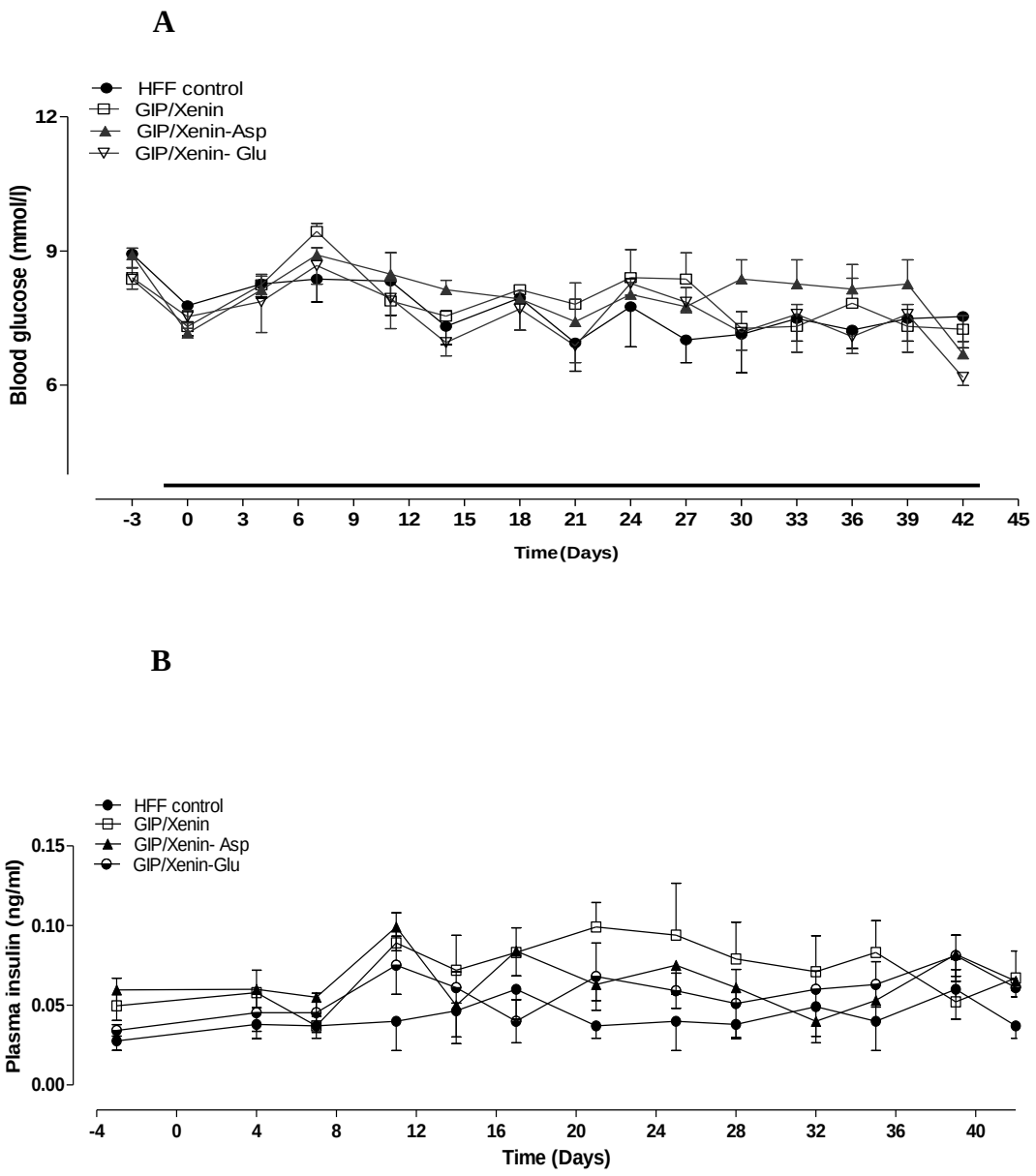

(A) Blood glucose and (B) plasma insulin were measured for 3 days before and 42 days during once daily treatment with saline vehicle (0.9%w/v NaCl), GIP/Xenin, GIP/Xenin-Asp and GIP/Xenin-Glu (each peptide at 25 nmol/kg bw). Values represent means ± SEM for 7 mice.

Figure 6.4 Effects of once daily administration of GIP/Xenin, GIP/Xenin-Asp and GIP/Xenin-Glu for 42 days on (A) glucose tolerance and (C) plasma insulin response to glucose in high fat fed mice

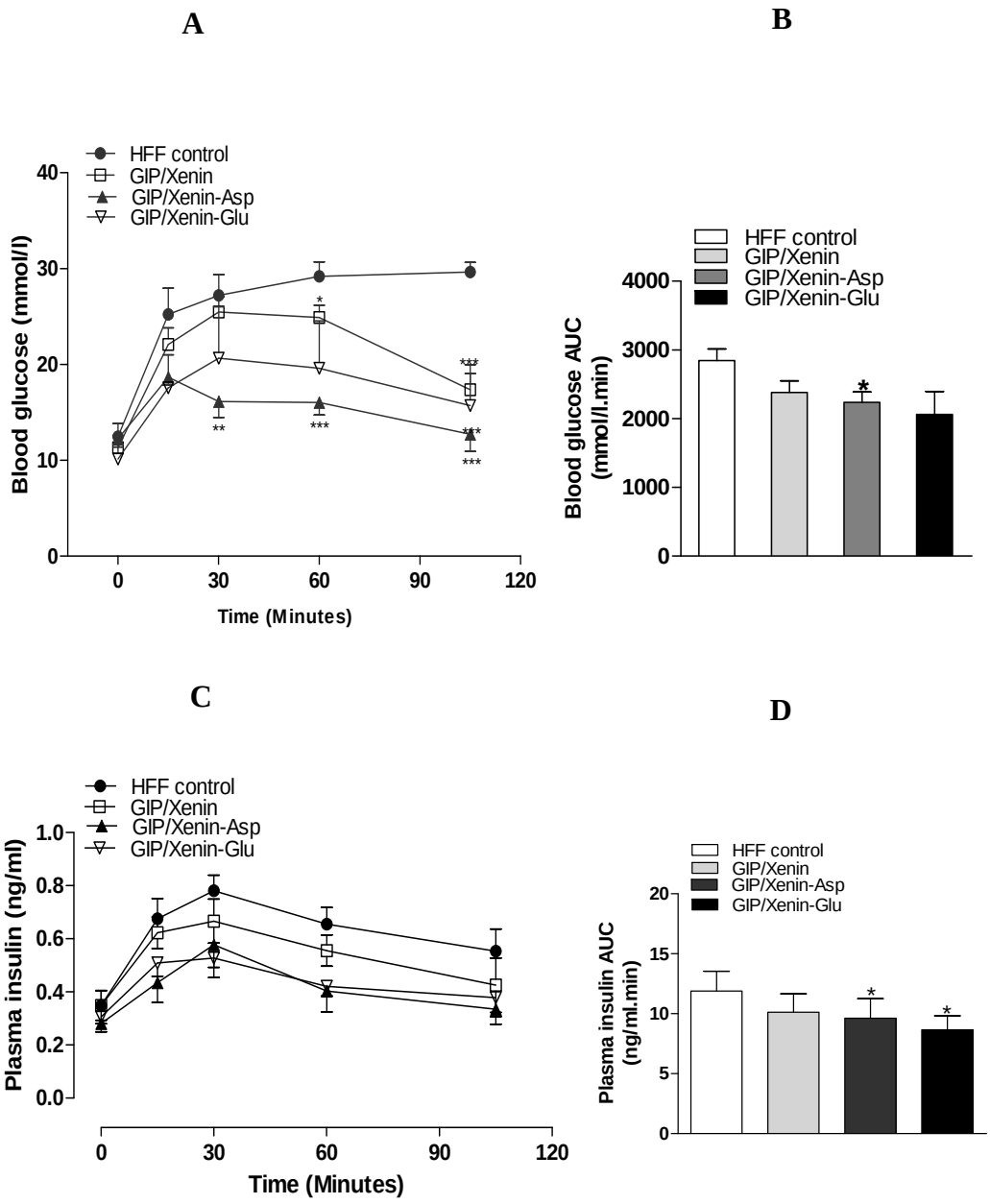

Tests were conducted after once daily treatment with saline, GIP/Xenin, GIP/Xenin-Asp and GIP/Xenin-Glu (each peptide at 25 nmol/kg bw) for 42 days. (A) Blood glucose (C) plasma before and after i.p injection of glucose (18 mmol/kg bw) alone in 18 hour fasted mice. (B,D) AUC values for for 0-105 min are shown. Values are mean ± S.E.M for 7 mice per group. *p< 0.05, **p< 0.01, ***p< 0.001 compared with high fat fed control.

Figure 6.5 Effects of once daily administration of GIP/Xenin, GIP/Xenin-Asp and GIP/Xenin-Glu for 42 days on insulin sensitivity high fat fed mice

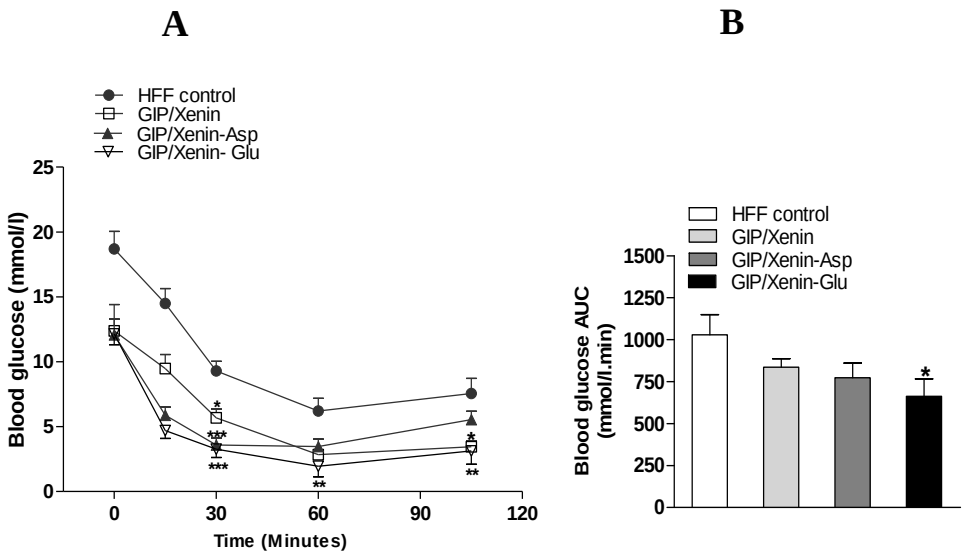

Following 42 days treatment with saline, GIP/Xenin, GIP/Xenin-Asp and GIP/Xenin-Glu (each peptide at 25 nmol/kg bw), insulin (25 U/kg bw) was injected intraperitoneally (at t=0) in non-fasted mice to assess insulin sensitivity. (A) Blood glucose and (B) blood glucose AUC values for 0-105 min are shown. Values represent means ± SEM for 7 mice. *p< 0.05, **p< 0.01 and ***p< 0.001 compared to high fat fed control.

Figure 6.6 Effects of once daily administration of GIP/Xenin, GIP/Xenin-Asp and GIP/Xenin-Glu for 42 days on (A) whole body bone mineral density (BMD), (B) whole body bone mineral content (BMC), (C) femur bone mineral density (BMD) and (D) femur bone mineral content (BMC) in high fat fed mice

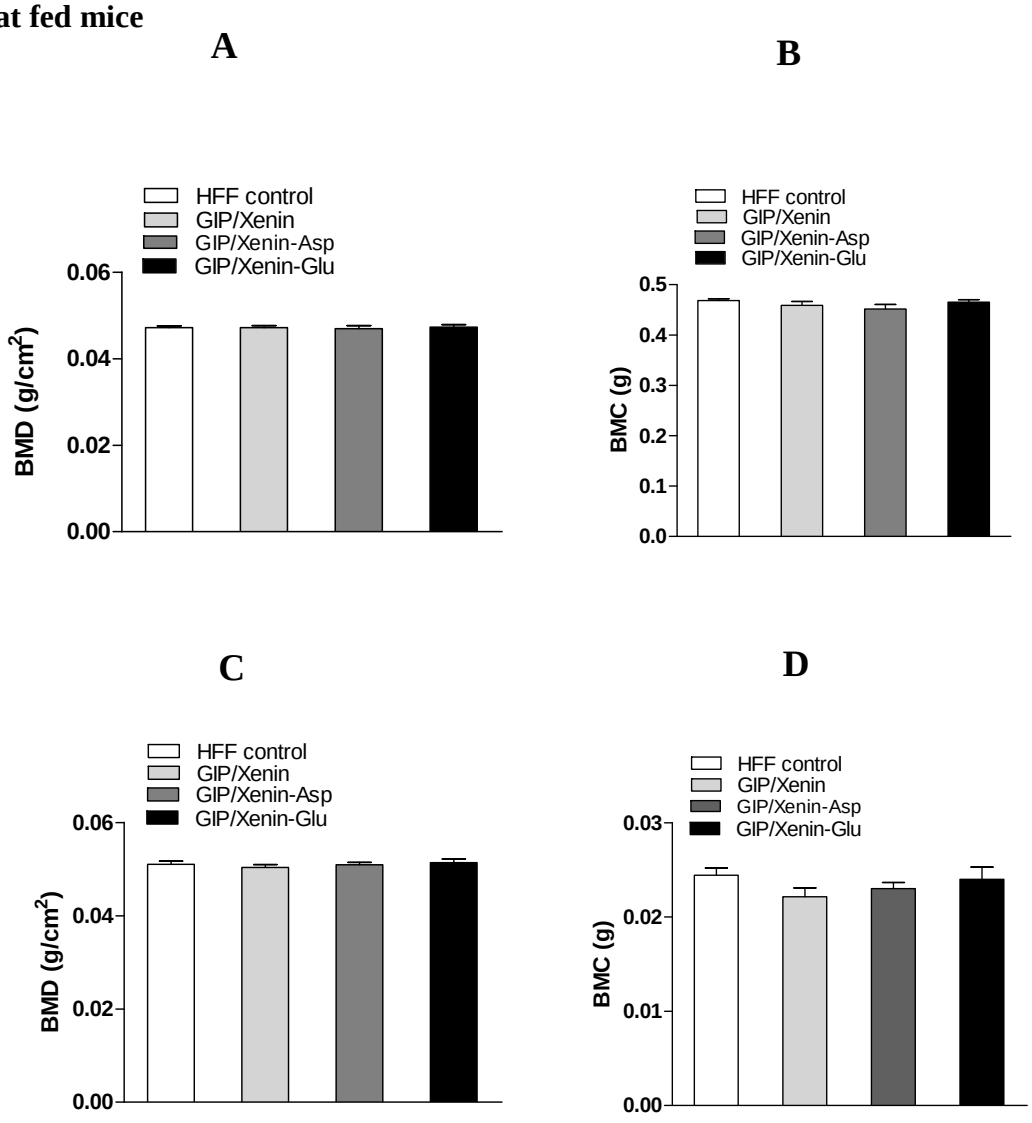

(A) Whole body bone mineral density (BMD) and (B) whole body bone mineral content (BMC), (C) femur BMD and (D) femur BMC as measured by DEXA scanning in high fat fed mice following 42 days treatment with GIP/Xenin, GIP/Xenin-Asp and GIP/Xenin-Glu (each peptide at 25 nmol/kg bw). Values represent means ± SEM for 7 mice.

Figure 6.7 Effects of once daily administration of GIP/Xenin, GIP/Xenin-Asp and GIP/Xenin-Glu for 42 days on lumbar spine (A) bone mineral density (BMD) and (B) bone mineral content (BMC) in high fat fed mice

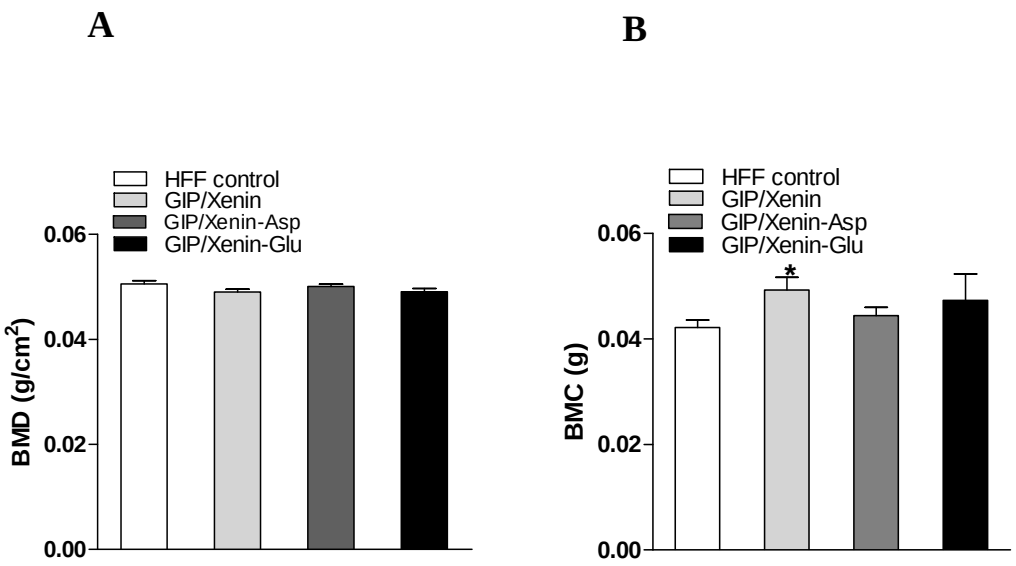

Lumbar Spine (A) Bone mineral density (BMD) and (B) bone mineral content (BMC) as measured by DEXA scanning in high fat fed mice following 42 days treatment with GIP/Xenin, GIP/Xenin-Asp and GIP/Xenin-Glu. Values represent means ± SEM for 7 mice. $^{*}p< 0.05$ compared to high fat fed control.

Figure 6.8 Effects of once daily administration of GIP/Xenin, GIP/Xenin-Asp and GIP/Xenin-Glu for 42 days on tibia (A) bone mineral density (BMD) and (B) bone mineral content (BMC) in high fat fed mice

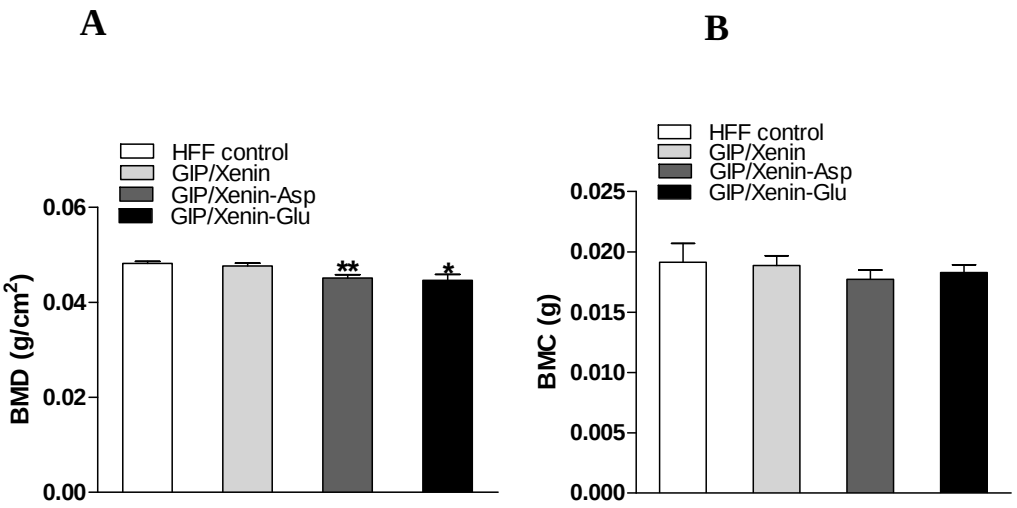

Tibia (A) Bone mineral density (BMD) and (B) bone mineral content (BMC) as measured by DEXA scanning in high fat fed mice following 42 days treatment with GIP/Xenin, GIP/Xenin-Asp and GIP/Xenin-Glu. Values represent means ± SEM for 7 mice. $^{*}p< 0.05$, $^{**}p<0.01$ compared to high fat fed control.

Figure 6.9 Effects of once daily administration of GIP/Xenin, GIP/Xenin-Asp and GIP/Xenin- Glu for 42 days on whole-bone mechanical properties of femoral cortical bone in high fat fed mice

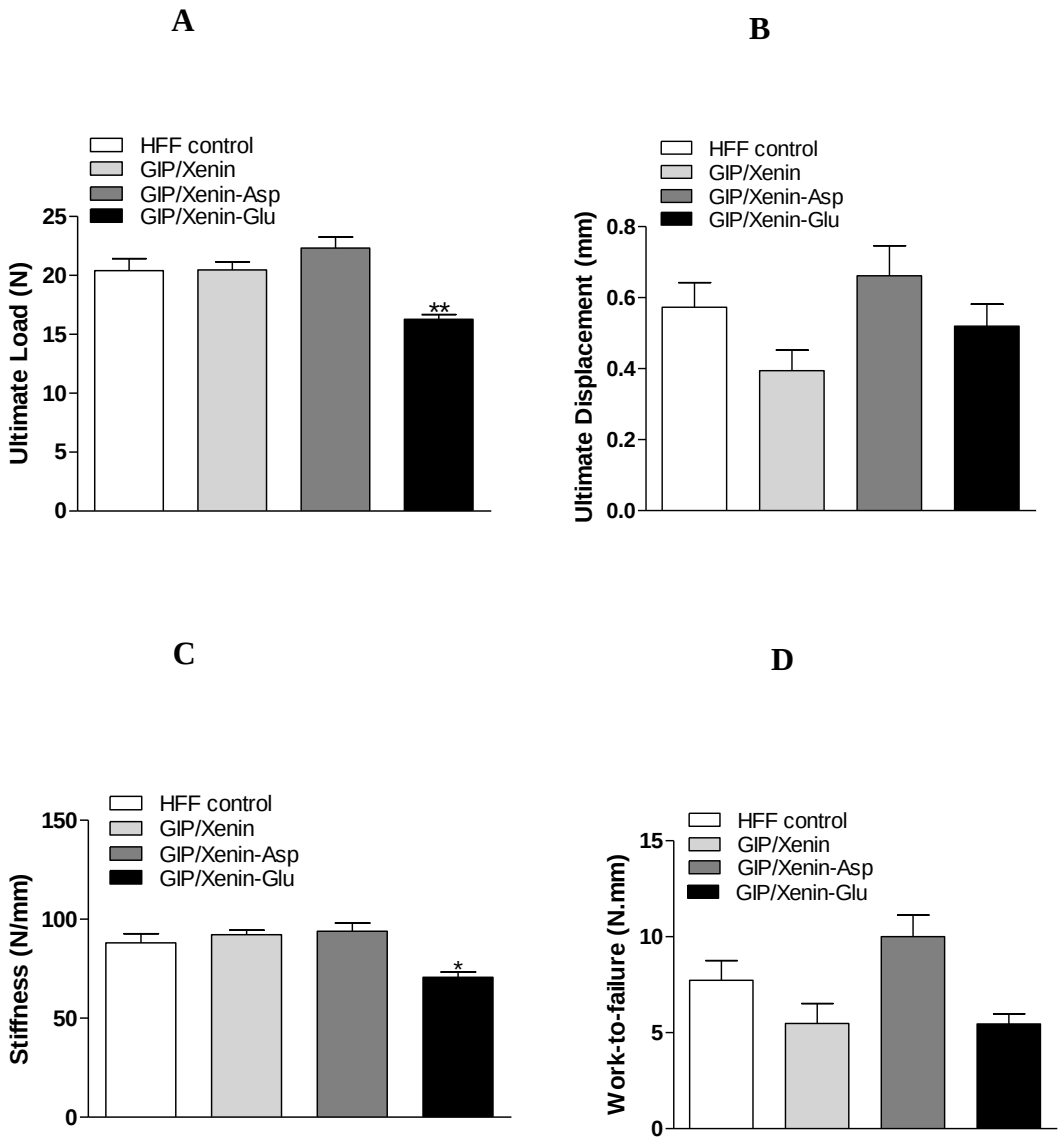

Parameters were obtained following 3-point bending tests after 42 days once daily administration of GIP/Xenin, GIP/Xenin-Asp and GIP/Xenin- Glu (each at 25 nmol/kg b.w) in high fat fed mice. Values are mean ± S.E.M for 7 mice. *p< 0.05, **p< 0.01 compared to high fat fed control.

Figure 6.10 Effects of once daily administration of GIP/Xenin, GIP/Xenin-Asp and GIP/Xenin-Glu on trabecular bone mass and microarchitecture in high fat fed mice

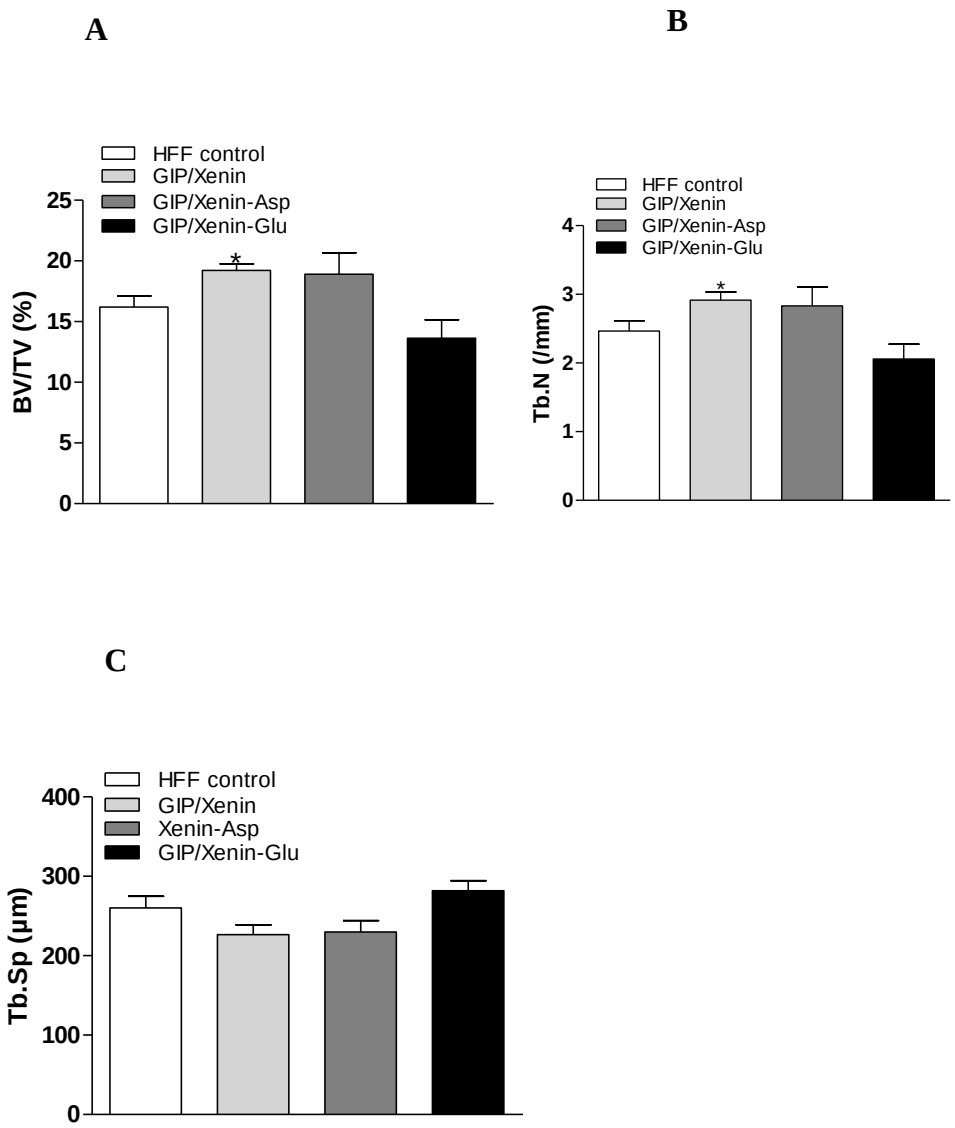

Parameters were obtained from a microtomography scan of tibia following 42 days once daily administration of saline (0.9%, w/v, NaCl), GIP/Xenin, GIP/Xenin-Asp and GIP/Xenin-Glu (each at 25 nmol/kg b.w). Values are mean ± S.E.M for 7 mice. *$p<0.05$ compared with high fat fed control.

Figure 6.11 Effects of once daily administration of GIP/Xenin, GIP/Xenin-Asp and GIP/Xenin-Glu on cortical bone microarchitecture in high fat fed mice

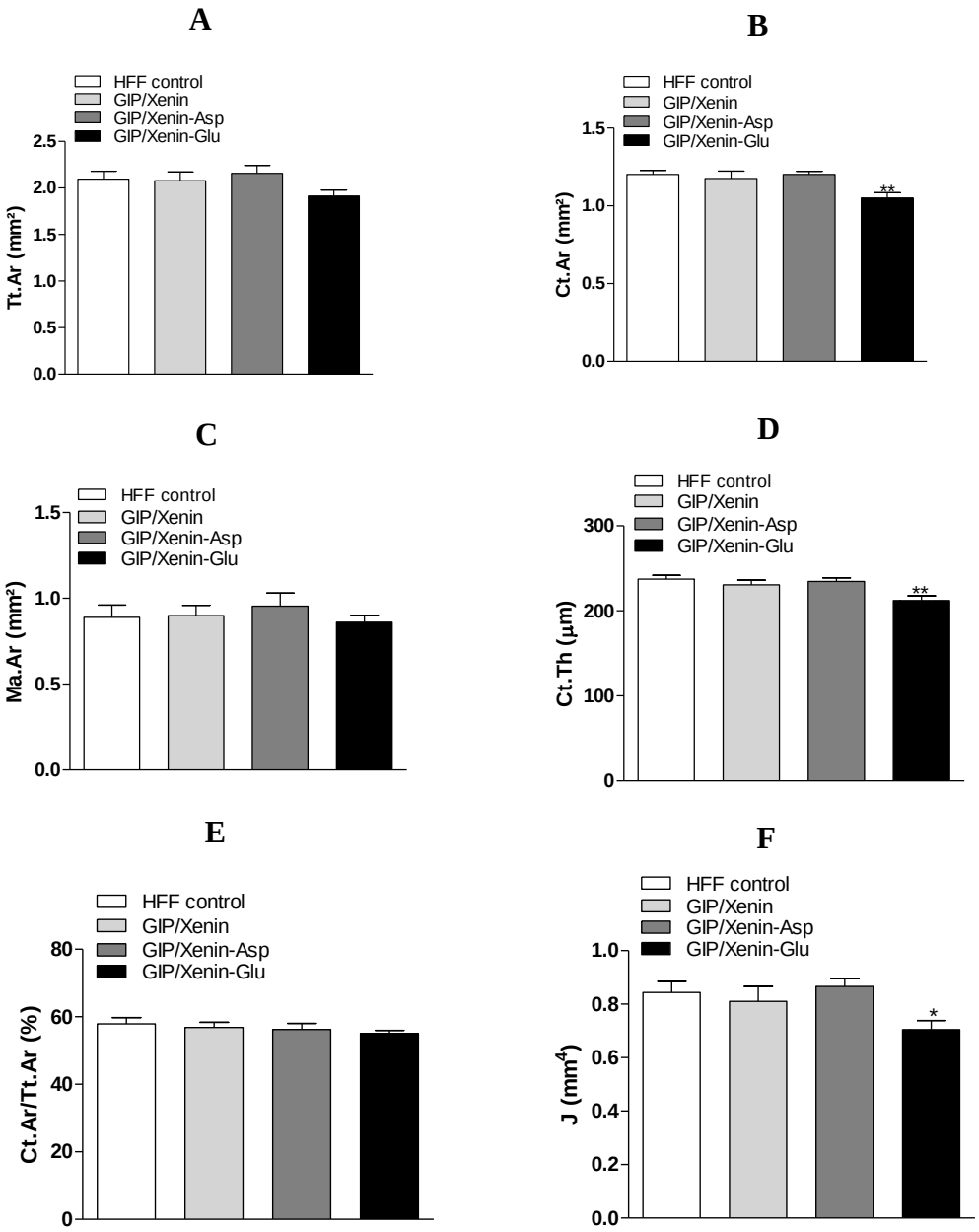

Images of cortical bone were obtained from a microtomography scan of tibia following 42 days once daily administration of saline (0.9%, w/v, NaCl), GIP/Xenin, GIP/Xenin-Asp and GIP/Xenin-Glu (each at 25 nmol/kg b.w). Cortical bone was located 3 mm below growth plate and Total area (A), cortical area (B), bone marrow diameter (C) cortical thickness (D), bone mineralisation and moment of inertia (F) were measured. Values are mean ± S.E.M for 7 mice. *$p<0.05$, **$p<0.01$ compared to normal high fat fed control.

Figure 6.12 Effects of GIP/Xenin, GIP/Xenin-Asp and GIP/Xenin-Glu on nanomechanical properties of cortical bone matrix in high-fat fed mice

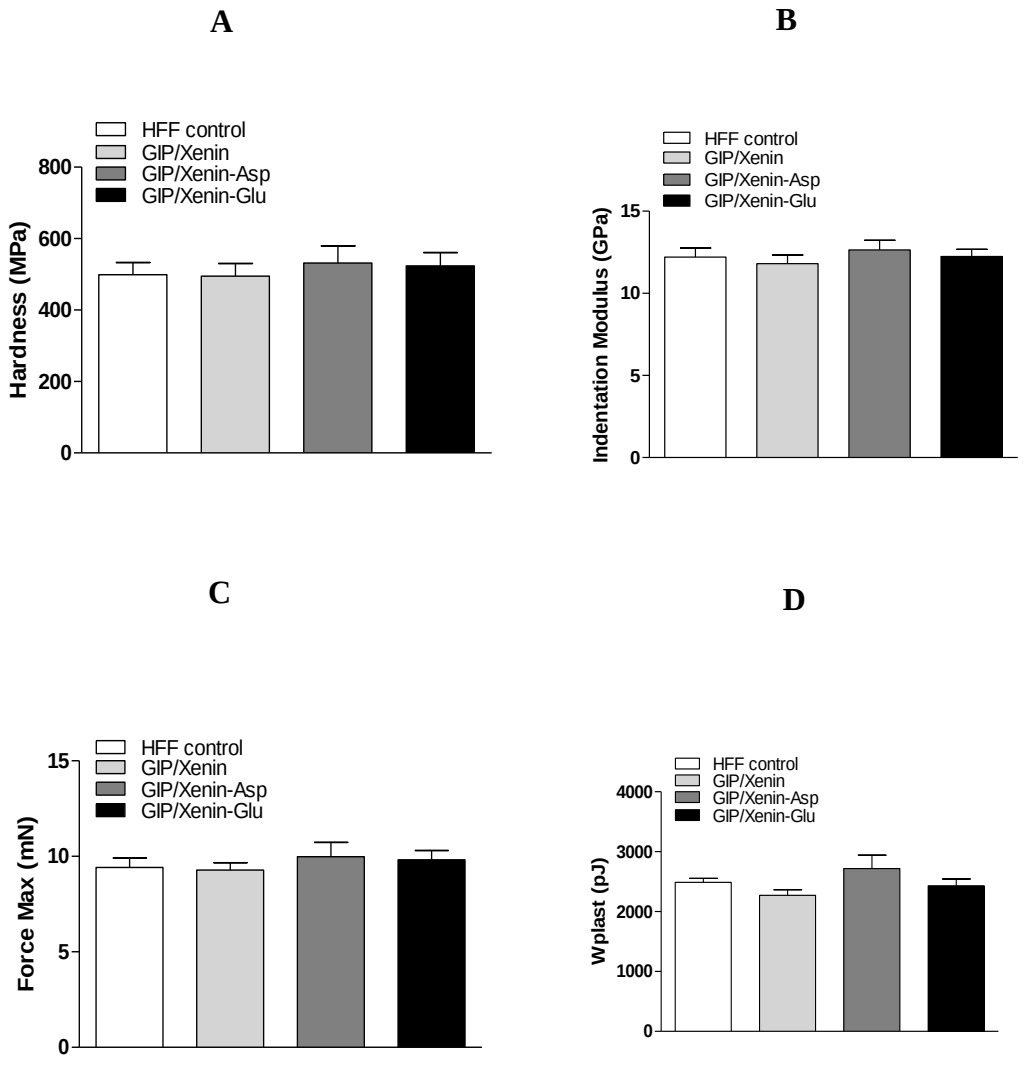

Parameters were measured by nanoindentation following 42 days once daily administration of saline (0.9%, w/v, NaCl), GIP/Xenin, GIP/Xenin-Asp and GIP/Xenin-Glu (each at 25 nmol/kg b.w). Values are mean ± S.E.M for 7 mice.

Figure 6.13 Effects of once daily administration of GIP/Xenin, GIP/Xenin-Asp and GIP/Xenin-Glu on cortical bone mineral density distribution (BMDD) in high-fat fed mice

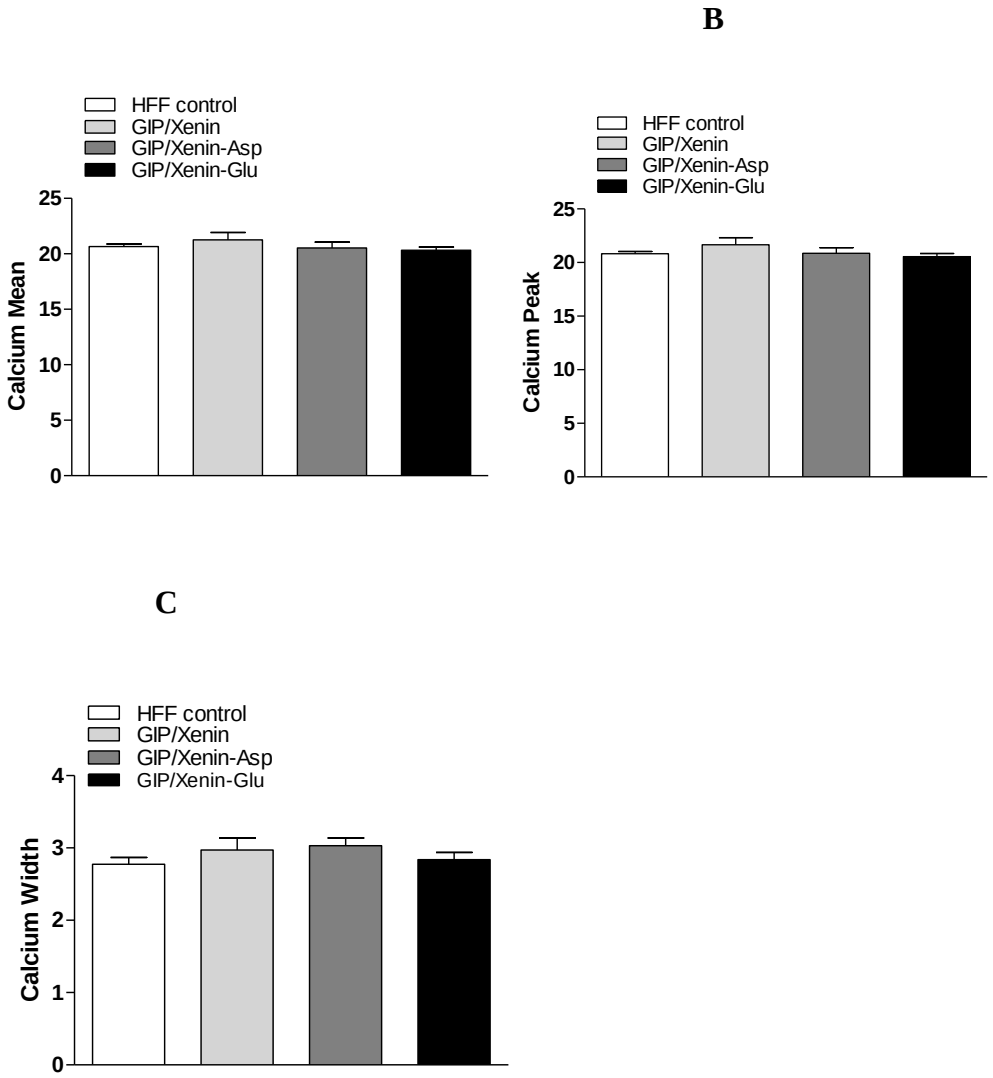

Bone mineralisation at cortical bone was measured by quantitative backscattered electron imaging following 42 days once daily administration of saline (0.9%, w/v, NaCl), GIP/Xenin, GIP/Xenin-Asp and GIP/Xenin-Glu (each at 25 nmol/kg b.w). Values are mean ± S.E.M for 7 mice.

Figure 6.14 Effects of once daily administration of GIP/Xenin, GIP/Xenin-Asp and GIP/Xenin-Glu on bone tissue

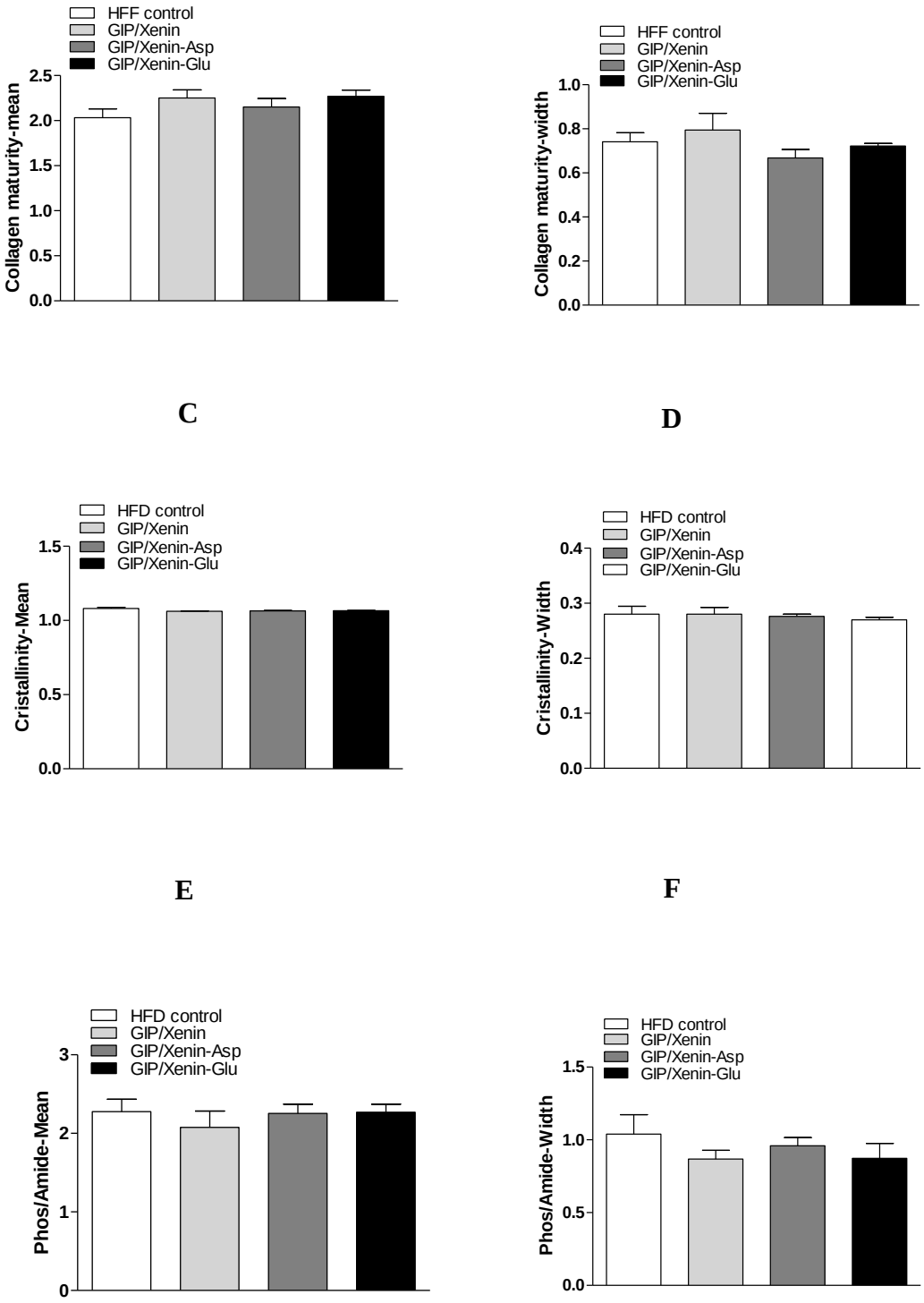

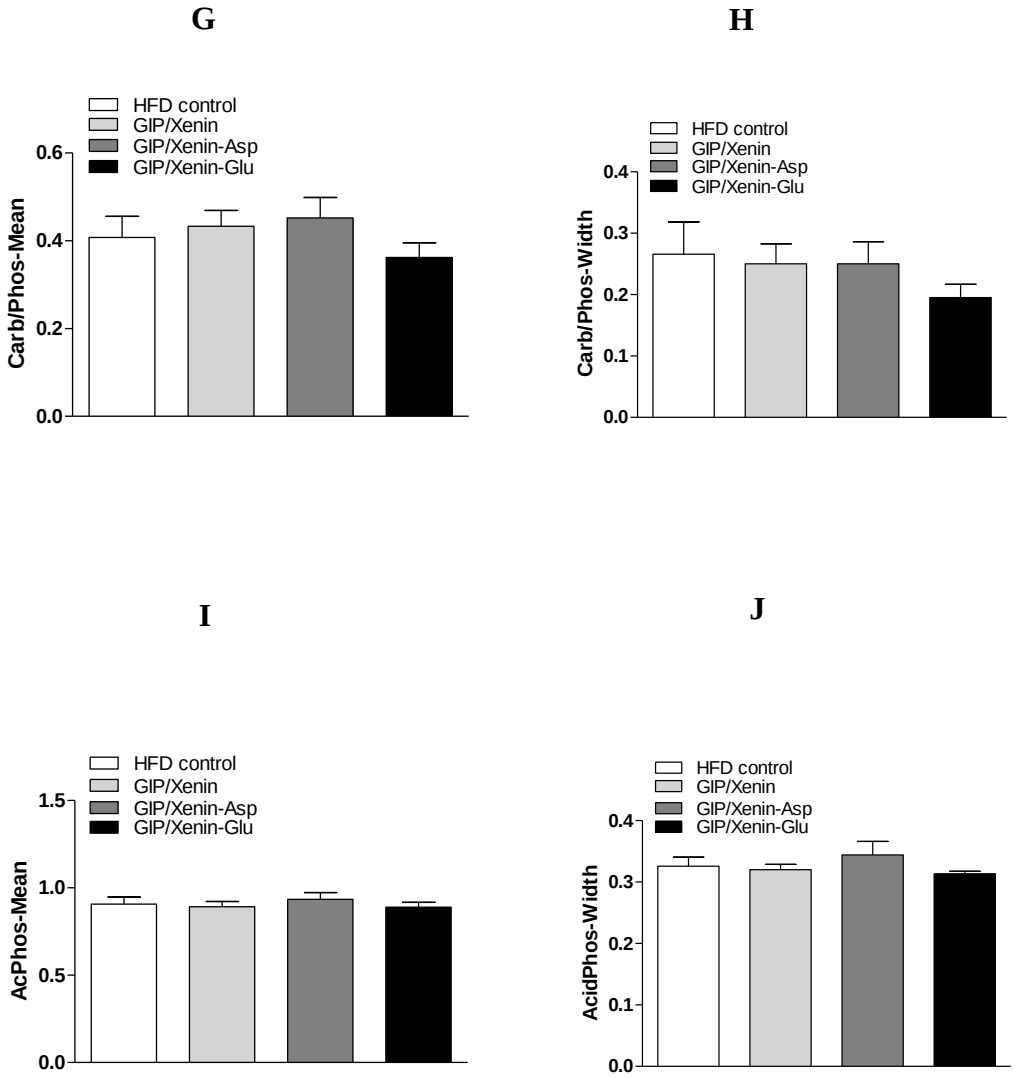

(A) Collagen maturity-mean, (B) collagen maturity width, (C) crystallinity-mean, (D) crystallinity-width, (E) phosphate/amide ratio mean, (F) phosphate/amide ratio-width, (G) carbon/phosphate ratio-mean, (H) carbon/phosphate ratio-width (I) acid phosphate mean and (J) acid phosphate with were measured by infrared spectroscopy following 42 days once daily administration of saline (0.9%, w/v, NaCl), GIP/Xenin, GIP/Xenin-Asp and GIP/Xenin-Glu (each at 25 nmol/kg b.w). Values are mean ± S.E.M for 7 mice.

Chapter 7

General Discussion

7.1 Overview

Diabetes mellitus is characterised by high blood glucose levels during which the pancreas is unable to synthesise sufficient insulin, or the body is unable to effectively utilise it (Moon *et al*. 2017). Diabetes mellitus is metabolic syndrome and it is a chronic, progressive incompletely understood disease (Chaudhury *et al*. 2017). Diabetes causes huge economic burden to the society (Pradeepa & Mohan 2017). The two main forms of diabetes include type 1 diabetes mellitus (T1DM) and type 2 diabetes mellitus (T2DM). T1DM is mostly seen in young individuals and is mainly characterised by inability of pancreatic beta cells to produce sufficient insulin and accounts for 10 % of cases of diabetes worldwide (International Diabetes Federation, 2014). T2DM is mainly seen in aged individuals, but also now increasingly in the young, and it is mainly characterised by ineffective utilisation of insulin and accounts for 90% of the cases of diabetes (Powers *et al*. 2017). Several complications of diabetes are very well known along with severe bone impairments and an increase in fracture risk (Sanches *et al*. 2017). However, there are inconsistencies in bone mineral content (BMC) and bone mineral density (BMD) measurements in T1DM and T2DM patients (Oei *et al*. 2015, Moayeri *et al*. 2017). Nonetheless, there is no doubt that diabetes plays an important role in increasing bone fracture risk (Russo *et al*. 2016).

In the recent years, there has been growing interest in understanding impact of diabetes on bone fractures and develop new therapeutic approaches for treatment of fractures (Morley *et al*. 2017). The major factors responsible for bone fractures risk are discussed in Section 1.1.3. Several studies have identified the insulinotropic incretin hormones, GIP and GLP-1, to have beneficial effects on bone (Hu *et al*. 2016, Hansen *et al*. 2017, Mabilleau *et al*. 2013, Mabilleau *et al*. 2014, Meiczkowska *et al*.

2015, Mabilleau 2017) opening a new arena of incretins and bone biology.

In this thesis, the potential of incretin based therapies as a treatment option against bone fractures was assessed. In particular, the impact of acidic olgionucleotide tagging of these peptides was employed (Dalal & Jana 2017), in order to preferentially direct the peptides towards bone. Bone-specific peptides (D-Ala^2)GIP, (D-Ala^2)GIP-Asp, (D-Ala^2)GIP-Glu, (D-Ala^2)GLP-1, (D-Ala^2)GLP-1-Asp, (D-Ala^2)GLP-1-Glu, Xenin-25[Lys^{13}PAL], Xenin-25[Lys^{13}PAL]-Asp, GIP/Xenin, GIP/Xenin-Asp, GIP/Xenin-Glu were designed and tested.

The main experiments in this thesis includes, i*n vitro* studies in sarcoma osteogenic SAOS-2 cells as well as assessing effects of the peptides in glucose homeostasis and bone quality in a high-fat fed diabetic mouse model. Bone quality was assessed using sophisticated imaging techniques to examine bone microarchitecture, tissue material properties, bone mass and bone strength to gain deeper understanding of bone mechanics.

7.2 *In vitro* studies with GIP, GLP-1, xenin and GIP/Xenin hybrid analogues

GIP, secreted from enteroendocrine K-cells and GLP-1, secreted from L-cells, although primarily regarded as insulin-releasing hormones (Kim & Sandoval 2017), are both known to play important roles in bone remodelling (Mabilleau *et al*. 2016, Seino & Yabe 2013, Lepsen *et al*. 2015, Zhao *et al*. 2017). There is no published evidence of an action of xenin on bone however; xenin is known to potentate biological action of GIP (Martin *et al*. 2016). Hence, there is a possibility that xenin might have some effect on bone, either directly or indirectly through GIP. Initially the insulinotropic activity of all peptides was examined in BRIN BD11 cells to confirm retention of bioactivity. The results were in

harmony with the previous studies that have reported similar findings (Holst *et al.* 2016, Martin *et al*. 2016, Hasib *et al*. 2017, Parthsarthy *et al*. 2016). As it is widely reported that GIP receptors are present on the bone (Garg *et al.* 2015), the sarcoma osteogenic SAOS-2 osteoblast cell line was used. Alkaline phosphatase activity was increased from 24 to 72 h after incubation with GIP analogues. The results were in agreement with previous studies which showed direct effects of GIP on osteoblasts (Pujari-Palmer *et al*. 2016, Lee *et al.* 2016, Mabilleau *et al*. 2013). Similar results were obtained with regards to GLP-1 and GIP/Xenin hybrid peptides. These peptide also enhanced TGF-β and IGF-1 release from SAOS-2 cells. Xenin did not show any activity regarding alkaline phosphatase, TGF-β and IGF-1 release. As such, further investigation is needed regarding effects of xenin on bone. IGF-1 is known for its dual action as it helps in proliferation and differentiation of bone cells. For example, positive effects of IGF-1 on bone mineralisation have been reported (Giustina *et al* 2008, Xian *et al*. 2012). Regarding the cAMP assay, direct effects of GIP and GLP-1 on SAOS-2 cells were observed indicating activation of cAMP signaling pathways, as seen in other cell lines (Hansen *et al*. 2017). In GIP/Xenin hybrid peptides, cAMP production was seen but that could be mainly due to activation of GIP receptors (Hasib *et al*. 2016). Importantly, bone-specific tagged oligopeptides retained their biological activity in BRIN BD11 and SAOS-2 cell lines. The findings from strongly reiterate the possibility of using these analogues as potential therapeutic option for bone fractures.

7.3 *In vivo* and bone assessment studies with GIP family peptides

Glucose dependent insulinotrpic polypeptide (GIP) is secreted by entero-endocrine K cells (Yamane *et al*. 2016). It is already known that GIP receptors are present on bone cells (Bollag *et*

al.2000, Zhong *et al* 2007). GIP has direct positive beneficial effects on bone (Hansen *et al*. 2017). Various studies have been carried out which focus on the aspect of using GIP as a therapeutic option for treatment of fragility fractures (Mabilleau *et al*. 2015, Mansur *et al*. 2016).

There was no effect on body weight and food intake in high-fat fed mice. Glucose was significantly reduced by day 42. Tolerance towards glucose was enhanced by (D-Ala^2)GIP-Asp. DEXA analysis was performed on all the mice and revealed no difference in overall, femoral and lumbar BMD and BMC. However, BMC assessment of tibia, revealed that BMC was increased ($p<0.01$) suggesting the potential benefits of (D-Ala^2)GIP-Asp. These findings are in harmony eith the previous study (Varela *et al*. 2017).

MicroCT was performed to determine cortical area, bone mineralisation, moment of inertia and cortical thickness. Cortical thickness and total area was enhanced in the mice treated with (D-Ala^2)GIP-Asp. The rest of the parameters remain unchanged in the mice treated (D-Ala^2)GIP and (D-Ala^2)GIP-Asp. Previous studies highlighted similar findings backing the idea of positive effects of GIP on bone (Mansur *et al*. 2015, Lee *et al*. 2016). A recent review suggested GIP has dual action on bone, to improve bone strength and bone integrity (Mabilleau 2017). Cortical thickness was reduced in the mice treated with (D-Ala^2)GIP-Asp, and interestingly it has been reported that hyperglycemia causes alterations and modifications in bone collagen (Poundarik *et al*. 2015).

Infrared spectroscopy was used to perform analysis of collagen cross-linking, crystallinity of hydroxyapaptite, degree of mineralisation, degree of carbonate substitution and content of acid phosphate. Out of which collagen cross-linking was enhanced significantly in the mice treated with (D-Ala^2)GIP and

(D-Ala^2)GIP-Asp. Positive effects of GIP on collagen cross-linking suggest GIP plays an important role in improving bone strength at tissue level (Mieczkowska *et al*. 2015, Mansur *et al*. 2016). The rest of the parameters were not affected by the treatment. These findings reveal that bone biology is goverened by different factors andfurther assessment of bone biomechanics is necessary.

7.4 *In vivo* and bone assessment studies with Xenin family peptides

Xenin is co-secreted with GIP from K-cells and it is already reported that xenin augments the biological activity of GIP (Martin *et al*. 2016, Hasib *et al*. 2017). Based on this fact, there is a possibility that xenin might affect bone metabolism because it is well known that GIP has positive effects on bone metabolism (Garg *et al*. 2015, Mantelmacher *et al*. 2017). However, to date, there is absolutely no evidence that demonstrates direct effects of xenin on bone. Indeed, data reported in Chapter 3 in this thesis might also suggest lack of direct effects.

In these studies, we found that both the xenin peptides had no impact on body weight or food intake in lean and high-fat fed mice. Xenin-25[Lys^{13}PAL] did not show any effect on glucose or insulin levels in lean mice, but significantly reduced circulating glucose in high fat fed mice. DEXA analysis revealed interesting findings regarding Xenin-25[Lys^{13}PAL] and Xenin-25[Lys^{13}PAL]-Asp in lean and high-fat fed mice. In high-fat fed mice, Xenin-25[Lys^{13}PAL] increased whole body BMC, with no effect of Xenin-25[Lys^{13}PAL]-Asp. Lumbar BMC was increased by Xenin-25[Lys^{13}PAL] and Xenin-25[Lys^{13}PAL]-Asp, whereas tibial BMC was increased only by Xenin-25[Lys^{13}PAL] treatment. In lean mice, lumbar BMD was decreased while tibial BMC was increased by Xenin-25[Lys^{13}PAL]. These differences regarding BMC and BMD reveal that xenin possibly differentially

affects each bone region, indicating the need for further detailed study. However, it should be remembered that inconsistencies are observed in T2DM patients as BMD is unchanged, or slightly elevated, in these patients despite increased bone fracture risk (Asokan *et al*. 2017). However, bone quality does not merely depend upon BMC and BMD but on many other factors such as microarchitecture, bone matrix composition and biomechanical strength that play an important role in overall bone quality and integrity (Christiana Zidrou 2016).

In this regard, the number of trabeculae and trabecular bone volume were reduced by Xenin-25[Lys^{13}PAL] in lean control mice, with increased trabecular separation suggesting a negative impact of xenin on bone under normal physiological conditions. Regarding high fat fed mice, microcomputed tomography results revealed reduction in bone volume and number of trabeculae with increased trabecular separation after treatment with Xenin-25[Lys^{13}PAL] and Xenin-25[Lys^{13}PAL]-Asp. Cortical bone parameters did not show any changes after treatment with both Xenin-25[Lys^{13}PAL] and Xenin-25[Lys^{13}PAL]-Asp. Xenin-25[Lys^{13}PAL] induced significant benefits on the nanomechanical properties of cortical bone including increase in hardness, indentation modulus and force. Based on the results, it is evident that Xenin-25[Lys^{13}PAL]-Asp did not possess any real positive effects on the bone rather, it decreased collagen maturity in high-fat fed mice. However, fatty acid derivation of Xenin-25[Lys^{13}PAL] and Xenin-25[Lys^{13}PAL]-Asp, might obstruct the actions of acidic oligopeptide tagging to deposit the peptide in bone, likely through stearic hindrance (Narayana *et al*. 2015). Despite this, Xenin-25[Lys^{13}PAL] and Xenin-25[Lys^{13}PAL]-Asp did possess beneficial metabolic effects and most importantly Xenin-25[Lys^{13}PAL] showed some positive effects in diabetic bone, even though the results were inconsistent under normal physiological conditions. Detailed studies are still required to

fully understand the effects of xenin on bone biology, and whether related analogues can be used as potential therapeutic options for treatment against bone fractures.

7.5 *In vivo* and bone assessment studies with GIP/Xenin hybrid family peptides

There is compelling evidence that suggests glucose-dependent insulinotropic polypeptide (GIP) has positive effects on bone (Mabilleau *et al*. 2016, Christensen *et al*. 2017). Xenin is known to potentiate the action of GIP (Martin *et al*. 2016, Gault *et al*. 2015), and a GIP/Xenin hybrid peptide has recently been characterised (Hasib *et al*. 2017). This hybrid peptide combines GIP and xenin activity into one molecule making it very unique and use it as a therapeutic option for diabetic disorders. The addition of six C-terminal acidic L-Asp and L-Glu amino acid residues by using acid oligopeptide tagging is believed to make peptides more specific towards bone by encouraging its binding to hydroxyapaptite (Ulbrich *et al*. 2016). No changes were seen in non-fasted plasma glucose and insulin levels in high-fat fed mice with these drugs. The results somewhat contradict findings from the previous study with GIP/Xenin (Hasib *et al*. 2017). The possible explanation could be due to number of factors such as frequency of the peptide administration, dose of the peptide and type of diabetic model. Bone-specific analogues- GIP/Xenin-Asp and GIP/Xenin-Glu did improve glucose homeostasis and insulin sensitivity, which is in harmony with the previous studies (Hasib *et al*. 2017). These results suggested that the C-terminal additions (GIP/Xenin-Asp and GIP/Xenin-Glu) did not alter the pharmacological activity of GIP/Xenin. DEXA analysis revealed that GIP/Xenin enhanced lumbar BMC while GIP/Xenin-Asp and GIP/Xenin-Glu increased tibial BMD. Again, some small inconsistencies were observed regarding BMC and BMD, as reported in the Chapter 5. However, the importance of these measurements in diabetes is questionable (Asokan *et al*. 2017).

Microcomputed tomography revealed that GIP/Xenin treated mice had increased trabeculae number and trabecular bone volume. These results were in accordance with the previous studies with GIP (Gaudin-Audrain *et al*. 2012). Interestingly, GIP/Xenin-Asp and GIP/Xenin-Glu did not have any significant effect on trabecular parameters. This might be because either the peptide was deposited excessively in bone, or reduced circulating levels of the peptides. GIP/Xenin-Glu evoked deleterious effects on cortical bone geometry, suggesting altered biological action of GIP/Xenin hybrid molecules. Infrared spectroscopy analysis revealed no significant changes regarding collagen maturity, crystallinity of the bone tissue, phosphate/amide ratio, carbon/phosphate ratio and acid phosphate. The possible explanation could be duration of the study, age of the mice, strain of the mice and timing of injections. There are many factors that govern overall bone integrity and bone quality such as microarchitecture, bone mineralisation and bone mass. Taken together, GIP/Xenin and GIP/Xenin-Asp demonstrated a positive impact on bone health in diabetic high fay fed mice. Hybrid peptides have opened up a whole new frontier in terms of therapeutics, and future studies are required to look into the potential therapeutic options for diabetic bone disorders.

7.6 Overall impact of oligopeptide tagging on bone parameters

The effects of oligopeptide tagging were encouraging. Diabetic mice treated with tagged peptide- (D-Ala^2)GIP-Asp had augmented bone marrow diameter and cortical thickness alongwith total area. These results were in harmony with the previous studies which report a positive impact of gastric inhibitory polypeptide (GIP) on bone biology (Mabilleau *et al*. 2016). No positive effect of Xenin tagged peptides was seen on different bone parameters. On the contrary, xenin tagged peptide-Xenin-25[Lys^{13}PAL]-Asp, showed reduction in number of

trabeculae as well as increase in tibial separation suggesting xenin might have negative effects on bone biology. However, more studies are needed to be performed in order to confirm this effect. The hybrid peptide- GIP/xenin-Asp increased bone marrw diameter and cortical thickness. MicroCT analysis revealed that trabecular bone volume and number of trabeculae were also augmented in the mice treated with GIP/Xenin peptide. However, there are some contradictions in the results with these tagged peptides, with some positive some negative findings findings. One thing is clear, that bone biology is extremely complex process with many players in the game, making it difficult for researchers to draw a perfect strategy to combat bone fractures. Nonetheless, one cannot deny the fact that diabetes does impact bone biology with increase risk in bone fractures (Nilsson *et al*. 2017), suggesting further studies are required to assess tagged oligopeptides (Narayana *et al*. 2015) as potential therapeutic option for treatment of bone fractures.

There are different labeling and statining techniques to assess molecular activities in the bone. Resorption, bone formation and mineralisation can be studied with the help of staining techniques (Erben *et al*. 2017). Established techniques include fluorochrome labeling with alizarin red S to analyse calcium deposition and sirus red stainin to determine presence pof collaen in the bone (Segnani *et al*. 2015). A study carried out by Takahashi-Nishioka in 2008 demonstrated that fluorescein-labeled L-Asp hexapeptide localised only in the bone and not any other tissue in mice. Indeed, the peptide was detected in the bone even after 14 days of administration suggesting specificity and affinity of tagged peptides to hydroxyapaptite making them strong contenders as potential therapeutic treatment for bone (Takahashi-Nishioka *et al*. 2008). This type of analyses would be extremely useful in the current studies.

7.7 Oligopeptide tagging and its impact on blood glucose, body weight, food intake and insulin sensitivity

(D-Ala^2)GIP and (D-Ala^2)GIP-Asp tagged peptides did not have any any effect on body weight and food intake in high-fat fed mice but did have reduced blood glucose at the end of experiment. (D-Ala^2)GIP-Asp enhanced tolerance. Similar findings were seen with xenin treated mice with no effect on body weight and food intake. It is already reported that xenin induces appetite suppression (Kaji *et al*. 2017) but only with higher dose than the dose used in the study. Xenin-25[Lys^{13}PAL] showed improved glucose tolerance and insulin sensitivity in accordance with the previous studies (Gault *et al*. 2015, Martin *et al*. 2016 and Hasib *et al*. 2017). Xenin did not have any effect on bone biology suggesting there is a need for further investigation. However, no changes were observed in insulin and non-fasted plasma glucose levels in high-fat fed mice. These findings were contradictory to the previous studies (Hasib *et al*. 2017). There are many factors such as dose and frequency of the peptide administered as well as type of the diabetic model used in the study. GIP/Xenin analogues improved glucose tolerance and enhanced insulin sensitivity. These findings were in harmony with previous studies (Hasib *et al*. 2017). Overall, bone-targeting peptides designed through addition of six C-terminal acidic L-Asp and L-Glu amino acid residues, did not impede upon the metabolic benefits of the parent peptides.

7.8 Role for oligopeptides peptides for bone disorders beyond diabetes

Targeted drug delivery to the bone can be achieved by acidic homopeptides (Nishioka *et al*. 2006). It was reported that fluorescence-labelled acidic amino acid (L-Asp & L-Glu) containing six amino acid residues show strong affinity towards hydroxyapatite which is major component of bone (Takahasi-

Nishioka *et al*. 2008). Osteoporosis is common problem in aged women, particularly after menopause (Kling *et al*. 2013). Estrogen has anabolic efects on bone through estrogen-receptor mediated mechanisms (Manolagas *et al*. 2013). Tagging of estradiol with L-Asp hexapeptide exerted positive osteogenic effects on the bone without adverse effects on any other organ (Stapelton *et al*. 2017). In case of levofloxacin, which is used in treating chronic osteomyelitis; similar results were obtained when levofloxacin was tagged with L-Asp hexapeptide suggesting positive beneficial effects of oligopeptide tagging (Philips *et al*. 1988, Mader *et al*. 1990). Tissue-nonspecific alkaline phosphatase (TNSALP) is present in bone, kidney, liver and adrenal tissue (Michael P White 2016). The deficiency of TNSALP results in hypophosphatasia and leads to defective bone minealisation (Meaah *et al*. 2017). Studies conducted previously showed that enzyme replacement therapy was not suitable option because of the adverse effects on other vital organs (Whyte *et al*. 1984, Whyte *et al*. 1986). Another study recommended continous delivery of high doses of TNSALP to initiate bone minelisation process (Murshed *et al*. 2005). L-Asp tagging of TNSALP induced positive effects on bone quality wih enhanced bioactivity and increase in bone minealsation (Orimo 2010). It is clear from these different studies that acidic oligopeptide tagging is efficient for achieving bone specific targeted drug delivery. There are concerns related to the use of tagged peptides mainly because of alterations in pharmacokinetic and biological properties (Saeui *et al*. 2017). Other factors such as biological activity, blood clearance and distribution to visceral organs could also be important, especially due to their increased hydrophilicity (Takahashi-Nishioka *et al*. 2008). However, taken together these observations suggest a promising future for tagged acidic oligopeptides.

Future prospects and conclusion

The data in this thesis includes *in-vitro* studies with bone specific GIP, GLP-1, xenin and GIP/Xenin analogues in sarcoma osteogenic SAOS2 cells as well as use of high-fat fed mice model to study *in-vivo* effects of these bone specific analogues. This thesis also includes bone assessment results which were performed using highly sophisticated and advanced imaging techniques such as QBEI, nanoindentation, three-point bending and FTIRI. The findings of this thesis highlight beneficial effects of incretin-based mimetics on bone. Further assessment is necessary to develop potential therapeutic treatment options against bone impairements.

The summary of future work is as follows:

1. More studies need to be carried out to highlight the safety, efficacy and tolerability of GIPR agonists, GLP-1R agonists, and hybrid analogues.

2. Clinical trials need to be undertaken in order to study the effects of insulin treatment on bone in T2DM patients.

3. As diabetes is multifactorial in nature. Several pathways come into play indiabetes. In order to target these pathways, double or triple-acting agonists, cocktails or hybrid stable analogues need to be developed.

4. Deeper understanding is required regarding mechanism of action of GIPR, GLP-1 and hybrid analogues on bone

In conclusion, the findings of this thesis highlights the use of incretin-based mimetics as new therapeutic approach for the treatment of fragility fractures associated with type 2 diabetes. This thesis will provide valuable information that can be used to design future studies and provide deeper insight in diabetes and bone biology. Very few clinical tirlas have been carried out to understand impact of type 2 diabetes on bone. Hence, this work will serve as platform to deisgn clinical trials to study effects of different incretin-based drugs on bone and help people who are fighting against diabetes.

Chapter 8

References

Abdulameer SA, Sulaiman SAS, Hassali MA, Subramaniam K, & Sahib MN 2012 Osteoporosis and type 2 diabetes mellitus: what do we know, and what we can do? *Patient Preference and Adherence* **6** 435–448.

Adamska E, Ostrowska L, Górska M & Krętowski A 2014 The role of gastrointestinal hormones in the pathogenesis of obesity and type 2 diabetes. *Przeglad Gastroenterologiczny* **9** 69–76.

Adil M, Khan RA, Kalam A, Venkata SK, Kandhare AD, Ghosh P & Sharma M 2017 Effect of anti-diabetic drugs on bone metabolism: Evidence from preclinical and clinical studies. *Pharmacological Reports* **69** 1328-1340.

Ali GY, Abdelbary EE, Albualia WH, AboelFetoh NM &AlGohary EH 2017 Bone mineral density & bone mineral content in Saudi children, risk factors and early detection of their affection using dual-emission X-ray absorptiometry (DEXA) scan Egyptian Pediatric Association Gazette **65** 65-71.

Alikhani M, Alikhani Z, Boyd C, MacLellan CM, Raptis M, Liu R, Pischon N, Trackman PC, Gerstenfeld L & Graves DT 2007 Advanced glycation end products stimulate osteoblast apoptosis via the MAP kinase and cytosolic apoptotic pathways. *Bone* **40** 345-353.

Althage MC, Ford EL, Wang S, Tso P, Polonsky KS, Wice BM (2008) Targeted ablation of glucose-dependent insulinotropic polypeptide-producing cells in transgenic mice reduces obesity and insulin resistance induced by a high-fat diet. *Journal of Biological Chemistry* **283** 18365–18376.

Amalia G, Melania G & Ralph DF 2017 Glucose kinetics: an update and novel insights into its regulation by glucagon and GLP 1. *Current Opinion in Clinical Nutrition & Metabolic Care* **20** 300–309.

Amatya C, Radichev IA, Ellefson J, Williams M & Savinov AY 2017 Self Transducible Bimodal PDX1-FOXP3 Protein Lifts Insulin Secretion and Curbs Autoimmunity, Boosting Tregs in Type 1 Diabetic Mice. *Molecular Therapy* In Press.

Anderson LJ, Tamayose JM & Garcia JM 2017 Use of growth hormone, IGF-I, and insulin for anabolic purpose: Pharmacological basis, methods of detection, and adverse effects. *Molecular and Cellular Endocrinology* In press.

Anishkumar C, Rashmi M & Khan T 2016 Novel Therapeutic Targets for Management of Type-2 Diabetes Mellitus. *Immunology, Endocrine & Metabolic Agents in Medicinal Chemistry (Formerly Current Medicinal Chemistry - Immunology, Endocrine and Metabolic Agents)* **16** 18-30.

Arnold M, Zhao S, Ma S, Giuliani F, HansenU, Cobb JP, Abel RL, & Boughto O 2017Microindentation – a tool for measuring cortical bone stiffness? *Bone and Joint Research* **6** 542 549.

Asokan AG, Jaganathan J, Philip R, Soman RR, Sebastian ST & Pullishery F 2017 Evaluation of bone mineral density among type 2 diabetes mellitus patients in South Karnataka. *Journal of Natural Science, Biology & Medicine* **8** 94–98.

Athauda D and Foltynie T 2016 The glucagon-like peptide 1 (GLP) receptor as atherapeutic target in Parkinson's disease: mechanisms of action. *Drug Discovery Today* **21** 802-818.

Atkinson MA & Eisenbarth GS 2001 Type 1 diabetes: new perspectives on disease pathogenesis and treatment. *The Lancet* **358** 221-229.

Badieh J & Mary EB 2016 Clinical pharmacy: Hypoglycaemia in elderly patients with type 2 diabetes mellitus: a review of risk factors, consequences and prevention. *The Australian Journal of Pharmacy* **97** 71-75.

Balcerczyk A , Chriett S & Pirola L 2017 Insulin Action, Insulin Resistance, and Their Link to Histone Acetylation *Handbook of Nutrition, Diet and Epigenetics* 1-22 .

Bart Clarke B 2008 Normal Bone Anatomy and Physiology *Clinical Journal of American Society of Nephrology* **3** 131–139.

Basile KJ, Johnson ME, Qianghua Xia Q & Grant SFA 2014 International Genetic Susceptibility to Type 2 Diabetes and Obesity: Follow-Up of Findings from Genome-Wide Association Studies. *Journal of Endocrinology* **2014** 1-13.

Bassett JHD, Van der Spek A, Gogakos A & Williams GR 2012 Quantitative x-ray imaging of rodent bone by faxitron. *Bone Research Protocols, Methods in Molecular Biology* **816** 499-506.

Baumgard LH, Hausman GJ & Fernandez MVS 2016 Insulin: pancreatic secretion and adipocyte regulation. *Domestic Animal Endocrinology* **54** 76-84.

Beata Lecka-Czernik 2017 Diabetes, bone and glucose-lowering agents: basic biology. *Diabetologia* **60** 1163–1169.

Berlier JL, Kharroubi I, Zhang J, Dalla Valle A, Rigutto S, Mathieu M, Gangji V & Rasschaert J 2015 Glucose-Dependent Insulinotropic Peptide Prevents Serum Deprivation Induced Apoptosis in Human Bone Marrow-Derived Mesenchymal Stem Cells and Osteoblastic Cells. *Stem Cell Review* **11** 841- 851.

Bhavya S, Lew PS & Mizuno TM 2017 Central action of xenin affects the expression of lipid metabolism-related genes and proteins in mouse white adipose tissue. *Neuropeptides* **63** 67-73.

Billings LK, Hsu YH, Ackerman RJ, Dupuis J, Voight BF, Rasmussen-Torvik LJ, Hercberg S, Lathrop M, Barnes D, Langenberg C, Hui J, Fu M, Bouatia-Naji N, Lecoeur C, An P, Magnusson PK, Surakka I, Ripatti S, Christiansen L, Dalgard C, Folkersen L, Grundberg E, Eriksson P, Kaprio J, Ohm KK, Pedersen NL, Borecki IB, Province MA, Balkau B, Froguel P, Shuldiner AR, Palmer LJ, Wareham N, Meneton P, Johnson T, Pankow JS, Karasik D, Meigs JB, Kiel DP & Florez JC 2012 Impact of common variation in bone-related genes on type 2 diabetes and related traits. *Diabetes* **61** 2176-2186.

Bolen S, Feldman L, Vassy J, Wilson L, Yeh HC, Marinopoulos S, Wiley C, Selvin E, Wilson R, Bass EB & Brancati FL 2007 Systematic Review: Comparative Effectiveness and Safety of Oral Medications for Type 2 Diabetes Mellitus. *Annals of Internal Medicine* **147** 386-399.

Bollag RJ, Zhong Q, Phillips P, Min L, Zhong L, Cameron R, Mulloy AL, Rasmussen H, Qin F, Ding KH & Isales CM 2000 Osteoblast-derived cells express functional glucose dependent insulinotropic peptide receptors. *Endocrinology* **141** 1228-1235.

Bonjour JP, Benoit V, Pourchaire O, Rousseau B & Souberbielle JC 2011 Nutritional approach for inhibiting bone resorption in institutionalized elderly womenwith vitamin D insufficiency and high prevalence of fracture. *Journal of Nutrition, Health Aging* **15** 404-409.

Bortolin RH, Freire Neto F P, Arcaro CA, Bezerra JF, da Silva FS, Ururahy, MAG, Souza KS, dC Lima, Luchessi, AD, Lima FP, Lia Fook MV, da Silva BJ, Almeida MdG, Abreu, BJ, de Rezende, L. A. & de Rezende AA 2017 Anabolic Effect of Insulin Therapy on the Bone: Osteoprotegerin and Osteocalcin Up-Regulation in Streptozotocin-Induced Diabetic Rats. *Basic Clinical Pharmacology & Toxicology* **120** 227–234.

Budi EH, Muthusamy BP & Derynck R 2015 The insulin response integrates increased TGF-β signaling through Akt-induced enhancement of cell surface delivery of TGF-β receptors. *Science Signaling* **29** 1-37.

Camp E, .Anderson PJ, .Zannettinobd ACW & Gronthos S 2017 Tyrosine kinase receptor c-ros-oncogene 1 mediates TWIST-1 regulation of human mesenchymal stem cell lineage commitment. *Bone* **94** 98-107.

Campbell JE & Drucker DJ 2013 Pharmacology, Physiology, and Mechanisms of Incretin Hormone Action. *Cell Metabolism* **17** 819-837.

Caprio M, Infante M, Calachini M, Mammi C & Fabbri A 2017 Vitamin D: not just the bone. Evidence for beneficial pleiotropic extraskeletal effects. Osteosarcopenia: where bone, muscle, and fat collide. *Eating and Weight Disorders* **28** 2781–2790.

Carbone EJ, Rajpura K, Allen BN, Cheng E, Ulery BD & Lo KWH 2017 Osteotropic nanoscale drug delivery systems based on small molecule bone targeting moieties. *Nanomedicine: Nanotechnology, Biology and Medicine* **13** 1337-47.

Carsten Posovszky & Martin Wabitsch 2015 Regulation of Appetite, Satiation, and Body Weight by Enteroendocrine Cells. Part 1: Characteristics of Enteroendocrine Cells and Their Capability of Weight Regulation. *Hormone Research inPaediatrics* **8** 1–10.

Castro PA, Dias DA, Veloso MN & Zezell DM 2017 "Biochemical Evaluation of Bone Submitted to Ionizing Radiation by ATR FTIR Spectroscopy," in Conference on Lasers and Electro Optics, OSA Technical Digest (online) (Optical Society of America, 2017), paper JTu5A.4.

Cavalli L, Guazzini A, Cianferotti L, Parri S, Cavalli T, Metozzi A, Giusti F, Fossi C, Black DM & Brandi ML 2016 Prevalence of

osteoporosis in the Italian population and main risk factors: results of BoneTour Campaign. *BMC Musculoskeletal Disorders* **17** 1-11.

Cavin JB, Bado A & Gall ML 2017 Intestinal Adaptations after Bariatric Surgery: Consequences on Glucose Homeostasis. *Trends in Endocrinology & Metabolism* **28** 354–364.

Ceccarelli E, Guarino EG, Merlotti D, Patti A, Gennari L, Nuti R & Dotta F 2013 Beyond Glycemic Control in Diabetes Mellitus: Effects of Incretin-Based Therapies on Bone Metabolism. *Frontiers in Endocrinol*ogy *(Lausanne)* **4** 1- 12.

Cha DS, Vahtra M, Ahmed J, Kudlow PA, Mansur RB, Carvalho AF & McIntyre RS 2016 Repurposing of Anti-Diabetic Agents for the Treatment of Cognitive Impairment and Mood Disorders. *Current Molecular Medicine* **16** 465-473.

Chandran M 2017 Diabetes Drug Effects on the Skeleton. *Calcified Tissue International* **100** 133–149.

Chapter 11 – Biomarkers and Their Use in Nutrition Intervention Nutrition in the Prevention and Treatment of Disease (Fourth Edition).2017217–234.

Chapter 4 – Bone metabolism Kline G, Orton D, Sadrzadeh H 2017Endocrine Biomarkers Clinicians and Clinical Chemists in Partnership.157–180.

Chaudhury A, Duvoor C, Reddy Dendi VS, Kraleti S, Chada A, Ravilla R, Marco A, Shekhawat NS, Montales MT,Kuriakose K, Sasapu A, Beebe A, Patil N, Musham CK, Lohani GP & Mirza W 2017 Clinical Review of Antidiabetic Drugs: Implications for Type 2 Diabetes Mellitus Management. *Frontiers in Endocrinology (Lausanne)* **8** 1-12.

Chen W, Wang G, Yung BC, Liu G, Qian Z & Chen X 2017 Long Acting Release Formulation of Exendin-4 Based on Biomimetic Mineralization for Type 2 Diabetes Therapy. *ACS Nano* **11** 5062–5069.

Chon S & GautierAn JF 2016 Update on the Effect of Incretin-Based Therapies on β-Cell Function and Mass. *Diabetes Metabolism Journal* **40** 99-114.

Choudhury SM, Tan TM & Bloom SR 2016 Gastrointestinal hormones and their role in obesity. *Current Opinion in Endocrinology Diabets and Obesity* **23** 18-22.

Christensen MB 2016 Glucose-dependent insulinotropic polypeptide: effects on insulin and glucagon secretion in humans. *Danish Medical Journal* **63** pii: B5230.

Christensen MB, Lund A, Calanna S Jørgensen NR, Holst JJ, Vilsbøll T & Knop FK 2017 Glucose-Dependent Insulinotropic Polypeptide (GIP) Inhibits Bone Resorption independently of Insulin and Glycemia *The Journal of Clinical Endocrinology & Metabolism* **103** 288-294.

Colhoun HM, Livingstone SJ, Looker HC, Morris AD, Wild SH, Lindsay RS, Reed C, Donnan PT, Guthrie B, Leese GP, McKnight J, Pearson DWM, Pearson E, Petrie JR, Philip S, Sattar N, Sullivan FM, McKeigue P 2012. Hospitalised hip fracture risk with rosiglitazone and pioglitazone use compared with other glucose-lowering drugs. *Diabetologia* **55** 2929-2937.

Collins FL, Kim SM, McCabe LR & Weaver CM 2017 Intestinal Microbiota and Bone Health: The Role of Prebiotics, Probiotics, and Diet. In: Smith S., Varela A., Samadfam R. (eds) Bone Toxicology. *Molecular and Integrative Toxicology Springer, Cham* 417-443.

Dang L, Liu J, Li F, Wang L, Li D, Guo B, He X, Jiang F, Liang, Liu B, Badshah SA, He B, Lu J, Lu C, Lu A & Ge Zhang 2016 Targeted Delivery Systems for Molecular Therapy in Skeletal Disorders. *International Journal of molecular Sciences* **17** 1 15.

Daniel H & Zietek T 2015 Joan Mott Prize 2015 Joan Mott Prize Lecture Lecture Taste and move: glucose and peptide transporters in the gastrointestinal tract. *Experiment Physiology* **100** 1441–1450.

De Laet C, Kanis JA, Odén A, Johanson H, Johnell O, Delmas P, Eisman JA, Kroger H, Fujiwara S, Garnero P, McCloskey EV, Mellstrom D, Melton LJ 3rd, Meunier PJ, Pols HA, Reeve J, Silman A & Tenenhouse A 2005 Body mass index as a predictor of fracture risk: a meta-analysis. *Osteoporosis International* **16** 1330-1338.

Deacon CF & Lebovitz HE 2016 Comparative review of dipeptidyl peptidase-4 inhibitors and sulphonylureas. *Diabetes Obesity and Metabolism* **8** 333–347.

Dempster DW, Compston JE, Drezner MK, Glorieux FH, Kanis JA, Malluche H, Meunier PJ, Ott SM, Recker RR & Parfitt AM 2013 Standardized nomenclature, symbols, and units for bone histomorphometry: A 2012 update of the report of the ASBMR Histomorphometry Nomenclature Committee. *Journal of Bone and Mineral Research* **28** 2-17.

Dilana A, Richardb W, Patrik B & Foltynie Thomas 2017 Is Exenatide a Treatment for Parkinson's disease? *Journal of Parkinson's Disease* **7** 451-458.

Drucker DJ 2016 Evolving Concepts and Translational Relevance of Enteroendocrine Cell Biology. *The Journal of Clinical Endocrinology & Metabolism* **101** 778–786.

Duan Y, Beck TJ, Wang XF & Seeman E 2003 Structural and biomechanical basis of sexual dimorphism in femoral neck fragility has its origins in growth and *aging. Journal of Bone and Mineral Research* **18** 1766-1774.

Duarte AI, Candeias E, Correia SC, Santos RX, Carvalho C, Cardoso S, Plácido A, Santos MS, Oliveira CR & Moreira PI 2013 Crosstalk between diabetes and brain: Glucagon-like peptide-1 mimetics as a promising therapy against neurodegeneration. *Biochemica et Biophysica Acta* **4** 527-554.

Duez H, Cariou B & Staels B 2012 DPP-4 inhibitors in the treatment of type 2 diabetes. *Biochemical Pharmacology* **83** 823-832.

Effoe VS, Carnethon MR, Echouffo-Tcheugui JB, Chen H, Joseph JJ, Norwood AF & Bertoni AG 2017 The American Heart Association Ideal Cardiovascular Health and Incident Type 2 Diabetes Mellitus Among Blacks: The Jackson Heart Study. *Journal of the American Heart Association* **6** 1-14.

Egger A, Kraenzlin ME & Meier C 2016 Effects of Incretin-Based Therapies and SGLT2 Inhibitors on Skeletal Health. *Current Osteoporosis Reports* 14 345 350.

El-Tawdy AH, Ibrahim EA, Sakhawy EM & Morsy TA 2016 Review on Bone Disease (osteoporosis) in Diabetes Mellitus. *Journal of the Egyptian Society of Parasitology* **46** 223-234.

Erben RG, Jolette J, Chouinard L & Boyce R 2017 Application of Histopathology and Bone Histomorphometry for Understanding Test Article-Related Bone Changes and Assessing Potential Bone Liabilities. In: Smith S, Varela A, Samadfam R. (eds) Bone Toxicology. *Molecular and Integrative Toxicology Springer* In Press.

Erik Gylfe 2016 Glucose control of glucagon secretion—'There's a brand-new gimmick every year'. *Upsala Journal of Medical Sciences* **121** 120-132.

Erin MB, McNerny, Gong B, Morris MD & Kohn DH 2015 Bone fracture toughness and strength correlate with collagen cross-link maturity in a dose-controlled lathyrism mouse model. *Journal of Bone and Mineral Research* **30** 446–455.

Faienza MF, Luce V, Ventura A, Colaianni G, Colucci S, Cavallo L, Grano M & Brunetti G 2015 Skeleton and Glucose Metabolism: A Bone-Pancreas Loop. *International Journal of Endocrinology* **2015** 1-7.

Fajardo RJ, Karim L, Calley VI & Bouxsein ML 2014 A Review of Rodent Models of Type 2 Diabetic Skeletal Fragility. *Journal of Bone & Mineral Research* **29** 1025–1040.

Fan T, Yu X, Shen B & Sun L 2017 Peptide Self-Assembled Nanostructures for Drug Delivery Applications. *Journal of Nanomaterials* **2017** 1-16.

Fan Y, Jun-ichiHanai, Le PT, RuiyeBi, Maridas D, Mambro VD, Figueroa CA, Kir S, Zhou X, Mannstadt M, Baron R, Bronson RT, Horowitz MC, Wu JY, Bilezikian JP, Dempster DW, Rosen CJ & Lanske B 2017 Parathyroid Hormone Directs Bone Marrow Mesenchymal Cell Fate. *Cell Metabolism* **25** 661-672.

Fareed M, Salam N, Khoja AT, Mahmoud MA & Ahamed M 2017 Life Style Related Risk Factors of Type 2 Diabetes Mellitus and Its Increased Prevalence in Saudi Arabia: A Brief Review. *International Journal of Medical Research & Health Sciences* **6** 125-132.

Farlay D, Panczer G, Rey C, Delmas P, and Boivin G 2010 Mineral maturity and crystallinity index are distinct characteristics of bone mineral *Journal of Bone* and Mineral Metabolism ***28*** 433–445.

Ferreira AM, Gentile P, Chiono V & Ciardelli G 2012 Collagen for bone tissue regeneration. *Acta Biomaterialia* **8** 3191-3200.

Feurle GE, Hamscher G, Kusiek R, Meyer HE & Metzger JW 1992 Identification of xenin, a xenopsin-related peptide, in the human gastric mucosa and its effect on exocrine pancreatic secretion. *The Journal of Biological Chemistry* **31** 22305 22309.

Florencio-Silva R, da Silva Sasso GR, Sasso-Cerri E, Simões MJ & Cerri PS 2015Biology of Bone Tissue: Structure, Function, and Factors That Influence Bone Cells. *Biomed Research Intermnational* **2015** 1-17.

Fourmy D 2017 Hybrid peptides in the landscape of drug discovery. *Peptides* 90 A1-A2.

Fujita K, Tokuda H, Yamamoto N, Kainuma S, Kawabata T, Sakai G, Kuroyanagi G, Matsushima-Nishiwaki R, Harada A, Kozawa O & Otsuka T 2017 Incretins amplify TNF-α stimulated IL-6 synthesis in osteoblasts: Suppression of the IκB/NF-κB pathway. *International Journal of Molecular Medicine* **39** 1053- 1060.

Fujita Y, Yanagimachi T, Takeda Y, Honjo J, Takiyama Y, Abiko A, Makino Y & Haneda M 2016 Alternative form of glucose dependent insulinotropic polypepide and its physiology. *Journal of Diabetes Investigation* **7** 33–37.

Furman BL 2012 The development of Byetta (exenatide) from the venom of the Gila monster as an anti-diabetic agent. *Toxicon: Official Journal of the International Society on Toxinology* **59** 464-471.

Gallagher EJ, Alikhani N, Tobin-Hess A, Blank J, Buffin NJ, Zelenko Z, Tennagels N, Werner U & LeRoith D 2013 Insulin Receptor Phosphorylation by Endogenous Insulin or the Insulin Analog AspB10 Promotes Mammary Tumor Growth Independent of the IGF-I Receptor. *Diabetes* **62** 3553-3560.

Garcia-Gil M, Pierucci F, Vestri A & Meacci, E 2017 Crosstalk between sphingolipids and vitamin D3: potential role in the nervous system. *British Journal of Pharmacology* **174** 605–627.

Garg MK & Kharb S 2013 Dual energy X-ray absorptiometry: Pitfalls in measurement and interpretation of bone mineral density.

Indian Journal of Endocrinology & Metabolism **17** 203-210.

Gasbjerg LS, Gabe MBN2, Hartmann B2, Christensen MB3, Knop FK4, Holst JJ2, Rosenkilde MM 2017 Glucose-dependent insulinotropic polypeptide (GIP) receptor antagonists as anti-diabetic agents. *Peptides* **100** 173-181.

Gaudin-Audrain C, Irwin N, Mansur S, Flatt PR, Thorens B, Basle M, Chappard D & Mabilleau G 2013 Glucose dependent insulinotropic polypeptide receptor deficiency leads to modifications of trabecular bone volume and quality in mice. Bone **53** 221–230.

Gault VA, Flatt PR, Bailey CJ, Harriott P, Greer B, Mooney MH & O'Harte FPM 2002 Enhanced cAMP generation and insulin releasing potency of two novel Tyr1-modified enzyme resistant forms of glucose-dependent insulinotropic polypeptide is associated with significant antihyperglycaemic activity in spontaneous obesity-diabetes. *Biochemical Journal* **367** 913 920.

Gault VA, Martin CM, Flatt PR, Parthsarathy V & Irwin N 2015 Xenin 25[Lys13PAL]: a novel long-acting acylated analogue of xenin 25 with promising antidiabetic potential. *Acta Diabetologica*. **52** 461-471.

Gilbert MP & Pratley RE 2015 The Impact of Diabetes and Diabetes Medications on Bone Health *Endocrine Reviews* **36** 194 213.

Gilor C, Rudinsky AJ & Hall MJ 2016 New approaches to Feline Diabetes Mellitus: Glucagon-like peptide-1 analogs. *Journ l of Feline Medicine and Surgery* **18** 733-743.

Godinho R, Mega C, Teixeira-de-Lemos E, Carvalho E, Teixeira F, Fernandes R, & Reis F 2015 The Place of Dipeptidyl Peptidase-4 Inhibitors in Type 2 Diabetes Therapeutics: A "Me Too" or "the Special One" Antidiabetic Class? *Journal of Diabetes Research* **2015** 1-28.

Gögebakan O, Osterhoff MA, Schüler R, Pivovarova O, Kruse M, Seltmann AC, Mosig AS, Rudovich N, Michael Nauck & Pfeiffer AFH 2015 GIP increases adipose tissue expression and blood levels of MCP-1 in humans and links high energy diets to inflammation: a randomised trial. *Diabetologia* **58** 1759–1768.

Gourion-Arsiquaud S, Lukashova L, Power J, Loveridge N, Reeve J & Boskey A L 2013 Fourier transform infrared imaging of femoral neck bone: Reduced heterogeneity of mineral-to-matrix and carbonate-to-phosphate and more variable crystallinity in treatment-naive fracture cases compared with fracture-free controls. *Journal of Bone & Mineral Research* **28** 150–161.

Graff IE, Øyen J, Kjellevold M, Frøyland L, Gjesdal CG, Almås B, Rosenlund G & Lie Ø 2016 Reduced bone resorption by intake of dietary vitamin D and K from tailor-made Atlantic salmon: a randomized intervention trial. *Oncotarget* **7** 69200–69215.

Graham KL, Sutherland RM, Mannering SI, Zhao Y, Chee J, Krishnamurthy B, Thomas HE, Lew AM & Kay WH 2012 Pathogenic Mechanisms in Type 1 Diabetes: The Islet is Both Target and Driver of Disease. *Review of Diabetic Studies* **9** 148–168.

Greco EA, Lenzi A & Migliaccio S 2016 The pathophysiological basis of bone tissue alterations associated with eating disorders. *Hormone Molecular Biology and Clinical Investigation* **28** 121 132.

Green B & Flatt PR 2007 Incretin hormone mimetics and analogues in diabetes therapeutics. *Best Practice & Research Clinical Endocrinology & Metabolism* **21** 497-516.

Green, B, O'Harte, FPM, Greer, B, Harriott, P & Flatt, PR 2001 N terminally modified GLP-1(7-36)amide is resistant to dipeptidyl peptidase-IV degradation whilst maintaining insulinotropic action. *Proceedings of the Nutrition Society* **60** 154A.

Greiner TU & Bäckhed F 2016 Microbial regulation of GLP-1 and L cell biology. *Molecular Metabolism* **5** 753–758.

Grieve D, Robinson E, Tate M, Green B & McDermott B 2016, 'Glucagon-like peptide-1 based therapies as a novel approach for chronic heart failure' Scottish Cardiovascular Forum-Annual Conference, Belfast, United Kingdom, 06/02/2016 06/02/2016.

Grieve DJ, Cassidy RS & Green BD 2009 Emerging cardiovascular actions of the incretin hormone glucagon-like peptide-1: potential therapeutic benefits beyond glycaemic control? *British Journal of Pharmacology* **157**1340-1351.

Haider A, Haider S, Han SS & Kang IK 2017 Recent advances in the synthesis, functionalization and biomedical applications of hydroxyapatite: a review. *RSC Advances* **7** 7442-7458.

Halade GV, Rahman MM, Williams PJ & Fernandes G 2010 High fat diet-induced animal model of age-associated obesity and osteoporosis. *The Journal of* Nutritional Biochemistry 21 1162 1169.

Hampson G, Evans C, Petitt RJ, Evans WD, Woodhead SJ, Peters JR & Ralston SH 1998 Bone mineral density, collagen type 1 a 1 genotypes and bone turnover in premenopausal women with diabetes mellitus. *Diabetologia* **41** 1314-1320.

Hamrick MW, Pennington C, Newton D, Xie D & Isales C 2004 Leptin deficiency produces contrasting phenotypes in bones of the limb and spine. *Bone* **34** 376- 383.

Hamscher G, Meyer HE & Feurle GE 1996 Identification of proxenin as a precursor of the peptide xenin with sequence homology to yeast and mammalian coat protein alpha. *Peptides* **17** 889-893.

Hanna A, Connelly KA, Josse RG & McIntyre RS 2015 The non glycemic effects of incretin therapies on cardiovascular outcomes, cognitive function and bone health. *Expert Review of Endocrinology & Metabolism* **101** 101-114.

Hansen MSS, Tencerova M, Frølich J, Kassem M & Frost M 2017 Effects of gastric inhibitory polypeptide, glucagon-like peptide 1 and glucagon likepeptide-1 receptor agonists on Bone Cell Metabolism. *Basic & Clinical Pharmacology & Toxicology* **122** 25-37.

Hao Z, Song Z, Huang J, Huang K, Panetta A, Gu Z & Jun Wu 2017 The scaffold microenvironment for stem cell based bone tissue engineering *Biomaterials Science* **5** 1382-1392.

Hasib A, Ng MT, Gault VA, Khan D, Parthsarathy V, Flatt PR & Irwin N 2017 An enzymatically stable GIP/xenin hybrid peptide restores GIP sensitivity, enhances beta cell function and improves glucose homeostasis in high-fat-fed mice. *Diabetologia* **60** 541–552.

Heise T, Pieber TR, Danne T, Erichsen L & Haahr H 2017 A Pooled Analyses of Clinical Pharmacology Trials Investigating the Pharmacokinetic and Pharmacodynamic Characteristics of

Fast-Acting Insulin Aspart in Adults with Type 1 Diabetes *Clinical Pharmacokinetics* **56** 551-559.

Henriksen DB, Alexandersen P, Bjarnason NH, Vilsbøll T, Hartmann B, Henriksen EE, Byrjalsen I, Krarup T, Holst JJ & Christiansen C 2003 Role of gastrointestinal hormones in postprandial reduction of bone resorption. *Journal of Bone and Mineral Research* **18** 2180-2189.

Hillier TA, Causley JA, Rizzo JH, Pedula KL, Ensrud KE, Bauer DC, Lui LY, Vesco KK, Black DM, Donaldson MG, LeBlanc E & Cummings SR 2011 The WHO Absolute Fracture Risk Models (FRAX): Do Clinical Risk Factors Improve Fracture Prediction in Older Women Without Osteoporosis? *Journal of Bone & Mineral Research* **26** 1774–1782.

Hirschfeld HP, Kinsella R & Duque G 2017 Vitamin D: not just the bone. Evidence for beneficial pleiotropic extraskeletal effects. *Eating and Weight Disorders - Studies on Anorexia, Bulimia and Obesity* **22** 27–41.

Holst JJ, Pedersen J, Wewer A, Jacob N & KF Krag 2017 The Gut: A Key to the Pathogenesis of Type 2 Diabetes? Metabolic Syndrome and Related Disorders. Metabolic Syndrome and Related Disorders **15** 259-262.

Hu XK, Yin XH, Zhang HQ, Guo CF & Tang MX 2016 Liraglutide attenuates the osteoblastic differentiation of MC3T3 E1 cells by modulating AMPK/mTOR signaling. *Molecular Medicine Reports* **14** 3662-3668.

Hussain MA, Akalestou E & Song WJ 2016 Inter-organ communication and regulation of beta cell function. *Diabetologia* **59** 659–667.

Hutchison AT, Wittert GA & Heilbronn LK 2017 Matching Meals to Body Clocks—Impact on Weight and Glucose Metabolism. *Nutrients* **9** 1-10.

Iepsen EW, Lundgren JR, Hartmann B, Pedersen O, Hansen T, Jørgensen N R, Jensen JB, Holst JJ, MSigne S & Torekov SM 2015 GLP-1 Receptor Agonist Treatment Increases Bone Formation and Prevents Bone Loss in Weight Reduced Obese Women. *The Journal of Clinical Endocrinology & Metabolism* **100** 2909–2917.

Irwin N & Flatt PR 2015 New perspectives on exploitation of incretin peptides for the treatment of diabetes and related disorders. *World Journal of Diabetes* **6** 1285–1295.

Irwin N, Green BD, Mooney MH, Greer B, Harriott P, Bailey CJ, Gault VA, O'Harte FPM & Flatt PR 2005a A novel, long-acting agonist of glucose-dependent insulinotropic polypeptide suitable for once-daily administration in type 2 diabetes. *Journal of Pharmacology and Experimental Therapeutics* **314** 1187-1194.

Jackuliak P & Payer J 2014 Osteoporosis, Fractures, and Diabetes. *International Journal of Endocrinology* **2014** 1-10.

Janssens K, Dijke PT, Janssens S & Hul WV 2005 Transforming growth factor beta1 to the bone. Endocrine Reviews **6** 743-774.

Janzer M, Larbig G, Kübelbeck A, Wischnjow A, Haberkorn U & Mier W 2016 Drug Conjugation Affects Pharmacokinetics and Specificity of Kidney Targeted Peptide Carriers. *Bioconjugate Chemistry* **27** 2441–2449.

Jiang C, Zurick K, Qin C & Bernards MT 2017 Probing the influence of SIBLING proteins on collagen-I fibrillogenesis and denaturation. Connect Tissue Res **14** 1-13.

Jiang S, Zhai H, Li D, Huang J, Zhang H, Li Z, Zhang W & Xu G 2016 AMPK dependent regulation of GLP1 expression in L-like cells. *Journal of Molecular Endocrinology* **57** 151-160.

Jiao H, Xiao E & Graves DT 2015 Diabetes and Its Effect on Bone and Fracture Healing. *Current Osteoporosis Reports* **13** 327–335.

Kainuma S, Tokuda H, Fujita K, Kawabata T, Sakai G, Rie Matsushima-Nishiwaki, Harada A, Kozawa O & Takanobu Otsuka 2016 Attenuation by incretins of thyroid hormone stimulated osteocalcin synthesis in osteoblasts. *Biomed Reports* **5** 771–775.

Kaji I, Akiba Y, Kato I, Maruta K, Kuwahara A & Kaunitz JD 2017 Xenin Augments Duodenal Anion Secretion via Activation of Afferent Neural Pathways. Journal of Pharmacology and Experimental Therapeutics **361** 151-161.

Kanazawa I 2015 Osteocalcin as a hormone regulating glucose metabolism. *World Journal of Diabetes* **25** 1345–1354.

Karpiński M, Popko J, Maresz K, Badmaev V & Stohs SJ 2017 Roles of Vitamins D and K, Nutrition, and Lifestyle in Low-Energy Bone Fractures in Children and Young Adults . *Journal of the American College of Nutrition* **36** 399-412.

Kathleen JM, Barrish JO, Jeffrey L. Neul & Glaze DG 2014 Low Bone Mineral Mass Is Associated with Decreased Bone Formation and Diet in Females with Rett Syndrome. *Journal of Pediatric Gastroenterology and Nutrition* **59** 386–392.

Kazafeos K 2011 Incretin effect: GLP-1, GIP, DPP4. *Diabetes Research Clinical Practise* **93** S32-S36.

Kerckhofs G, Durand M, Vangoitsenhoven R, Marin C, Van der Schueren B, Carmeliet G, Luyten F P, Geris L & Vandamme K 2016 Changes in bone macro- and microstructure in diabetic obese mice revealed by high resolution microfocus X-ray computed tomography. *Scientific Reports* **6** 1-13.

Khan MH, Nabavi SM & Habtemariam S. Anti-diabetic potential of peptides: Future prospects as therapeutic agents. *Life Sciences* In Press.

Kieffer TJ, McIntosh CHS & Pederson RA 1995 Degradation of glucose-dependent insulinotropic polypeptide and truncated glucagon-like peptide 1 in vitro and in vivo by dipeptidyl peptidase IV. *Endocrinology* **136** 3585-3596.

Kim DS, Choi H, Wang Y, Luo Y, Hoffer BJ & Greig NH 2017 A New Treatment Strategy for Parkinson's Disease through the Gut–Brain Axis. *Cell Transplantation* **26** 1560–1571.

Kim KS & Sandoval DA 2017 Endocrine Function after Bariatric Surgery. *Comprehensive Physiology* **7** 783–798.

Kim KS, Lee IS, Kim KH, Park J, Kim Y, Choi JH, Choi JS & Jang HJ 2017 Activation of intestinal olfactory receptor stimulates glucagonlike peptide-1 secretion in enteroendocrine cells and attenuates hyperglycemia in type 2 diabetic mice. Scientific Reports **7** 1-11.

Kini U & Nandeesh BN Physiology of bone formation, remodeling and metabolism In Radionuclide and Hybrid Bone Imaging, Fogelman, I.; Gnanasegaran, G.; van der Wall, H., Eds. Springer: Berlin, 2012; Chapter 2, 29−57.

Kling JM, Clarke BL & Sandhu NP 2014 Osteoporosis Prevention, Screening, andTreatment: A Review. Journal of Womens Health **23** 563–572.

Kodama S, Fujihara K, Ishiguro H, Horikawa C, Ohara N, Yachi Y, Tanaka S, Shimano H, Kato K, Hanyu O & Sone H 2017 Unstable bodyweight and incident type 2 diabetes mellitus: A meta-analysis. *Journal of DiabetesInvestigation* **8** 501-509.

Kõks S, Dogan S, Tuna BG, Navarro HG, Potter P, Vandenbroucke RE 2016 Mouse models of ageing and their relevance to disease. *Mechanisms of Ageing and Development* **160** 41-53.

Kolb H & Herrath M 2017 Immunotherapy for Type 1 Diabetes: Why Do Current Protocols Not Halt the Underlying Disease Process? *Cell Metabolism* **25** 233-241.

Koole C , Reynolds CA, Mobarec JC, Hick C, Sexton PM & Sakmar TP 2017 Genetically encoded photocross-linkers determine the biological binding siteof exendin-4 peptide in the N-terminal domain of the intact human glucagonlike peptide-1 receptor (GLP-1R). *The Journal of Biological Chemistry* **292**7131-7144.

Kourkoumelis N, Lani A & Tzaphlidou M 2012 Infrared spectroscopic assessment of the inflammation-mediated osteoporosis (IMO) model applied to rabbit bone. *Journal of Biological Physics* **38** 623–635.

Krishnan A & Muthusami S 2017 Hormonal alterations in PCOS and its influence on bone metabolism. *Journal of Endocrinology* **232** 99-113.

Kuo TR & Chen CH 2017 Bone biomarker for the clinical assessment of osteoporosis: recent developments and future perspectives. *Biomarker Research* **5** 1-9.

Kyoji Ikeda & Sunao Takeshita 2014 Factors and Mechanisms Involved in the Coupling from Bone Resorption to Formation: How Osteoclasts Talk to Osteoblasts? *Journal of BoneMetabolism* **21** 163–167.

Langsford D, Steinberg A & Dwyer KM 2017 Diabetes Mellitus Following Renal Transplantation: Clinical and Pharmacological Considerations for the Elderly Patient. *Drugs & Aging* **34** 589–601.

Lecka-Czernik B, Moerman EJ, Grant DF, Lehmann JM, Manolagas SC & Jilka RL 2002 Divergent effects of selective peroxisome proliferator-activated receptor γ2 ligands on adipocyte versus osteoblast differentiation. *Endocrinology* **143**2376-2384.

Lee JH, Kang MS, Mahapatra C & Kim HW 2016 Effect of Aminated Mesoporous Bioactive Glass Nanoparticles on the Differentiation of Dental Pulp Stem Cells. *PLoS ONE* **11.**

Lee KS, Hong SH & Bae SC 2002 Both the Smad and p38 MAPK pathways play a crucial role in Runx2 expression following induction by transforming growth factor-beta and bone morphogenetic protein. Oncogene **21** 7156-7163.

Lee S, & Lee DY 2017 Glucagon-like peptide-1 and glucagon-like peptide-1 receptor agonists in the treatment of type 2 diabetes. *Annals of Pediatric Endocrinology and Metabolism* **22** 15–26.

Lee WC, Guntur AR, Long F &Rosen CJ 2017 Energy Metabolism of the Osteoblast: Implications for Osteoporosis. *Endocrine Reviews* **38** 255–266.

Lee YS & Jun HS 2014 Anti-diabetic actions of glucagon-like peptide-1 on pancreatic beta-cells. *Metabolism* **63** 9-19.

Leeuwen VJ, Koes BW, Paulis WD, & Middelkoop MV 2017 Differences in bone mineral density between normal-weight children and children with overweight and obesity: a systematic review and meta-analysis. *Obesity Reviews* **18** 526–546.

Li R, Xu W, Luo S, Xu H, Tong G, Zeng L, Zhu D & Weng J 2015 Effect of exenatide,insulin and pioglitazone on bone metabolism in patients with newly diagnosed type 2 diabetes. *Acta Diabetologica* **52** 1083-1091.

Li Y, Li L & Hölscher C 2016 Incretin-based therapy for type 2 diabetes mellitus is promising for treating neurodegenerative diseases. *Reviews in the Neurosciences* **27** 689-711.

Lindgren O, Pacini G, Tura A, Holst J, Deacon C & Ahrén B 2015 Incretin Effect After Oral Amino Acid Ingestion in Humans. *The Journal of Clinical Endocrinology & Metabolism* **3** 1172–1176.

Lips P 2001 Vitamin D deficiency and secondary hyperparathyroidism in the elderly; consequences forbone loss and fractures and therapeutic implications. *Endocrionoly Review* **22**: 477-501.

Lorenz M, Lawson F, Owens D, Raccah D, Roy-Duval C, Lehmann A, Perfetti R & Blonde L 2017 Differential effects of glucagon like peptide-1 receptor agonists on heart rate. *Cardiovascular Diabetology* **16** 1-10.

Lu N, Sun H, Yu J, Wang X, Liu D, Zhao L, Sun L, Zhao H, Tao B & Liu J 2015 Glucagon-like peptide-1 receptor agonist Liraglutide has anabolic bone effects in ovariectomized rats without diabetes. *PLoS ONE* 10e0132744.

Luo G, Liu H & Lu H 2016 Glucagon-like peptide-1(GLP-1) receptor agonists: potential to reduce fracture risk in diabetic patients? *British Journal of Clinical Pharmacology* **81** 78–88.

M.Weivoda, Youssef SJ & Oursler MJ 2017 Sclerostin expression and functions beyond the osteocyte. *Bone* **96** 45-50.

Mabilleau G 2017 Interplay between bone and incretin hormones: A review.*Morphologie* **10** 9-18.

Mabilleau G, Pereira M & Chenu C 2017 Novel skeletal effects of glucagon-like peptide-1 (GLP-1) receptor agonists. *Journal of Endocrinology* **236** 29-42.

Mabilleau G, Perrot R, Mieczkowska A, Boni S, Flatt PR, Irwin N & Chappard D 2016 Glucose-dependent insulinotropic polypeptide (GIP) dose-dependently reduces osteoclast differentiation and resorption. *Bone* **91** 102-112.

MacDonell R, Hamrick MW & Isales CM 2016 Protein/amino-acid modulation of bone cell function. *Bone Key Reports* **5** 1-7.

Mader JT, Cantrell JS & Calhoun J 1990 Oral ciprofloxacin compared with standard parenteral antibiotic therapy for chronic osteomyelitis in adults. *Journal of Bone & Joint Surgery America* **72** 104-110.

Madiraju AK, Erion DM, Rahimi Y, Zhang XM, Braddock D, Albright RA, Prigaro BJ, Wood JL, Bhanot S, MacDonald MJ, Jurczak M, Camporez JP, Lee HY, Cline GW, Samuel VT, Kibbey RG & Shulman GI 2014 Metformin suppresses gluconeogenesis by inhibiting mitochondrial glycerophosphate dehydrogenase. *Nature* **510** 542-546.

Manolagas SC, O'Brien CA & Almeida M 2013 The role of estrogen and androgen receptors in bone health and disease. *Nature Reviews Endocrinology* **9** 699-712.

Manske SL, Zhu Y, Sandino C and Boyd SK 2015 Human trabecular bone microarchitecture can be assessed independently of density with second generation HR-pQCT. *Bone* **79** 213-221.

Maria Goretti M. Penido G and Alon US 2012 Phosphate homeostasis and its role in bone health. *Pediatric Nephrology* **27** 2039-2048.

Martin CM, Gault VA, McClean S, Flatt PR & Irwin N 2012 Degradation, insulin secretion, glucose-lowering and GIP additive actions of a palmitate derivatised analogue of xenin-25. *Biochemical Pharmacology* **8** 312-319.

Martin CM, Parthsarathy V, Hasib A, Ming T. Ng, McClean S, Flatt PR, Gault VA,& Irwin N 2016 Biological Activity and Antidiabetic Potential of C Terminal Octapeptide Fragments of the Gut-Derived Hormone Xenin. *PLoS One* **11** e0152818.

Martin CM, Parthsarathy V, Pathak V, Gault VA, Flatt PR & Irwin N 2014 Characterisation of the biological activity of xenin-25 degradation fragment peptides. *Journal of Endocrinology* **221** 193-200.

Marvaniya HM & Patel HU 2017 Role of dipeptidyl peptidase-iv (dpp 4) inhibitor in the management of type 2 diabetes *World journal of Pharmacy and Pharmaceutical Sciences* **6** 551-566.

Matsuo K & Irie N 2008 Osteoclast–osteoblast communication. *Archives of Biochemistry and Biophysics* **473** 201-209.

Mayfield K, Siskind D, Winckel K, Russell AW, Kisely S, Smith G & Hollingorth S 2016 Glucagon-like peptide-1 agonists combating clozapine associated obesity and diabetes. *Journal of Psychopharmacology* **30** 227-236.

Mazella J, Béraud-Dufour S, Devader C, Massa F & Coppola T 2012 Neurotensin and its receptors in the control of glucose homeostasis. *Frontiers in Endocrinology* **3** 1-7.

McClenaghan NH, Barnett CR, Ah-Sing E, Abdel-Wahab YHA, O'Harte FPM, Yoon TW, Swanston-Flatt SK & Flatt PR 1996 Characterization of a Novel Glucose-Responsive Insulin

Secreting Cell Line, BRIN-BD11, Produced by Electrofusion. *Diabetes* **45** 1132-1140.

McIntosh CHS 2008 Incretin-based Therapies for Type 2 Diabetes. *Canadian Journal of Diabetes* **32** 131-139.

MD, Siminerio L & Vivian E 2017 Diabetes Self-management Education and Support in Type 2 Diabetes: A Joint Position Statement of the American Diabetes Association, the American Association of Diabetes Educators, and the Academy of Nutrition and Dietetics. *The Diabetes Educator* **43** 40 – 53.

Meah F, Basit A, Emanuele N & Emanuele MA 2017 *Clinicical Reviews in Bone Mineral Metabolism* **15** 24-36.

Meece J 2017 The Role of the Pharmacist in Managing Type 2 Diabetes with Glucagon-Like Peptide-1 Receptor Agonists as Add-On Therapy. *Advances in Therapy* **34** 638–657.

Meier C, Schwartz AV, Egger A & Lecka-Czernik B 2016 Effects of diabetes drugs on the skeleton. *Bone* **82** 93-100.

Mells JE & Anania FA 2013 The Role of Gastrointestinal Hormones in Hepatic Lipid Metabolism. *Seminars Liver Disease* **33** 343–357.

Melton LJ, Leibson CL, Achenbach SJ, Therneau TM & Khosla S 2008 Fracture Risk in Type 2 Diabetes: Update of a Population Based Study. *Journal of Bone & Mineral Research* **23** 1334–1342.

Meng J, Ma X, Wang N, Jia M, Bi L, Wang Y, Li M, Zhang H, Xue X, Hou Z, Zhou Y, Yu Z, He G & Luo X 2016 Activation of GLP-1 Receptor Promotes Bone Marrow Stromal Cell Osteogenic Differentiation through β-Catenin. *Stem Cell Reports* **6** 579-591.

Merkus FW, Verhoef JC, Romeijn SG & Schipper NG 1991 Absorption enhancing effect of cyclodextrins on intranasally administered insulin in rats. *Pharmaceutical Research* **8** 588-592.

Miazgowski T & Czekalski S 1998 A 2-year Follow-up study on bone mineral density and markers of bone turnover in patients with long-standing insulin dependent diabetes mellitus. *Osteoporosis International* **8** 399–403.

Mieczkowska A, Bouvard B, Chappard D & Mabilleau G 2015 Glucose dependent insulinotropic polypeptide (GIP) directly affects collagen fibril diameter and collagen cross-linking in osteoblast cultures. *Bone* **74** 29-36.

Mieczkowska A, Irwin N, Flatt PR, Chappard D & Mabilleau G 2013 Glucose dependent insulinotropic polypeptide (GIP) receptor deletion leads to reduced bone strength and quality. Bone **56** 337-342.

Mieczkowska A, Mansur S, Bouvard B, Flatt PR, Thorens N, Irwin N, Chappard D & Mabilleau G 2015 Double incretin receptor knock-out (DIRKO) mice present with alterations of trabecular and cortical micromorphology and bone strength. *Osteoporosis International* **26** 209-218.

Millar PJB, Pathak V, Moffett RC, Pathak NM, Bjourson AJ, MJO'Kane, Flatt PR & Gault VA 2016 Beneficial metabolic actions of a stable GIP agonist following pre-treatment with a GLT2 inhibitor in high fat fed diabetic mice. *Molecular and Cellular Endocrinology* **420** 37-45.

Miller B, Spevak L, Lukashova L, Javaheri B, Pitsillides AA, Boskey A, BouGharios G & Carriero A 2017 *Calcified Tissue International* **100** 631-640.

Mirošević G, Blaslov K, Naranđa F, Plećko M, Radošević JM &Vrkljan M 2017 The emerging role of incretins in the pathophysiology of insulin resistance in type 1 diabetes. *Endocrine Oncology and Metabolism* **3** 90-96.

Moayeri A, Mohamadpour M, Mousavi SF, Shirzadpour E, Mohamadpour S & Amraei M 2017 Fracture risk in patients with type 2 diabetes mellitus and possible risk factors: a systematic review and meta-analysis. *Therapeutics & Clinical Risk Managagement* **13** 455–468.

Moon MK, Hur KY, Ko SH, Park SO, Lee BW, Kim JH, Rhee SY, Kim HJ, Choi KM & Kim NH 2017 Committee of Clinical Practice Guidelines of the Korean Diabetes Association. Combination Therapy of Oral Hypoglycemic Agents in Patients with Type 2 Diabetes Mellitus. Diabetes Metabolism Journal **41**357-366.

Moonschi FH, Hughes CB, Mussman GM, Fowlkes JL, Richards CI & Popescu I 2017 *Acta Diabetologica* **54** 1-14.

Morley JE, Abbatecola AM & Woo J 2017 Management of Comorbidities in Older Persons with Type 2 Diabetes. *The journal of Post-Acute and Long-Term Care medicine* **18** 639-645.

Mosenzon O, Wei C, Davidson J, Scirica BM, Yanuv I, Rozenberg A, Hirshberg B, Cahn A, Stahre C, Strojek K, Bhatt DL & Raz I 2015 Incidence of Fractures in Patients With Type 2 Diabetes in the SAVOR-TIMI 53 Trial. *Diabetes Care* **38** 2142-2150.

Müller TD, Finan B, Clemmensen C, DiMarchi RD &Tschöp MH 2017 The New Biology and Pharmacology of Glucagon. *Physiological Reviews* **97** 721-766.

Muppidi A, Zou H, Yang PY, Chao E, Sherwood L, Nunez V, Woods AK, Schultz PG, Lin Q & Shen W 2016 Design of Potent and Proteolytically Stable Oxyntomodulin Analogs. *ACS Chemical Biology* **11** 324–328.

Murshed M, Harmey D, Millán JL, McKee MD & Karsenty G 2005 Uniquecoexpression in osteoblasts of broadly expressed genes accounts for the spatial restriction of ECM mineralization to bone. *Genes Development* **19** 1093- 1104.

Muruganandan S & Sinal CJ 2014 The impact of bone marrow adipocytes on osteoblast and osteoclast differentiation. *IUBMB Life* **66** 147–155.

Muscogiuri G, A.DeFronzo R, Gastaldelli A & Holst JJ 2017 Glucagon-like Peptide1 and the Central/Peripheral Nervous System: Crosstalk in Diabetes. *Trends in Endocrinology & Metabolism* **28** 88-103.

Napoli N, Chandran M, Pierroz DD, Abrahamsen B, Schwartz AV & Ferrari SL 2017 Mechanisms of diabetes mellitus-induced bone fragility. *Nature Reviews Endocrinology* **13** 208–219.

Narayana VK, Tomatis VM, Wang T, Kvaskoff D & Meunier FA 2015 Profiling of Free Fatty Acids Using Stable Isotope Tagging Uncovers a Role for Saturated Fatty Acids in Neuroexocytosis. *Chemical Biology* **19** 1552-1561.

Nauck MA 2014 Update on developments with SGLT2 inhibitors in the management of type 2 diabetes. *Drug Design Development and Therapy* **8** 1335-1380.

Newman MR & Benoit DSW 2016 Local and targeted drug delivery for bone regeneration. *Current Opinion in Biotechnology* **40** 125-132.

Nicolai J, Albrechtsen W, Kuhre RE, Pedersen J, Knop FK & Holst JJ 2016 The biology of glucagon and the consequences of hyperglucagonemia. Biomarkers in Medicine **10** 1141–1151.

Nilsson, AG, Sundh, D, Johansson, L, Nilsson, M, Mellström, D, Rudäng, R, Zoulakis, M, Wallander, M, Darelid, A. & Lorentzon, M. 2017 Type 2 Diabetes Mellitus Is Associated With Better Bone Microarchitecture But Lower Bone Material Strength and Poorer Physical Function in Elderly Women: A Population-Based Study. *Journal of Bone & Mineral Research* **32** 1062–1071.

Nishioka T, Tomatsu S, Gutierrez MA, Miyamoto K, Trandafirescu GG, Lopez PLC, Grubb JH, Kanai R, Kobayashi H, Yamaguchi S, Gottesman GS, Cahill R, Noguchi K & Sly WS 2006 Enhancement of drug delivery to bone: Characterization of human tissue-nonspecific alkaline phosphatase tagged with an acidic oligopeptide. *Molecular Genetics & Metabolism* **88** 244–255.

Nongonierma AB & FitzGerald RJ 2017 Features of dipeptidyl peptidase IV (DPP IV) inhibitory peptides from dietary proteins. *Journal of Food & Biochemistry* **94** 79-89.

Nuche-Berenguer B, Portal-Núñez S, Moreno P, González N, Acitores A, López Herradón A, Esbrit P, Valverde I & Villanueva Peñacarrillo ML 2010 Presence of a functional receptor for GLP-1 in osteoblastic cells, independent of the cAMP linked GLP-1 receptor. *Journal of Cellular Physiology* **225** 585-592.

Nyman JS, Granke M, Singleton RC & Pharr GM 2016 Tissue-level Mechanical Properties of Bone Contributing to Fracture Risk. *Current Osteoporosis Reports* **4** 138–150.

O'Connor EM & Durack E 2017 Osteocalcin: The extra-skeletal role of a vitamin K dependent protein in glucose metabolism. *Journal of Nutrition & Intermediary Metabolism* **7** 8-13.

Oei L, Rivadeneira F, Carola Zillikens M & Oei EHG 2015 Diabetes, Diabetic Complications, and Fracture Risk. *Current Osteoporos Reports* **13** 106-115.

O'Harte FPM, Ng MT, Lynch AM, Conlon JM & Flatt PR 2016 Novel dual agonist peptide analogues derived from dogfish glucagon show promising in vitro insulin releasing actions and antihyperglycaemic activity in mice. *Molecular and Cellular Endocrinology* **431** 133-144.

Ooms ME, Lips P, Van Lingen A & Valkenburg HA 1993 Determinants of bone mineral density and risk factors for osteoporosis in healthy elderly women. *Journal of Bone and Mineral Research* **8** 669-675.

Orimo H 2010 The mechanism of mineralization and the role of alkalinephosphatase in health and disease. *Journal of Nippon Medical School* **77** 4-12.

Osterhoff G, Morgan EF, Shefelbine SJ, Karim L, Laoise M. McNamara & Peter Augat P 2016 Bone mechanical properties and changes with osteoporosis. *Injury* **47** 11–20.

Otter S & Lammert E 2016 Exciting Times for Pancreatic Islets: Glutamate Signaling in Endocrine Cells. *Trends in Endocrinology & Metabolism* **27** 177-188.

Pais R, Gribble F & Reimann F 2016 Stimulation of incretin secreting cells. *Therapeutic Advances in Endocrinology and Metabolism*. **7** 24–42.

Palermo A, D'Onofrio L, Buzzetti R, Manfrini S & Napoli N 2017 Pathophysiology of Bone Fragility in Patients with Diabetes. *Calcified Tissue International* **100** 122–132.

Palleria C, Leo A, Andreozzi F, Citraro R, Iannone M, Spiga R, Sesti G, Constanti A, De Sarro G, Arturi F & Russo E 2017 Liraglutide prevents cognitive decline in a rat model of streptozotocin-induced diabetes independently from its peripheral metabolic effects. *Behavioral Brain Research* **32**1 157-169.

Pan KY, Xu W, Mangialasche F, Fratiglioni L &Wang HX 2017 Work related psychosocial stress and the risk of type 2 diabetes in later life. *Journal ofInternal Medicine* **281** 601–610.

Patil AS, Sable RB and Kothari RM 2011 An update on transforminggrowth factor-β (TGF-β): sources, types, functions and clinical applicability for cartilage/bone healing. *Journal of Cell Physiology* **226** 3094-103.

Peacock SJ, Coats BR, Kirkland JK, Tanner CA & Garland T Jr & Middleton KM 2017 Predicting the bending properties of long bones: Insights from an experimental mouse model. *American Journal of Physical Anthropology* **00** 1–14.

Pederson RA & Brown JC 1976 The insulinotropic action of gastric inhibitory polypeptide in the perfused isolated rat pancreas. *Endocrinology* **99**: 780-785.

Pereira M, Jeyabalan J, Jørgensen CS, Hopkinson M, Al-Jazzar A, Roux JP, Chavassieux P, Orriss IR, Cleasby ME, Chenu C 2015 Chronic administration of Glucagon-like peptide-1 receptor agonists improves trabecular bone mass and architecture in ovariectomised mice. *Bone* **81** 459- 467.

Pérez-Sáez , José M, Sabina H, Daniel PA, Xavier N, María V, Dolores RP, Marisa M, Roberto G, Marta C, Adolfo DP & Julio P 2017 Bone Density, Microarchitecture, and Tissue Quality Long-term After Kidney Transplant. *Transplantation* **101** 1290–1294.

Peter AK, Crocini C & Leinwand LA 2017 Expanding our scientific horizons: utilization of unique model organisms in biological research. *The EMBO Journal* **36** 2311-2314.

Petit MA, Paudel ML, Taylor BC, Hughes JM, Strotmeyer ES, Schwartz AV, Cauley JA, Zmuda JM, Hoffman AR & Ensrud KE 2010 Bone mass and strength in older men with type 2 diabetes: the osteoporotic fractures in men study. *Journal of Bone and Mineral Research* **25** 285–291.

Phillips I, King A & Shannon K. 1988 In The quinolones, Andriole V.T., Ed.;Academic Press: New York 83-113.

Picke AK, Alaguero IG, Campbell GM, CCGlüerbJ.Salbach-Hirsch, Rauner M, Hofbauer LC& Hofbauerd C 2016 Bone defect regeneration and cortica bone parameters of type 2 diabetic rats are improved by insulin therapy. *Bone* **82** 108-115.

PontiSara F, Claudia G, Giuseppe S, Giuseppe B & Bazzocchi GA 2017 Imaging of diabetic bone. *Endocrine* **58** 426–441.

Poundarik AA, Wu PC, Evis Z, Sroga GE, Ural A, Rubin M & Vashishth D 2015 A direct role of collagen glycation in bone fracture. Journal *of the Mechanical Behavior of Biomedical Materials* **52** 120-130.

Powers MA, Bardsley J, Cypress M, Duker P, Funnell MM, Fischl AH, Maryniuk Pradhan B & Majhi C 2017 Pancreatic alpha cell dysfunction in diabetes mellitus and its management strategies. *Journal of Evidence Based Medicine & Healthcare* **4** 2775-2782.

Pradeepa R & Mohan V 2017 Prevalence of type 2 diabetes and its complications in India and economic costs to the nation. *European Journal of Clinical Nutrition* **71** 816-824.

Prasad RB *& Groop L 2015* Genetics of Type 2 Diabetes—Pitfalls and Possibilities. *Genes* **6** 87-123.

Preiato VL, Vicennati V, Gambineri A & Pagotto U The Endocrine Regulation of Energy and Body Weight. *Principles of Endocrinology and Hormone Action Part of the series Endocrinology*.

Pscherer S, Kostev K, Dippel FW & Rathmann W 2016 Fracture risk in patients with type 2 diabetes under different antidiabetic treatment regimens: a retrospective database analysis in primary care. *Diabetes Metabolic Syndrome & Obesity: Targets & Therapy* **9** 17–23.

Pujari-Palmer M, Pujari-Palmer S, Lu X, Lind T, Melhus H, Engstrand T, Karlsson Ott M, & Engqvist H 2016. Pyrophosphate Stimulates Differentiation, Matrix Gene Expression and Alkaline Phosphatase Activity in Osteoblasts. *PLoS One* **11** e0163530.

Qingqing W, Imam U, Yida M & Wang Z 2017 Peroxisome Proliferator-Activated Gamma (PPARγ) as a Target for Concurrent Management of Diabetes and Obesity-Related Cancer. *Current Pharmaceutical Design* **23** 3677-3688.

Quach D & Britton RA 2017 Gut Microbiota and Bone Health. *Advances in Experimental Medicine and Biology* **1033** 47-58.

Räkel A, Sheehy O, Rahme E & LeLorier J 2008 Osteoporosis among patients with type 1 and type 2 diabetes. *Diabetes & Metabolism* **34** 193-205.

Raška Jr. I, Rašková M, Zikán V & Škrha J 2017 Prevalence and risk factors of osteoporosis in postmenopausal women with type 2 diabetes mellitus *Central European Journal of Public Health* **25** 3–10.

Rigato M & Fadini GP 2014 Comparative effectiveness of liraglutide in the treatment of type 2 diabetes. *Diabetes Metabolic Syndrome & Obesity: Targets & Therapy* **7** 107–120.

Robey PG, Young ME, Flanders KC, Roche NS, Kondaiah P, Reddi AH, Termine JD, Sporn MB & Roberts AB 1987 Osteoblasts Synthesize and respond to transforming growth factor-type beta (TGF-beta) in vitro. The Journal of Cell Biology **105** 457-463.

Romieu I, Dossus L, Barquera S, Blottière HM, Franks PW, Gunter M, Hwalla N, Hursting SD, Leitzmann M, Margetts B, Nishida C, Potischman N, Seidell J, Stepien M, Wang Y, Westerterp K, Winichagoon P, Wiseman M & Willett WC 2017 Energy balance and obesity: what are the main drivers? *Cancer Causes & Control* **28** 247-258.

Rouille Y, Bianchi M, Irminger J & Halban PA 1997a Role of the prohormone convertase PC2 in the processing of proglucagon to glucagon. *FEBS Letters* **413** 119-123.

Rubin KH, Abrahamsen B, Friis-Holmberg T, Hjelmborg V , Bech M, Hermann AP, Barkmann R, Glüer CC & KimBrixen 2013 Comparison of different screening tools (FRAX®, OST, ORAI, OSIRIS, SCORE and age alone) to identify women with increased risk of fracture. A population-based prospective study. *Bone* **56** 16-22.

Ruppert K., Cauley J., Lian Y, Zqoibor JC, Derby C & Solomom DH 2017 The effect of insulin on bone mineral density among women with type 2 diabetes: a SWAN Pharmacoepidemiology study. *Osteoporosis International* In Press.

Russo GT, Giandalia A, Elisabetta L. Romeo, Nunziata M, Muscianisi M, Ruffo MC, Catalano A & Cucinotta D 2016 "Fracture Risk in Type 2 Diabetes: Current Perspectives and Gender Differences," *International Journal of Endocrinology* **2016** 1-11.

Saeui CT, Liu L, Urias E, Morrissette-McAlmon J, Bhattacharya R & Yarema KJ 2017 Pharmacological, Physiochemical, and Drug-Relevant Biological Properties of Short Chain Fatty Acid Hexosamine Analogues Used in Metabolic Glycoengineering. *Molecular Pharmaceutics* In Press.

Samelson EJ, DemissieS, Cupples LA, Zhang X, Xu H, Liu C-T, Boyd SK., McLean RR, Broe, KE, Kiel DP & Bouxsein ML 2017

Diabetes and Deficits in Cortical Bone Density, Microarchitecture, and Bone Size: Framingham HR-pQCT Study. *Journal of Bone & Mineral Research* **33** 54-62.

Sarah L. Booth, Amanda Centi, Steven R. Smith & Caren Gundberg 2013 The role of osteocalcin in human glucose metabolism: marker or mediator? *Nature Reviews Endocrinology* **9** 43–55.

Sbaraglini ML, Molinuevo MS, Sedlinsky C, Schurman L, McCarthy AD 2014 Saxagliptin affects long-bone microarchitecture and decreases the osteogenic potential of bone marrow stromal cells. *European Journal of Pharmacology* **727** 8-14.

Schipper NG, Verhoef JC, De Lannoy LM, Romeijn SG, Brakkee JH, Wiegant VM, Gispen WH & Merkus FW 1993 Nasal administration of an ACTH(4-9) peptide analogue with dimethyl-beta-cyclodextrin as an absorption enhancer: pharmacokinetics and dynamics. *British Journal of Pharmacology* **110** 1335-1340.

Schipper NG, Verhoef JC, Romeijn SG & Merkus FW 1995 Methylated betacyclodextrins are able to improve the nasal absorption of salmon calcitonin. *Calcified Tissue International* **56** 280-282.

Schmidt FN, Zimmermann EA, Campbell GM, Sroga GE, Püschel K, Amling M, Tang SY, Vashishth D & Bussea B 2017 Assessment of collagen quality associated with non enzymatic cross-links in human bone using Fourier transform infrared imaging. *Bone* **97** 243-251.

Schwartz AV, Hillier TA, Sellmeyer DE, Resnick HE, Gregg E, Ensrud KE, Schreiner PJ, Margolis KL, Cauley JA, Nevitt MC, Black DM & Cummings SR 2002 Older women with diabetes have a higher risk of falls. *Diabetes Care* **25** 1749- 1754.

Schwartz AV, Sellmeyer DE, Ensrud KE, Cauley JA, Tabor HK, Schreiner PJ, Jamal SA, Black DM & Cummings SR 2000 Older women with diabetes have an increased risk of fracture: a prospective study. *The Journal of Clinical Endocrinology & Metabolism* **86** 32-38.

Segnani C, Ippolito C, Antonioli L, Pellegrini C, Blandizzi C, Dolfi A, & Bernardini A 2015 Histochemical Detection of Collagen Fibers by Sirius Red/Fast Green Is More Sensitive than van Gieson or Sirius Red Alone in Normal and Inflamed Rat Colon. *PLoS ONE* **10** e0144630.

Seino Y, Fukushima & Yabe D 2010 GIP and GLP-1, the two incretin hormones: Similarities and differences. *Journal of Diabetes Investigation* **1** 1-2.

Shaikh NS & Sawarkar SP 2017 Targeting Approaches for Effective Therapeutics of Bone Tuberculosis. *Journal of Pharmaceutical Microbiology* **3** 1-13.

Shanbhogue VV, Hansen S, Frost M & Jørgensen NR 2016 Compromised cortical bone compartment in type 2 diabetes mellitus patients with microvascular disease. *European Journal of Endocrinology* **174** 115-124.

Shanbhogue VV, Mitchell DM, Rosen CJ & Bouxsein ML 2016 Type 2 diabetes and the skeleton: new insights into sweet bones. *The Lancet Diabetes & Endocrinology* **4** 159-173.

Shapses SA & Sukumar D 2012 Bone Metabolism in Obesity and Weight Loss. *Annual Review of Nutrition* **32** 287–309.

Sheu Y, Amati F, Schwartz AV, .Danielson ME, Li X, Boudreau R & Cauley JA 2017 Vertebral bone marrow fat, bone mineral density and diabetes: The Osteoporotic Fractures in Men (MrOS) study. *Bone* **97** 299-305.

Shimazu-Kuwahara S, Harada N, Yamane S, Joo E, Sankoda A, Kieffer TJ & Inagaki N 2017Attenuated secretion of glucose dependent insulinotropic polypeptide (GIP) does not leviate hyperphagic obesity and insulin resistance in ob/ob mice. *Molecular Metabolism* **6** 288–294.

Sims NA & Martin JT 2015 Coupling Signals between the Osteoclast and Osteoblast: How are Messages Transmitted between These Temporary Visitors to the Bone Surface? *Frontiers in Endocrinology (Lausanne)* **6** 41.

Smith EP, An Zhibo, Wagner C, Lewis AG, Coen EB, Bailing Li, Mahbod P, Sandoval D, Perez-Tilve D, Tamarina N, Philipson LH, Stoffers DA, Seeley RJ & D'Alessio DA 2014 The role of β-cell GLP-1 signaling in glucose regulation and response to diabetes drugs. *Cell Metabolism* **19** 1050-1057.

Sosa DD & Eriksen EF 2017 Reduced Bone Material Strength is Associated with Increased Risk and Severity of Osteoporotic Fractures. An Impact Microindentation Study *Calcified Tissue International* **101** 34-42.

SparreUlrich AH, Gabe MN, Gasbjerg LS, Christiansen CB, Svendsen B & Hartmann B 2017 GIP(3–30)NH2 is a potent competitive antagonist of the GIP receptor and effectively inhibits GIP mediated insulin, glucagon, and somatostatin release. *Biochemical Pharmacology* **131** 78-88.

Stapleton M , Sawamoto K , Almériga-Díaz CJ , Mackenzie WG , Mason RW Orii T & Tomatsu S 2017 Development of Bone Targeting Drugs. *International Journal of Molecular Science* **18** 1-15.

Steinert RE, Feinle-Bisset C, Asarian L, Horowitz M, Beglinger B & Geary N 2017. Ghrelin, CCK, GLP-1, and PYY (3–36): Secretory Controls and Physiological Roles in Eating and Glycemia in Health, Obesity, and After RYGB. *Physiological Reviews* **97** 411-463.

Sterl K, Wang S, Oestricker L, Wallendorf MJ, Patterson BW, Reeds DN & Wice BM 2017 Metabolic responses to xenin-25 are altered in humans with Roux en-Ygastric bypass surgery. *Peptides* **82** 76-84.

Stewart A. Low, Jiyuan Yang & Jindřich Kopeček 2014 Bone-Targeted Acid Sensitive Doxorubicin Conjugate Micelles as Potential Osteosarcoma Therapeutics. *Bioconjugate Chemistry* **25** 2012 2020.

Strotmeyer ES, Cauley JA, Orchard TJ, Steenkiste AR & Dorman JS 2006 Middle aged premenopausal women with type 1 diabetes have lower bone mineral density and calcaneal quantitative ultrasound than nondiabetic women. *Diabetes Care* **29** 306-311.

Tahrani AA, Bailey CJ, Del Prato S & Barnett AH 2011 Management of type 2 diabetes: new and future developments in treatment. *The Lancet* **378** 182-197.

Takah shi-Nishioka T, Yokogawa K, Tomatsu S, Nomura M, Kobay shi S & Miyamoto K 2008 Targeted drug delivery to bone: pharmacokinetic and pharmacological properties of acidic oligopeptide-tagged drugs. *Current Drug Discovery Technologies* **5** 39-48.

Tang Y, Wu X, Lei W, Pang L, Wan C, Shi Z, Zhao L, Nagy TR, Peng X, Hu J, Feng X, Hul WV, Wan M & Cao X 2009 TGF-β1 induced migration of bone mesenchymal stem cells couples bone resorption with formation. *Nature Medicine* **15** 757-765.

Tatarkiewicz K, Hargrove DM, Jodka CM, Gedulin BR, Smith PA, Hoyt JA, LwinA, Collins L, Mamedova L, Levy OE, D'Souza L, Janssen L, Srivastava V, Ghosh SS & Parkes DG 2014 A novel long-acting glucose-dependent insulinotropic peptide analogue: enhanced efficacy in normal and diabetic rodents. *Diabetes, Obesity & Metabolism* **16** 75–85.

Taylor AI, Irwin N, McKillop AM, Patterson S, Flatt PR & Gault VA 2010 Evaluation of the degradation and metabolic effects of the gut peptide xenin on insulin secretion, glycaemic control and satiety. *Journal of Endocrinology* **207** 87-93.

Teitelbaum SL & Ross FP 2003 Genetic regulation of osteoclast development and function. *Nature Reviews Genetics* **4** 638 649.

Torekov SS, Harsløf T, Rejnmark L, Eiken P, Jensen JB, Herman AP, Hansen T, Pedersen O, Holst JJ & Langdahl BL 2014 A functional amino acid substitution in the glucose-dependent insulinotropic polypeptide receptor (GIPR) gene is associated with lower bone mineral density and increased fracture risk. *Journal of Clinical Endocrinology & Metabolism* **99** 729 733.

Tramutola A, Arena A, Cini C, Butterfield DA & Barone E 2017 Modulation of GLP-1 signaling as a novel therapeutic approach in the treatment of Alzheimer's disease pathology. *Expert Review of Neurotherapeutics* **17** 59- 75.

Turner CH 2006 Bone strength: current concepts. *Annals of the New York Academy of Sciences* **1068** 429-446.

Uccellatore A, Genovese S, Dicembrini I, Mannucci E & Ceriello A 2015 Comparison Review of Short-Acting and Long-Acting Glucagon-like Peptide-1 Receptor Agonists. *Diabetes Therapy* **6** 239–256.

Ugleholdt R, Poulsen MH, Holst PJ, Irminger J, Orskov C, Pedersen J, Rosenkilde MM, Zhu X, Steiner DF & Holst JJ 2006 Prohormone Convertase 1/3 Is Essential for Processing of the Glucose-dependent Insulinotropic Polypeptide Precursor. *Journal of Biological Chemistry* **281** 11050-11057.

Ulbrich K, Holá K, Šubr V, Bakandritsos A, Tuček J & Zbořil R 2016 Targeted Drug Delivery with Polymers and Magnetic Nanoparticles: Covalent and Noncovalent Approaches, Release

Control, and Clinical Studies. *Chemical Reviews* **116** 5338-5431.

Unnanuntana A, Gladnick BP, Donnelly E & Lane JM 2010 The assessment of fracture risk. *The Journal of Bone and Joint Surgery* **92** 743–753.

Upadhyay J, S A Polyzos SA, Perakakis N, Thakkar B, Paschou SA, Katsiki N, Underwood P, Park KH, Seufert J, Kang ES, Sternthal E, Karagiannis A & Mantzoros CS 2018 Pharmacotherapy of type 2 diabetes: An update. *Metabolism Clinical and Experimental* **78** 13 – 42.

Varela A, Chouinard L, Lesage E, Guldberg R, Smith SY, Kostenuik PJ &Hattersley G 2017. One year of abaloparatide, a selective peptide activator of the PTH1 receptor, increased bone mass and strength in ovariectomized rats. *Bone* **95** 143-150.

Varol C, Zvibel I, Spektor L, Mantelmacher FD, Vugman M, Thurm T, Khatib M, Elmaliah E, Halpern Z & Fishman S 2014 Long Acting Glucose-Dependent Insulinotropic Polypeptide Ameliorates Obesity-Induced Adipose Tissue Inflammation. *Journal of Immunology* **193** 4002-4009.

Vennin S, Desyatova A, Turner JA, Watson PA, Lappe JM, Recker RR & Akhtera MP 2017 Intrinsic material property differences in bon tissue from patients suffering low-trauma osteoporotic fractures, compared to matched non fracturing women. *Bone* **97** 233-242.

Verdelis K, Lukashova L, Atti E, Mayer-Kuckuk P, Peterson MGE, Tetradis S, Boskey AL & van der Meulen MCH 2011 MicroCT Morphometry Analysis of Mouse Cancellous Bone: Intra- and Inter-system Reproducibility. *Bone* **49** 580–587.

Vestergaard P 2007 Discrepencies in bone mineral density and fracture risk in patients with type 1 and type 2 diabetes - a meta analysis. *Osteoporosis International* **18** 427-444.

Vogt MT, Cauley JA, Kuller LH, Nevitt MC 1997 Bone mineral density and blood flow to the lower extremities: the study of osteoporotic fractures. *Journal of Bone and Mineral Research* **12** 283-289.

Wallander M, Axelsson KF, Nilsson AG, Lundh D & Lorentzon M 2017 Type 2 Diabetes and Risk of Hip Fractures & Non-Skeletal

Fall Injuries in the Elderly: A Study From the Fractures and Fall Injuries in the Elderly Cohort (FRAILCO). *Journal of Bone & Mineral Research* **32** 449–460.

Walter Ramsey& Carlos M. 2017 Isales Intestinal Incretins and the Regulation of Bone Physiology. *Advances in Experimental Medicine and Biology* **1033** 13- 33.

Wan Kim SW, Yanhui Lu, Elizabeth A Williams, Forest Lai, Ji Yeon Lee, Tetsuya Enishi, Deepak H Balani, Michael S Ominsky, Hua Zhu Ke, Henry M Kronenberg, Marc N Wein 2017 Sclerostin Antibody Administration Converts Bone Lining Cells Into Active Osteoblasts. *Journal of Bone and Mineral Research* **32** 892–901.

Wang Q, Yan J, Yang J & Li B 2016 Nanomaterials promise better bone repair. *Materials Today* **19** 451-463.

Wang T, Ma X, Tang T, Higuchi K, Peng D, Zhang R, Chen M, Yan J, Wang S, Yan D, He Z, Jiang F, Bao Y, Jia W, Ishida K & Hu C 2017 The effect of glucose-dependent insulinotropic polypeptide (GIP) variants on visceral fat accumulation in Han Chinese populations. *Nutrition & Diabetes* **7** 1-6.

Wang X, Chen J, Li L, Zhu CL, Gao J, Rampersad S, Bu L & Qu S 2017 New association of bone morphogenetic protein 4 concentrations with fat distribution in obesity and Exenatide intervention on it. *Lipids in Health & Disease* **16** 1-8.

Wang X, Lai Y, Helena HL, Zhijun N & Qin L 2015 Systemic Drug Delivery Systems for Bone Tissue Regeneration– A Mini Review. *Current Pharmaceutical Design* **21** 1575-1583.

Wang ZX, Lloyd AA, Burket JC, Gourion-Arsiquaud S & Donnelly E 2016 Altered distributions of bone tissue mineral and collagen properties in women with fragility fractures. *Bone* **84** 237-244.

Wasserman H & Gordon CM 2017 Bone Mineralization and Fracture Risk Assessment in the Pediatric Population. *Journal of Clinical Densitometry* **20** 389–396.

Watts NB, Bilezikian JP, Usiskin K, Edwards R, Desai M, Gary GL 2016 Effects of Canagliflozin on Fracture Risk in Patients With Type 2 Diabetes Mellitus. *The Journal of Clinical Endocrinology & Metabolism* **101** 157-166.

WC Oliver & GM Pharr 1992 An improved technique for determining hardness and elastic modulus using load and displacement sensing indentation experiments. *Journal of Materials Research* **7** 1564-1583.

Weaver RE, Donnelly D, Wabitsch M, Grant PJ & Balmforth AJ 2008 Functional expression of glucose-dependent insulinotropic polypeptide receptors is coupled to differentiation in a human adipocyte model. *International Journal of Obesity* **32** 1705–1711.

Weiner S & Wagner HD 1998 The material bone: structure-mechanical function relations. *Annual Review of Materials Science* **28** 271-298.

Wen X-X, Wang F-Q, Xu C, Wu Z-X, Zhang Y, Feng Y-F, Yan Y-B & Lei W 2015 Time Related Changes of Mineral and Collagen and Their Roles in Cortical Bone Mechanics of Ovariectomized Rabbits. *PLoS ONE* **10** e0127973.

Westberg-Rasmussen S, Starup-Linde J, Hermansen K, Holst JJ, Hartmann B, Vestergaard P & Gregersen S 2017 Differential impact of glucose administered intravenously or orally on bone turnover markers in healthy male subjects. *Bone* **97** 261-266.

White WB & Baker WL 2016 Cardiovascular Effects of Incretin Based Therapies. *Annual Review of Medicine* **67** 245-260.

Whitehouse WJ, Dyson ED & Jackson CK 1971 The scanning electron microscope in studies of trabecular bone from a human vertebral body. *Journal of Anatomy* **108** 481-496.

Whyte MP 2016 Hypophosphatasia — aetiology, nosology, pathogenesis, diagnosis and treatment. *Nature Reviews Endocinology* **12** 233–246.

Whyte MP, Magill HL, Fallon MD & Herrod HG 1986 Infantile hypophosphatasia: normalization of circulating bone alkaline phosphatase activity followed by skeletal remineralization. Evidence for an intact structural gene for tissue nonspecific alkaline phosphatase. *Journal of Pediatrics* **108** 82-88.

Whyte MP, McAlister WH, Patton LS, Magill HL, Fallon MD, Lorentz WB & Herrod HG 1984 Enzyme replacement therapy for infantile hypophosphatasia attempted by intravenous

infusions of alkaline phosphataserich Paget plasma: results in three additional patients. *Journal of Pediatrics* **105** 926-933.

Wice BM, Wang S, Crimmins DL, Diggs-Andrews KA, Althage MC, Ford EL, Tran H, Ohlendorf M, Griest TA, Wang Q, Fisher SJ, Ladenson JH and Polonsky KS 2010 Xenin-25 potentiates glucose-dependent insulinotropic polypeptide action via a novel cholinergic relay mechanism. *The Journal of Biological Chemistry* **285** 19842-19853.

Wientroub S, Eisenberg D, Tardiman R, Weissman SL & Salama R 1980 Isdiabetic osteoporosis due to microangiopathy? *Lancet* **316** 931-988.

Wilmot E & Idris I 2014 Early onset type 2 diabetes: risk factors, clinical impactand management. *Therapeutic Advances in Chronic Diseases* **5** 234–244.

Wolverton D & Blair M. 2017 Fracture risk associated with common medications used in treating type 2 diabetes mellitus. *American Journal of Health-System Pharmacy* **74** 1143-1151.

Wu T, Yu, S, Chen D & Wang Y 2017 Bionic Design, Materials and Performance of Bone Tissue Scaffolds. *Materials (Basel)* **10** 1-14.

Xian L, Wu X, Pang L, Lou M, Rosen CJ, Qiu T, Crane J, Frassica F, Zhang L, Rodriguez JP, Jia X, Yakar S, Xuan S, Efstratiadis A, Wan M & Cao X 2012 Matrix IGF-1 maintains bone mass by activation of mTOR in mesenchymal stem cells. *Nature Medicine* **18** 1095-1100.

Yamagishi S 2011 Role of advanced glycation end products (AGEs) in osteoporosis in diabetes. *Current Drug Targets* **12** 2096-2102.

Yamamoto M, Yamaguchi T, Nawata K, Yamauchi M & Sugimoto T 2012 Decreased PTH Levels Accompanied by Low Bone Formation Are Associated with Vertebral Fractures in Postmenopausal Women with Type 2 Diabetes. *The Journal of Clinical Endocrinology & Metabolism* **97** 1277-1284.

Yamane S, Harada N & Inagaki N 2016 Mechanisms of fat inducedgastric inhibitory polypeptide/glucose-dependent insulinotropic polypeptide secretion from K cells. *Journal of Diabetes Investigation* **7** 20-26.

Yan J & Charles JF 2017 Gut Microbiome and Bone: to Build, Destroy, or Both? *Current Osteoporosis Report* **15** 376-384.

Yan L, Nielsen FH, Sundaram S & Cao J 2017 Monocyte chemotactic protein-1 deficiency attenuates and highfat diet exacerbates bone loss in mice with Lewis lung carcinoma. *Oncotarget* **8** 23303-23311.

Yan X, Wu G, Qu Q, Fan X, Xu X & Liu N 2016 A Hybrid Peptide PTS that Facilitates Transmembrane Delivery and Its Application for the Rapid In vivo Imaging via Near-Infrared Fluorescence Imaging. *Frontiers in Pharmacology* **7** 1-10.

Yanagimachi T, Fujita Y, Takeda Y, Honjo J, Sakagami H, Kitsunai H, Takiyama Y, Abiko A, Makino Y, Kieffer TJ & Haneda M 2017 Dipeptidyl peptidase-4 inhibitor treatment induces a greater increase in plasma levels of bioactiveGIP than GLP-1 in non-diabetic subjects. *Molecular Metabolism* **6** 226-231.

Yang J, Oh YT, Wan D, Watanabe RM, Hammock BD & Youn JH Postprandial effect to decrease soluble epoxide hydrolase activity: roles of insulin and gut microbiota. *Journal of Nutritional Biochemistry* **49** 8-14.

Yang PY, Zoub H, Chaob E, Sherwood L, Nunezb V, Keeney M, Ghartey-Tagoe E, Ding Z, Quirinob H, Luo X, Welzel G, Chen G, Singh P, Woods AK, Schultz PG & Shen W 2016 Engineering a long-acting, potent GLP-1 analog for microstructure-based transdermal delivery. *Proceedings of National Academy of Sciences* **12** 4140-4145.

Yipei Chen, Jiabin Luan, Shen W, Kewen Lei, Lin Yu & Jiandong Ding 2016 Injectable and Thermosensitive Hydrogel Containing Liraglutide as a Long Acting Antidiabetic System. *ACS Applied Material Interfaces* **8** 30703- 30713.

Yokogawa K, Toshima K, Yamoto K, Nishioka T, Sakura N & Miyamoto K 2006 Pharmacokinetic advantage of an intran sal preparation of a novel antiosteoporosis drug, L-Asp hexapeptide-conjugated estradiol. *Biological & Pharmaceutical Bulletin* **29** 1229-1233.

Yumiko Oishi Y & Manabe I 2016 Macrophages in age-related chronic inflammatory diseases. *Aging & Mechanisms of Disease* **2** 1-8.

Yusta B, Baggio LL, Koehler J, Holland D, Cao X, Lee J. Pinnell, Johnson-Henry KC, Yeung W, Michael G. Surette, Bang KWA, Sherman PM & Drucker DJ 2015 GLP-1R Agonists Modulate Enteric Immune Responses Through the

Intestinal Intraepithelial Lymphocyte GLP-1R. *Diabetes* **64** 2537–2549.

Zhang JJJ, Hu P & Jacobsen LV 2011 The Pharmacokinetics, Pharmacodynamics, and Tolerability of Liraglutide, a Once Daily Human GLP-1 Analogue, After Multiple Subcutaneous Administration in Healthy Chinese Male Subjects. *The Journal of Clinical Pharmacology* **51** 1620 1627.

Zhang M, Xuan S, Bouxsein ML, von Stechow D, Akeno N, Faugere MC, Malluche H, Zhao G, Rosen CJ, Efstratiadis A & Clemens TL 2002 Osteoblast-specific knockout of the insulin-like growth factor (IGF) receptor gene reveals an essential role of IGF signaling in bone matrix mineralization. *Journal of Biological Chemistry* **277** 44005-44012.

Zhong Q, Itokawa T, Sridhar S, Ding K, Xie D, Kang B, Bollag WB, Bollag RJ, Hamrick M, Insogna K & Isales CM 2007 Effects of glucose-dependent insulinotropic peptide on osteoclast function. *American Journal of Physiology Endocrinology And Metabolism* **292** E543-E548.

Zhu C, Zhang W, Liu J, Mu B, Zhang F, Lai N, Zhou J, Xu A & Li Y 2017 Marine collagen peptides reduce endothelial cell injury in diabetic rats by inhibiting apoptosis and the expression of coupling factor 6 and microparticles. *Molecular Medicine Reports* **16** 3947-3957.

Zhuo Fu, Gilbert ER & Liu D 2013 Regulation of Insulin Synthesis and Secretion and Pancreatic Beta-Cell Dysfunction in Diabetes. *Current Diabetes Review* **9** 25–53.

Zurick KM, Qin C & Bernards MT 2012 Mineralization induction effects of osteopontin, bone sialoprotein, and dentin phosphoprotein on a biomimetic collagen substrate. *Journal of Biomedical Materials Research* **101A** 1571-1581.